Gene regulatory and pro-tumourigenic mechanisms of the bHLH-PAS Transcription Factor SIM2s

Alexandra Louise Farrall
B.Sc (Jurisprudence) (Hons.)

A thesis submitted in the fulfilment of the requirements for the degree of Doctor of Philosophy

Discipline of Biochemistry
School of Molecular and Biomedical Science
The University of Adelaide, Australia
21st May, 2009

Table of Contents

ABSTRACT

Single-minded 2 (SIM2), a class I basic Helix-Loop-Helix/PAS (bHLH/PAS) transcription factor, is essential for early development, and the short isoform (SIM2s) is selectively up-regulated in pancreatic and prostate tumours. Mechanistic role(s) for SIM2 that are essential for development and in these cancers is unknown, largely due to the fact that few *bona fide* target genes have been described for SIM2. SIM2 must heterodimerise with the obligate class II partner factor ARNT to regulate transcription. Surprisingly, these studies reveal SIM2 plays a role in the regulation of the ARNT homologues, ARNT1 and ARNT2. Two non-exclusive mechanisms were identified; enhanced protein stabilisation, and the specific increased transcription of *ARNT2*. The regulation of ARNT by a class I family member was found to be unique to the SIM homologues. These findings suggest novel insights into how elevated levels of SIM2s in tumours may confer increased transcriptional activities and/or increase the availability of the essential partner factor for other class I family members to promote their respective activities and functions in developmental and/or tumourigeneic processes. Furthermore, microarray studies in prostate DU145 cells identified the pro-cell death gene, *BNIP3* (Bcl-2/adenovirus E1B 19kDa interacting protein 3), as a novel target of SIM2s mediated repression. Further validation showed BNIP3 repression in several prostate and pancreatic carcinoma derived cell lines with ectopic expression of human SIM2s via SIM2s activities at the proximal promoter hypoxia response element (HRE), the site through which bHLH/PAS family member, Hypoxia-Inducible Factor 1α (HIF1α), induces *BNIP3*. SIM2s attenuates *BNIP3* hypoxic induction via the HRE, and increased hypoxic induction of *BNIP3* occurs with siRNA knockdown of endogenous SIM2s in prostate PC3AR+ cells. BNIP3 is implicated in hypoxia-induced cell-death processes. PC3AR+ cells expressing

ectopic SIM2s have enhanced survival upon treatment with hypoxia mimetics, DP and DMOG. LC3-II protein levels fail to induce in PC3AR+/SIM2s DMOG and hypoxia treated cells, suggesting SIM2s may attenuate autophagic cell-death processes, perhaps via BNIP3 repression. These data show, for the first time, SIM2s cross-talk on an endogenous HRE. SIM2s functional interference with HIF1α activities on *BNIP3* may indicate a novel role for SIM2s in promoting tumourigenesis. Moreover, SIM2 expression has previously been implicated in the Hedgehog (Hh) signalling pathway during mouse brain development. The Hh-pathway is known to promote pancreatic and prostate tumour growth, and these studies indicate that SIM2s is indeed implicated in promoting and/or maintaining Hh-signalling in cell lines of these cancer types. Likewise, aberrant Androgen Receptor (AR)-signalling is implicated in prostate tumour development, and androgen-independent AR activity is a hallmark of aggressive prostate cancer. Unexpectedly, SIM2s expression was found to up-regulate endogenous AR protein levels in prostate carcinoma PC3AR+ cells. Furthermore, SIM2s expression is associated with androgen-dependent wtAR-transcriptional responsiveness in these cells, and SIM2s co-immunoprecipitates with endogenous AR in a hormone independent manner. Together these data suggest, for the first time, that SIM2s may function as a co-activator, and concomitant with enhancing AR levels, aid AR-signalling in prostate cancer cells. In summary, these studies sought to identify molecular mechanisms by which aberrant levels of SIM2s expression in solid tumours of the prostate and pancreas may promote tumour development. Several novel mechanisms for SIM2s activities were identified which implicate SIM2s in tumour processes. Namely SIM2s was found to be implicated in:

1) promoting pro-tumourigeneic Hh and AR signalling pathways

2) regulation of the common partner factor ARNT, and

3) attenuation of hypoxically-induced cell-death processes in tumour cells via the direct transcriptional repression of the novel SIM2s target gene, *BNIP3*.

CANDIDATES DECLARATION

To the best of my knowledge, this work contains no material which has been accepted for the award of any other degree or diploma in any university or other tertiary institution, and to the best of my knowledge and belief, contains no material previously published or written by another person, except where due reference has been made in the text. I give consent to this copy of my thesis when deposited in the University Library, being made available for loan and photocopying, subject to the provisions of the Copyright Act 1968.

The author acknowledges that copyright of published works contained within this thesis (as listed below) resides with the copyright holder(s) of those works. I also give permission for the digital version of my thesis to be made available on the web, via the University's digital research repository, the Library catalogue, the Australasian Digital Theses Program (ADTP) and also through web search engines, unless permission has been granted by the University to restrict access for a period of time.

Alexandra Farrall

21st of May 2009

1. Woods, S., Farrall, A., Procko, C., & Whitelaw, M. The bHLH/Per-Arnt-Sim transcription factor SIM2 regulates muscle transcript myomesin2 via a novel, non-canonical E-box sequence. *Nucleic Acids Res.* 2008 Jun;36(11):3716-27

PUBLISHED & PRESENTED WORK ARISING FROM THIS THESIS

Publications:

1. Woods, S., Farrall, A., Procko, C., & Whitelaw, M. The bHLH/Per-Arnt-Sim transcription factor SIM2 regulates muscle transcript myomesin2 via a novel, non-canonical E-box sequence. *Nucleic Acids Res.* 2008 Jun;36(11):3716-27

2. Farrall, A., and Whitelaw, M. The HIF-1α inducible pro-cell death gene BNIP3 is a novel target of SIM2s repression via cross talk on the Hypoxia Response Element. *(Manuscript under peer review)*

Conferences and Symposia Presentations:

Published abstract:

Farrall, A., and Whitelaw, M. SIM2s functional interference with HIF1α-inducible expression of the pro-cell death factor BNIP3 - A novel target of SIM2s repression via the hypoxia response element. 2009 (*in press*) *Annals of the NYAS*.

Invited oral presentations:

1. Flinders University Medical School Seminar Series, SA, Australia, July 23rd, 2008
Presentation Title: "Is anything SIMple in tumourigenesis?: Putative role for the bHLH-PAS transcription factor, SIM2, in tumour progression through regulation of pro-apoptotic BNIP3" A. Farrall & M. Whitelaw

2. Network in Genes and Environment in Development [NGED] Forum:
Cross Disciplinary Workshop Attendance Award, 2007, June 13-15th 2007 - Palm Cove, QLD, Australia

Presentation Title: “NGED Epigenetics Workshop, QIMR, 2006: Investigating a putative role for the transcription factor SIM2 in tumourigenesis” A. Farrall & M. Whitelaw

Poster presentations:

1. Howard Hughes Medical Institute [HHMI]: Modern Technologies in Gene Expression Detection and Data Integration Course, July 2006

The University of Debrecen, Debrecen, HUNGARY

Poster: “Investigating a role for the transcription factor SIM2s in tumourigenesis” A. Farrall & M. Whitelaw

2. New York Academy of Sciences: “Hypoxia and Consequences: from Molecule to Malady” Conference, March 2009 – New York, NY, USA

Poster: “SIM2s functional interference with hif1α-inducible expression of the pro-cell death factor bnip3 - a novel target of SIM2s repression via the hypoxia response element” A. Farrall, & M. Whitelaw

3. 28th Lorne Genome Conference 2007 – Lorne, VIC, Australia

Millennium Science Student Poster Prize –

Poster presentation entitled “Investigating a role for the transcription factor SIM2 in tumourigenesis”. A. Farrall & M. Whitelaw

4. 20th Lorne Cancer Conference 2008 – Lorne, VIC, Australia

Poster: “Interplay of bHLH/PAS transcription factors in tumourigenesis: Single Minded 2 Competes with the Hypoxia Inducible Factor for Regulation of the Pro-apoptotic gene BNIP3” A. Farrall & M. Whitelaw

ACKNOWLEDGEMENTS

Firstly, to my supervisor and mentor Murray Whitelaw; thank you for all the insightful conversations, inspiring excitement and passion for science, and allowing me the opportunity to study and work in a supportive, stimulating and fun environment. I am particulary grateful for all the opportunities to extend my professional, and personal, development via study and work both at home and abroad. I am also grateful to Daniel Peet for inspired advice and many laughs, to Anne Chapman-Smith, for her patience and insight, and to Keryn Williams, for her encouragement and sincere interest in my professional development. I am particulary most thankful for the friendship and mentorship of Susi Woods, a brilliant mind with a big heart. I was honoured to be your 'partner in (SIM2) crime'! Fiona Whelan, my 'bay buddy' and friend; thanks for your quick wit and mind, all the daily laughs, science-talk, life-talk and encouragement along the way. It was wonderful to share the 'PhD journey' with you! I sincerely thank Margo van Bekkum and Colleen Bindloss for their friendship and brilliant technical assistance, and to all past and present Whitelaw and Peet Lab members, and many in the School of Molecular & Biomedical Science who have all been supportive friends and collegues and contributed to making a dynamic and fun work environment. Big thanks to Jo, Mike, Sebastian, Anne R, Dave, Andrew and Adrienne – the next carrier of the SIM2 torch, with your mind behind it, it will surley be bright! I am privileged to have had the opportunity to work with our collaborators Lorenz Poellinger and Katarina Gradin, a most patient teacher and friend, at the Karolinska Institutet in Stockholm, Sweden, also in collaboration with Helena Edlund and Elisabet Palsson at the Univeristy of Umeå, Sweden. I would also like to thank the staff of the Adelaide Microarray Centre. Importantly, my deepest thanks go my supportive parents, wonderful brothers and sisters, and friends for all the fun, love, friendship and understanding. Lastly, and most importantly, my heartfelt gratitude and appreciation goes to my husband Pelham; ever constant, ever understanding and supportive, and a source of inspiration and continued encouragement.

CHAPTER 1

Introduction

1.1 bHLH/PAS Family of Transcriptional Regulators – General background

The bHLH-PAS [basic Helix-Loop-Helix-Per-Arnt-Sim homology] transcription factors respond to a number of physiological and developmental cues such as hypoxic stress, exposure to xenobiotics, circadian rhythms and neurogenesis [1, 2]. Gene targeting studies in mice have revealed all bHLH-PAS family members are essential for development. Commonly, homozygous deletions are either embryonic lethal, or mice die shortly after birth due to developmental defects [1-3]. These factors form a subfamily of the evolutionarily conserved bHLH proteins, distinguished by the PAS domain juxtaposed to the bHLH at the N-terminus (**Figure 1.1**) (for review [4, 5]). The basic region binds the DNA, and the HLH is the primary dimerisation interface. The distinguishing PAS domain acts as a secondary dimerisation interface to the bHLH domain, and is also known to mediate a number of biochemical functions, including small molecule binding, contribution to DNA binding and target gene specificity [5-7].

In 1996 Hirose *et al* aligned the PAS regions of identified family members to date including, rat Arnt (Arylhydrocarbon Receptor Nuclear Transporter), Arnt homologues 1 and 2 from mouse, *drosophila melanogaster* Per, and the murine factors Single-minded (Sim), Arylhydrocarbon Receptor (AhR) and Hypoxia-Inducible Factor 1 alpha (HIF1α), and consequently were the first to identify that the family divided into two sub-groups [8]. bHLH/PAS proteins fall within one of two classes; class one (I) comprises, among others in mammals, the AhR (or Dioxin receptor DR), SIM and HIF-1α and NPAS4 (or NXF); class two (II) contains ARNT1 and ARNT2 [5, 8-10]. Class II members are able to homodimerise, whereas Class I heterodimerise with ARNT1 or ARNT2 to form transcriptionally functional heterodimers [4, 5, 11]. The molecular mechanisms which underpin activation of gene targets by these factors in response to environmental cues or stimuli are best characterised for HIF1α and AhR, in response to hypoxic stress or

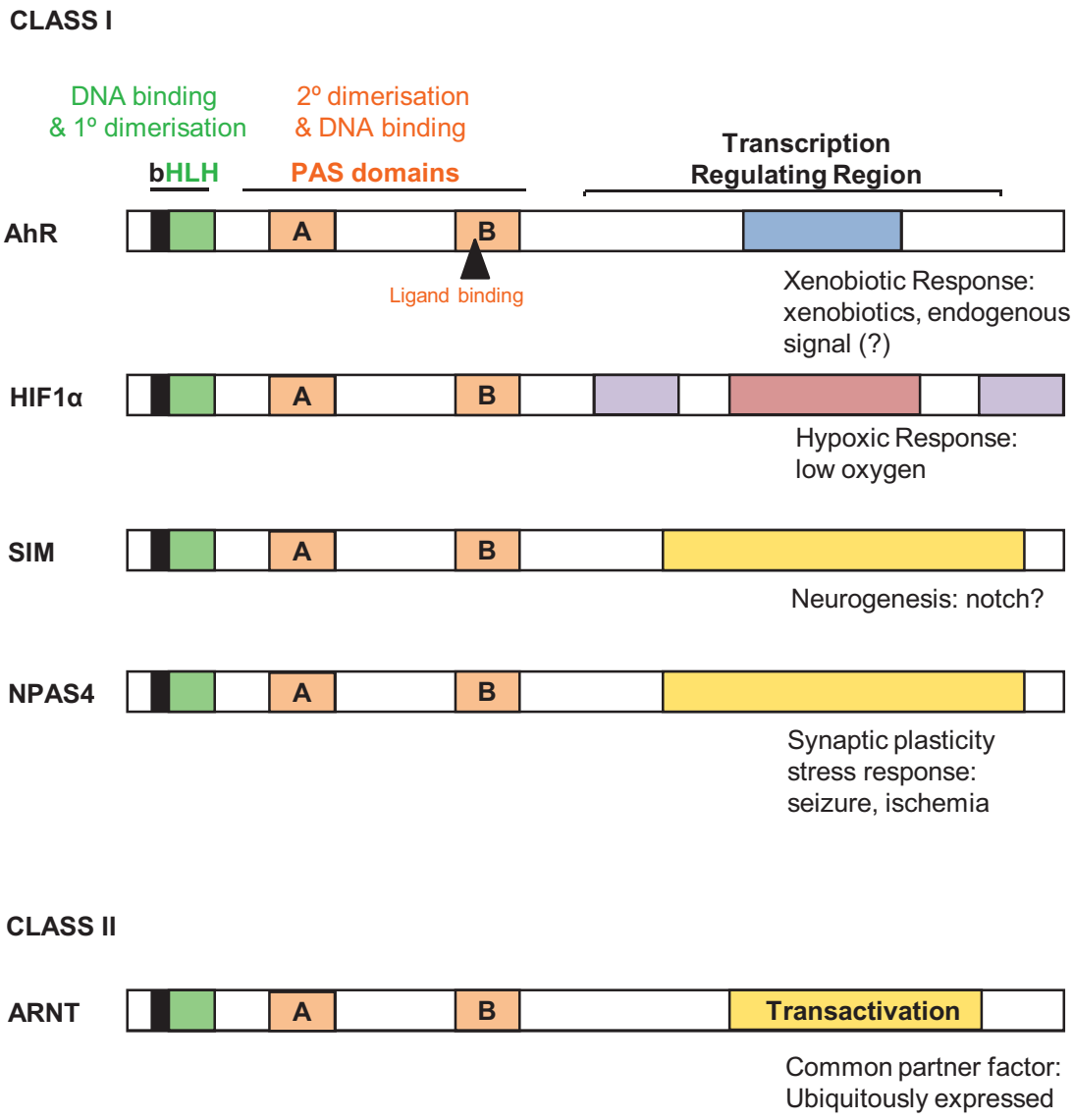

FIGURE 1.1: *Schematic example of conserved regions of the bHLH-PAS family of transcriptional regulators.*

Family members are characterised by the N-terminal basic-Helix-Loop-Helix (bHLH) DNA binding and 1° dimerisation domain, followed by two repeat PAS domains, PAS A and PAS B, also required for DNA-binding and a 2° dimerisation domain, followed by the C-terminal transcription regulating region. Class I family members all heterdimerise with the Class II family member, ARNT. Functional roles and mechanisms of activation and/or regulation are also indicated for the family members represented.

exposure to xenobiotics, respectively. The Hypoxia Inducible Factor (HIF) will be discussed in more detail as an example of a bHLH/PAS protein activated by an environmental signal, as it is one of the most studied, and consequently better understood, family members.

1.1.1. The Hypoxia Inducible Factor

The chronic response to low oxygen tension, or hypoxia, has been found to be largely mediated by the transcription inducing activities of the Hypoxia Inducible Factors, including HIF1α and a closely related non-redundant homologue, HIF2α [12-14], which drive the expression of many genes encoding proteins required for the hypoxic response; including those involved in vascularisation, erythropoiesis, the glycolytic pathway, and glucose uptake (for review see [12, 13]). These bHLH-PAS family members are stabilised and transcriptionally activated in hypoxic conditions via the inhibition of oxygen-dependent post-translational mechanisms (reviewed by [14]). In essence, the oxygen-dependent prolyl-hydroxylase (PHD) enzymes specifically hydroxylate two proline residues in the C-terminus of HIF in normoxic conditions [15]. Hydroxylation confers recruitment of VHL (von-hippel-lindau) protein, a component of the E3-ubiquitin ligase complex which subsequently poly ubquitylates HIF to format it for degradation via the proteosome [16-18]. During hypoxia, HIF remains non-hydroxylated to avoid VHL mediated degradation. Secondly, inhibition of the oxygen-dependent asparagine hydroxylase, Factor Inhibiting HIF (FIH), allows interaction between HIF and the transcriptional co-activator, CBP/p300 [19, 20]. Following stabilisation and activation of HIF in response to hypoxia, HIF/ARNT heterodimers initiate transcription via the hypoxia response element (HRE) DNA sequences 5'-C/TACGTG-3' in the regulatory regions of hypoxia responsive genes, including; *erythropoietin* (*EPO*) [21] and *vascular endothelial growth factor* (*VEGF*) [22]. These mechanisms of hypoxic stabilisation and activation of HIF are outlined in **figure 1.2**. Interestingly, oxygen-independent

mechanisms of HIF regulation have also been reported and are gradually becoming better understood (reviewed in [23], also see [24] further discussed in **Chapter 6**).

1.2 The Single-minded (SIM) bHLH/PAS Family Members

First identified in *Drosophila melanogaster*, *dSim* has been found to be a master regulator of cell lineage-specific development in the central nervous system (CNS) ([25-29]; for review see, [30]). Single minded orthologues have also been identified in a number of other organisms, including *xenopus,* zebrafish, rodents and humans [9, 31-38]. Two mouse and two human *Sim* genes have been isolated thus far through homology to *dSim*, and are termed *mSim1* and *mSim2,* and *hSIM1* and *hSIM2* respectively [9, 34-38]. These proteins share extremely high sequence conservation in the bHLH and PAS regions required for DNA-binding and partner factor heterodimerisation; where in comparison to dSim, both mouse and human Sim homologues share 87-90% and 69-70% identity in the bHLH and PAS regions respectively. Indeed, mouse and human Sim1 share approximately an overall 98% identity across these regions, and likewise mSim2 and hSIM2 share 99% amino acid identity [38][S. Woods, PhD Thesis 2004]. Such high levels of conservation in these regions required for DNA-binding and partner factor heterodimerisation begs the question as to how these non-redundant homologues might confer alternate (and specific) transcriptional responses, the answer to which remains to be determined.

Human *SIM1,* located on chromosome 6, produces a single transcript [38]. Conversely, human *SIM2*, located on chromosome 21, has had up to five different RNA species identified from northern blot analysis of RNA samples from human foetal kidney tissue and cultured neuro- and glio-blastoma and embryonic human kidney cell lines [38-40]. Alternative splicing produces a short Sim2 protein variant in mice and humans [38, 41]. The designated 'short' isoform of human SIM2 (SIM2short or SIM2s) studied here was

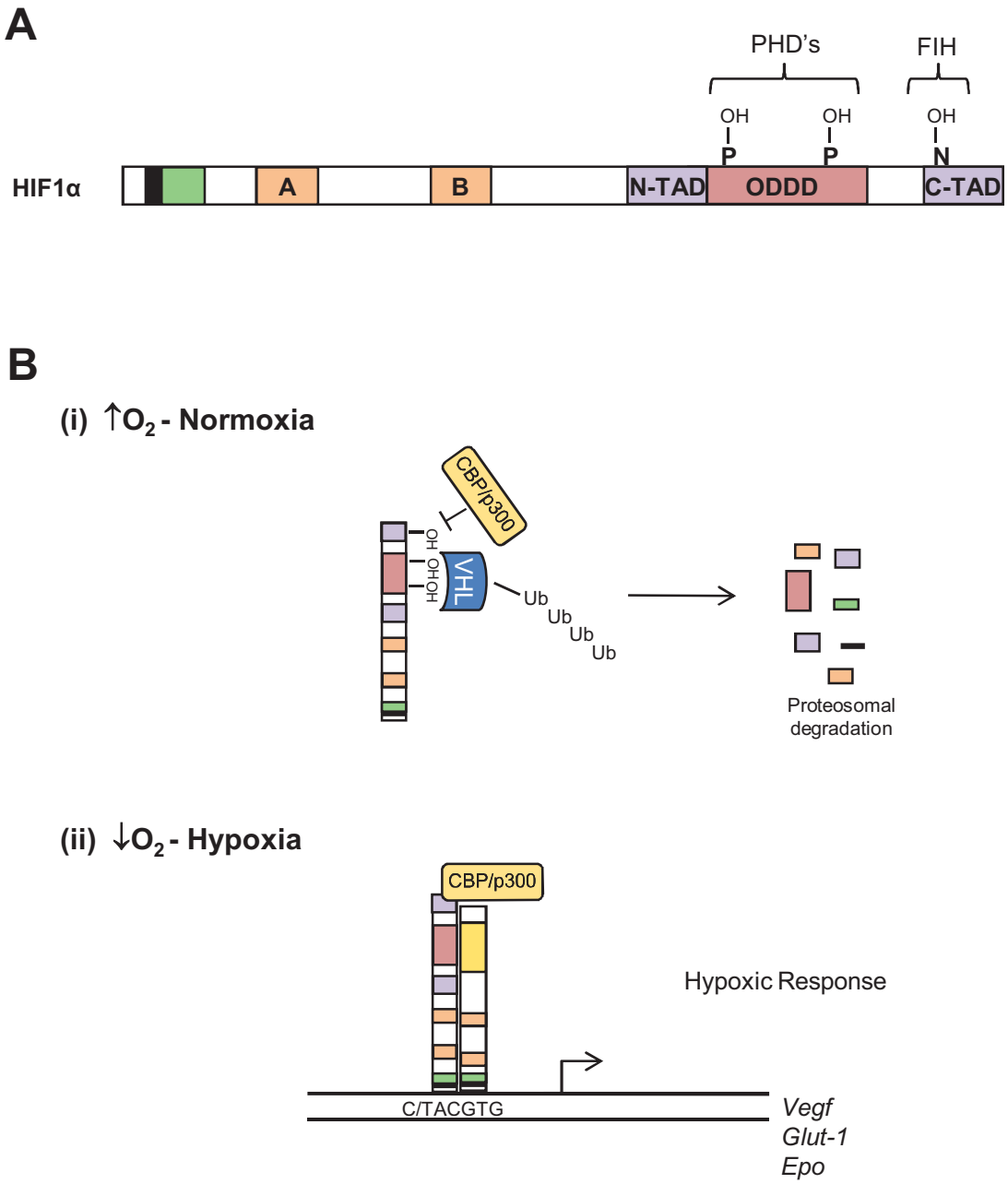

FIGURE 1.2: *The HIF1α and the Hypoxic Response.*

(A) Schematic of HIF1α indicating the carboxy terminal regulatory and transactivation domains; N-TAD & C-TAD, N and C-terminal activation domains, ODDD, oxygen dependent degradation domain. When oxygen is available, Proline (P) residues in the ODDD, and an Asparigine (N) in the C-TAD, are hydroxylated via the oxygen dependent PHD's (proyl hydroxylases) and FIH (factor inhibiting HIF), respectively. (B) (i) In normoxia, HIF1α-mediated transcription is inhibited as hydroxylation of HIF inhibits co-activator (CBP/p300) binding and results in VHL binding and poly-ubiquitination (Ub) of the protein and subsequent degradation via the proteasome. (C) In hypoxia (low oxygen tension), HIF1a is stabilised, and heterodimerises with ARNT and interacts with co-factors to mediate a transcriptional response via binding to the enhancer elements in target genes such as Vegf, Glut-1 and Epo.

identified using 3' RACE on foetal kidney mRNA and a foetal kidney cDNA library screen by Chrast and co-workers (1997). This arises from a 4.4 kb transcript and is due to an alternate read-through event into the last intron of *SIM2,* resulting in a 570 amino acid protein which contains only one of the two SIM2 repression regions and a final 44 residues of unique C-terminal sequence [38]. The full length 667 residue SIM2 'long' protein (SIM2Long or SIM2L) arises from the 6 kb transcript (**Figure 1.3**). The other 3.6, 3.0, and 2.7kb *SIM2* mRNA transcripts identified are yet to be studied further. How the minor divergence between C-termini of full length human SIM2L and SIM2s may confer alternate transcriptional activities or functions remains to be fully elucidated. More recently a short form of mouse Sim2 has been characterised. mSim2s is a 579 amino acid protein with an overall 87% amino-acid identity with human SIM2s. Interestingly however, the variable 'short' regions between the mouse and human orthologues are actually quite divergent, sharing only 20% amino acid homology [41]. How these differences may confer alternate transcriptional functions of Sim2s in mice and humans remains to be investigated.

Analyses of expression patterns of *Sim1* and *Sim2* in *xenopus*, zebrafish, chick, rodents and humans has provided a starting point to postulate functional roles for the Sim family members [31, 35, 36, 38, 39, 42, 43]. Each mammalian Sim homologue was found to have partially overlapping, but differing expression patterns and molecular properties. Most of our understanding comes from studies in mice as will be described in the following sections.

1.2.1. SIM expression patterns in development

Despite the broad screening for the Sims in various tissues and in wholemount sections of the developing embryo from zebrafish, mice and humans, the consensus overlap for expression for each homolog, as outlined in **Table 1.1**, is in essence refined to the brain, kidney and skeletal muscle. The gene expression of

mSim1 and *mSim2* overlap in some regions of the CNS, but is distinct in other regions. CNS development is common to both dSim and mSim [30]. Both mammalian homologues are functionally required for the development of several neuroendocrine lineages within the hypothalamus [39, 44, 45]. dSim expression has been reported to influence muscle development in the embryo [26] and mSim1 has also been identified as an early gene marker of presomitic mesoderm and lateral dermatome by its expression in the somites [46], suggesting a role for the Sim transcripts in muscle. Indeed, both transcripts are present in the developing and adult skeletal muscle [34, 47], and *Sim1* and *Sim2* expression is associated with limb muscle formation in the developing mouse and chick [42]. Interestingly, work from our laboratory in cultured cells has recently shown mSim2 to co-express with, and directly influence the gene expression of, the skeletal muscle factor Myomesin2 (Myom2) [48]. *Myom2* is differentially expressed and regulated during rodent muscle development in a tightly spatial-temporal manner [49-51]. Whether *Myom2* is directly targeted and regulated by the Sims during muscle development is yet to be tested experimentally.

Mammalian *Sim1* and *Sim2* transcripts are expressed in the adult and developing kidney [36, 38, 43], and as is found in developing limb muscle [42], the transcripts are expressed in a non-overlapping fashion [36]. *mSim1* is expressed to a lesser extent that *mSim2* in these tissues [35]. Early *mSim2* expression is also seen in the facial cartilage and palate, as well as trunk muscles and cartilage, ribs, vertebrae and lung [34-36, 39, 46]. All human homologues (*SIM2s*, *SIM2L* and *SIM1*) have also been reported to be co-expressed in heart, testis and tonsil tissues [43]. Human *SIM2s* and *SIM2L* were also detected in the normal tissue cDNAs of adult prostate, breast and lung, and foetal heart [38, 40, 43, 52, 53]. Human *SIM1* expression is present in many of the same tissues as *SIM2*, except *SIM2* is exclusive in the lung and prostate and *SIM1* is expressed exclusively in bone marrow, placenta, liver (adult and foetus), ovary and pancreas [43]. Recently, an *mSim1* equivalent has been identified in the brain and kidney of zebrafish, (delineated here as, *zSim1*) [32]. However, the zebrafish kidney is yet to be screened for the recently identified mSim2 equivalent, which

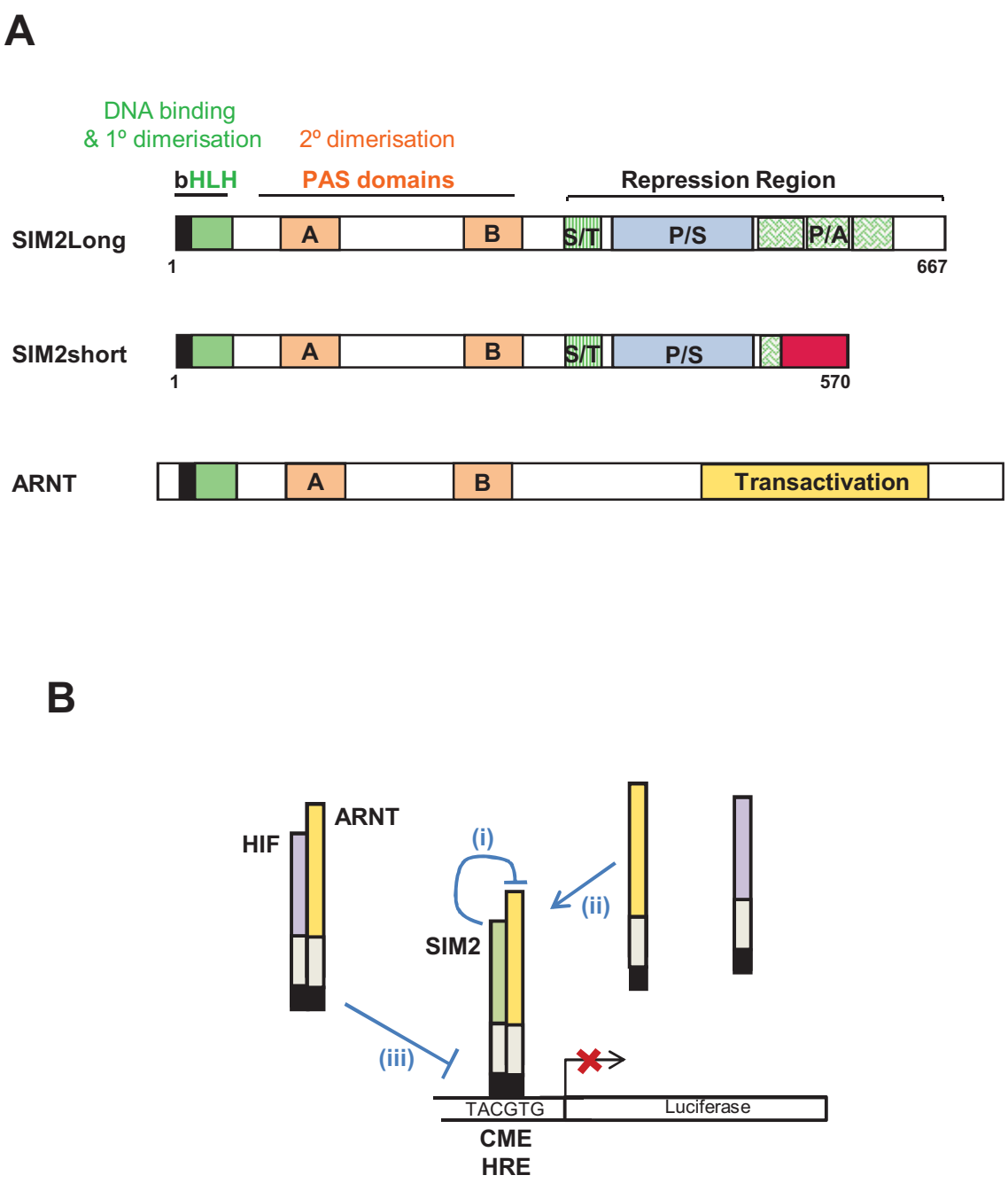

FIGURE 1.3: *Human SIM2 isoforms and known mechanisms of SIM2-mediated repression.*

(A) The C-terminal repression region of SIM2 contains serine/threonine (S/T), proline/serine (P/S) and proline/alanine (P/A) rich regions. The final 44 amino acids of the short isoform (570 residues) of SIM2 (SIM2s) contains unique sequence (highlighted in red) to the P/A-rich repressive region in the C-terminus of the 667 amino acid long isoform (SIM2L). (B) *In vitro* synthetic promoter driven reporter studies have shown SIM2 to repress transcription via (i) repression of the transactivational properties of ARNT, (ii) inhibit HIF1α/ARNT transcription via the sequesteration ARNT from HIF1α, and (iii) DNA-binding cross-talk on the HRE. Refer Woods *et al* 2002, JBC. **227**: 10236-43.

	ZEBRAFISH		MOUSE		HUMAN	
	Embryo	**Adult**	**Embryo**	**Adult**	**Embryo**	**Adult**
SIM1	Brain *kidney*	No studies as yet	Brain CNS *Kidney tubules* *Somites (early muscle)* Genital eminence Dermis	Hypothalamus *Kidney* *Skeletal muscle*	Hypothalamus *Kidney* Liver	Hypothalamus Tonsil *Kidney* Testis *Skeletal muscle* Heart Bone marrow Breast Placenta Liver Ovary *Pancreas*
SIM2	*Pancreas* *Intestine*	No studies as yet	Brain *Kidney* Craniofacial - palate Ribs *Skeletal muscle* Vertebrae Lung Limbs	Hypothalamus *Kidney* Lung *Skeletal muscle*	Hypothalamus *Kidney* *Skeletal muscle* Heart	Hypothalamus Tonsil *Kidney* Testis *Skeletal muscle* Lung Heart *Prostate*
SIM2-short	(yet to be found)		*Kidney* *Skeletal muscle*		*Kidney* *Skeletal muscle* Heart	Tonsil *Kidney* Testis *Skeletal muscle* Lung Heart Breast *Pancreatic, Colon* and *Prostate* tumours

TABLE 1.1: *Summary of expression patterns of the Single minded family members in zebrafish, mouse and humans.*

Expression patterns determined from a combination of wholemount *in situ* and RT-PCR approaches. *Italics* – main consensus of expression of both homologues.
See section 1.2 for reference details

was found in the pancreas and intestine (delineated here as, *zSim2*) [33]. Interestingly, the zSim2 equivalent, which shares approximately 96% amino acid identity in the bHLH-PAS region with mSim2, shares only 18% C-terminal amino acid identity with that of mSim2 [33]. Bioinformatic alignment of the two zebrafish Sims however, shows 54% predicted amino acid identity (data not shown). Functional roles for the Sims in zebrafish remain to be determined.

1.2.2. Targeted Deletion Studies

Homozygous null mutation of *single-minded* in *D. Melanogaster* is embryonic lethal and characterised by the failure of CNS cell development and defective ventral muscle patterning [25, 26, 28, 54, 55]. Loss of *mSim1* results in animal death shortly after birth, concurrent with hypocellularity of neuroendocrine lineages in the hypothalamus [45]. Heterozygote *mSim1* mice show that disruption of developing hypothalamic neuroendocrine pathways can cause obesity [56], and that importantly, haploinsufficiency of *Sim1* results in hyperphagic feeding behaviour [57]. Interestingly *mSim2* expression, which overlaps with *mSim1* in the PVN (paraventricular nucleus) of the hypothalamus, also contributes to hypothalamic development and neuroendocrine hormone gene expression, however, it appears to do so downstream of mSim1 [44]. Two targeted disruption studies of *mSim2* have shown that *mSim2*$^{-/-}$ mice have developmental defects distinct from *mSim1*$^{-/-}$ mice, however, phenotypic discrepancies due to loss of *mSim2* in these mice exist between the two studies [3, 58]. Both studies concur that the postnatal death of *mSim2*$^{-/-}$ mice within days after birth is due to breathing failure, despite marked differences in phenotype. Goshu *et al* (2002) attribute failure of lung inflation to compromised structural components required for breathing, including rib protrusions, abnormal vertebrae, diaphragm hypoplasia, pleural mesothelium tearing and abnormal muscle attachments. Shamblott and co-workers however, see in their F_2 double mutant mice severe defects in craniofacial architecture, especially in the palate which they report as contributing to the aerophagia. Interestingly, the

founder mouse was identical for each study, the only difference being that the F_1 heterozygous female used in the Goshu *et al* (2002) study was backcrossed for five generations, prior to selecting for the double mutant. The *mSim2*$^{-/-}$ mice in both studies displayed disrupted phenotypes in regions that corresponded to normal mSim2 expression patterns [3, 58], and hence both models may provide insight into mSim2 regulation and function in differing genetic backgrounds.

1.2.3. Activation and Regulation of SIM

There is little comprehension of the regulatory and activation mechanisms of Sim. dSim and the mammalian Sim homologues are predominantly nuclear proteins, and nuclear localisation signals (NLS) have been identified in both human SIM1 and SIM2 [54, 55, 59, 60]. Where activation and controlled cytoplasmic-nuclear shuttling of other bHLH/PAS family members occurs in response to a ligand or external environmental cue, the restricted spatial and temporal expression pattern appears to control the activity of each Sim [30].

The activation of *dSim* gene expression has been found to be under the control of Twist, Dorsal and Notch, whereas repression is mediated by by Su(H) (Supressor of Hairless) and Hairless, requiring the co-repressors Groucho (Gro) and CtBP (C-terminal Binding Protein) [61-67]. Snail also plays a direct role in the repression, and the Notch-dependent activation, of *dSim* expression in the embryo [62, 67-69]. Interestingly, where Notch signalling is required for activation of *dSim* expression, both mouse and human *Sim2* expression, reported specifically for the expression of the short isoforms, is repressed by active NOTCH signalling, and also C/EBPβ, in human breast cancer MCF-10A cells and mouse mammary tissue [70]. As NOTCH signalling has not been directly correlated to Sim1 expression in mice or humans, it remains to be determined if mechanisms of Notch-mediated regulation of *Sim* are conserved for both mammalian

homologues. A small 60bp region (-1385 to -1325) in the promoter of human *SIM2* has been shown to strongly confer the transcriptional activation of *SIM2* expression, in which the authors have identified consensus binding sites for E2F, c-Myb and E47 transcriptional regulators [40], although the identification of a specific regulatory factor(s) responsible for transactivation at this particular region remains to be shown. Studies in mice have also revealed that Sonic Hedgehog (Shh) expression, and signalling, also contributes to *mSim2* in the developing forebrain [71], yet the mechanism(s) by which this occurs also remains to be defined. In summary, there are yet to be any reports unifying, or providing any insight into how and in what context, these currently independently identified mechanisms may co-ordinate the expression and regulation of the *SIM2* gene. However, it is interesting to note that in *Drosophila* Delta to Notch signalling de-represses dE2F1 inhibition to drive proliferation during eye development, where Delta expression requires secreted Hedgehog (dHh) protein [72]. Furthermore, c-Myb and C/EBP co-operate with a Notch-related protein, GABP, to drive *mNE* (neutrophil elastase) promoter activity in mouse fibroblast NIH3T3 cells [73]. Perhaps together these studies may provide a model to investigate how various factors may interact and co-ordinate to regulate *Sim(2)* expression in mice and *Drosophila*.

Even less is understood about the direct mechanisms of *Sim1* expression and regulation, bar the interesting report from *in vitro* studies that the *mSim1* promoter contains a DR/Arnt2 responsive xenobiotic response element (XRE), and that *in vivo*, *mSim1* expression appears to be elevated in the hypothalamus and kidney of mice three days following treatment with dioxin [74].

Although this thesis is concerned with investigating mechanisms controlling gene transcription and function mediated by the SIM2 protein - ie 'downstream' of *SIM2* gene expression and regulation - further knowledge of these latter processes would also greatly aid further work and an understanding of the function of SIM2 in development, and as discussed later, in disease.

1.2.4. Molecular Mechanisms and Properties of the Single-minded Proteins

Partnered with Tango (Tgo, the *Drosophila* Arnt ortholog, referred to hereafter as dArnt), nuclear dSim can both activate midline gene expression and repress lateral CNS gene expression, the latter indirectly via activating the expression of repressive factors [27, 54, 75]. Thus dSim has only been reported to act as a transcriptional activator but is able to both positively and negatively regulate lineage-specific transcription. The DNA consensus sequence recognised by dSim/dArnt is an asymmetric E-Box-like sequence, 5'-(G/A)(T/A)ACGTG-3', termed the CNS midline enhancer element (CME) [76]. dSim regulation of the gene *slit* is conferred via a single CME DNA binding site has been identified within the intronic CNS midline enhancer of *slit* [77], whereas multiple functional CME enhancer sequences have been found in the regulatory regions of *toll*, *breathless* and *dSim* itself [76, 78]. Functional dSim/dArnt CME enhancers identified to date contain the core 5'-ACGTG-3' element.

The molecular mechanisms and functions of the mammalian Sim homologues in mice and humans remain largely unknown. There is some understanding about the transcriptional properties of Sim1, perhaps more so of Sim2. Nuclear localisation signals have been identified in hARNT, hSIM1 and hSIM2, which are found to be nuclear [60, 79], as are human and mouse SIM2s [41, 80-82], and mSim1 and mSim2 [59]. Like other Class I bHLH/PAS family members, the mSim1 and mSim2 proteins do not homodimerise but bind the common bHLH/PAS partner factors Arnt, and Arnt2 [8, 9, 34, 35, 46, 47]. Sim2 is able to heterodimerise with Arnt2 in *in vitro* systems to activate transcription of reporter genes [41, 46], however, unlike mSim1/mArnt2, which has been shown to function for the specific development of the hormone secretory regions of the hypothalamus [83, 84], no endogenous function for the Sim2/Arnt2 heterodimer has been identified. As

mentioned in the previous section (section 1.2.3) a signalling mechanism(s) that affects the localisation and/or dimerisation of the SIMs with ARNT partner factors is yet to be found.

The search to discern direct target genes of the mammalian SIM family members is rapidly progressing with the utilisation of advancements in computer based bioinformatics tools and microarray technology. Liu and colleagues (2003) recently published microarray data potentially identifying 268 downstream target genes of mSim1/mArnt2 in a neuroendocrine tumour cell context [83]. However, *bona fide* direct target genes for the mSim1/mArnt complexes remain to be established. Only in the last year has direct gene targets of Sim2/Arnt emerged [48, 82]. Indications of the transcriptional properties and what the endogenous DNA-binding response element(s) may be, for the mammalian SIMs came largely from reporter gene studies. Mouse and human SIM proteins are able to bind DNA via the core [underlined] 5'-(T)ACGTG-3' CME in the presence of Arnt or Arnt2 in reporter gene studies driven by a synthetic promoter [8, 9, 41, 46, 84]. Contrary to earlier *in vitro* studies indicating mSim2L to be a transcriptional repressor [34, 36, 59], it has recently emerged that SIM2 is also capable of activating transcription in an ARNT-transactivation-domain-dependent manner [41, 48]. The molecular mechanisms that differentiate between these two transcriptional outcomes remains to be determined, however in the case of Sim2s may be part due to the loss of one of the C-terminal repression domains (**Figure 1.3A**) [41]. This transactivation outcome may also be conferred via the context of specific DNA-binding elements, as studies by Woods and colleagues (2008), including work from this thesis, have identified a novel mammalian SIM/ARNT non-canonical E-Box DNA binding element, 5'-AACGTG-3' in the endogenous promoter of the novel human target gene *Myomesin 2* (*MYOM2*). We have termed this the S2RE (SIM2 Response Element) Specifically, this site was identified following studies in which the transcriptional control was first found to be conferred from an element within the 1.3kb promoter sequence directly upstream of the start of transcription. Several putative SIM2 DNA-binding site elements were found containing the core 5'-ACGTG-3' motif, particularly two 5'-AACGTG-3' sites. Interestingly, site-

directed mutagenesis studies of these putative elements in the 1.3kb promoter of *hMYOM2*, from 5'-AACGTG-3' to mutant 5'-AAAAAG-3' motifs, revealed that both transiently expressed mSIM2L and hSIM2s were able to mediate transactivation of luciferase reporter gene expression solely via one of these sites (site 1) in HEK293A cells (**Figure 1.4A**). Moreover, stably expressed hSIM2s.myc was only found to be bound to DNA at site 1, and not site 2, of the endogenous *hMYOM2* promoter in HEK293A cells (**Figure 1.4B**)[48]. No genes prior to this study have shown mammalian SIM2 to confer transcriptional control via direct DNA-binding activities at this novel non-canonical E-Box sequence. It is via this site that the long and short isoforms of SIM2 *activate* gene expression via the transactivation domain of ARNT [48].

Despite the loss of one of the repression regions, SIM2s has recently been shown to confer transcriptional repression via direct binding on the promoter of the newly identified target gene, *SLUG* [82]; however, the exact DNA-binding element and mechanism of this repression are yet to be defined. Three mechanisms have been previously identified by which Sim2 acts as a transcriptional repressor. The transactivational property of Arnt is silenced in the mSim2/Arnt complex by the repression activity found in the carboxy terminus of mSim2 [9, 46] (**Figure 1.3A & Bi**). Murine Sim2 can also repress transcription of reporter genes by interfering with the transactivating mSim1/Arnt and HIF-1α/Arnt heterodimers, via sequestering Arnt [9, 46] (**Figure 1.3Bii**). Furthermore, the DNA binding basic regions of the mammalian SIMs and HIF-1α are highly conserved and the mSim2/Arnt complex can also act as a repressor through competition for the hypoxia response element (HRE) from HIF-1α, which also contains the core 5'-ACGTG-3' [59] (**Figure 1.3Biii**). Conversely, the mSim1/Arnt heterodimer acts as a transcriptional activator on this same response element in synthetic reporter studies [59]. Existing literature on mSim1 activity contains data which appears contradictory, but this may be indicative of the transcriptional activity of mSim1 being context dependent [34, 35, 83]. Model reporter gene transfection studies indicate that, as is for Sim2, the activation properties of the mSim1/Arnt heterodimer may be largely due to the presence of Arnt [46, 59].

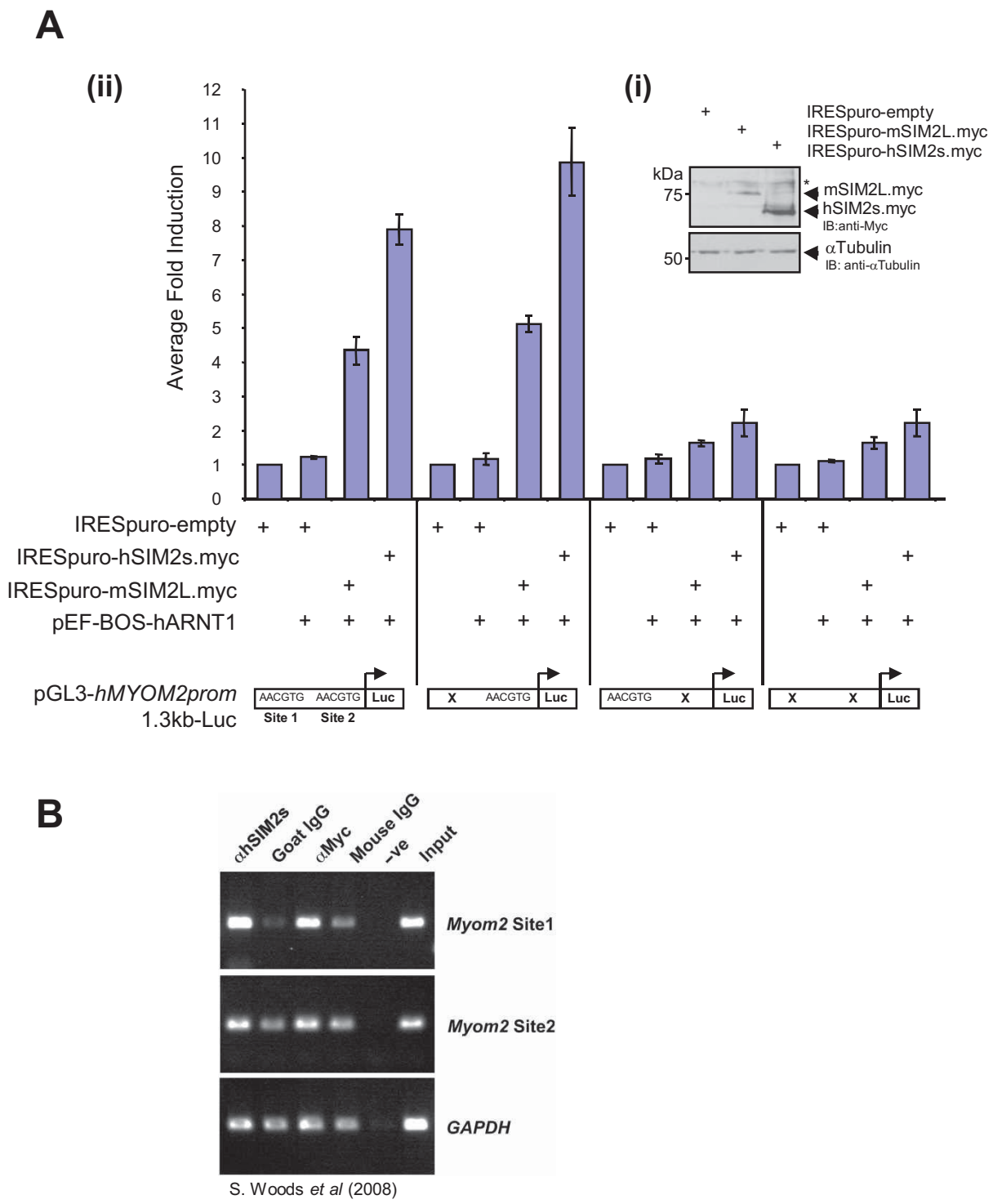

Figure 1.4: *Both mSIM2L and hSIM2s activate hMYOM2 promoter via binding a novel non-canonical e-box sequence, 5'-AACGTG-3'.*

(A) (i) Western analysis of transient expression of IRESpuro-mSIM2L.myc and -hSIM2s.myc in HEK293A cells (50µg WCE) which (ii) determined by dual luciferase reporter analysis confer transcriptional activation of luciferase gene expression driven by the hMyom2 1.3kb promoter via the 5'-AACGTG-3' site 1, normalised to pRL-SV40. Binding-site mutations indicated. Average fold induction shown for three independent experiments (n=3). Error bars SD. (B) Chromatin extracts from HEK293A cells stably expressing ARNT1 and Myc-epitope tagged hSIM2s were immunoprecipitated with antibodies recognising hSIM2s (αhSIM2s) or the Myc tag (αMyc) or an equal amount of the non-specific immunoglobulin controls (Goat IgG and Mouse IgG). DNA eluted from the chromatin immunoprecipitations was examined by PCR amplification using primers designed to amplify the Site 1 or Site 2 sequences from the Myom2 promoter or the control GAPDH sequence. Input contains DNA isolated from the chromatin extract and –ve indicates a control eluate in which no chromatin extract was added to the immunoprecipitation. Published in; Woods, Farrall, Procko & Whitelaw (2008) *Nuc. Acid. Res.* 36(11):3716-27

1.3 SIM2 and Disease

1.3.1. SIM2 and the eitology of Downs Syndrome

Human *SIM2* is located in the Downs Syndrome critical region (DSCR) of chromosome (Ch) 21. Similarly, *mSim2* maps to chromosome 16 which is syntenic to the DSCR of Ch 21 in humans [35, 36, 38, 39, 85-87]. Downs Syndrome (DS) is caused by the presence of three partial or whole copies of chromosome 21 in humans. Overexpression of *mSim2* has been utilised for constructing a biochemical paradigm to aid elucidation of the role of mSim2 in development and disease [71, 86]. The effects of ectopic *mSim2* expression are of interest since the chromosomal location and expression pattern of mSim2 in the mouse suggests human SIM2 as a candidate gene in the etiology of DS [35, 36, 39, 40, 85, 87, 88]. Chen *et al* (1995) were the first to identify human SIM2 in chromosome 21 and propose it as a dosage contributor to DS due to the cited data of expression making it feasible for contributing to craniofacial defects and mental retardation seen in humans [87]. Mice trisomic for an artificial bacterial chromosome encoding *mSim2* display no obvious histopathological abnormalities, however, like in previous partial trisomy Chr 16 mouse models of DS, they observed increased sensitivity to pain and anxiety related reduced exploratory behaviour [86] and impaired learning and memory [89], hence causing it to be postulated that SIM2 may play a role in mental retardation of DS [40, 87]. Supporting a role for SIM2 in the etiology of DS is the expression of mSim2 in tissues affected by DS. These include the developing forebrain [88], ribs, vertebrae, kidney, skeletal muscle of limbs, and craniofacial structures [34-36, 38, 40, 46, 86]. Interestingly, the gross anatomy of lung, heart, gut, skeletal muscle and kidney in the trisomic mice for *mSim2* was unchanged compared to normal littermates [86]. How SIM2 expression may affect the etiology of DS remains to be determined [88, 90].

1.3.2. SIM2 and Cancer

The emphasis on discerning a role for SIM2 in the pathology of DS has shifted in light of more recent data linking SIM2s with the progression and severity of certain forms of solid tumours, and consequently the expression status of SIM2s is emerging as an interesting candidate for a solid tumour marker. Select up-regulation of SIM2s has been identified in solid tumours of the pancreas, colon and prostate [43, 80, 81, 91-94]. These are three of the most lethal of human cancers (see review [95]). Although the focus has mainly been on SIM2s in these tumour types, *SIM2L* mRNA has also been found to be expressed in tumours and tumour derived cell lines of the pancreas [43] and in prostate tumours [81], but not, or at much lower levels [40], in corresponding normal cell lines or benign tissue samples, respectively. Indeed, several independent microarray studies find *SIM2* to be consistently up-regulated gene in prostate tumours, compared to corresponding benign tissue [81, 93, 94]. *SIM2* over-expression in human pancreatic carcinoma samples and derived cell lines compared to normal ductal epithelium controls has also recently been found in the most comprehensive genome wide analysis to date [96]. Compellingly, Halverson and colleagues (2007) find approximately 43% of prostate tumours have elevated SIM2s protein levels, which significantly correlates to increased tumour aggression and a dramatic drop in estimated survival, thus the authors propose SIM2s levels as a novel marker of aggressive prostate cancer. Studies by Narayanan and colleagues have strongly linked SIM2s expression with the survival of tumour derived cell lines of the pancreas and colon where antisense mediated knockdown of SIM2s in cell culture and mouse xenograft models results in cell death and a decrease in tumour size [43, 52, 80, 91]. Conversely however, *SIM2s* has recently been found to be repressed in breast cancer tumours [53]. In contrast to the colon and pancreatic tumour derived cell lines tested, loss of SIM2s in MCF7 breast cancer cells correlates to cell survival via the activation of SLUG mediated EMT (epithelial mesenchymal transition) [53, 82]. Whether

changes in SIM2s expression levels are required for tumour growth and/or tumour maintenance, and how SIM2s expression and transcriptional activities fit into the molecular profile of disease progression, is in need of further investigation.

1.4 Thesis Aims and Approaches

The studies of this thesis sought to identify the molecular mechanisms by which aberrant levels of SIM2s expression in solid tumours of the prostate and pancreas may promote tumour development. This was approached predominantly in two ways. Firstly, by the identification of novel SIM2s direct target genes as means to identify a functional role(s) for SIM2s in tumour progression, and understand potential differential molecular mechanisms of transcriptional activities of the long and short isoforms of SIM2 in gene regulation. And secondly, via investigating how the activities of SIM2s may be implicated in known tumour promoting signalling pathways. The context of these aims and approaches will be introduced and discussed in more detail within each 'Results' chapter (**Chapters 3, 4, 5** and **6**) to follow.

CHAPTER 2

Materials and Methods

2.1 Abbreviations

5’-Aza-dC	5-aza-2'-deoxycytidine
Amp	Ampicillin
AhR	arylhydrocarbon receptor
AMV	avian myeloblastosis virus
APS	ammonium persulphate
AR	Androgen Receptor
ATP	Adenosine triphosphate
βME	β-mercapto-ethanol
BSA	bovine serum albumin
bp	base pair
cDNA	coding deoxyribonucleic acid
DMOG	dimethyloxallyl glycine
DMSO	dimethylsulphoxide
°C	degrees Celsius
cds	coding sequence
C-	carboxy-
ctrl	control
DAPI	4',6-diamidino-2-phenylindole
DHT	dihydrotestosterone
DMEM	Dulbecco's modified Eagle's medium
DMF	dimethylformamide
DNA	deoxyribonucleic acid
dNTP	deoxynucleotide triphosphate
Dox	Doxycyline
DP	2, 2' Diprydyl
ds	double stranded
DTT	dithiothreitol
EDTA	ethylene diamine tetra-acetic acid
EtBr	ethidium bromide
EtOH	ethanol
FA	formaldehyde
FCS	fœtal calf serum
FITC	fluorescein isothiocyanate
Ha	Haemagglutinin
HEPES	4-(2-Hydroxyethyl)piperazine-1-ethanesulfonic acid
HIF	Hypoxia inducible facot
h	hour
HRE	Hypoxic Response Element
HRP	Horseradish peroxidase
IF	immunofluoresence
IGEPAL	IGEPAL CA-360

Ig	Immunoglobulin
IP	immunoprecipitation
IPTG	isopropyl-β-D-thiogalactopyranoside
kDa	kiloDalton
L	Litre
LB	Luria broth
µl	microlitre
ml	milliltre
min	minute
M	molar
mAmp	mini-Amps
mM	millimolar
OD	optical density
O/N	overnight (typically 16h)
N-	amino-
NEB	New England Biolabs
PAGE	polyacrylamide gel electrophoresis
PBS	phosphate buffered saline
PCR	polymerase chain reaction
PFA	paraformaldehyde
PMSF	phenylmethyl sulphonyl fluoride
Puro	Puromycin
PVDF	Polyvinylidene Fluoride
RNA	ribose nucleic acid
RO	reverse osmosis
rpm	revolutions per minute
RPMI	Roswell Park Memorial Inst.
RT	room temperature
S2RE	SIM2 Response Elment
SIM	Single minded
siRNA	small interfering RNA
shRNA	short hairpin RNA
SAP	Shrimp alkaline phosphatase
SDS	sodium dodecyl sulphate
sec	second
TBE	Tris/borate/EDTA
TE	Tris/EDTA
TEMED	N,N,N^1,N^1-tetramethyl-ethylenediamine
TES	*N*-tris(hydroxymethyl)methyl-2-aminoethane sulphonic acid
Tween-20	polyoxyethylene-sorbitan monolaurate
V	volt
v/v	volume per volume

WCE	whole cell extract	XRE	xenobiotic response element
w/v	weight per volume		

2.2 Materials

2.2.1 General materials and specialised equipment

ITEM	MAIN SUPPLIER
3MM chromatography paper	Whatman
AnaeroGen™ Sachet	Oxoid
StepOne Plus Real-time PCR system	Applied Biosystems
Bioruptor	Diagenode
Bottle-top filters - 500ml, 0.22 or 0.45 µM	Corning
Cryomold	Tissue-tek
Cryotube™ vials	Nunc™
Disposable pipettes (2, 10 and 25 ml)	Falcon
Flip-cap tubes - 1.5ml	Eppendorf
Flip-cap tubes - 1.7ml low retention	Axygen
Glass pipettes	Chase Instruments
Luminometer, Glomax	Promega
Luminometer, TD 20/20	Turner designs
Microscope slides (1 - 1.2mm thick)	Sail Brand
Minisart syringe top 0.2 or 0.45 µM filters	Sartorius
Needles, various guage	Terumo®
Nitrocellulose	Pall Corporation

Protran nitrocellulose transfer membrane	Schleicher & Schuell
PVDF	BIO-RAD
Scalpel blades	Swann Morton®
Screwcap tubes 5, 10, 50ml	Falcon
Sealed plastic containers (Hypoxia Chamber)	Supermarket standard
Sigmacote	SIGMA-ALDRICH
Spectramax plate reader	Molecular Devices
Syringes, various volumes	Becton Dickinson
Tissue culture vessels, various	Falcon
X-ray film	AGFA

2.2.2 Chemicals and Reagents

All chemicals and reagents were of analytical grade or of the highest purity available. The majority of common laboratory materials were obtained from SIGMA-ALDRICH Inc. Specialized reagents and their suppliers are listed below.

5'-Aza-dC	SIGMA-ALDRICH
Acrylamide (acryl/bis 29:1)	Astral Scientific
Alpha-MEM	Invitrogen/Gibco BRL™
ATP	SIGMA-ALDRICH
Agarose, DNA grade	SIGMA-ALDRICH
Amp	SIGMA-ALDRICH
Apoprotinin	SIGMA-ALDRICH
APS	BDH Chemicals

Bacto-agar	Difco Labs
Bacto-tryptone	Difco Labs
Betaine (5M)	SIGMA-ALDRICH
Benchmark pre-stained protein markers	Invitrogen™
Bestatin	SIGMA-ALDRICH
BIGDYE™ Versions 3 to 6	Amersham
BioTaq reaction buffer, 10x	Bioline
Bisbenzimide stain (Hoechst 33258)	SIGMA-ALDRICH
Blastacidin	Invitrogen
BSA	SIGMA-ALDRICH
Bradford protein assay reagent	BIO-RAD
Bromophenol blue	SIGMA-ALDRICH
Cyclohexamide	SIGMA-ALDRICH
DAPI	Invitrogen/GIBCO
DHT (100mM stcok in EtOH)	Gift, W. Tilley, Hanson Centre,SA.
DMEM	Invitrogen/Gibco BRL™
DMOG	Chemicon
DP	SIGMA-ALDRICH
DMSO	SIGMA-ALDRICH
DNA 1kb Plus Ladder	Life Technologies
dN6 Random hexamers	Geneworks
dNTPs (25mM each)	Finnzymes
Dox	SIGMA-ALDRICH
DP	SIGMA-ALDRICH

DTT	SIGMA-ALDRICH
EDTA	SIGMA-ALDRICH
EtBr	SIGMA-ALDRICH
FA	BDH AnalaR
FCS	JRH Biosciences
Formamide	BDH AnalaR
Fugene 6	Roche Molecular Biochemicals
Galactolight substrates	Applied Biosystems
Glycine	Amresco
Horse Serum	CSL
Hydroquinone	SIGMA-ALDRICH
Hygromycin	Invitrogen
IGEPAL	SIGMA-ALDRICH
Imidazole	SIGMA-ALDRICH
IPTG	SIGMA-ALDRICH/BioVectra
LiCl (8M)	SIGMA-ALDRICH
LipofectAMINE™ 2000	Invtrogen/Gibco BRL™
MG132	BioMol
Mineral oil	BIO-RAD
OCT	Tissue-tek
Oligofectamine	Invitrogen
Passive lysis buffer, 4x	Promega
PFA	SIGMA-ALDRICH
PIPES	SIGMA-ALDRICH

Pfu Turbo polymerase buffer, 10X	Stratagene®
PMSF	SIGMA-ALDRICH
Protease Cocktail Inhibitor (100x)	SIGMA-ALDRICH
Protein (Bradford) Assay Reagent , 4x	BIO-RAD
rec-protein G-sepharose	Zymed
Protein-G agarose/salmon sperm DNA	Upstate
Puromycin	SIGMA-ALDRICH
Rapid ligation buffer, 2x	Promega
Restriction enzyme reaction buffers	New England Biolabs
RPMI-1640	Invitrogen/Gibco BRL™
RNaseZAP™	Ambion
RNAZol B	Tel-Test Inc.
Shrimp Alkaline Phosphatase Buffer, 10x	Amersham Pharmacia
SDS	SIGMA-ALDRICH
Skim milk powder	Diploma (supermarket)
Sodium azide	SIGMA-ALDRICH
Sodium bisulphite	SIGMA-ALDRICH
SUPERase-In™	Ambion
T4 DNA ligase buffer, 10x	New England Biolabs
T4 DNA polymerase buffer, 10x	New England Biolabs
Taq polymerase reaction buffer, 10x	New England Biolabs
TEMED	SIGMA-ALDRICH
TRI-Reagent	Ambion
Tris	Amresco

Triton X-100	SIGMA-ALDRICH
Trypan Blue	SIGMA-ALDRICH
Trypsin-EDTA	Invitrogen/Gibco BRL™
Tween-20	SIGMA-ALDRICH
WST-1 reagent	ROCHE
X-Gal	BioVectra
Zeocin	Invitrogen

2.2.3 Commerically available kits

All kits used as per manufacturers' instructions/recommendations.

Galactolight β-galactosidase Luciferase Reporter Assay	Applied biosystems
Dual Luciferase™ Reporter Assay System	Promega
Imobilon™ Western Chemilumenescent reagents	Millipore
Luciferase Assay System	Promega
QIAprep spin Mini-prep Kit	QIAGEN
Qiafilter Midi Plasmid Prep kit	QIAGEN
Qiaquick PCR Purification kit	QIAGEN
QIAquick Gel Extraction Kit	QIAGEN
RNeasy Mini-prep Kit	QIAGEN
PureLink Genomic DNA Purification Kit	Invitrogen
pGem-T® Easy Vector System	Promega
Quickchange site-directed mutagenesis kit	Stratagene
SlowFade Light Antifade kit	Molecular Probes/Invitrogen

Superscript III cDNA synthesis kit	Invitrogen
SuperSignal Westpico ECL reagents	Pierce
BIOTAQ DNA polymerase PCR kit	Bioline
Ez-ChIP Kit	Upstate

2.2.4 Enymes

BIOTAQ DNA polymerase	Bioline
Double stranded DNA restriction enymes	NEB
Platinum SYBR Green qPDR Supermix-UDG reagent	Invitrogen
Platinum Pfx DNA polymerase	Invitrogen
PfuTurbo® DNA polymerase	Stratagene
Shrimp alkaline phosphatase	USB
Taq DNA Polymerase	NEB
T4 DNA ligase	Geneworks

2.2.5 Antibodies

Unless specified, all antibodies are purified.

Details of dilution and incubation conditions used for western blot and/or IF analysis provided below where applicable.

2.2.5.1 Primary Antibodies

anti-Actin rabbit polyclonal (Sigma); WB 1:1000/2% skim-milk/PBS-T – 1h RT.

anti-Alpha-Tubulin rat polyclonal (Serotec); WB 1:1000/1% skim-milk/PBS-T – 1h RT.

anti-AR rabbit polyclonal (Santa Cruz); WB 1:500/2% skim-milk/PBS-T – O/N 4°C.

anti-ARNT MA515 mAb (Affinity BioReagents); 1:100 (of 1:20 stock) 2% skim-milk/PBS-T – 2hrs RT

anti-ARNT1#51 [59] and anti-ARNT1#30 rabbit polyclonal sera raised against the N- (residues 1-142) and C- (last 34 residues) termini of human ARNT1, respectively. Dr. M. Whitelaw; WB 1:500 or 1:400, respectively, 5% skim-milk/PBS-T - O/N 4°C.

anti-ARNT1 goat polyclonal (Santa Cruz); used for IP only.

anti-ARNT2 rabbit polyclonal (Santa Cruz); WB 1:500/1% skim-milk/PBS-T – O/N 4°C.

anti-BNIP3 Ana40 mAb (Sigma); WB 1:1000-1500/5% skim-milk/TBS-T – 1.5-3hrs RT.

anti-GLI1 rabbit polyclonal (Santa Cruz); IF only 1:200 in 1% BSA/TBS-T block solution O/N at 4°C.

anti-HIF1α mAb (BD Biosciences); WB 1:400/2% skim-milk/PBS-T – 3.5hrs RT.

anti-HIF1α rabbit polyclonal (ab2185, Abcam); used for ChIP only.

anti-HIF1α-CAD #207 rabbit polyclonal sera [97]; WB 1:1000/2% skim-milk/PBS-T – O/N 4°C

obtained from the laboratory of Prof. J. Pouysségur, CNRS UMR6543, University of Nice, France, was used for detection of mouse HIF1α.

anti-IgG goat polyclonal (Santa Cruz) isotype match to anti-hSIM2s for ChIP negative control only.

anti-IgG rabbit polyclonal (Upstate) isotype match to anti-HIF1α for ChIP negative control only.

anti-IPF, rabbit polyclonal – IF only, 1:400/1% BSA/TBS-T O/N 4°C. Kind gift from Prof. H. Edlund, University of Umeå, Sweden.

anti-LC3B rabbit polyclonal (Abcam); WB 1:500/2% skim-milk/PBS-T – 90min at RT.

anti-Myc rabbit polyclonal (Abcam); WB 1:5000/2% skim-milk/PBS-T – 1.5-3hrs RT.

anti-RPT1 (AhR) MA1-514 mAb (Affinity BioReagents); WB 1:1000/2% skim-milk/PBS-T - O/N 4°C.

anti-SHH goat polyclonal (Santa cruz); WB 1:500/2% skim-milk/PBS-T – O/N 4°C

anti-hSIM2s goat polyclonal (Santa Cruz); used for IP, ChIP and WB 1:500/2% skim-milk/PBS-T – O/N 4°C, also IF were a dilution 1:50 in 1% BSA/TBS-T block solution was applied O/N at 4°C.

anti-SQSTM1/p62 mAb (Santa Cruz); WB 1:500/2% skim-milk/PBS-T- O/N 4°C

Note: For sequential immunoblot detection of proteins on the same membrane, order of antibodies optimised for non-interference of previously used antibody in a manner corresponding to the animal in which the antibody was generated: commonly- 1st, mouse; 2nd, rabbit; 3rd, goat; 4th, rat. Incubation time periods for immunoblot detection, with gentle mixing/orbital shaking, listed above with each antibody.

2.2.5.2 Secondary Antibodies

Horseradish peroxidase-conjugated secondary antibodies used were anti-goat, anti-mouse, anti-rabbit (Pierce), and anti-rat (Dako), used routinely at 1:5000-10000/1-2% skim-milk/PBS-T, or TBS-T were appropriate, typically 1hr at RT for immunoblot (see below, **section 2.3.4.4**)

Alexa-fluor-labelled-594 and -488 secondary antibodies used for immunofluoresence were anti-goat, anti-mouse, anti-rabbit (all from Invitrogen), typically used at a dilution of 1:1000/1% BSA/TBS-T, incubated on tissue section for 1hr at RT.

.

2.2.6 Solutions

2.2.6.1 General solutions and buffers

Cyclohexamide	1mg/ml, dissolved in water, stored at -20°C
DAPI (5mg/ml)	10mg dissolved in 2ml MQ-water. Working stock 1mg/ml (1000x).
DNA load buffer (6x)	50% (v/v) glycerol, 0.01% (w/v) bromophenol blue, 0.01% (w/v) xylene cyanol, 0.1mM EDTA pH 8.0.
DMOG	Dissolved in DMSO to 1M (1000x stock)
DP	Dissolved in DMSO to 100mM (1000x stock)

IF block solution	1% BSA/TBS-T
IP buffer	250mM NaCl, 20mM HEPES pH 8.0, 0.1% Igepal, 1mM EDTA
IPTG (1M)	0.238g dissolved in 1ml MQ-water.
LB	1% (w/v) bacto-tryptone (Difco), 0.5% (w/v) yeast extract (Difco), 1% (w/v) NaCl. NaOH used to adjust pH to 7.0.
Mouse tail tip Lysis Buffer	50mM Tris pH 7.5, 0.1M EDTA, 0.1M NaCl, 1% SDS
PBS	20mM NaPhosphate pH 7.6 and 137mM NaCl.
PBS-T	PBS plus 0.1% (w/v) Tween-20.
PFA (4%)	4g dissolved in 100ml of boiling (by microwaving) PBS + 25µl of 5M NaOH. Stored at 4°C for up to 2 days.
Ponseau Stain	0.5% Poncaeu S (w/v), 1% glacial acetic acid (v/v) in MQ-water.
Reaction Buffer (RB) (10x)	250mM Tris pH 9.0, 160mM $(NH_4)SO_4$
RIPA cell extract buffer	150mM NaCl, 1.0% Igepal, 0.5% sodium deoxycholate, 0.1% SDS, 50mM Tris pH 8.0.
SDS load buffer (4x)	50mM Tris pH 6.8, 20mM DTT, 8% (w/v) SDS, 40% (v/v) glycerol and 0.01% (w/v) bromophenol blue.
Separation Buffer (4x)	1.5M Tris, 0.4% (w/v) SDS, 1M HCl used to adjust pH to 8.8.
SOC	0.1ml 1M $MgSO_4$, 0.1ml 1M $MgCl_2$, 0.2ml 20% (w/v) glucose and 9.6ml LB.
Stacking buffer (4x)	0.5M Tris, 0.4% (w/v) SDS, 1M HCl used to adjust pH to 6.8.
TBE	216g Trizma base, 110g Boric acid and 18.6g EDTA plus water to 1L and pH adjusted to 8.3 using NaOH
TBS	50mM Tris pH 7.5, 150mM NaCl
TBS-T	TBS plus 0.1% (w/v) TritonX-100
TE (100x)	121.1ml of 1M Trizma base and 37.22ml of 0.1M EDTA upto 1L with water.

Whole Cell Extract Buffer	20mM HEPES, 0.42M NaCl, 0.5% (v/v) Igepal, 25% (v/v) Glycerol, 0.2mM EDTA, 1.5mM $MgCl_2$. pH adjusted with NaOH to 7.8. 1xPI cocktail and 1mM DTT added fresh.
Western blot block solution	10% skim-milk/PBS-T or TBS-T
Western Transfer Buffer	Semi-dry: 25mM Tris pH 8.4, 0.25M glycine and 20% Methanol. Wet: 48mM Tris, 1.93M glycine, 0.01% SDS and 20% Methanol.
X-gal (50mg/ml)	Dissolved in DMF, stock stored at -20°C.

2.2.6.2 ChIP Solutions:

Nuclear Isolation Buffer	5mM PIPES pH 8 adjusted with KOH, 85mM KCl, 0.5% Igepal and 1xPIs
SDS Lysis Buffer	1% SDS, 10mM EDTA, 50mM Tris pH 8.1.
Dilution buffer	16.7mM Tris-HCl pH 8.1, 1.2mM EDTA, 167mM NaCl,0.01% SDS, 1.1% Triton X-100
Low salt wash buffer	20mM Tris-HCl pH 8.1, 2mM EDTA, 150mM NaCl, 0.1% SDS, 1% Triton X-100
High salt wash buffer	20mM Tris-HCl pH 8.1, 2mM EDTA, 500mM NaCl, 0.1% SDS, 1% Triton X-100
LiCl wash buffer	0.25M LiCl, 110mM Tris pH 8.1, 1mM EDTA, % Igepal-CA630, 1% deoxycholic acid (sodium salt)
Elution buffer	100mM $NaHCO_3$, 1% SDS
Proteinase K	600ug Proteinase K in 60µl of 50mM Tris-HCl pH 8.0, 10mM $CaCl_2$

2.2.7 Primers and oligonucleotides

Typically, primers synthesised by Geneworks, SA, Australia

2.2.7.1 Sequencing

BS Reverse primer	5'-AACAGCTATGACCATG-3'	(pBSK)
Puro Vector Sense	5'-AGTTCAATTACAGCTCTT-3'	(pEF/IRESpuro)
Puro Vector Antisense	5'-AACGTTAGGGGGGGGGGA-3'	(pEF/IRESpuro)
Antisense pEF-BOS	5'-GGCCCTCTAGATGCATG-3'	(pEF-BOS)
pGL3reverse	5'-GCCGGGCCTTTCTTTATG-3'	(pGL3-promoter)
Cam primer 1	5'-GCTCTTACGCGTGCTAGC-3'	(pGL3-promoter)
Luc27C (reverse)	5'-TATGCAGTTGCTCTCCAG-3'	(Firefly Luciferase)
CMV Forward	5'- CGCAAATGGGCGGTAGGCGTG -3'	(pcDNA5/FRT/TO)
BGH Reverse	5'-TAGAAGGCACAGTCGAGG-3'	(pcDNA5/FRT/TO)

2.2.7.2 cDNA and Semi-Quantitative RT-PCR primer sequences

5'- 3'	**Sense**	**Antisense**
hSIM2s [52]	TGGAGGACCGCCTTGTCTACCT	GCCCAAAGCGTGAGGGTTCTGTCT
hSIM2L [52]	TGCCCTTCGTGCTGCTCAACTACC	AGGAAACCAAGCCCCCAGCA
hARNT1 [52]	TCTGTCATGTTCCGGTTCCGGTCT	TCAAGGGGCTTGCTGTGTTCTGGT
hARNT2	ATGATGAGCTCAGCCTCTGC	AGAAAACGGTGGAAACATGC
mARNT2	CCTTCAGCTCTTCCGTGG	TCTGGGCAGTAGAAGCCT
hMMP16	GTAAAGCTATTCGCCGTGCC	CACTGTCGGTAGAGGTCTTG
hXAGE-1	CAAACACAGAACCACACAGCCA	ACCAGCTTGCGTTGTTTCAGC
hPTPRR	CCATTGGCTGTCAACAGCTG	CAGCAGCTCATCCAGTCATC
hPTP-SL	TTAGAAAGCCTGGGACCTGC	GCAAAACAGAAAGTCCGACG
hPTPBR7	GCAAACACTATGCGGAGAGC	TTGATGTGCACTTGCTGGGG
hPSA	ATGAGCCTCCTGAAGAATCG	GCACACAGCATGAACTTGGT
hS100P	ATGACGGAACTAGAGACAGCCATGGGC	GGAATCTGTGACATCTCCAGCGCATCA
hTMEFF2	AACTCTCGAGATCATGCGCG	ACGCAAGTCACAGTGTCTCC
hBTG1	CCGTGTCCTTCATCTCCAAG	TTTGGAAGGGCTCGTTCTGC
hHSPA10/8	AAACGTCTGATTGGACGCAG	GCACGTTTCTTTCTGCTCCA
hGAGEB1	AGAGAGGATGAGGGAGCATC	CAGCCTGAACCATTTCAGCG

hPHLDA1 /TDGA51	GATCACGCTGCAGATGGTGC	TCCCACTTCCTCAAGTCCTC
hIER3 /IEX-1	ATGTGTCACTCTCGCAGCTG	AAGCCTTTTGGCTGGGTTCG
hSPOCK2	CGTCCATCTCGCAGTACAGC	CGCCTGTTGCTCCAGCTTAC
hEREG	ATGGAGATGCTCTGTGCCGG	CAGACTTGCGGCAACTCTGG
hBNIP3	GACGGAGTAGCTCCAAGAGC	CTGGTGGAGGTTGTCAGACG
mBNIP3	CAGCATGAATCTGGACGAAG	TCCAATGTAGATCCCCAAGC
hARv1	ACTGAGGAGACAACCCAGAAG	ATTGGTGAAGGATCGCCAGC
hSHH [98]	CAGCGACTTCCTCACTTTCC	GGAGCGGTTAGGGCTACTCT
hGLI1 [98]	TACTCACGCCTCGAAAACCT	GTCTGCTTTCCTCCCTGATG
hIHH [98]	CCCCCTCCACTCCAATAAAT	AAAATTCTCCCATGGGCTTC
hSMO [98]	TTACCTTCAGCTGCCACTTCTACG	GCCTTGGCAATCATCTTGCTCTTC
GAPDH (m&h)	GGAGCCAAAAGGGTCATC	ACCACCCTGTTGCTGTAG

2.2.7.3 Real-time qPCR primers

5' - 3'	**Sense**	**Antisense**
hSIM2s	GGGTCAGGTCTGCTCGTG	AAGCGTGAGGGTTCTGTCTC
hSIM2L	AGCAGCTCGTCTCCAGCTAA	GTGTCCTCGCCGAACCTG
hARNT2	TGAAGTGTTCCAGGACATGC	AGAAAACGGTGGAAACATGC
hBNIP3	TGCTGCTCTCTCATTTGCTG	GACTCCAGTTCTTCATCAAAAGGT
hPOLR2a	GAGAGTCCAGTTCGGAGTCCT	CCCTCAGTCGTCTCTGGGTA

2.2.7.4 ChIP primers (gDNA)

5' - 3'	**Sense**	**Antisense**
HUMAN		
hARNT2 promoter -7500 S2RE site 1	TGTCCCTGTTGTTCTCCAAG	CCATCCCTTTGTCTCTTCCA
hARNT2 promoter -7100 CME/E-box site 2	AACAAGGGGAAAGCAGGAAT	CCCACCAATTATGCTCCAGT
hARNT2 promoter -6550 E-box site 3	GAACAGGCATGTGACTCGAA	ACCAGGCATCTGGACTTCAC
hARNT2 promoter -2340 E-box site 4	ATTGTGCGTAGCCCAGTTCT	ACTTCCCAAGTCTGGAGTCG

MOUSE		
mBNIP3 Proximal promoter HRE	CGGTCCACTTCTGCATTAGA	CACTGGACTGAGGGACAAGG
mBNIP3 Intron 1 S2RE site 1	GAACGTGCTGGGTAAGTGCT	CATCAGGAAGTGGCAACAAA
mBNIP3 Intron 1 S2RE site 2	TGGAGGAGGATCCTGTTGAC	AATCCCAGCACTAGGGAGGT
mACTIN intron 1 [99]	CGGTGTGGGCATTTGATGA	CGTCTGGTTCCCAATACTGTGTAC
mChromosome 7 (3kb upstream of *mBNIP3*)	GGGGAGGGAGTTTTTGAGAC	TGTGTCAGGATCTGGGTTCA

2.2.7.5 gDNA primers

For identification of hSIM2s transgenic mice: see ***Chapter 6.***

1. mIPF1 5'3 (sense): 5'-GGG AAG AGG AGA TGT AGA CTT -3'
2. hSIM2s antisense #2: 5'-TTG GAG CAG GTG GTG -3'
3. mIPF1-AR (antisense): 5'-GAGCTGAGCTGGAAGGT-3'

Primers 1 & 2 give a 790bp product for transgene. Primers 1 & 3 gDNA control PCR gives 700bp amplicon.

(E. Palsson, University of Umeå, Sweden)

hARNT2 promoter- ChIP studies see **section 2.2.7.4** for primer sequences.

mBnip3 promoter – generating promoter reporter constructs see **section 2.2.8.3** below, and ChIP primers (promoter and intron 1) see **section 2.2.7.4** above.

2.2.7.6 gDNA bisulphite specific primers

methBNIP3prmHRE LEFT: 5'-TTTTTTTATTAGTAGGATGGAAAGA -3'

methBNIP3prmHRE RIGHT: 5'- AAAAAACTCACAAAACAAAAC -3'

2.2.7.7 Primers for cDNA synthesis

Oligo-dT_{15} primer	Promega or Geneworks
Random Hexamers (dN6)	Geneworks

2.2.7.8 siRNA oligonucleotides and shRNA oligonucleotides

All siRNA oligonucleotides were chemically synthesized by Qiagen. siControl and siSIM2s-1759 were labeled with 3'Alexafluor546 used to assess transfection efficiency into cells. siControl: 5'-aacgtacgcggaatacaacga-3' [100]; siScrambled: 5'- gtactaccgttgttataggtg-3' (sequence ex. Ambion); siSIM2s-1759: 5'-aaccctcacgctttgggcaaa-3'; siSIM2s-2a: 5'-ctgtgctttcttgctctcaat-3'. SIM2s-2a siRNA oligonucleotide was generated by Qiagen, using their proprietary HP Flexible siRNA design service. All others designed using online algorithms provided by Qiagen, Ambion siRNA Target finder, and/or using Xcel siRNA design template written by Maurice Ho. See below **section 2.2.11**, Bioinformatic resources.

Primers designed and used to generate construction of stable integrated tet-inducible shRNA expression [101] in DU145 cells. shSIM2s-1759; 19mer target sequence of siRNA in lowercase and underlined, loop sequence in uppercase. shSIM2s_1759_F: 5' – TTCAAGAGA<u>tttgcccaaagcgtgagggtt</u>tttttacccagc – 3', shSIM2s-1759-R: 5' – aaaTCTCTTGAA<u>tttgcccaaagcgtgagggtt</u>gatctctatcac – 3'. All subcloning, generation of recombinant expression vectors for lentiviral infection and generation of stably integrated shRNA DU145 cell lines, by C. Bindloss.

2.2.8 Plasmids

2.2.8.1 Cloning vectors

pBluescript (pB) KS and pBSK.

2.2.8.2 Mammalian Expression vectors

Plasmids generated by others

pEF-BOS-cs - J. Langer, Robert Wood Johnson Medical School, New Jersey USA.

pEF-IRESpuro [102] source vector for pEF-IRESpuro6 with modified multiple cloning site used for all work contained in this thesis, generated by D. Peet.

pEF/mSIM2s(Myc)$_2$/IRESpuro and *pEF/mSIM1(Myc)2/IRESpuro* – S. Woods [59].

(any such vectors using this backbone are referred to hereafter as, ie; mSIM2.myc-IRESpuro and mSIM1.myc-IRESpuro, respectively)

pEF-BOS-hARNT1v3.HA – R. Kewely, as described in [59].

hHIF1α(no tag)-IRESpuro – D. Lando [20].

hAhR-pEF-BOS – M. Kleman.

pDR-hSIM1 - S. Antonarkis, Laboratory of Human Molecular Genetics, Department of Genetics and Microbiology and 2GraduateProgram of Cellular and Molecular Biology, Geneva University Medical School, 1211 Geneva, Switzerland; [38]. Sequence identifier Genbank accession number: U70212.

hGLI1-pBKS – (GLI1 cDNA -79 to 3522) Gift from Dr. Bert Volgelstein, The Howard Hughes Medical Institute & Sidney Kimmel Comprehensive Cancer Center, Baltimore, USA [103].

Tet-inducible tH1 promoter driven shRNA lentiviral vectors were a kind gift from Dr. S. Barry, Children's Health Research Institute, SA, Australia [101].

Plasmids I have made during the course of this PhD

hSIM2s.myc-IRESpuro (corrected) - Source clone hSIM2s.myc (2xMyc tag) in IRESpuro (original clone) made by S. Woods. Single nucleotide site mutation(C->T) resulted in an A -> V mutation at amino acid 63. This was corrected using a site-directed mutagenesis splice-overlap PCR approach using Pfu turbo DNA polymerase. Step 1: PCR amplification and purification of the N-terminus of hSIM2 using primers; SIM2-

1NheF; 5'-CTAAGCTAGCATGAAGGAGAAGTC-3', and the reverse primer hSIM2-68R; 5'-GGCTGTCCCCACGCGTCTCCTAAAC-3', which incorporated the corrected nucleotide (underlined). Step 2: PCR amplification of approximately 350bp c-term of site mutation, using a forward primer also incorporating corrected nucleotide (underlined), hSIM2-59F; 5'-GTTTAGGAGACGCGTGGGGACAGCC-3', with SIM2-184R; 5'- GTGGATGACCTTGTATCC-3'. Step 3: Purified PCR products (which overlap in sequence 12-13bp either side of the corrected nucleotide) together provide the template for splice-overlap PCR, using primers SIM2-1NheF and SIM2-184R. Step 4: Resulting 552bp PCR product of corrected sequence following splice-overlap PCR then restriction digested with Nhe1/Sac1. Step 5: Corrected N-terminal sequence subcloned back into Nhe1/Sac1 digested hSIM2s.myc-IRESpuro original backbone to create corrected hSIM2s.myc-IRESpuro - verified by sequencing. All references to hSIM2s.myc in this thesis are of this corrected hSIM2s.myc clone. Use of this clone recently published [48].

hSIM2L.myc-IRESpuro - Subcloned out of hSIM2L.myc-FRT/TO (see below) Nhe1/EcoRv and ligated into myc-IRESpuro) backbone cut Nhe1/EcoRV (excised hSIM2s cds from hSIM2s.myc-IRESpuro).

hGLI1-IRESpuro - Human GLI1 cDNA excised from hGLI1-pBKS Sal1/Xba1 and ligated into Xho1(Sal1 compatible end)/Xba1 pEF/IRESpuro backbone. Full length sequencing confirmation of cds. Aligns with Genbank accession number clone: NM_005269.

Tet-inducible cDNA expression – using the Flp-In™ T-Rex™ System form Invitrogen.

Expression vectors: pcDNA5/FRT/TO©, and *pOG44*

hSIM2s.myc-FRT/TO - 1.7kb coding sequence insert subcloned into vector AflII/Not1 from similarly digested source vector hSIM2s.myc-IRESpuro.

hSIM2L.myc-FRT/TO (and cloning of human SIM2L cDNA) - Using primers hSIM2s-sense [80] (see **section 2.2.7.2** above) and hS2LEcoRVRev: 5'- CAATGATATCCCTCCCGTTGGTGATGATGAC-3', PCR amplified

the carboxy-terminus of endogenous SIM2L from human skeletal muscle cDNA using Platinum Pfx DNA polymerase (Invitrogen) (see **section 2.3.2.3** below for furter detail). PCR product then restriction digested with BamH1/EcoRV. hSIM2s.myc-FRT/TO also digested BamH1/EcoRV to remove 'short' specific C-terminus, which was replaced with the 'Long' specific cloned C-terminus to create hSIM2L.myc cDNA insert of approximately 2kb. Cloned hSIM2L c-term same sequence as Genbank accession number: U80456.

hHIF1α(not tag)-FRT/TO - HIF1α cds 2.6kb insert subcloned into vector BamH1/EcoRV using BamH1/Pml1 insert from source vector hHIF1α(notag)-pEF-BOS..

hAhR(no tag)-FRT/TO - hAhR 2.7kb cds insert subcloned into vector EcoRV/Not1 from source vector hAhR(no tag)-IRESpuro.

Made by others:

hSIM1.myc-FRT/TO - Subcloning of hSIM1 cDNA from pDR-hSIM1 into FRT/TO carried out by A. Raimondo.

2.2.8.3 Reporter Plasmids

pGL3-basic-Firefly luciferase – no promoter or enhancer sequences (Promega).

pGL3-promoter-Firefly luciferase - with minimal SV40 promoter (Promega).

pRLSV40 - Renilla luciferase internal control plasmid with minimal SV40 promoter (Promega).

pRLTK – Renilla luciferase internal control plasmid with minimal thymidine kinase promoter [104].

pCMX-beta-galactosidase – Beta-galactosidase reporter plasmid under the control of the CMX promoter used as an internal normalising control for enhancer/promoter driven Firefly luciferase expression (gift D. Dowhan, Diamantia Institute, Australia.)

PB3-luciferase – pGL3basic vector containing 3 repeats of the *Probasin* androgen responsive minimal promoter (gift W. Tilley, Hanson Research Institute, Australia).

8x3'GliBS-p δ51-LucII – Synthetic enhancer of consecutive 8x3'Gli binding sites (BS) – 5'- GAACACCCA-3' - to drive Firefly luciferase expression (gift from Dr. Hiroshi Sasaki, Laboratory of Developmental Biology, Institute for Molecular and Cellular Biology, Osaka University, Japan) [105]. Empty vector control needed (pδ510LucII) for 8x3'Gli3BS-Luciferase reporter (**Chapter 6, section 6.4.2**), thus removed the Gli binding site (BS) enhancers with BamH1/BamH1 restriction digestion, followed by re-ligation of the vector backbone.

1.3kb Myom2promoter-Luciferase – C. Proco & S. Woods [48].

Plasmids I have made during the course of this PhD

1kb mBnip3promoter-Luciferase and DNA binding site mutants

1.2kb of the mouse BNIP3 promoter was amplified from NIH3T3 genomic DNA, made using Purelink Genomic DNA purification Kit (Invitrogen), using Pfu Turbo polymerase (Stratagene) as per manufacturers' instructions. Primers; sense: 5- ATGAGGAGCTCTTGGGGAACTATGGGTCAAC -3', and antisense: 5'-GTATCGCTAGCAGCAAGCCAGGGGTAAAGAT -3'. Subcloned Sac1/Nhe1 into pGL3-Basic vector (with technical assistance from M. van Bekkum). 1kb mBnip3 promoter was then excised and ligated into native pGL3basic, Xho1/Xho1. Site directed mutagenesis of mBnip3 regulatory region HRE 5'-CACGTG-3' and S2RE 5'-AACGTG-3', binding sites to mutant 5'-AAAAAG-3' sites, was carried out using the following primers: HRE; mBnip3promHREmut_F: 5 '-CCGGCGCACGCGCCGAAAAAGCCACACGCTCCC-3', mBnip3promHREmut_R: 5 '- GGGAGCGTGTGGCTTTTTCGGCGCGTGCGCCGG-3 '. S 2 R E ; mBnip3promS2REmut_F: 5 '- GTACTGGGGACAGAACCAGATCTGAAAAAGCTGGGTAAGTGCTC-3', mBnip3promS2REmut_R: 5'- GAGCACTTACCCAGCTTTTTCAGATCTGGTTCTGTCCCCAGTAC-3', using Quickchange site-directed mutagenesis kit.

1.3kb Myom2-mutant S2RE site 1 (and site 2) -promoter-Luciferase

Using Quickchange site-directed mutagenesis kit, 'Site 1' and 'Site 2' S2RE (5'-AACGTG-3') binding sites within the 1.3kb Myom2promoter-Luciferase plasmid were mutated. Site 2 mutant construct previously generated by S. Woods. To obtain single S2RE site 1 and double mutant constructs of the 1.3kb Myom2 promoter in pGL3bsic, the following primers were used for site directed mutagenesis, S2RE site 1; forward: 5'-GCCTCTGATACCCCAGTGTGAGAAAAAGGAGTTTCTTAAGGC-3', reverse 5'-GCCTTAAGAAACTCCTTTTTCTCACACTGGGGTATCAGAGGC-3', using either the native 1.3kb Myom2promoter- or 1.3kb Myom2promoterSite2mutant-pGL3basic plasmid templates, respectively.

2.2.9 Bacterial strain

DH5α: This strain of *E.Coli* was used for the propogation and subcloning of DNA. [Genotype: Φ80*lac*ZΔM15, *rec*A1, *end*A1, *gyr*A96, *thi*-1, *hsd*R17(r_K^-,m_K^+), *sup*E44, *rel*A1, *deo*R, Δ(*lac*ZYA-*arg* F)U169].

2.2.10 Cultured mammalian cell lines

Unless specified, cell lines originally obtained from ATCCC-derived Discipline of Biochemistry, School of Molecular & Biomeical Science, The University of Adelaide, cell line stocks.

Mouse fibroblast NIH3T3, and embryonic carcinoma P19 cells.

Human embryonic kidney HEK293A (Kind gift from Prof. K. Williams, Flinders University, Australia)

HEK293 Flp-In™ TRex™ (Invitrogen)

Human carcinoma derived cell lines: Prostate; DU145, PC3AR+ and LNCaP (kind gifts from W. Tilley, Hanson Centre); Pancreatic; PANC-1, CAPAN-1, CFPAC (kind gift from Prof. Lorenz Pollinger, Karolinska Institute, Sweden).

2.2.11 Electronic Bioinformatic Resources

Human and mouse genomic DNA sequence data obtained from online database, BLAT - http://genome.brc.mcw.edu/cgi-bin/hgBlat.

'TESS' (Transcription Element Site Search) online software utilised to search for putative SIM2 DNA-binding sites as described; http://www.cbil.upenn.edu/cgi-bin/tess/tess?RQ=SEA-FR-Query.

Bioinformatic epigenetic analysis of corresponding region of the human [-1162 to +538] and mouse [-1120 to +580] *BNIP3* regulatory regions was performed using 'Methprimer' and 'EMBL EMBOSS' online software; www.urogene.org/methprimer/index1.html; http://www.ebi.ac.uk/emboss/cpgplot/index.html., respectively.

siRNA oligonucleotide design: Independent online design algorithm tools used from both Qiagen (www.qiagen.com) and Ambion (www.ambion.com), also designed in reference to rational siRNA design rules using the Xcel siRNA design template written by Maurice Ho, http://ihome.ust.hk/~bokcmho/siRNA/siRNA.html.

Genomic DNA primers designed with online software, Primer3 (http://frodo.wi.mit.edu/cgi-bin/primer3/primer3_www.cgi), or Methprimer (as above).

Oncomine™ Research online microarray database - http://www.oncomine.org/

2.3 Methods

2.3.1 Bacterial culture

Aseptic technique was utilised for handling of bacterial cultures.

2.3.1.1 Growth and maintenance of bacteria

Bacteria were grown in liquid cultures of LB, or on solid media, LB plus 1.5% (w/v) bacto-agar (Difco), supplemented with antibiotic for selection of transformed bacteria when appropriate – 100ug/ml ampicillin (Amp) or Amp mimetic carbenicillian. Typically, cultivation from frozen stocks was carried out by using aseptic technique streaking cells directly from a frozen stock onto a solid medium growth plate with the aim to obtain a single colony for continued growth following incubation of the plate O/N at 37°C.

Frozen stocks of overnight cultures of transformed DH5a bacteria mixed with final concentration of 16-20% Glycerol were stored at -80°C.

2.3.1.2 Preparation of Chemically Competent (CC) DH5α for Heat Shock Transformation

[Cells were prepared by others by the following protocol]

LB agar plates were streaked from frozen stock of bacteria and allowed to grow O/N at 37°C. The following day 500ml of LB was inoculated with the freshly plated bacteria. Liquid cultures were grown at 37°C with shaking till an OD_{600} of 0.4-0.6 was obtained. Liquid cultures in growth flasks were chilled on ice for 10min, then cultures were transferred to sterile 500ml screw cap centrifuge bottles and centrifuged for 10min at 3000rpm/4°C. Cell pellets were gently resuspended in 200ml (40% of the original culture volume) of ice cold TFBI and incubated in ice for 10min. Following a second 10min spin at 3000rpm/4°C, cell pellet was gently resuspended in 0.04 volumes of ice cold TFBII (20ml) and incubated on ice for 15min. 100-200µl of cells were aliquoted into pre-chilled (on ice) labelled microfuge tubes, and then snap frozen in a dry ice/EtOH

bath, then stored at -80°C. Typical competency was between $5x10^6$-10^7 cfu (colony forming units)/µg of plasmid (circular) DNA.

TFBI solution: 30mM Potassium Acetate (KAc), 0.1M Rubidium Chloride (RbCl), 10mM Calcium Chloride ($CaCl_2(2H_2O)$), 50mM Manganese Chloride ($MnCl_2(4H_2O)$), 15% (v/v) Glycerol. pH adjusted with 0.2M glacial acetic acid to 5.8, then filter sterilised.

TFBII solution: 10mM MOPS(acid), 75mM Calcium Chloride, 10mM Rubidium Chloride, 15% (v/v) Glycerol. Potassium Hydroxide (0.1M) used to adjust pH to 6.5, then filter sterilised.

2.3.1.3 Heat Shock Transformation of CC DH5α Bacteria

Prior to transformation, CC bacteria were taken from -80°C and allowed to thaw on ice for 10-20minutes.

With Intact plasmid:

Typically 10-50ng of purified plasmid DNA was gently mixed with 30-50ul of CC bacteria and incubated on ice for 5-10min. This was followed by a brief incubation of the mix at 42°C (heat shock) for 60-90sec, then back on ice for 2min. Mix was then resuspended in SOC to a final volume of no more than 150ul, then plated onto a LB agar plate containing Amp antibiotic and incubated at 37°C O/N.

Pre-thawed and then re-frozen to -80C samples of CC bacteria were commonly used for this protocol.

With Ligation mix:

5-7µl of ligation reaction (see **2.3.3.11**) was gently mixed with 50-100µl of CC bacteria and incubated on ice for 20min in a microfuge tube. The mix was then heat shocked at 42°C for 2min, then chilled on ice for 2min. 200-400µl of SOC was added to mix and incubated with gentle constant inversion/agitation (on a rotary wheel) at 37°C for 45min. Cells were then centrifuged at 6500rpm for 15sec, and supernatant removed such that 150µl remained in which to resuspend the pellet prior to plating onto a pre-warmed LB(Amp) agar plate. Plates were then incubated O/N at 37°C. Previously unthawed CC bacteria were always used for this protocol.

2.3.2 Manipulation of Nucleic acids

2.3.2.1 Preparation of plasmid DNA

Plasmid DNA was propagated by the transformation and growth of CC DH5α (see **2.3.1.3**). Plasmid DNA was then extracted from overnight liquid growth cultures of transformed bacteria as per the standard protocol of Qiagen mini and midi plasmid kits (see product information for commercially available kits **2.2.3**).

2.3.2.2 PCR from Plasmid template using Pfu Turbo

The high fidelity DNA polymerase PfuTurbo was used to generate PCR products ultimately used for protein expression. As per manufacturers' recommendations for reaction conditions using 1-10ng of plasmid DNA template in a 25µl reaction, standard PCR program was 35x cycles of 94°C 30sec, 55-60°C 30sec, 72°C 1min.

2.3.2.3 Cloning human SIM2L C-term using Platinum Pfx DNA polymerase

The high fidelity DNA polymerase Pfx (Invitogen) was used for the cloning of the c-terminal region (940bp) of human SIM2L from human skeletal muscle cDNA. As per manufacturers' instructions, using1µl of cDNA template, 40xPCR cycles of 94°C 30sec, 56°C 30sec, 68°C 1min, using primers hSIM2sSense [80] and hSIM2LEcoRV-Rev. Optimised PCR reaction conditions used 2x PCR_x Enhancer Solution (Invitrogen) to obtain single amplicon of expected size. (see section further further sub-cloning details).

2.3.2.4 PCR from genomic DNA template using Biotaq DNA polymerase

See section **2.3.5.2** for PCR amplification of bisulphite converted gDNA.

See **section 2.3.9** for PCR amplification of ChIP enriched (sheared) gDNA.

2.3.2.5 Semi-quantitative RT-PCR

Typically, semi-quantitative RT-PCR (sqRT-PCR) in a 25µl reaction volume using 1µl of cDNA template was performed using Biotaq DNA polymerase as per manufacturers' instructions, plus final concentration of 1M betaine, or Taq DNA polymerase in 1xRB PCR reaction buffer. Primers used see **sections 2.2.7.2** and **2.2.7.3**. General PCR program: denature 94°C for 5', then limiting cycles of 94°C, 30"; 60°C, 30"; 72°C, 30". Limiting cycle numbers for each primer set, relevant to each cell line, can be found in the appropriate figure legends. Single PCR amplicons were separated by 1% (w/v) TBE agarose gel electrophoresis stained with ethidium bromide (EtBr) and visualised by UV detection.

2.3.2.6 Quantitative Real-Time RT-PCR

Quantitative real-time RT-PCR (qPCR) was carried out using Platinum SYBR Green qPDR Supermix-UDG reagent as per manufacturers' instructions, and PCR performed in triplicate 15µl reactions, using 1µl of cDNA template per reaction, performed and analysed using StepOne Plus Real-time PCR system and 'QGene' analysis software [106].

2.3.2.7 Restriction digestion of plasmid or purified PCR product

Typically, 1-5U of restriction enzyme per 1µg of purified DNA was used for digestion in compliance with the recommendations of the NEB catalogue and technical reference book (updated annually).

2.3.2.8 Dephosphorylation of linear double stranded DNA

Final concentration of 1xSAP buffer was added to purified digested DNA with 1U (1µl) of the Shrimp Alkaline Phosphatase (SAP) enzyme, and mixed well. Sample incubated at 37°C for 30-45min, followed by

15min at 70°C to heat inactivate the enzyme. Dephosphorylated DNA then used for downstream applications.

2.3.2.9 Electrophoretic separation and visualisation of nucleic acids

EtBr stained 0.75-2.5% (w/v) TBE agarose gel electrophoresis was used for the separation, and subsequent UV light visualisation using a UV transilluninator, of nucleic acids.

2.3.9.10 DNA purification from enzymatic reactions

Following PCR or enzymatic digestion, DNA was purified using the Qiaquick PCR purification Kit (Qiagen) as per manufacturers' protocol.

2.3.2.11 DNA purification from Agarose gels

Linearised DNA to be purified was carefully excised from the agarose gel with a scalpel blade using UV transillumination to show EtBR stained DNA, then purified using the Qiaquick Gel purification kit (Qiagen) as per manufacturers' instructions.

2.3.2.12 Ligation of purified DNA fragments

Typically, ratios of insert:vector backbone of 3:1 and 5:2 were used as calculated by the Promega equation:

((ng of vector x kb size of insert)/kb size of vector)x(insert/vector ratio) = ng of insert needed

Purified and dephosphorylated linearised vector and insert DNA was mixed together with final concentration of 1x ligation buffer and 1U of T4 DNA ligase in 10µl, and incubated O/N at 16°C, or for longer periods at 4°C.

2.3.2.13 Purification of genomic DNA

Mammalian cultured cells:

Purelink Genomic DNA purification Kit was used for the purification of mammalian gDNA from cultured cells (DU145) as per manufacturers' instructions. Purified gDNA stored at -20°C.

From mouse tail samples:

Tail tips (1-2mm) samples from 3 week old pups were incubated in 300µl Mouse tail tip lysis buffer plus 15µl of 10mg/ml Proteinase K dissolved in the same lysis buffer O/N at 56°C. Following a brief vortex, remaining un-dissolved solid material (cartilage and hair etc) was removed from the soluble material with a pipette or separated by 10 min spin at 14 000 rpm at RT, and S/N removed to a new tube. Genomic DNA was then precipitated with the addition of 0.7 volumes of isopropanol, and mixed by gentle inversion approximately 6 times. Sample was then spun for 1min at max speed and S/N removed from gDNA pellet. Pellet was then washed with 200µl of 70% EtOH, followed by 1min spin at max speed. S/N was removed and pellet air-dried for 30-40 min, then 100µl of 1xTE added to pellet and allowed to stand at RT O/N (min) to dissolve gDNA. Samples then stored at 4°C. 1µl used for template in 25µl PCR reaction.

2.3.3.14 Isolation of Total RNA

Total RNA was chloroform extracted from cells lysed with Tri-reagent as per manufacturers' instructions from mammalian cultured cells or frozen tissue. Equal volume of 70% EtOH was added to the collected aqueous phase, containing RNA, which was then purified and eluted from Qiagen RNAeasy mini columns as per manufacturers' instructions. 0.5-1ug of total RNA visualised by UV light detection following EtBR stained agarose gel electrophoresis. Quality of extracts assessed by the apparent ratio of 28S:18S ribosome bands (2:1 expected) and lack of any evidence of degradation.

2.3.2.15 cDNA synthesis from mRNA in total RNA extracts

Typically, cDNA was synthesised from 1-2µg of total RNA using Superscript III (Invitrogen) reverse transcriptase, utilising a protocol adapted from manufacturers' recommendations. In essence, total RNA diluted in 8µl of MQ, to which 1µl of Oligo-DT_{15} (500ng/ul stock), 1µl of random hexamers (dN6, 300ng/ul stock) and 2µl of 5mM dNTP mix, mixed by brief vortex and incubated at 65°C for 5min, to allow primer annealing, then 1min on ice. Then, 4µl of 5xFirst-strand buffer, 1µl 0.1M DTT, 2µl SUPERase-In™ (20U/µl stock) and 1µl of Superscript III are added to make a final reaction volume of 20µl. Reaction mixed by brief vortex, followed by brief spin, and incubated at RT for 5min before 60-90min incubation at 50°C for cDNA synthesis. Synthesis was stopped by heat inactivation of the enzyme at 70°C for 15mins. If 1µg total RNA template was used for synthesis reaction, cDNA made up to 25µl with TE. If 2µg total RNA used for cDNA synthesis template, cDNA sample made upto 50µl with TE. Note; for directly comparative samples, the same amount of total RNA template and reaction conditions were used to control for synthesis efficiency. Typically, 1µl of cDNA used per 25µl PCR reaction for semi-quantitative RT-PCR, or 1µl per 15µl qPCR reaction.

2.3.4 Microarray

Two independently derived polyclonal LNCaP or DU145 cell lines with stable ectopic expression of myc tagged human SIM2s, and two independently derived polyclonal Control (empty-vector) puromycin resistant cell lines, were each grown in duplicate 75cm^2 flasks, maintained in usual growth conditions and allowed to reach 80-90% confluency prior to harvesting. Total RNA was extracted using Tri-Reagent (Ambion) and purified using Qiagen RNeasy mini kit. For both LNCaP and DU145 cell lines, 20ug of purified total RNA for each sample, 8 samples in total, representing 2xControl, 2xSIM2s polyclonal cell lines, each grown in duplicate (see **Figure 4.1**, **Chapter 4**) from which independent RNA extracts were made, was supplied to

the Adelaide Microarray Facility (Adelaide, SA, Australia), who performed all cDNA synthesis and dye labelling reactions. Labelled cDNA was subsequently hybridised to a human 19K oligonucleotide array chip (Adelaide Microarray Facility, SA, Australia). All data compilation and statistical analysis was completed by the Adelaide Microarray Facility.

2.3.5 Epigenetic methods: Detection of gDNA methylation by bisulphite conversion

All methods below were carried out wearing powder free gloves, using nuclease free plastic ware, plugged pipette tips, in a 'plasmid-free' and 'PCR-product' free area to avoid 'DNA' cross-contamination to which this protocol is highly susceptible. The following protocols were carried out INDEPENDENTLY in triplicate, n=3. Method supplied by Prof. E. Whitelaw & Dr. S. Chong at QIMR, Australia.

2.3.5.1 Bisulphite conversion of gDNA

Day One: Sodium bisulphite hydroquinone conversion solution made fresh. Note; sodium bisulphite powder stock must be used within 2 months of opening. The following recipe is enough for six samples: Do not airate solution at anypoint, gentle mixing required. Firstly, 2.7g of Sodium bisulphite (Sigma) was dissolved in 5ml of MQ-water standing at RT with the occasional very gentle swirl-rotation to mix, typically this took up to 90mins. Meanwhile, the 4.4mg/ml hydroquinone solution was made, ie: 0.22g in 50ml of MQ-water. This dissolved easily. Carefully, 333µl of 4.4mg/ml hydroquinone solution and 200µl of 10M NaOH was added to the dissolved soldium bisulphite in 5ml and mixed by gentle inversion only. Previously un-thawed purified gDNA stored at -20°C since its preparation was thawed at RT, then immediately put on ice. gDNA extracts were then quantified by spectrometry and 1µg of gDNA aliquots were taken and made up to 100µl with MQ-water for conversion and kept on ice. No gDNA control samples were also included. For denaturation of

gDNA prior to conversion, 3M NaOH was prepared fresh from 10M NaOH stock. 300µl of 3M NaOH was added to 1µg of gDNA in 100µl of MQ-water in a well sealed 1.5ml eppendorf tube and incubated in a 55°C water bath for 30min. Then, 900ul of the conversion solution added to denatured gDNA (final volume 1.3ml) and overlayed with mineral oil, and incubated for 20hrs in 55°C waterbath.

Day Two: Desalting DNA clean-up and desulphonation. Nearly all mineral oil was carefully removed from each (1.3ml) sample (including no gDNA control) which was then subsequently cleaned-up using Qiaquick PCR purification kit as per manufacturers' instructions. gDNA was eluted from columns with 2x40µl MQ-water pH 8.0, giving a final eluate volume of 80µl. 8µl of freshly made 3M NaOH from 10M stock, was then added to each sample, gently mixed, and incubated at for 15min in a 37°C waterbath. After which, gDNA was then EtOH precipitated by adding 44ul of 6M ammonium acetate and 450ul of 100% EtOH, mixed gently, and incubated at -80°C for 30min. Samples were then spun in a microcentrifuge at 14000rpm for 15min at 4°C, supernatant carefully removed from precipitated DNA pellet with a pipette, and gently washed with 150ul 70% EtOH, followed by another 14000rpm spin at 4C. EtOH wash carefully removed and gDNA pellet allowed to air dry. gDNA was then dissolved gently in 30µl of MQ-water pH 8.0 with heating at 70°C for 90sec. Converted gDNA samples then stored at -20°C till used for PCR.

2.3.5.2 Bisulphite converted specific gDNA PCR

Specific amplification of bisulphite converted gDNA of the human *BNIP3* proximal promoter region containing the HRE was carried out using the bisulphite specific primers; methBnip3prmHRE LEFT and methBnip3prmHRE R (see **section 2.2.9.6**) and BIOTAQ DNA polymerase, as per manufacturers' recommendations, in a 50µl reaction volume including 1.5µl of 10uM stock of each primer, 2µl of 5mM dNTP mix and 2.5U of BIOTAQ DNA polymerase. Two rounds of 35xcycles of PCR using an annealing temperature of 60°C and with changes in reaction conditions modified as follows. Round 1 PCR: 3µl of

bisulphite converted gDNA sample for PCR template, 3mM $MgCl_2$; Round 2 PCR utilised 2µl of round 1 PCR as template, buffer adjusted to 6mM $MgCl_2$. 50mM stock of $MgCl_2$ used. Half (25µl) of the round 2 PCR reaction was subjected to 1% (w/v) agarose TBE gel electrophoresis and resultant single PCR amplicon was agarose gel purified and stored at -20°C.

2.3.5.3 Combined bisulphite restriction analysis (COBRA)

This protocol is used to assess the efficiency of conversion. 5'-CCCAAA-3' in native gDNA becomes 5'-TTTAAA-3' upon complete conversion creating a Dra1 restriction site. Such a site was contained within the mBnip3 promoter region under investigation. Complete digestion of the round 2 PCR product with Dra1, as shown by an expected change in size, indicates complete conversion. The remaining 25µl of round 2 PCR reaction mix was subjected to restriction digestion with Dra1 as per NEB recommendations, and then subjected to EtBr stained 1% agarose (w/v) TBE gel electrophoresis and visualisation with UV-light.

2.3.5.4 Ligation of bisulphite converted specific PCR amplicon into pGem-Teasy vector and generation of individual clones for sequencing analysis

Utilising the 3'-A-overhang following PCR using a Taq polymerase, 3µl of gel purified bisulphite converted round 2 PCR product was ligated into 1µl pGem-Teasy vector using 1µl T4 DNA ligase with 2xRapid Ligation buffer in 10µl, incubated overnight at 16°C. Next day, 40µl of chemically competent DH5α heat shock transformed with 5 µl of the ligation reaction and then plated onto solid 10cm diameter LB media plates supplemented with 100 µl of 0.1M IPTG and 40 µl of 50 mg/ml X-gal. Single colonies then individually selected and cultured for propagation and plasmid purification. Mimimum of 5 individual clones arising from a single conversion were analysed by sequencing for detection of methylation. Clones were deemed individual due to variations in methylation patterns or sites of conversion (see **Chapter 5**).

2.3.5.5 Treatment with 5'-Aza-dC

DU145/SIM2s.myc cells were plated in a 6-well tray, and the next day at approximately 30% confluency, complete growth media was supplemented with 0, 1, 5 or 10 μM 5'-Aza-dC, and cells were further incubated for 48h prior to harvesting for WCE.

2.3.6 Cell culture

Handling of all cell cultures and materials was done with sterile aseptic technique, in a UV sterilised laminar flow fume hood.

2.3.6.1 Thawing and generation of frozen cell line stocks

Vials of cells removed from liquid nitrogen or -80°C stocks thawed immediately in 37°C water bath and then resuspended in pre-warmed (RT or 37°C) complete growth media. Media replaced 24h later, then maintained as usual. Typically, frozen stocks generated by resuspending cell pellet to 1-2x10^7 cells/ml in 90% growth media + 10% DMSO freezing medium and aliquoting into Nunc® Cryo-tubes and freezing to -80°C. 1ml vials of cells frozen to -80°C were then be transported on dry ice to liquid nitrogen long term storage.

2.3.6.3 Routine maintenance of cell lines

Human pancreatic, and prostate carcinoma derived cells were maintained in RPMI-1640 (Gibco) supplemented with final concentration of 1mM sodium pyruvate (Gibco), and mouse NIH3T3 and P19 cells were maintained in Dulbecco's modified Eagle's medium (Invitrogen), and Alpha-MEM (Gibco), respectively.

HEK 293 cells (293F and 293A) were grown in DMEM. All growth media supplemented with 10% foetal bovine serum (FBS, Gibco) and cells routinely maintained at 37°C, 5% CO_2.

2.3.6.4 Hypoxic culture conditions

Cells grown in 10cm dishes, or 6- and 24-well trays, were sealed in a hypoxia chamber with a hypoxia sachet to achieve <1% Oxygen (O_2) and incubated as usual for the designated number of hours (8, 16 or 44h) prior to harvesting for experimental analyses. Percent O_2 concentration using this system was determined utilising the oxygen sensing device from Teledyne Analytical Instruments (model AX3001) to actually be ≤ 0.2%, however is stated at <1% hereafter. Prolonged 'hypoxia' (18, 36 and 44h) was induced using or 1mM DOMG, or 100μM DP, compared to DMSO vehicle control treatment, from 1000x stocks.

2.3.6.5 Transient Transfection

Transfection of cells for the transient cDNA expression were all carried out using Fugene 6, and the protocol optimised, as per manufacturers' instructions. Typically a ratio of 3μl of Fugene6 for every 1μg of plasmid DNA, was used.

2.3.6.6 Cell lines engineered for stable integration of cDNA (transgene) expression constructs

For constitutive stable ectopic expression: Subconfluent cells were transfected using Fugene6 (Roche) as per manufacturer's instructions. To produce stably transfected polyclonal lines, subconfluent cells were transfected with blank pEF/IRESpuro or pEF/IRESpuro vector containing the cDNA expression sequence, ie: hSIM2s.myc-IRESpuro, and were selected and expanded with up to 10μg/ml puromycin.

For inducible expression using the HEK293 Flp-In™ TRex™ (Invitrogen) System: Cell lines were developed as per the recommendations of the manufacturer. In brief, 293F cells were maintained with complete DMEM growth media supplemented with 100μg/ml zeocin. For generation of inducible polyclonal

isonic cell lines, zeocin selection was removed and subconfluent (60%) cells in a 6cm dish were transfected by usual method using Fugene6 with 200ng of the FRT-TO-Flp-In-cDNA expression construct with 1800ng of the Flp-recominbase vector, pOG44. Antibiotic resitance selection for successful integration of the expression construct was carried out with 15µg/ml Blasticidin and 200µg/ml Hygromucin. Cells were treated with 1-5ug/ml Dox for inducing cDNA expression for the time stipulated.

2.3.6.7 WST-1 survival/growth assay

PC3AR+ cells were seeded at $1.3x10^4$ cells/well (100µl) in 96 well trays, and allowed to adhere overnight. Cells were then treated for the indicated hours with either DMSO vehicle control, DMOG or DP. At time of harvest 10µl WST-1 reagent was added to the wells as per manufacturers' instructions. Cells were then incubated in usual growth conditions and incubation time with WST-1 reagent was optimised according to manufacturers' instructions. WST-1 signal was measured at 450nm on a Spectramax plate reader (Molecular Devices) after 20, 40, 60 and 90minutes incubation with the reagent to determine linear range of the signal. 40min time point was used. Data represented as percent of cell survival (mitochondrial activity) of respective DMSO vehicle treated puromycin resistant Control, or SIM2s.myc cells, at each time point.

2.3.6.8 siRNA treatment

All siRNA oligonucleotides were chemically synthesized (Qiagen). 100nM of siRNA oligos were transfected into 25-30% confluent cells using Oligofectamine as per manufacturers' instructions, and repeated 24 hours later. Transfection efficiency of siRNAs was assessed using 3'Alexafluor549 labelled siRNA oligonucleotides. Cells were then harvested 72 hours after first transfection for analysis. Or, DU145 cells, transduced with lentiviral vector containing tet-inducible shRNA sequences for targeting SIM2s and scrambled control (generated with technical assistance from C. Bindloss), were treated with doxycycline for 72hrs, then harvested. Target sequences for siRNA oligonucleotides are listed above (**section 2.2.9.7**).

2.3.6.9 Dual Luciferase/Renilla or Beta-galacosidase Reporter assays

Transient transfection of 293A or NIH3T3 cells at 50% and 30% confluency, respectively, in 24-well tray format was performed using Fugene6 (Roche) as per manufacturer's instructions. Each transfection contained equal final DNA levels, including 100-150ng of pGL3basic luciferase reporter construct with equal concentration of pCMX-beta-galactosidase (gift D. Dowhan) or pGL3-Renilla in a 10:1 ratio pGL3-Luciferase:pGL3-Renilla, with 100-150ng of hSIM2s or mSIM2L expression vector, with or without 10ng carboxy-terminal heamagglutinin tagged hARNT1. Mouse 1kb Bnip3promoter reporter studies: 24 hours later NIH3T3 cells were either harvested or subjected to an additional incubation for 16 hours in a hypoxia chamber. Human 1.3kb Myom2 promoter reporter studies: 293A cells were incubated for 48hrs post transfection before harvesting. Cells were lysed with 100µl 1xPassive Lysis Buffer.

Luciferase/Beta-gal assays: 10µl of each lysate was analysed in 96 well tray format for measurement of luciferase activity, using 50µl Luciferase Assay Substrate (Promega) (Luciferase light emmision immediately measured using the Glomax luminometer), followed by incubation with the Galacto-light substrates (Applied Biosystems): 70µl Galacto-light, 1 hour incubation, then addition of 100µl Galacto-light Accelerator, for immediate analysis of control beta-galactosidase for normalisation, as per manufacturer's instructions, using the Promega Glomax luminometer system.

Luciferase/Renilla assays: 5-10µl of lysate analysed as per Promega Dual Luciferase Assay protocol. In brief, 25ul of LARII reagent mixed with lysate to measure Firefly luciferase levels, followed by the addition of 25ul of Stop'n'Glo for an independent measure of Renilla luciferase levels for normalisation. Light emission data collected using the TD 20/20 Luminometer.

2.3.7 Mice and mouse tissue preparation

Transgenic mice for ectopic expression of hSIM2s in the pancreas were generated by Prof. H. Edlund and E. Palsson, and maintained in animal house facility of the University of Umeå, Sweden.

Animals were killed by ethically approved methods and tissue was dissected and supplied for analysis by the technical assistance of others at the University of Umeå, and at the Karolinska Institute, Sweden.

2.3.7.1 Preparation of fresh frozen tissue sections for IF

The following protocol was optimised for maintaining pancreatic tissue morphology.

Freshly harvested mouse pancreatic tissue was placed in a Cryomold suspended in OCT (Tissue-tek) gel, carefully wrapped in aluminium foil, and parcels then snap frozen in liquid nitrogen and stored at -80°C. Frozen tissue blocks were transported on dry ice to -20°C Cryostat in which tissue sections (<10µm) were cut from the frozen tissue bocks and gently placed onto glass Superfrost-plus slides. Tissue sections were only allowed to dry onto slides for 5-10min at RT, then fixed immediately with freshly made 4% PFA for 10min at RT. (Further details of following IF protocol are in **section 2.3.8.6**).

2.3.8 Protein analysis

2.3.8.1 Preparation whole cell extracts and quantitation of protein yields

Media aspirated off adherent cells grown in 6-well trays, rinsed with cold PBS, and ice cold WCE buffer or RIPA buffer, with freshly added 1xPI cocktail and 1mM DTT, added directly to adherent cells. Tray rocked at 4°C for 10min, lystate and cellular debris collected into a 1.5ml tube and further incubated at 4°C on an orbital shaker, followed by a 35-40min 14 000xrpm centrifugation in a microcentrifuge at 4°C. Cleared whole cell extracts collected to a new tube and stored at -80°C. Similar process applied to cell pellets collected using trypsin. Cells treated in a hypoxia chamber were removed from the chamber, harvested and

lysed all at 4°C. Volume of WCE or RIPA buffer used for lysis at a minimal 2.5:1 WCEB:cell (pellet) volume, v/v, ratio. (References from which protocol adapted [59, 107]).

Poretin yields were determined by Bradford protein assay (BIORAD) as per manufactiurers instructions, calculated from OD_{600} measures with reference to a BSA concentration standard curve.

2.3.8.2 Immunoprecipitation

0.5mg of WCE was diluted to ~1.6µg/µl in IP buffer plus fresh 1x Protease Inhibitor (PI) cocktail from 100x stock, then pre-cleared using rec-proteinG-sepharose. Pre-cleared diluted WCE was then mixed with 2ug of goat polyclonal hSIM2s or IgG control antibodies, or no antibody, and mixed gently for 1h at 4°C. Protein-antibody complexes were then conjugated to the rec-proteinG-sepharose for 2h with gentle mixing at 4°C, followed by 4x washes with IP buffer. Final pellet was resuspended in SDS load buffer, boiled, and separated by 8% SDS-PAGE, followed by transfer to nitrocellulose for immunoblot analyses as described below.

2.3.8.3 Denaturing gel electrophoresis

Denaturing SDS-PAGE was used for the separation of proteins for western (immunoblot) analyses. Typically, gels were prepared on the previous day using the Biorad mini-gel apparati, and once set stored at 4°C wrapped in moist paper towel and plastic. The (bottom) separating gel (8-13.5%) containing;1x Separation buffer, 8-13.5% (v/v) acrylamide [29:1, acrylamide:bisacrylamide], 0.08% (v/v) TEMED and 0.08% (w/v) APS, was overlayed with 20% (v/v) EtOH immediately after pouring and allowed to set at RT. Once set, the EtOH was removed and top of gel rinsed with RO-water, and the (top) stacking gel containing 1xStacking buffer, 4.5-5% acrylamide, 0.08% (v/v) TEMED and 0.08% (w/v) APS, was poured over the bottom gel, and comb to form wells in the top gel set in place. Set gel was then assembled in the Biorad gel

running apparatus with 1xGTS running buffer. Typically, 35-50ug of whole cell protein extract (see **2.3.8.1**) in 1xSDS load buffer were boiled at 96C for 5-10min, briefly centrifuged, then loaded into wells with a fine (blunt) needle syringe. Commonly, gel electrophoresis took 90-120min at 100-110V constant at RT.

2.3.8.4 Western Blot

Protein transfer to nitrocellulose or PVDF membrane

Following SDS-PAGE, proteins from the denaturing SDS gels were transferred to PVDF or nitrocellulose membrane (8cm x 10cm) using a wet transfer system at 4°C, typically 70mins at constant 250mA, or with a semi-dry electroblotter at RT, typically 25min at 25 volts, as per manufacturers' instructions, with appropriate buffers (see **section 2.2.6.1**).

Ponceau staining of membrane

Efficiency of protein transfer was sometimes assessed by incubating the membrane with Ponceau stain immediately post-transfer and before 'blocking'. After 2-3min/RT/gentle rocking incubation of the stain, membrane was washed several times with MQ-H_2O to reveal clearly visible red protein bands above the background. Stain is subsequently removed following blocking of the membrane (see below).

Immunoblot chemiluminescent detection of protein

Membranes were 'blocked' in a 10% skim-milk/PBS-T or TBS-T solution for minimum 60min/RT/gentle rocking, followed by incubation with primary antibodies (dilutions and incubation times and temperatures described in **section 2.2.5**) with gentle rocking, or orbital shaking. Following incubation with primary antibody, membranes were washed 3x with PBS-T for 5min at RT with gentle rocking, then incubated for 45-60min with appropriate secondary antibody at RT with gentle rocking, or orbital shaking. Membranes were then washed again 3x with PBS-T for 5min at RT with gentle rocking, air-dried and on a flat surface, chemiluminescent reagents added directly to the 'protein' surface of the membrane and incubated for 5mins

using Super Signal, or 1min using Imobilon chemiluminesence reagents. Membranes were then blotted dry between two pieces of whatman paper, then exposed to film, and developed.

2.3.8.5 Chemiluminescent quantification using ImageQuant v 5.2

Quantification of chemiluminesent immunoblot data was done using ImageQuant v5.2 (Molecular Dynamics) software, analysed with XCEL, and normalised to loading controls, including alpha-tubulin and primary antibody non-specific background bands. Details of quantification and normalisation controls described within appropriate figure legends.

2.3.8.6 Assesment of protein half life

Subconfluent cells were treated ith 60ug/ml cyclohexamide (CHX) for the time periods indicated. For several time points individual wells were treated such that the slongest treatment time was applied first, then through to the shortest time point applied, for even confluency of cells at the time WCE were harvested. Equal amounts of protein for each time point of CHX treatment were separated by SDS-PAGE followed by western blot analysis. Quantification of relative protein levels was carried out as described in **section 2.3.8.5.**

2.3.8.7 Immunofluoresence of fresh frozen tissue sections

Following the fixation of tissue on glass slides (see **section 2.3.7.1**) pancreatic tissue samples then gently washed with TBS-T, then blocked with 1% BSA/TBS-T block solution for 60-90min at RT. Slides were then wiped clean and dry around tissue samples (were needed a Pap pen was used to border samples) and 1° antibody solution, typically diluted 1:50-400 in block solution, was applied to the slide (usually 150µl/slide) and left to incubate O/N at 4°C in a humid chamber. Following 3x washes with TBS-T, 1:1000/1% BSA/TBS-T diluted alexa-fluor-labelled secondary antibodies were applied to tissue samples incubated for

1hr at RT. Slides were then washed 3x TBS-T, slides were prepared for mounting and mounted using the SlowFade Light Antifade kit, which included a 10min incubation at RT with Equilibration Buffer and then mounted with the Antifade aqueous mounting medium which also contained the nuclei counterstain, DAPI, and then covered with a glass slide, and stored in a humid chamber at 4°C till analysed. If mounting media without DAPI was used, DAPI was applied diluted with the secondary antibody. Analysis and images were obtained by confocal microscopy.

2.3.9 Chromatin immunoprecipitation

This protocol was carried out using powder free gloves, plugged pipette tips, nuclease free solutions, polypropylene and/or low retention tubes.

Subconfluent DU145 or NIH3T3 cells were grown in a 75cm^2 flask or 10cm dish with or without 8 hours of hypoxia were fixed with final concentration of 1% Formaldehyde (Sigma) added to growth media, gentle swirl to mix, for 10 minutes at RT, stopped by 128mM final concentration of 1.67M glycine. Cells were then harvested using a cell scraper and collected into 50ml conical bottom tube, and spun at 1500rpm for 5min. Media containing inactivated formaldehyde is gently poured off cell pellet, which is then washed once with 10ml ice-cold PBS, spinning at 1500rpm for 5' on a table centrifuge to gently pellet the cells and PBS wash gently aspirated off cell pellet. Cell pellet then resuspended gently in 1ml ice-cold PBS and trasferredto a 1.5ml eppendorf tube, followed by 2xbreif pulse spins to 4000rpm in microfuge at 4°C, before PBS wash gently removed from cell pellet. Cells were then lysed in freshly made Nuclear Isolation Buffer for 10min at RT, with 4x brief vortex of samples during that time to aid lysis. Following a 5min 4000rpm spin at 4°C in a microcentrifuge, the nuclear pellet from approximately 2x10^6 cells (for one IP sample) was then resuspended in 200µl freshly made SDS lysis sonication buffer plus 1xPIs as per Ez-ChIP kit protocol

(Upstate), and snap frozen in an ethanol/dry ice bath, samples were then stored at -80°C for a few hours, or long term if not to be used the same day. Typically, 1x10cm dish of 80-90% confluent NIH3T3 cells is enough for 3xIPs, therefore, the nuclear pellet was resuspend in 600µl of SDS lysis buffer, then aliquoted to 200ul samples for sonication. Either the same day, or the next, nuclear pellets in sonication buffer were thawed and then sonicated using the Bioruptor (Diagenode), set on high for 30" on/30" off for 7.5-10 minutes, in an ice-cold water bath. After sonication, samples were transferred on ice to be immediately spun at 12000rpm for 15min at 4C. 180µl of soluble chromatin (supernatant) can be easily collected from each 200µl sonication aliquot. At this time, a 20-30µl sample of the soluble chromatin was taken to assess sonication efficiency. To do so, the sample of soluble chromatin was incubated overnight at 65°C in a well sealed tube to reverse the crosslinks. After which an equal volume of water and Proteinase K to a final concentration of approximately 0.8µg/ul (ie: 2.5µl of 20mg/ml stock to 60µl of diluted chromatin) was added and the sample incubated at 42°C for three hrs. Sheared gDNA was then purified with Qiagen QIAquick columns as manufacturers' protocol and eluted with 30µl of kit elution buffer (10mM Tris, pH 8.5), quantified by spectrometry, and ~1µg of purified sheared gDNA subjected to EtBR stained 1% agarose gel electrophoresis to determine predominant size of sheared gDNA. Ideally, a predominance of 200-500bp was sought, and obtained, via optimisation of nuclear pellet 'concentration', volume and sonication time.

Following the collection of soluble chromatin, ChIP was then performed as per Ez-ChIP protocols with salmon sperm blocked protein-G resin (Upstate), using 2µg of goat polyclonal anti-hSIM2s (Santa Cruz), goat-polyclonal IgG (Santa Cruz), rabbit polyclonal anti-HIF1α (ab2185, Abcam), and rabbit polyclonal IgG (Upstate) antibodies for immunoprecipitations. Eluted ChIP DNA, using freshly made ChIP elution buffer, was purified using Qiagen DNA purification Spin column, and then analysed by PCR, using BIOTAQ polymerase as per manufacturer's instructions, supplemented with 1M betaine (Sigma). Typically 2µl of purified gDNA was used as template in a 25µl reaction, including 1µl of each 10µM primer and 1U of

BIOTAQ. **See section 2.2.7.4** for ChIP primer sequences. PCR program used as described above, using 35-40x cycles. PCR products visualised by UV-light detection following EtBR stained 2.5% agarose (w/v) TBE gel electrophoresis.

CHAPTER 3

SIM2 stabilisation and regulation of its obligate partner factor, ARNT

3.1 INTRODUCTION

3.1.1 Arylhydrocarbon Receptor Nuclear Translocator (ARNT): Expression and transcription inducing activities

Murine Arylhydrocarbon Receptor Nucelar Translocator Arnt (or Arnt1) and Arnt2 are close homologues, and share an overall 54% amino acid similarity between mouse, rat and humans (**Figure 3.1**). The region of highest shared homology is in the bHLH-PAS N-terminus, with 81% in mice [8], and overall 80.2% between mouse, rat and human (**Figure 3.1**). Analysis of truncated mutants of mArnt2 in growth studies in yeast revealed a C-terminal trans-activation domain (TAD) in the last 37 amino acids which is relatively conserved to the Arnt1 trans-activation domain [8, 108], and overall approximately 60% in mice, rats and humans, whereas the rest of the carboxy-terminus after the PAS domain is divergent, sharing only 39% homology in humans and rodents (**Figure 3.1**) [8, 109].

ARNT1 is ubiquitously expressed, whereas the homologue ARNT2 has a highly restricted expression pattern, mainly in the brain and kidney [5, 8, 110, 111] and only lowly expressed in muscle during embryonic development [111]. Targeted deletion of *Arnt1* results in embryonic lethality between E9.5 and E10.5 with signs of disrupted foetal development including defects in neural tube closure, embryonic placenta vascularisation and angiogenesis of the yolk sac and brachial arches [112, 113]. *Arnt2*-deficient mice die shortly after birth and are characterised by impaired hypothalamic development [2, 114]. These characteristics phenocopy the mSim1 knockout mouse and is concordant with the hypothesis that Arnt2/Sim1 functions as a heterodimer *in vivo* [2, 84]. Interestingly, others report that no difference in embryonic CNS development was observed between wildtype and *Arnt2*$^{-/-}$ mice [114], which is also in contrast to a previous report for Arnt2 being required for rat PC12 neuronal cell survival [109].

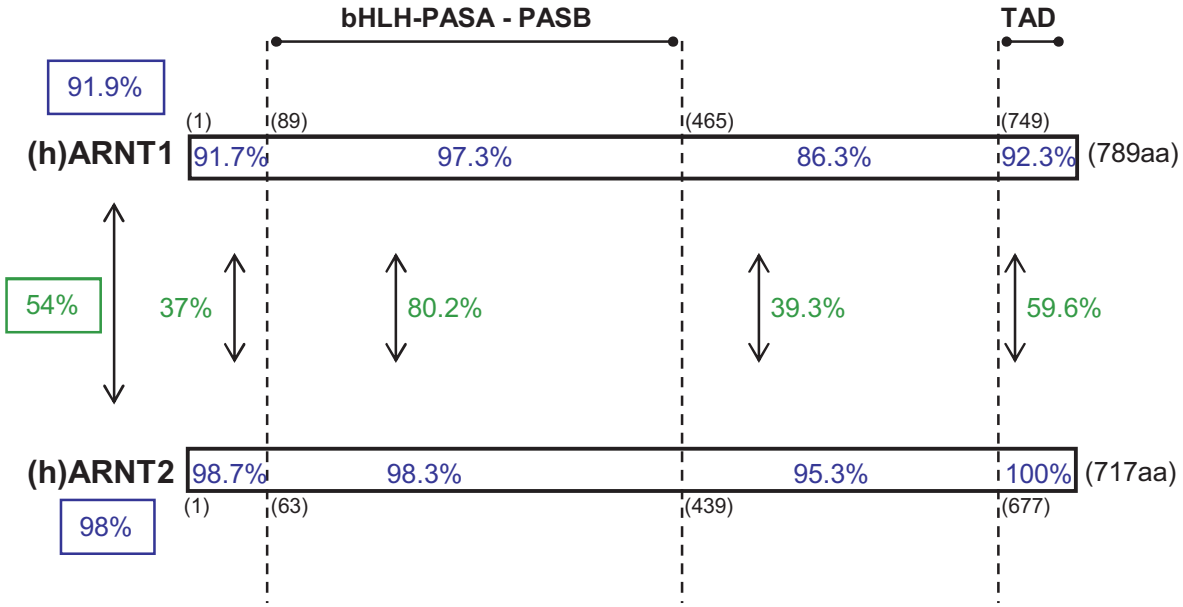

FIGURE 3.1: *Shared amino acid homology of ARNT1 and ARNT2 orthologues in human, mouse and rat*.

Overall shared amino acid homology between human, mouse and rat orthologues of ARNT1 and ARNT2 shown (boxed values). Average percent (%) shared homology of human, rat and mouse for each homologue in blue. Average % homology between ARNT1 (A1) and ARNT2 (A2) of human, rat and mouse in green, and marked with arrows. N-terminal basic Helix-Loop-Helix-PAS (bHLH-PAS) region and C-terminal transactivation domain (TAD) marked. Accession numbers used for alignments: hA1 = NM_001668; hA2 = NM_014862; mA1 = NM_001037737; mA2 = NM_007488; rA1= NM_012780; rA2 = NM_012781. Amino acid (aa) residue numbers indicated within brackets ( ). References: Hirose et al (1996) Mol. & Cell Biol. 16(4):1706-1 and Drutel et al (1996) Biochem. Biophys. Res. Comm. 225; 333-339.

Arnt1 and Arnt2 are partially redundant before E8.5 as discerned from genetic interaction studies by Keith and colleagues crossing compound heterozygote *Arnt1*$^{+/-}$, *Arnt2*$^{+/-}$ mice, where severe under-representation or absence of the expected Mendelian distribution of embryos with less than two wild-type alleles of either *Arnt1* or *Arnt2*, in any combination before E8.5, was found. Thus the authors suggest a model for a dose-dependent requirement for either *Arnt* to fulfil essential overlapping functions before E8.5, whereafter the requirement for *Arnt1* becomes more critical for development [114]. The nature of these overlapping functions for *Arnt1* and *Arnt2* remain to be determined, however, insights into their overlapping, and evidence for their unique, transcriptional roles are apparent in their interactions as bHLH-PAS class II obligate partner factors for class I family members such as HIF1α and AhR in response to hypoxia and xenobiotics, respectively [5, 114, 115]. In particular, through binding HIF1α, both Arnt1 and Arnt2 are able to induce expression of endogenous HIF1α/Arnt target genes, such as *Glut-1*, *Vegf* and *Pgk,* and induce expression of hypoxic response element (HRE) driven reporter genes [114, 115]. Although *Vegf* and *Pgk* are only induced 75% of wildtype levels in Arnt2-/- neurons after 16h hypoxia, major disruptions in the vascular endothelial network observed in *Arnt1*-/- mice are not found in the *Arnt2*-/- mice, indicating that *Vegf* expression levels are effectively normal in *Arnt2*-deficient mice [114]. In contrast however, due to a single amino acid difference in the PASB region, unlike Arnt1, Arnt2 is unable to bind ligand activated AhR to induce expression of xenobiotic response element (XRE) driven reporter gene, and endogenous AhR/Arnt1 *CYP1A1* expression [115, 116].

Transiently expressed Arnt1 has been found to form homodimers which bind and activate transcription of reporter genes via palindromic enhancer (E-box) 5'-CACGTG-3' elements in the promoter [5, 117]. However, until only recently there had been no reports of endogenous targets of the homodimer, and hence the *in vivo* relevance and function of Arnt/Arnt was unclear. Insight into the endogenous transcriptional activities of the Arnt homodimer recently emerged from Arpiainen *et al* (2007) in the first, and thus far only,

report of active Arnt homodimer regulating gene expression. Transcription of the *Cytochrome P450* (*Cyp) 2a5* gene was increased upon the binding of Arnt/Arnt to an E-box in the promoter of *Cyp2a5* [118]. Arnt2 has also been shown to homodimerise in yeast two-hybrid experiments [8, 34]. Transient expression of Arnt2 in Arnt1- and Arnt2-deficient Hepa-1 c4 cells results in the transactivation of a reporter gene driven by the *Cyp1a1* promoter indicating that Arnt2 homodimers may be able to regulate *Cyp1a1* gene expression [8]. In contrast, in a study by others stable ectopic expression of Arnt2 in the same Arnt-deficient Hepa-1 c4 cells had no effect on the endogenous levels of *Cyp1a1* gene expression as measured by real-time PCR [115]. Thus, as was initially so for Arnt1, in the absence of any reports of endogenous target genes for the Arnt2 homodimer, the possible physiological relevance or function of Arnt2/Arnt2 in gene regulation remains unclear.

3.1.2 Regulation of ARNT

Very little is understood about the mechanisms of regulation of ARNT1, and nothing about ARNT2, at the protein level. In recent years, two studies have emerged with novel insights into the mechanisms of ARNT1 protein regulation via interactions with non-bHLH-PAS proteins and how the consequent changes in ARNT1 stability via these interactions impacts on its role as an obligate bHLH-PAS partner factor. In particular, Kang and co-workers (2006) found BRCA1 to modulate AhR/ARNT1 xenobiotic (TCDD) stress induced induction of *CYP1A1* and *CYP1B1* in breast cancer MCF-7 cells. Their findings suggest BRAC1 interacts with ARNT1, without which ARNT1 becomes de-stabilised upon treatment with TCDD and xenobiotic stress-inducible gene expression is attenuated [119]. Also, treatment of Hep3B cells with curcumin, a putative tumour inhibitor, has been shown to promote destabilisation and proteasomal degradation of ARNT1 (where *ARNT1* mRNA remains unchanged), resulting in the inhibition of HIF1α activities as measured by the attenuation of induction of HIF1α regulated genes such as *EPO* and *VEGF* [120].

However, endogenous ARNT1 levels remain unchanged upon treatment with the proteasome inhibitor MG132 in curcumin-untreated Hep3B cells in this study [120], consistent with a previous report by others in mouse adrenal Y1 cells [121], indicating that proteasomal degradation is not the usual mechanism of ARNT1 degradation. There may be a number of possible mechanisms that ensue in response to stressors or stimuli that contribute to regulating the stability of ARNT1. There is a dearth of knowledge on the cues and mechanisms for the transcriptional regulation of *ARNT1* and *ARNT2*. The only definitive indication of upregulation of *ARNT1* was observed in a recent study by Arpianen and co-workers (2007), where both *ARNT1* mRNA and protein was found to be increased in murine primary hepatocytes cultured for 24h following liver perfusion [118]. The mechanisms that resulted in this upregulation of *ARNT1* however, remain to be investigated. In all there have been very few studies exploring possible mechanisms of regulation for Arnt1 or Arnt2, largely due to the belief that they function only as generic partner factors for the Class I bHLH/PAS factors.

3.1.3 The role of ARNT as a regulator of bHLH-PAS family members

Although mechanisms that function to regulate and stabilise ARNT remain to be fully investigated, roles for ARNT in the regulation of class I bHLH-PAS family members have been described. The expression, and thus the transcriptional activities, of ARNT have been implicated in the gene regulation of class I bHLH-PAS family members by Gunton and co-workers (2005), who reported a down regulation in expression of *AhR*, *HIF1α* and *HIF2α* mRNAs upon siRNA-mediated knockdown of endogenous ARNT1 in Min6 cells [122], however, the mode of this regulation remains unknown. Better understood are the recent findings indicating a role for ARNT in the regulation of HIF1α at the protein level. Although ARNT is not thought to be required for hypoxic stabilisation of HIF1α [123], ARNT1 has long been implicated in the oxygen-independent stabilisation and regulation of HIF1α [24, 124]. Initial insights into regulatory cross-talk between these

bHLH-PAS family members were first observed by Forsythe *et al* (1996) upon analysis of Hepa-1 c4 ARNT-deficient cells subjected to hypoxic growth conditions. These experiments showed little hypoxic induction of endogenous HIF1α in the nucleus compared to the greatly enhanced hypoxic induction of HIF1α in Hepa-1 c4 cells with ectopic expression of Arnt1, or in Hepa-1 c4 revertant (Arnt-proficient) RB13 and wild-type Hepa-1 cells, suggesting that HIF1α may not be stable without ARNT [22]. Consistent with this observation, others have shown that transiently expressed full-length HIF1α, and a novel ubiquitously expressed isoform of HIF1α, HIF1α^{417}, have enhanced protein levels upon co-transfection of ARNT1 in HEK293 cells [124]. Cyclohexamide treatment studies in HEK293 cells with transient expression of HIF1α^{417} and/or ARNT1, showed that the half-life of HIF1α^{417} was greatly prolonged in direct correlation of ARNT1 co-expression [124]. Recent work by Isaacs *et al* (2004) have also demonstrated in human renal carcinoma 786-O cells that co-expression of ARNT1 greatly enhances the half-life of transiently expressed full length HIF1α. In addition, siRNA-mediated knockdown of endogenous ARNT1 resulted in a dramatic reduction in HIF1α levels, demonstrating that the regulation of HIF1α is dependent on ARNT1 levels in these cells [24]. As 786-O cells are VHL-deficient HIF1α is not degraded via the oxygen dependent VHL-mediated ubquitination and degradation pathway in these cells [5]. Therefore the oxygen-independent mechanism of ARNT1 stabilisation of HIF1α in these cells was identified to be via the ability of the ARNT1 bHLH-PAS region to compete with the molecular chaperone Hsp90 for binding to HIF1α, whereby ARNT1 binding attenuated the proteasomal degradation of HIF1α mediated via the Hsp90 pathway [24]. This mode of stabilisation conferred through the bHLH-PAS interaction of ARNT1 with HIF1α may also account for the ARNT-dependent stabilisation of the HIF1α^{417} splice variant, which due to a premature stop contains only one of two sites of prolyl hydroxylation and no oxygen dependent degradation domain (ODDD) [124] required for VHL-mediated degradation [5].

3.1.4 The regulation of bHLH-PAS class II family member ARNT by class I family members?

The oxygen-independent regulation of HIF1α by ARNT1 [22, 24, 124] provides a precedent for regulation of a class I bHLH-PAS family member by a class II bHLH-PAS family member. However, as there are yet to be any reports of a class I family member being implicated in the gene or protein regulation of *ARNT*, thus the cross-regulation of these family members appears to be one way. Indeed, data thus far showing *Arnt2* mRNA levels to remain unchanged upon hypoxic treatment of cultured murine embryonic hippocampal and cortical neurons [125] does not indicate a role for HIF1α in the gene regulation of *Arnt2*. Likewise, endogenous ARNT1 protein levels are seen to remain unchanged in a number of cell lines treated with hypoxia (thus stabilising and activating HIF1α) [22, 59, 123, 126], and upon TCDD treatment to activate AhR [121, 126]. Taken together, these data support the established notion that the expression and activities of class I bHLH-PAS family members HIF1α and AhR do not affect (class II) ARNT levels. Indeed, as ARNT is ubiquitously and constitutively expressed [5, 8, 127], and in light of these observations, the protein levels of ARNT have been specifically utilised as a loading control for western blot analyses [59, 121]. It was upon implementation of using ARNT1 levels as a loading control for immunoblot experiments in the course of these studies that the surprisingly unexpected and novel reciprocal cross-regulatory relationship between bHLH-PAS class II family member SIM and ARNT was revealed. This chapter will discuss these novel findings and subsequent work conducted to further understand and elucidate the mechanism(s) of what turns out to be an apparently SIM-specific relationship with the regulation of ARNT.

3.2 RESULTS & DISCUSSION

3.2.1 Manipulating SIM2s expression results in correlating changes in ARNT1 protein levels in prostate carcinoma DU145 and LNCaP cells

A minimum of three independently derived polyclonal cell lines for either empty-vector puromycin control (Control), or stable ectopic expression of carboxy-terminal myc tagged human SIM2s (SIM2s.myc), were derived from human prostate carcinoma DU145 and LNCaP cells for microarray studies aimed at identifying novel putative targets of SIM2s (as discussed in **Chapter 4**). Upon western blot analysis of endogenous ARNT1 protein levels in these polyclonal cell lines a dramatic increase in ARNT1 protein (~87kDa) was observed in cell lines with stable ectopic expression of SIM2s.myc compared to Control cell lines (**Figure 3.2A**). To assess whether the increase in protein was due to an increase in message levels *ARNT1* mRNA levels were analysed by semi-quantitative RT-PCR. This analysis revealed, however, no change in *ARNT1* mRNA levels with stable ectopic expression of SIM2s.myc compared to empty-vector controls in independently derived polyclonal cell lines (**Figure 3.2B**). This indicates that there may be a possible post-transcriptional mechanism of ARNT1 regulation correlating to SIM2s expression.

It is notable in **figure 3.2A** the appearance of higher molecular weight products of ectopically expressed SIM2s.myc, particulary in this figure in the samples derived from the LNCaP cell lines. This material was commonly observed following western blot analysis of SIM2s.myc, to varying levels of detection, in all cell lines made for stable, transient, or inducible expression of SIM2s throughout the studies for this thesis. Reports by others provide evidence for the nature of the post-translational modification (PTM) that may account for these higher molecular weight species of SIM2, namely Okui *et al* (2005) reported the poly-ubiquitination of transiently expressed SIM2 in human embryonic kidney 293 cells, and treatment of cells with the proteosome inhibitor MG132 prevented degradation of SIM2 [128]. Non-ubiqutinated SIM2 is the

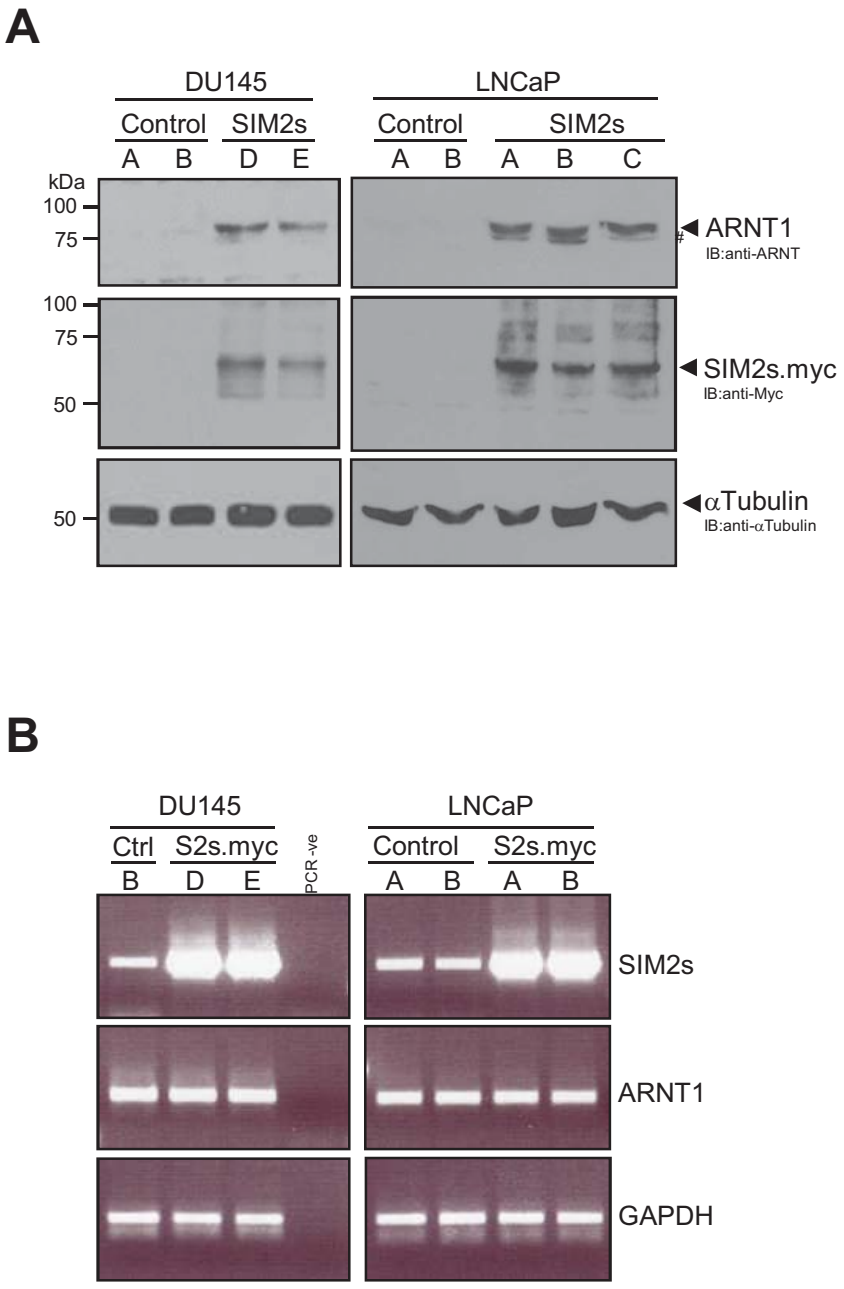

FIGURE 3.2: *(A) Stable ectopic expression of SIM2short.myc correlates with an increase in endogenous ARNT1 protein levels however, (B) ARNT1 mRNA levels remain unchanged in human prostate carcinoma DU145 and LNCaP cells across independently derived polyclonal cell lines compared to empty-vector Control (Ctrl) polyclonal cell lines.*

(A) 50µg WCE were separated by 8% SDS-PAGE followed by sequential immunoblotting of proteins as marked. # = cross reactivity of anti-ARNT (ARNT1 87kDa) mAb with ARNT2 (lower band ~75kDa). (B) Semi-quantitative RT-PCR single amplicons visualised following EtBr stained 1% agarose gel electrophoresis. Limiting cycles of PCR used: GAPDH 25x, ARNT1 25x, SIM2s 40x.

predominant species detected and the presence of modified SIM2 does not affect the ability to investigate and assess the functionality of the SIM2 isoforms as part of transcriptional complexes in cell culture based studies [48, 59][and the work of this thesis]. Consequently, further studies into alternate possible forms of PTMs of SIM2 were not persued for this thesis, and the presence or absence of detectable higher molecular weight forms of ectopically expressed SIM2 will not be discussed.

The increase in ARNT1 protein was initially observed using the commercially available mouse monoclonal anti-ARNT MA-515 antibody (from Affinity BioReagents). Two alternate independently derived rabbit polyclonal antibodies generated in our laboratory, one against the C-terminus of ARNT1, anti-ARNT1 #30 (last 34 residues), and the other to the N-terminus (residues 1-142) #51, also detected increased ARNT1 protein in DU145/SIM2s.myc cells (**Figure 3.3**). Further, siRNA oligonucleotide mediated knockdown of stable ectopic SIM2s.myc (using siSIM2s-1759 siRNA) in DU145 and LNCaP cells resulted in the reduction of ARNT1 protein (**Figure 3.4**) by western analysis compared to scrambled siRNA control treated cells, confirming that ectopic SIM2s.myc expression is indeed associated with the increase in endogenous ARNT1 protein. To assess if this observation is indicative of an endogenous function for SIM2s in these cells, puromycin resistant control DU145 cells were treated for siRNA knockdown of endogenous SIM2s using the SIM2s-specific siRNA oligonucleotide, siSIM2s-1759, which successfully knocks-down ectopic SIM2s protein (**Figure 3.4**). A clear reduction in ARNT1 protein was observed in siSIM2s-1759 treated, compared to scrambled siRNA control treated, DU145/Control cells (**Figure 3.5A**). To date, (and not for want of testing and in-house development), there are no commercially available antibodies that detect endogenous SIM2s protein by western analysis, thus detection of siRNA-mediated knockdown of endogenous SIM2s protein is unable to be assessed. However, semi-quantitative RT-PCR analysis of endogenous *SIM2s* mRNA levels in siRNA oligonucleotide treated cells from a duplicate experiment (harvested for total RNA), shows there is a decrease in *SIM2s* mRNA with siSIM2s-1759 treatment

compared to scrambled siRNA control oligonucleotide treatment (**Figure 3.5B**), which correlates to the reduction in ARNT1 protein observed (**Figure 3.5A**). Consistent with the observation that SIM2s expression has no impact on *ARNT1* mRNA levels; no change in *ARNT1* mRNA was observed with siSIM2s-1759-mediated knockdown of endogenous SIM2s in DU145/Control or LNCaP/Control cells (**Figure 3.5B**). Together these data indicate an endogenous role for SIM2s in the regulation of ARNT1 at the protein, but not message, level in DU145 cells.

The reduction in ARNT1 protein on siRNA-mediated knockdown of endogenous SIM2s in DU145 cells (**Figure 3.5A**) suggests that there is a requirement for SIM2s expression in the regulation of ARNT1 protein in these cells. This supports the observation of increased ARNT1 protein levels upon ectopic expression of SIM2s.myc in many independently derived polyclonal cell lines, and across several different carcinoma derived cells, as not being an artefact of prolonged constitutive stable expression of randomly integrated (and potentially several copies of) SIM2s cDNA(s). However, to address this latter issue more closely, human embryonic kidney 293 cells engineered to allow inducible expression of cDNA from a defined single locus, the 293Flp-TRex® cells (293F, Invitrogen), were exploited for controlled expression studies of SIM2s.myc and analysis of ARNT1 protein levels. ARNT1 protein levels were seen to increase with 12 hours of 1µg/ml doxycycline (Dox) induced expression of SIM2s.myc, and these levels remained unchanged from 18 to 24 hours of induced expression compared to un-induced (UI) controls (**Figure 3.6A**, panel i). This effect was not enhanced by increased Dox concentration to 5ug/ml, nor longer SIM2s.myc induction times of up to 48h (**Figure 3.6B**, panel i). These data further support the emerging model of a close association between SIM2s expression and the regulation of ARNT1 protein levels from these studies.

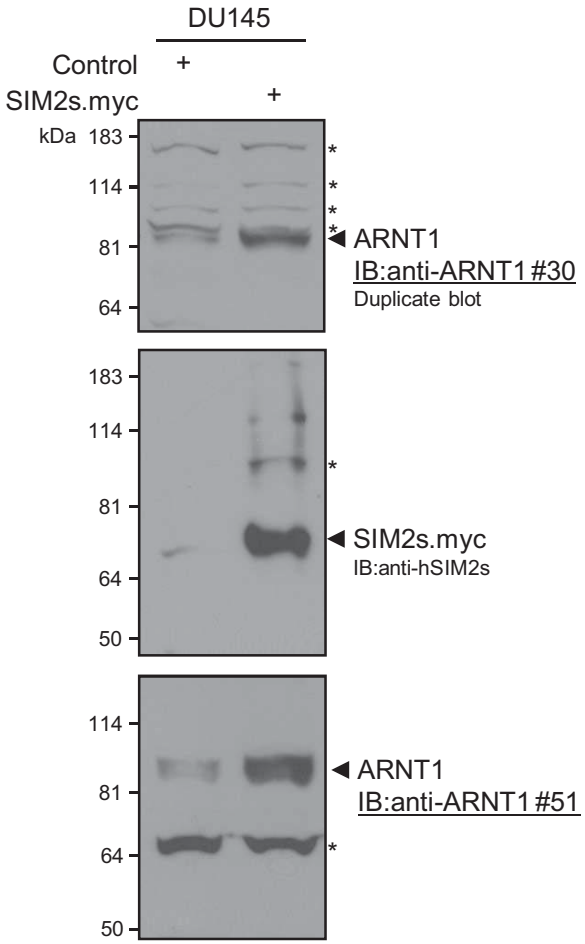

FIGURE 3.3: *Increased endogenous ARNT1 (87kDa) protein levels upon stable SIM2s.myc expression is also detectable by independent rabbit polyclonal antibodies directed against the last 34 C-terminal amino acids and the N-terminal first 142 amino acids of human ARNT1, anti-ARNT1 #30 & #51 respectively, in human prostate DU145 carcinoma polyclonal cell lines.*

70µg whole cell extract were separated by 8% SDS-PAGE in duplicate, followed by immunoblot detection of proteins as indicated. * = non-specific background bands.

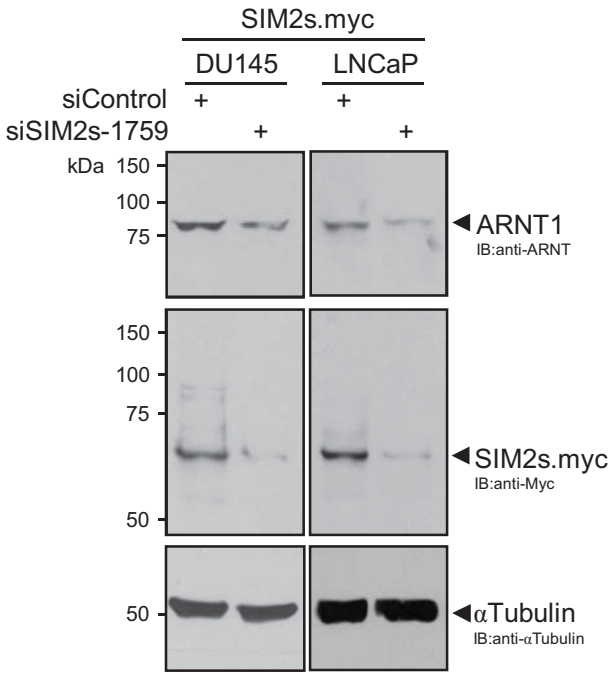

FIGURE 3.4: *Endogenous ARNT1 protein levels decrease on siRNA knockdown of ectopic SIM2s.myc in prostate carcinoma DU145 and LNCaP cells.*

Cells were treated 2x100nM siRNA, 24hrs apart, total treatment time 72hrs before cells were harvested for either WCE or total RNA. 50µg WCE were separated by 8% SDS-PAGE and subjected to sequential immunoblot analysis for proteins as marked. Representative of minimum n=2-3 each cell line.

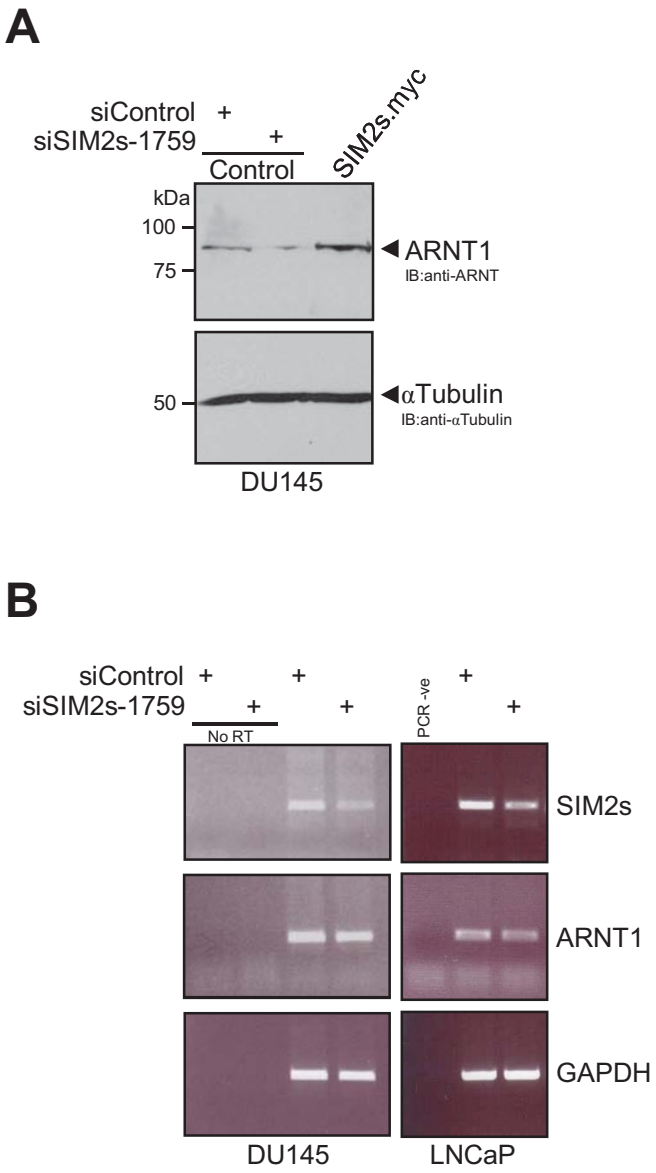

FIGURE 3.5: *(A) Endogenous ARNT1 protein levels decrease upon siRNA knockdown of endogenous SIM2s, however, (B) ARNT1 mRNA levels remain unchanged in prostate carcinoma DU145 and LNCaP cells.*

Cells were treated 2x100nM siRNA, 24hrs apart, total treatment time 72hrs before cells were harvested for either WCE or total RNA for cDNA synthesis from duplicate experiments. (A) 50µg WCE were separated by 8% SDS-PAGE and subjected to sequential immunoblot analysis for proteins as marked. Representative n=2. (B) RT-PCR analysis of independent experiments. Note: *GAPDH* and *ARNT1* mRNA detected with limiting 25x cycles of PCR, however, 33x used for detection of *SIM2s* mRNA.

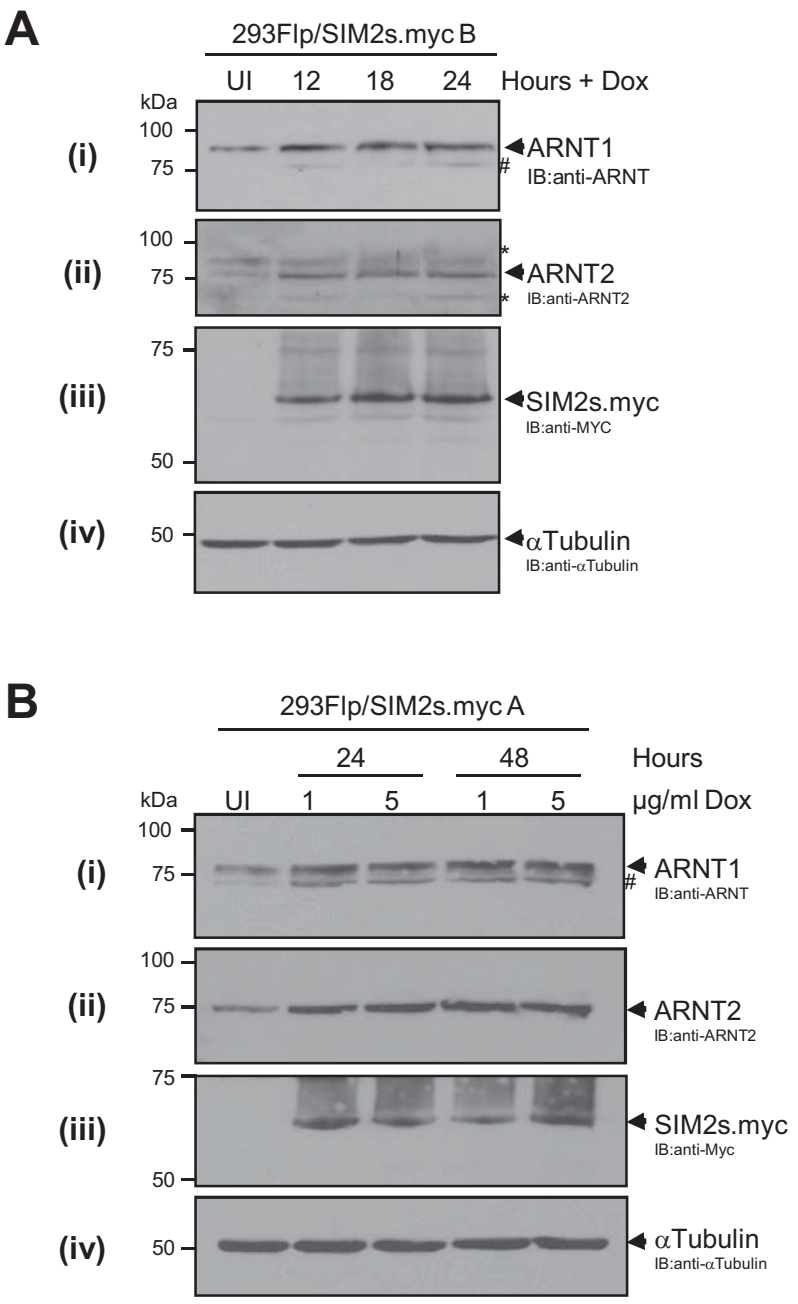

FIGURE 3.6: *ARNT1 and ARNT2 protein levels increase upon induction of SIM2s.myc in 293Flp-TRex® cells after (A) 12h of 1ug/ml Doxcycline (Dox) induced expression of SIM2s.myc, and (B) is not further enhanced by increased Dox treatment or prolonged expression of SIM2s.myc.*

Subconfluent cells were treated with 1 or 5ug/ml Dox for the hours indicated. WCE were then made and 50µg separated by 8% SDS-PAGE, followed by sequential immunoblot detection of proteins as indicated, panel sets i, ii, iii, iv. UI = uninduced. # = cross-reactivity of anti-ARNT with ARNT2 (75kDa). * = non-specific background bands.

In summary, these data show for the first time that SIM2s expression closely correlates to the regulation of ARNT1 protein levels, specifically that SIM2s expression appears to be required for the post-transcriptional mechanism(s) that results in the increased ARNT1 protein.

3.2.2 Increase in ARNT1 and ARNT2 protein levels upon stable SIM2s.myc expression in human carcinoma, and mouse fibroblast, derived cell lines

SIM2s expression being implicated in the regulation of ARNT1 protein levels described here is the first report of a class I bHLH-PAS family member being involved in protein regulation of a class II family member. Where the identification of increased ARNT1 protein (~87kDa) was detected using the anti-ARNT MA-515 mAb, curiously, a faint lower band at ~75kDa was also sometimes observed with immunoblot analysis of ARNT1 in LNCaP and 293F whole cell extracts (**Figures 3.2A, & 3.6**, panels sets i, respectively, marked with a # symbol). This monoclonal antibody was generated against a peptide corresponding to the C-terminal 34 amino acids of the human ARNT1 transactivation domain. Bioinformatic sequence analyses reveals that this region shares high amino acid sequence similarity (61.7%) to the ARNT1 homologue, ARNT2 (**Figure. 3.7**), thus it is possible, however previously unreported, that ARNT2 is detectable using this antibody. As Arnt2 has a calculated MW of ~75kDa, it may indeed be the fainter band sometimes observed below ARNT1 (~87kDa) following SDS-PAGE separation of protein extracts and immunoblot analyses. Interestingly, these indications of ARNT2 protein were observed to be enhanced where SIM2s was ectopically expressed, thus the potential up-regulation in ARNT2 protein levels upon SIM2s ectopic expression was assessed using an ARNT2 specific rabbit polyclonal antibody. An increase in ARNT2 protein was confirmed in 293F/SIM2s.myc upon Dox induction of SIM2s.myc expression (**Figure 3.6**, panel sets ii). ARNT2 protein levels were also specifically assessed in LNCaP/SIM2s.myc and DU145/SIM2s.myc cell lines, and enhanced ARNT2 protein observed compared to respective puromycin-resistant control cell

lines (**Figure 3.8A**) along with ARNT1. Increased ARNT1 protein was also found in a third prostate carcinoma PC3AR+ cell line upon stable ectopic expression of SIM2s.myc, however, ARNT2 protein was not detected (**Figure 3.8A**). RT-PCR analysis of *ARNT2* mRNA in PC3AR+ cells revealed that *ARNT2* is not expressed in the cells (**Figure 3.9A**).

The correlation between ARNT1 and ARNT2 (collectively referred to as ARNT hereafter) regulation and SIM2s has been observed in both human prostate and kidney derived cell lines, indicating that the mechanism(s) of this association may be indicative of a general function of SIM2s, and not restricted to prostate carcinoma derived cells lines. To further support this notion, ARNT levels in human pancreatic carcinoma derived cell lines, PANC-1, CFPAC, and HPAC, with or without stable ectopic expression of SIM2s, were analysed. Consistent with that observed in prostate carcinoma and embryonic kidney 293F cells, both ARNT1 and ARNT2 protein levels were elevated in SIM2s.myc expressing pancreatic carcinoma cell lines (**Figure 3.8B**). Indeed, stable ectopic expression of human SIM2s.myc in mouse fibroblast NIH3T3 cells also resulted in an increase in endogenous Arnt1 and Arnt2 protein levels (**Figure 3.8C**).

3.2.3 *ARNT2* may be a novel direct target of SIM2s transcription

Consistent with that observed previously in prostate carcinoma cell lines, semi-quantitative RT-PCR analysis of CFPAC and PANC-1 SIM2s.myc over-expressing cell lines showed no change in *ARNT1* mRNA levels (**Figure 3.9A**), further indicating that the increase in ARNT1 protein observed in these cells upon SIM2s.myc expression is perhaps a general a post-transcriptional phenomena. Surprisingly, however, semi-quantitative RT-PCR assessment of *ARNT2* mRNA in prostate DU145 and LNCaP, and pancreatic CFPAC, cells with stable expression of SIM2s revealed up-regulation of *ARNT2* message (**Figure 3.9A**). A quantitative assessment of *ARNT2* mRNA levels following siSIM2s-2a-mediated knockdown of endogenous

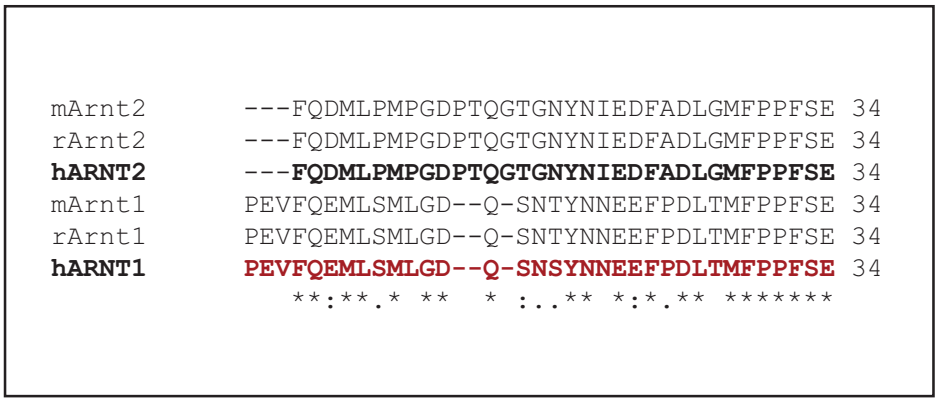

FIGURE 3.7: *C-terminal 34 amino acids of the hARNT1 transactivation domain (TAD) used for the generation of the mouse monoclonal anti-ARNT MA-515 antibody (Affinity BioReagents) in red, and shared amino acid homology of the TAD of ARNT1 and ARNT2 orthologues in human, mouse and rat.*

Bioinformatic clustalW alignments showing overall shared homology between human, mouse and rat orthologues. 21/34 amino acids (61.7%) in hARNT1 (in bold) share exact homology with hARNT2 (also in bold). Accession numbers used for alignments: hA1 = NM_001668; hA2 = NM_014862; mA1 = NM_001037737; mA2 = NM_007488; rA1= NM_012780; rA2 = NM_012781. References: Hirose et al (1996) Mol. & Cell Biol. 16(4):1706-1 and Drutel et al (1996) Biochem. Biophys. Res. Comm. 225; 333-339.

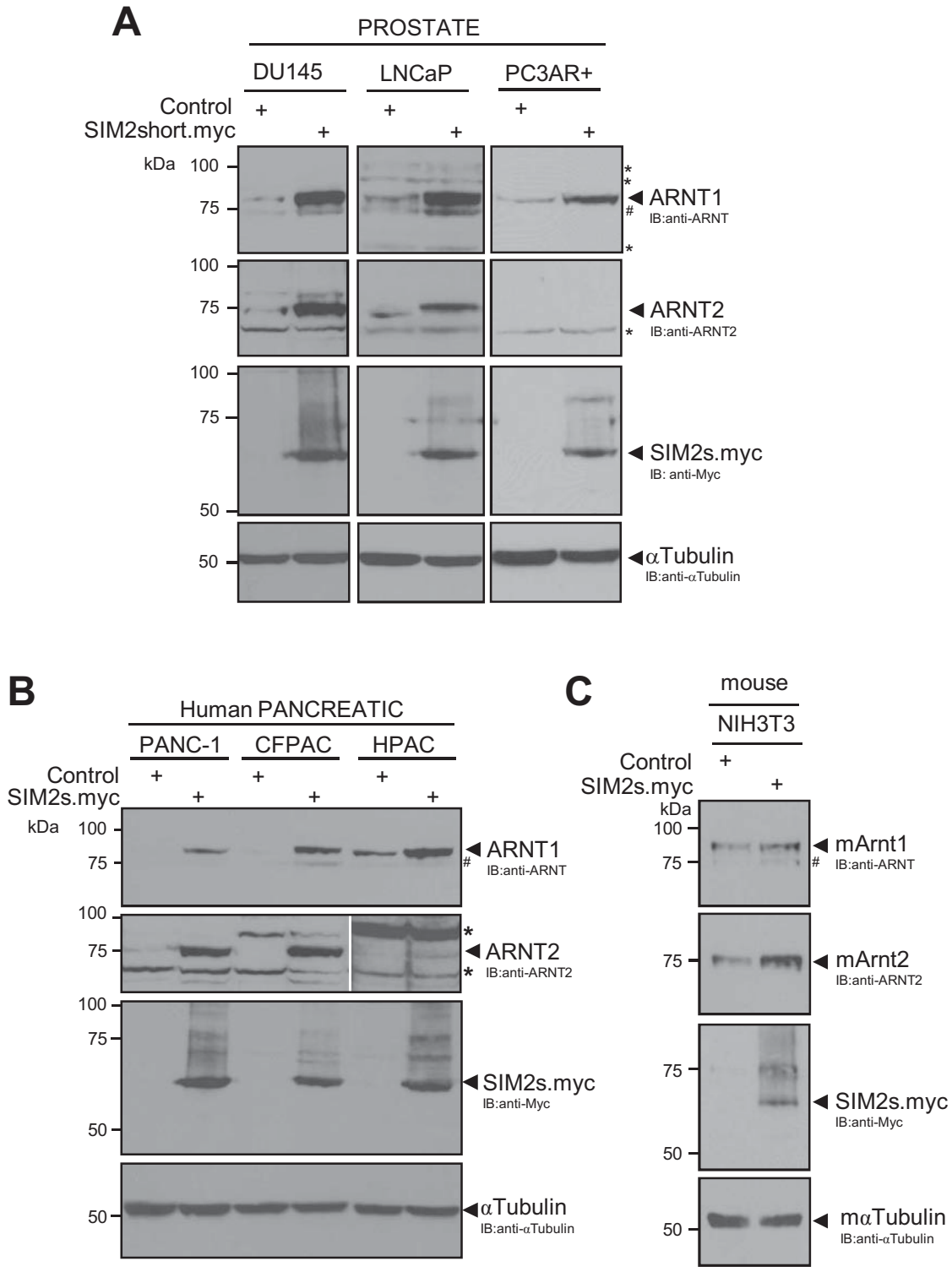

FIGURE 3.8: *Increase in endogenous protein levels of both ARNT1 and ARNT2 are observed in human (A) prostate DU145, LNCaP, and (B) pancreatic PANC-1, CFPAC & HPAC carcinoma, and (C) mouse NIH3T3 fibroblast, derived cell lines upon stable ectopic expression of human SIM2s.myc (myc tagged). Note: ARNT2 is not expressed in prostate carcinoma PC3AR+ cells, thus only an increase in ARNT1 is observed with ectopic SIM2s.myc expression (A).*

Whole cell extracts from human (50µg) and mouse (35 µg) cells were separated by 8% SDS-PAGE followed by sequential immunoblot of proteins as marked. # = cross reactivity of anti-ARNT (ARNT1 87kDa) antibody to ARNT2 (75kDa).. * = non-specific background bands. Representative of minimum two independent analyses of each cell line.

SIM2s in human prostate carcinoma DU145 cells (n=3) strongly suggests that SIM2s may play an endogenous role in regulation of *ARNT2* mRNA expression levels (**Figure 3.9B**). This was supported by data obtained in a preliminary study of the effects of siSIM2s-1759-mediated knockdown of endogenous SIM2s in LNCaP human prostate cancer cells (**Figure 3.9C**). These findings indicate that the increase in ARNT2 protein observed in relation to SIM2s expression arises from an alternate mechanism(s) to that for ARNT1 as the increase in translated product in DU145, LNCaP and CFPAC cells is likely due to increased *ARNT2* mRNA levels in SIM2s.myc expressing cells.

There are no reports of *ARNT2* regulation. Here, endogenous ARNT2 expression levels were shown to be intimately linked to endogenous SIM2s levels in DU145 cells (**Figure 3.9B**), suggesting a requirement for SIM2s expression in the regulation of *ARNT2* mRNA levels. Interestingly, expression studies in rodents further support the notion that Sim2 is up-stream of Arnt2 regulation. There is a distinctive pattern of overlapping expression of Sim2 and Arnt2 in the kidney of adult rodents [34, 109-111]. *In situ* expression studies in developing mouse kidney indicate that *Sim2* expression, first detected at E10.5 and in tubules by E12.5 [25], precedes that of *Arnt2*, for which the earliest reports are at E13 [111] and in the tubules by E15.5 [110]. Thus, *Sim2* expression appears to be upstream of *Arnt2* gene expression in the developing kidney, and may be indicative of the endogenous temporal requirement of Sim2 expression for subsequent expression and regulation of Arnt2. Whether SIM2 expression is required to mediate direct transcriptional regulation of ARNT2 was investigated next. The presence of putative SIM2/ARNT binding sites in the regulatory region of ARNT2 (**Figure 3.10A**) highlights the possibility that SIM2 may, via binding these sites, control direct transcriptional regulation of *ARNT2*.

Bioinformatic searches of 10kb 5' and 12kb 3' from the start of the first exon of *ARNT2* in human and mouse identified several potential binding sites for SIM2s/ARNT transcriptional activities (**Figure 3.10A**). These

sites contain the core 5'-ACGTG-3' found in recently identified SIM2 target genes during the course of these studies, as discussed in **Chapter 1** and **Chapter 5**, and sites found to be SIM2 responsive in synthetic promoters, including the classical CME (central midline element) 5'-TACGTG-3', the canonical palindromic E-box (and HRE) 5'-CACGTG-3' (refer to **Chapter 5**), and the novel SIM2 Response Element (S2RE) 5'-AACGTG-3' [9, 41, 48, 59] (**Figure 3.10A**). These are all possible sites through which SIM2s/ARNT may regulate *ARNT2* expression. Few identical sites are conserved in a positional manner between mouse and human promoters however, there is the striking conservation of a S2RE and E-box, clustered within 400-600bp of each other in the regions around 9-10kb, and 7-8kb, respectively, 5' of the first exon (**Figure 3.10**A, marked with a δ symbol), and in the human promoter, these two sites actually includes an overlapping CME/E-box (5'-GTGCACGTA-3') and is also associated with another palindromic E-box 550bp downstream. These sites are labelled 1, 2, and 3 in **Figure 3.10A**. Similarly, postionally conserved sequences containing the core 5'-ACGTG-3' were also found a little over 2kb upstream of the start of exon 1 in both the mouse and human *ARNT2* promoters (**Figure 3.10A**, marked with a # symbol, and termed site 4 in human promoter). Furthermore, two S2REs are also clustered within 1kb of each other inside the first intron (**Figure 3.10**, marked with an asterix). To directly assess if SIM2s may be regulating the expression of human *ARNT2* via transcriptional activities at the promoter, possible SIM2s DNA-binding at the putative promoter sites 1-4 was examined by chromatin immunoprecipitation (ChIP) from human prostate DU145/SIM2s.myc cells. Although subtle, SIM2s was found at the palindromic E-box site 4 (**Figure 3.10B**, compare lane 3 to control lane 2), but not at the further upstream identical E-box sequences at site 3 or at site 2, nor was there any indication of SIM2s associated with the DNA at the S2RE (site 1) (**Figure 3.10B**) (representative of n=2 independent experiments). These data indicate that SIM2s-mediated regulation of ARNT2 protein levels may indeed be at the level of transcription, as found here in DU145 cells, where *ARNT2* mRNA levels are intimately linked with SIM2s expression. Further studies are required to confirm if *ARNT2* is indeed a direct target of SIM2s transcription, and moreover another example of SIM2s capability

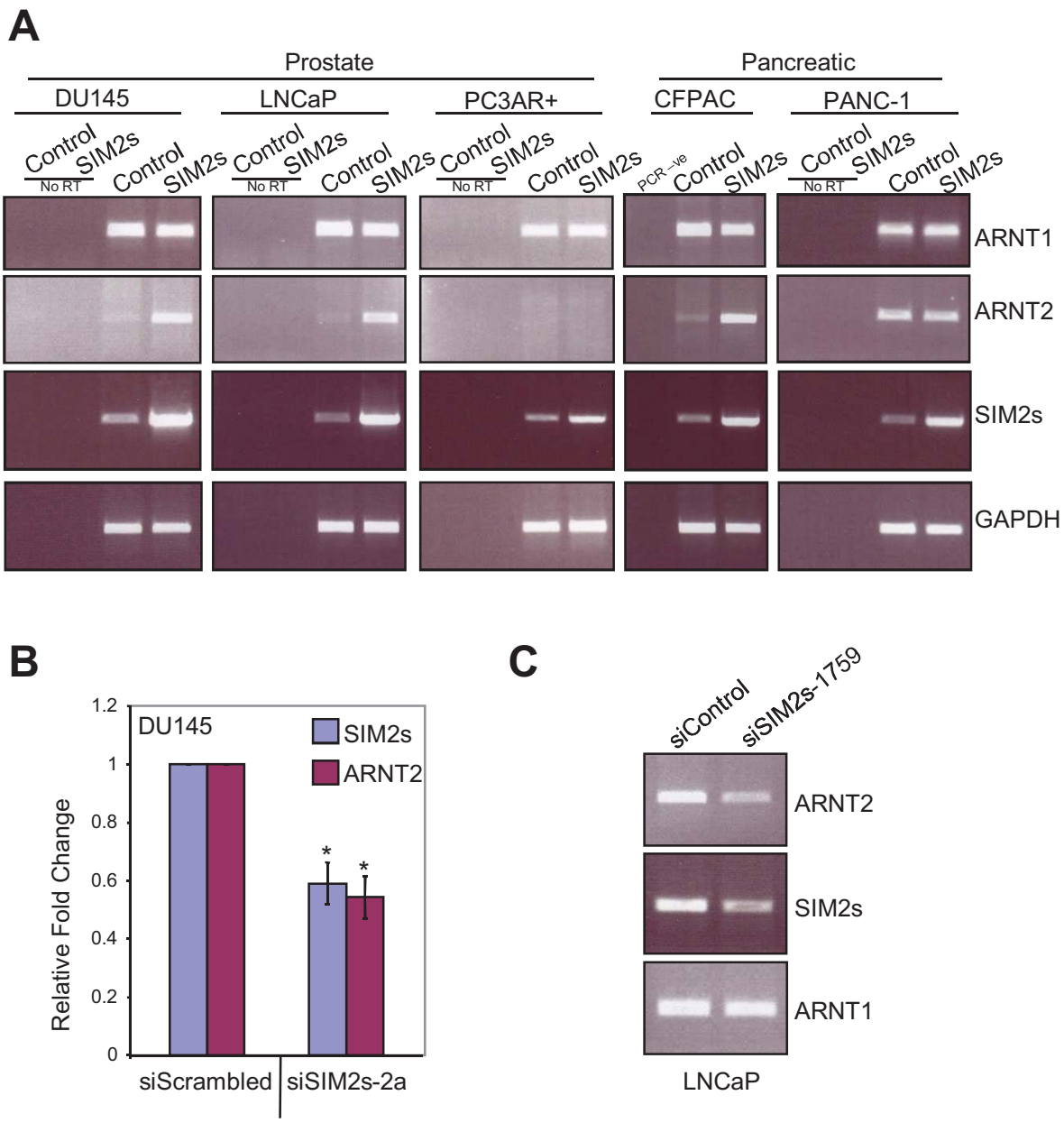

FIGURE 3.9: *ARNT2 is a putative target of SIM2s-mediated mechanisms of regulation. (A) Where endogenous ARNT1 mRNA levels remain unchanged in prostate and pancreatic carcinoma cell lines upon stable ectopic expression of SIM2s.myc compared to control, endogenous ARNT2 mRNA levels increase in DU145, LNCaP and CFPAC cells. (B and C) Endogenous ARNT2 mRNA levels are reduced concomitant with siRNA-mediated knockdown of endogenous SIM2s in prostate carcinoma LNCaP and DU145 cells.*

(A) Semi-quantitative RT-PCR; limiting PCR cycles used as follows for each primer set: GAPDH 25x, SIM2s 35x, except DU145 40x, ARNT1 25x, except PANC-1 using 30x; ARNT2 30x, except PANC-1 38x and CFPAC 35x. ARNT2 is not expressed in PC3AR+ cells, 40x PCR cycles used. Control represents IRESpuro-empty vector Control derived cell lines, except for CFPAC where the parent cell line was used. (B) Quantitative-PCR assessment of the fold-change in *ARNT2* or *SIM2s* mRNA levels following induced expression of siSIM2s-2a in DU145 cells for 72hrs. n=3 independent experiments. Error bars SEM. Unpaired, two-tailed Students T-Test used. Significance * $P \leq 0.029$. (C) siRNA mediated knockdown in LNCaP cells: 2x100nM siRNA oligonucleotide transfections 24h apart, total RNA harvested 72h after first treatment. sqRT-PCR, cycles; ARNT1 25x, ARNT2 35x, SIM2s 33x. Single amplicons of expected size identified following 1% EtBr stained agarose gel electrophoresis. Representative preliminary experiment only.

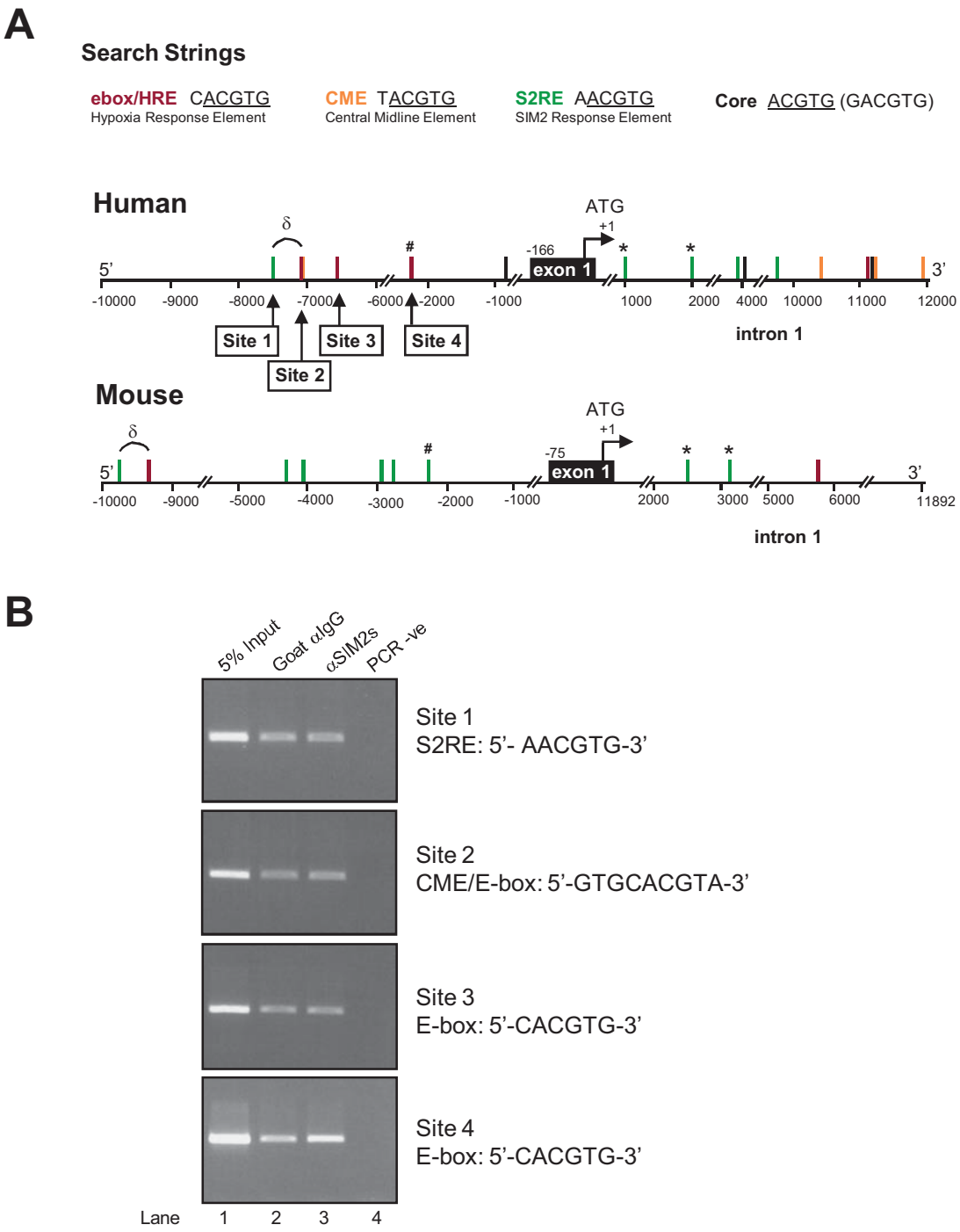

FIGURE 3.10: *Is the human ARNT2 gene a direct target of SIM2s transcriptional activities? ChIP studies indicate DNA binding of SIM2s at the canonical E-Box 5'-CACGTG-3' approximately 2kb downstream of the start of the hARNT2 gene, but not at other identified putative binding sites, including identical E-box sequences, further upstream.*

(A) Bioinformatic search for putative sites for SIM2/ARNT binding 10kb upstream, and ~12kb into the first intron, of the gene ARNT2, in human and mouse. Genomic DNA sequences were obtained following human and mouse BLAT analyses of ARNT2, accession numbers: NM_014862 and NM_007488, respectively. [human/mouseBLAT online software: http://genome.ucsc.edu/cgi-bin/hgBlat]. Genomic sequences were then searched using online software TESS [Transcription Element Search System: http://www.cbil.upenn.edu/cgi-bin/tess/tess] for potential sites for SIM2/ARNT heterodimer binding. Search strings used, and identified positions are indicated, as are genomic DNA 1000bp intervals to and from the ATG translation start site (+1) in exon 1. Start of exon 1 indicated. δ = Conserved sequences similarly clustered close together. # = Sites conserved in a positional manner containing core 5'-ACGTG-3'. Putative sites 1 to 4 for ChIP analysis indicated. (B) PCR analysis of ChIP of SIM2s of binding activities on the human *ARNT2* promoter from human prostate DU145/SIM2s.myc cells. Representative n=2.

to mediated transactivation of gene expression as found for the regulation of *Myom2* [48]. This study also raises interesting questions regarding binding site recognition and specificity of SIM2s, as particular to this context it remains to be determined why SIM2s appears to show a preference for one of three identical binding sequences.

The presence of conserved canonical E-box sequences highlights the possibility that ARNT (1 and 2) homodimers, enriched due to increased protein levels upon SIM2s.myc expression, may have the capacity to also regulate *ARNT2* transcription through this site as a downstream effect of SIM2s expression, perhaps incojunction with, and/or interacting with, SIM2s/ARNT on the DNA. *In vitro* DNA binding studies of the bHLH-PAS factors performed in 1995 by Swanson and colleagues identified that ARNT homodimers prefer this canonical sequence 80% of time, however they have also been shown to bind the 5'-AACGTG-3' sequence [the sequence of the endogenous *Myom2* S2RE] the other 20% [129]. Thus the S2REs also identified in the *ARNT2* regulatory region could theoretically function as a site for ARNT homodimer DNA-binding. However, there are no reports to date of ARNT-self regulation. Moreover, co-immunoprecipitation experiments from DU145/SIM2s.myc and LNCaP/SIM2s.myc cells, where *ARNT2* mRNA is found to be increased, reveal that endogenous ARNT1 and ARNT2 protein, although in slight excess to SIM2s.myc in DU145 cells, predominantly co-immunoprecipitate with SIM2s.myc (**Figure 3.11**), thus formation of ARNT/ARNT homodimers is not evident in these cells. Hence, considered together, these observations suggest that any possible changes in *ARNT2* transcription that may arise from bHLH-PAS dimer DNA-binding activities would more likely arise from those of SIM2s/ARNT, than ARNT/ARNT on the *ARNT2* regulatory region.

In summary, the increase in ARNT protein levels upon ectopic expression of human SIM2s found across a number of different tissue-derived human and mouse cell lines indicates a general, and not cell type

specific, mechanism(s) of ARNT regulation that occurs as a function of SIM2s expression. Specifically, the increase in ARNT1 protein level appears to arise from a post-transcriptional mechanism(s) of enhanced stabilisation that requires SIM2s expression, whereas multiple, and perhaps not mutually exclusive, mechanisms for the direct regulation of *ARNT2* gene expression and regulation of protein levels appear to occur upon SIM2s expression.

3.2.4 Regulation of ARNT levels is specific to mammalian homologues of SIM, and not other bHLH/PAS family members, AhR and HIF1α

The long and short isoforms of SIM2 share high amino acid identity in their bHLH-PAS DNA-binding and ARNT dimerisation domains [38], thus the possibility exists that the two isoforms may perform similar, if not in certain contexts the same, functional roles. Consequently, the effect of human SIM2L expression on ARNT protein levels was also assessed in human prostate PC3AR+, DU145 and LNCaP cell lines. ARNT1 protein was also found to be highly increased upon stable expression of SIM2L.myc compared to controls (**Figure 3.12A**), and like that observed upon SIM2s expression, *ARNT1* mRNA levels remained unchanged upon SIM2L.myc expression in DU145 cells by semi-quantitative RT-PCR analyses (**Figure 3.12B**). ARNT2 protein levels were also observed to be dramatically enhanced in DU145 and LNCaP cells upon stable expression of SIM2L.myc, but not in PC3AR+ cells where ARNT2 is not found to be expressed (**Figures 3.8, 3.9,** & **3.12A**). Preliminary semi-quantitative and quantitative-real-time RT-PCR analysis also shows increased *ARNT2* mRNA levels upon SIM2L.myc expression in DU145 cells, like that seen previously in several SIM2s stable cell lines, compared to control cells (**Figures 3.12B & C**). Taken together, these data indicate that the long isoform of SIM2 may play a similar role, if not the same, as SIM2s, in the regulation of ARNT levels. The murine homologue to SIM2L (mSim2L), which shares overall 89.6% amino acid identity to human SIM2L [38], also showed an increase in endogenous ARNT1 protein

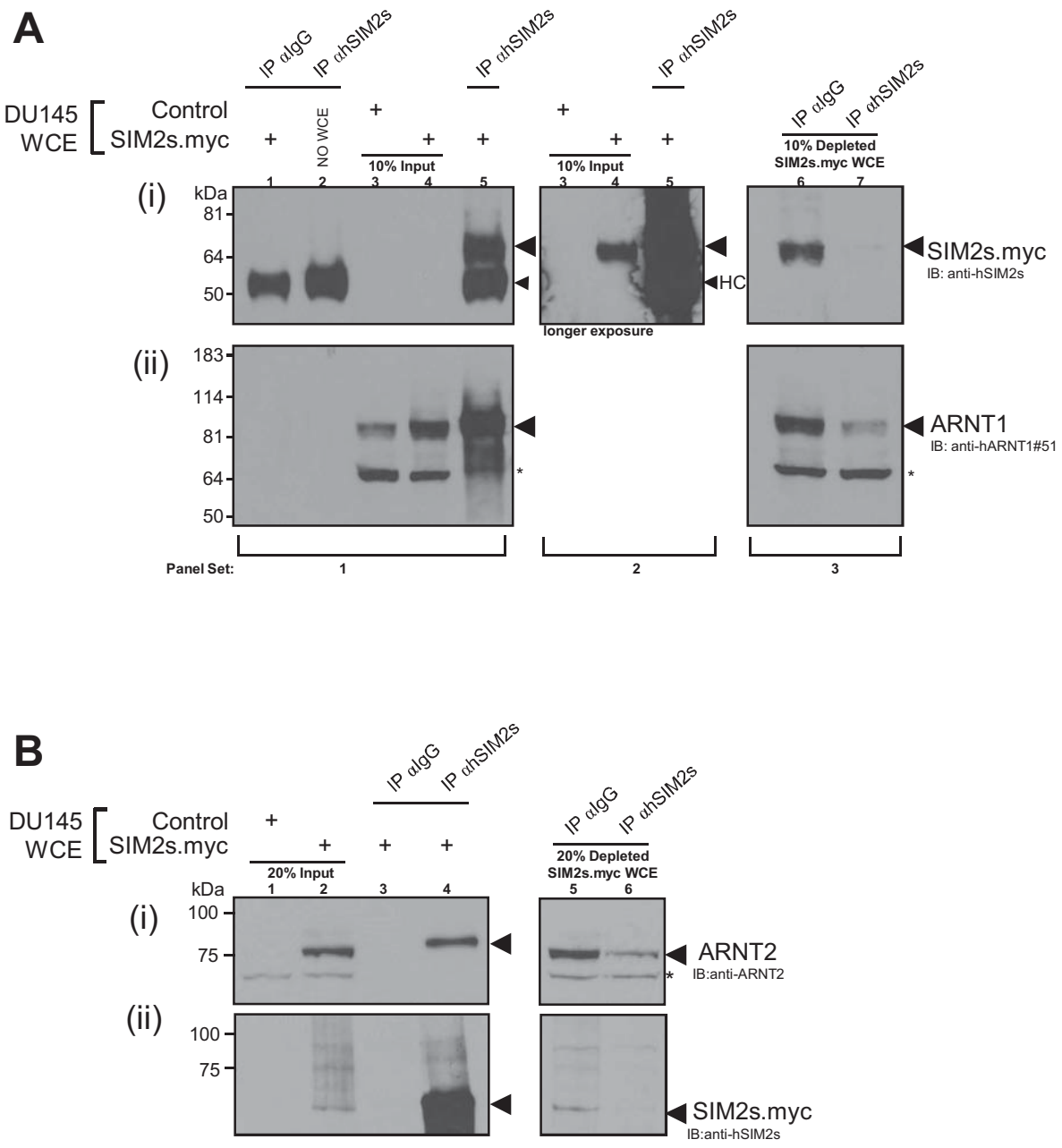

FIGURE 3.11: *Ectopic SIM2s.myc co-immunoprecipitates both endogenous partner factors ARNT1 and ARNT2, in human prostate DU145 (A & B), where they are in excess, and in LNCaP (C) cells.*

50µg of whole cell extract (WCE) representing 10 or 20% 'input' were separated by 8% SDS-PAGE with 10 or 20% 'depleted' supernatant and samples from immunoprecipitation of SIM2s from 0.5 or 0.25mg of DU145/SIM2s.myc and LNCaP/SIM2s.myc whole cell extracts using anti-hSIM2s antibody, compared to isotype IgG antibody, or no whole cell extract, immunoprecipitation controls. Immunoblot detection of proteins as indicated. (A) Immunoprecipitated SIM2s.myc shown in lane 5 [(i) panel set 1] above IgG HC. Longer exposure of anti-hSIM2s immunoblot lanes 3-5 [(i) panel set 2] shows 10% input levels of SIM2s.myc (lane 4). ARNT1 and ARNT2 levels remain in excess following immunodepletion of SIM2s.myc from DU145/SIM2s.myc WCE, (A) compare lanes 6 & 7, panel set 3, and (B) compare lanes 5 & 6, respectively. HC = heavy chain; * = non-specific background band. Representative n=2.

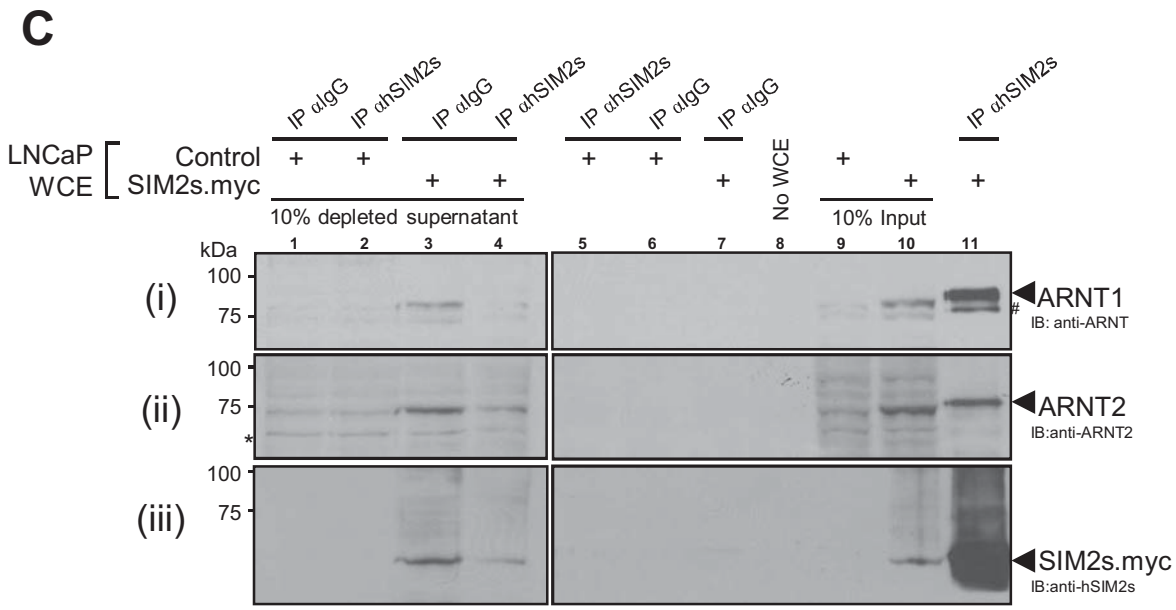

FIGURE 3.11 continued: *Ectopic SIM2s.myc co-immunoprecipitates both endogenous partner factors ARNT1 and ARNT2, in human prostate DU145 (A & B), where they are in excess, and in LNCaP (C) cells.*

(C) Ectopic SIM2s.myc co-immunoprecipitates with both endogenous ARNT1 and ARNT2 in LNCaP cells (lane 11), however, analysis of depleted supernatant (compare lanes 3 & 4)does not indicate if the partner factor is in excess to SIM2s.myc, or not. # = ARNT2 protein detection due to anti-ARNT antibody cross-reactivity. Representative n=2.

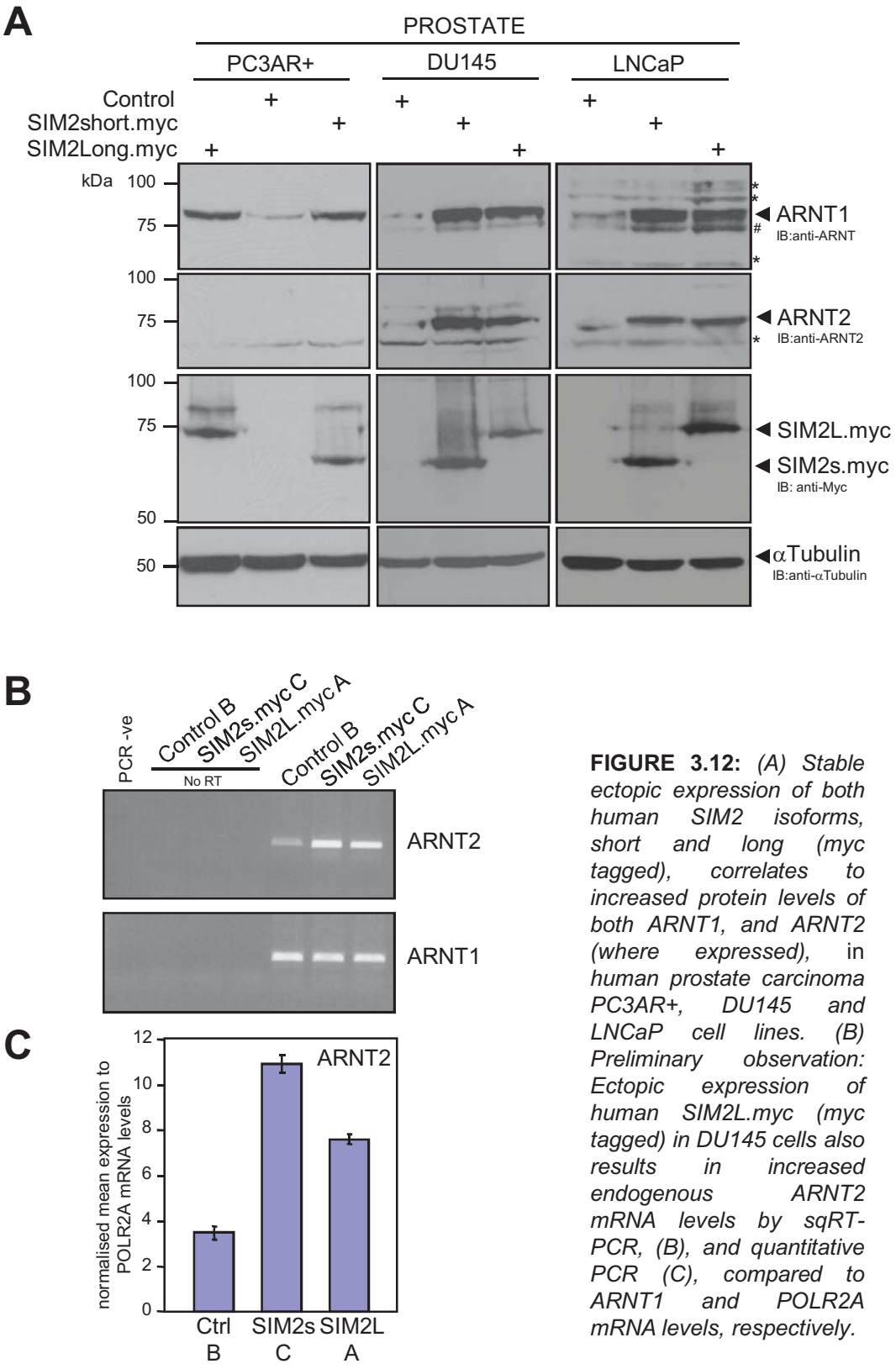

FIGURE 3.12: *(A) Stable ectopic expression of both human SIM2 isoforms, short and long (myc tagged), correlates to increased protein levels of both ARNT1, and ARNT2 (where expressed),* in *human prostate carcinoma PC3AR+, DU145 and LNCaP cell lines. (B) Preliminary observation: Ectopic expression of human SIM2L.myc (myc tagged) in DU145 cells also results in increased endogenous ARNT2 mRNA levels by sqRT-PCR, (B), and quantitative PCR (C), compared to ARNT1 and POLR2A mRNA levels, respectively.*

(A) 50µg of whole cell extract was separated by 8% SDS-PAGE followed by sequential immunoblots of proteins as marked. # = cross reactivity of anti-ARNT antibody to ARNT2 (75kDa). * = non-specific background bands. Representative of n=3 independent experiments for each cell line. Note: data shown here in (A), previously shown in part in figure 3.5.A. (B & C) Preliminary observation. cDNA synthesised from total RNA, and then subjected to semi-quantitative (B), and quantitative (C), RT-PCR, normalised to ARNT1 and POLR2a mRNA levels, respectively. Error bars, SEM of three replicate reactions.

levels in initial analyses of human prostate LNCaP cells stably expressing ectopic C-terminal myc-tagged mouse Sim2L (**Figure 3.13**). Interestingly, when the mouse Sim2 homologue, mSim1, which shares 89.4% amino acid identity in the N-terminal DNA binding and PAS domains and only 15.3% in the carboxy-regions [38], was stably over-expressed in LNCaP cells, an increase in endogenous ARNT1 protein was also observed in two independently derived polyclonal cell lines, compared to puromycin resistant controls (**Figure 3.13**). Immunoblot detection of ARNT1 in the LNCaP/mSim1.myc cells also indicates an increase in ARNT2 protein levels (~75kDa species, just below ARNT1 at ~87kD, **Figure 3.13**) due to the cross-reactivity of the anti-ARNT MA-515 antibody as discussed in section **3.2.1**, indicating that like SIM2, mSim1 may also play a role in the regulation of ARNT2 protein levels in these cells. Together this indicates that the regulation of ARNT levels may be a general function of both mammalian SIM homologues, by as yet undefined mechanisms.

Thus far the regulation of ARNT1 protein levels appears to be specific to SIM bHLH-PAS family members as there is an absence of any previous reports of a class I bHLH-PAS family member affecting the regulation of the class II bHLH-PAS family members, and common partner factors, ARNT1 and ARNT2. To analyse this more directly, 293F cells engineered for inducible expression of C-terminal myc epitope tagged human SIM2s, SIM2L, SIM1, and untagged Arylhydrocarbon Receptor (AhR) and Hypoxia Inducible Factor 1α (HIF1α) were used to assess and compare ARNT1 protein levels upon expression of these class I family members. As SIM2 is nuclear, due a nuclear localisation signal (NLS) sequence [59, 60], SIM2-mediated ARNT1 regulation is likely to be occurring through SIM2 activities in the nucleus, including potential DNA binding activities. With this in mind, 293F cells for ectopic AhR expression were co-treated with AhR activating ligand, YH439 [130], to allow for nuclear localisation of ectopic AhR, and potential DNA binding activities (**Figure 3.14B**) for the duration of the induced expression [1ug/ml doxycline (Dox) for 18.5 hours]. HIF1α is stabilised and translocates to the nucleus in hypoxic growth conditions [5, 123], thus to ensure

stabilisation of induced ectopic HIF1α and optimal activity, 293F/HIF1α cells were grown in hypoxic conditions (<1% O_2) for the duration of induced expression (**Figure 3.14C**). 293F cells engineered for induced expression of the human homologues of SIM were treated with 1ug/ml Dox for 18.5 hours and cultured in normal growth conditions (**Figure 3.14A**). Analysis of whole cell extracts showed the anticipated increase in ARNT1 protein levels upon induced expression of all three human SIM homologues, however strikingly, no change in ARNT1 protein levels upon induced ectopic expression of AhR and HIF1α, co-treated in their respective manners to optimise function (**Figure 3.14**). Thus consistent with the lack of any previous report of enhanced ARNT1 protein levels upon hypoxic induction of HIF1α, or associated with active AhR, endogenous ARNT1 protein levels did not increase upon induced expression and nuclear localisation (activation) of HIF1α and AhR as they did upon induction of SIM2 and SIM1 in these cells (**Figure 3.14**), supporting the emerging model of SIM-specific regulation of ARNT1.

3.2.5 Investigating post-transcriptional mechanisms of SIM2s-mediated increase of ARNT1 and ARNT2 proteins

Thus far these studies have indicated that SIM2-dependent increases in ARNT1 protein appear to arise from a post-transcriptional mechanism, as mRNA levels remain unchanged (refer **sections 3.2.1-3**).

Modes of regulation, that do not include increased transcription or mRNA stability, that may account for the elevated levels of ARNT1 and ARNT2 protein include enhanced translation and post-translational mechanisms of enhanced protein stability. To gain some insight into which of these mechanisms at the translation and post-translation level may account for SIM2s-dependent elevated ARNT protein levels, human prostate DU145 cells, with and without stable ectopic expression of SIM2s.myc were treated with the translation inhibitor cycloheximide (CHX). Chemiluminescent western blot analysis, and subsequent densitometric quantification from independent experiments (n=2-3), revealed a half-life ($t_{1/2}$) of

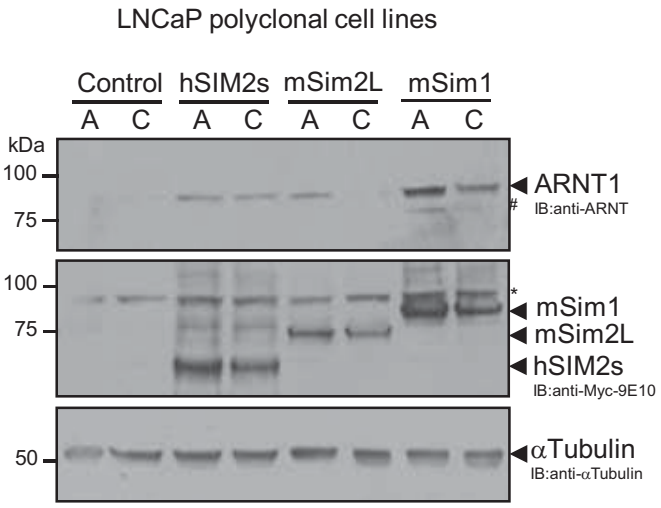

FIGURE 3.13: *(B) Like human SIM2s, stable ectopic expression of murine SIM2Long and SIM1 (myc tagged) homologues also correlates to an increase in endogenous ARNT1 protein levels, compared to puromycin resistant empty-vector controls, in independently derived polyclonal cell lines (labelled A & C for each empty-vector Control & SIM stable expression construct) of prostate carcinoma LNCaP cells.*

60µg of whole cell extract was separated by 8% SDS-PAGE, followed by sequential immunoblot analysis of proteins as marked. * = non-specific background band.

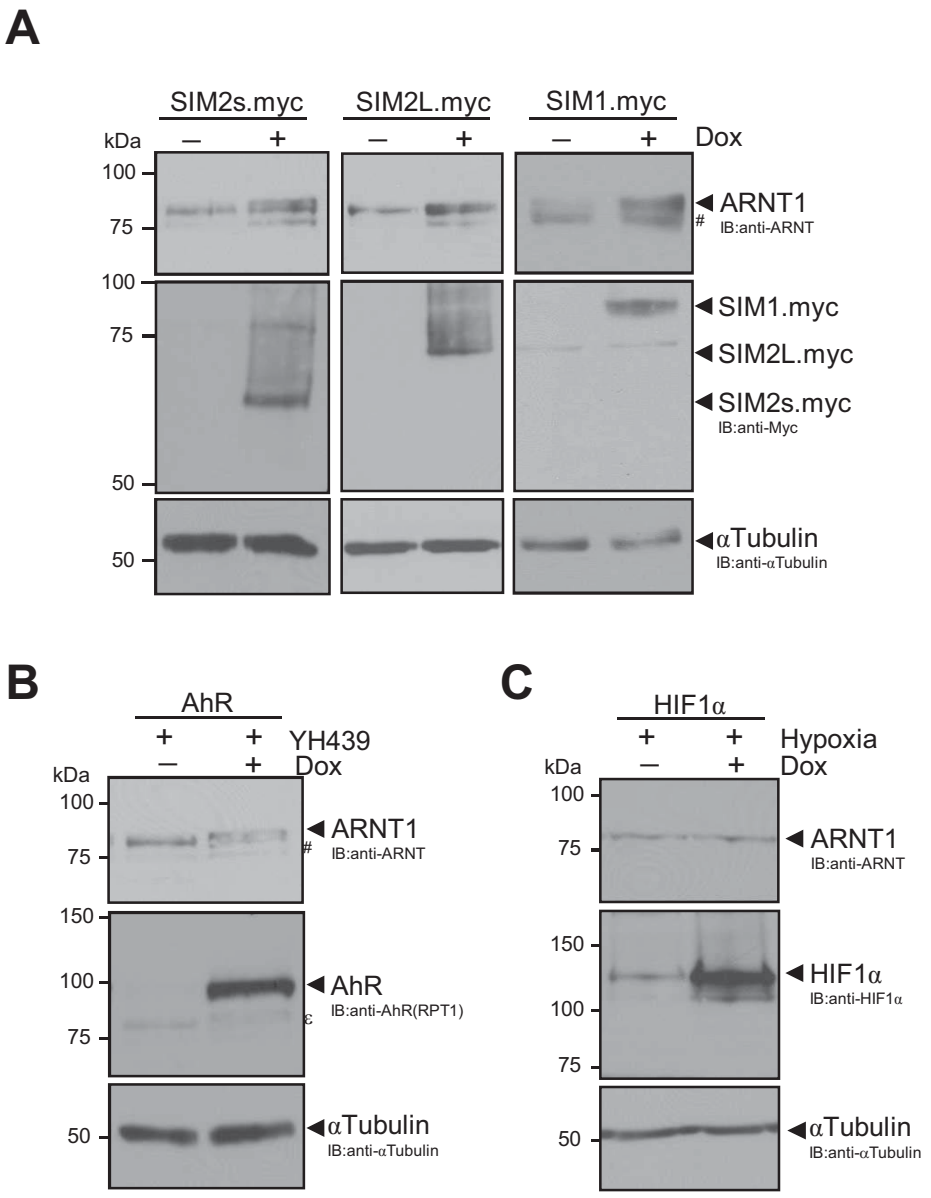

FIGURE 3.14: *Increase in protein levels of endogenous ARNT is specific to SIM bHLH-PAS family members.*

Whole cell extracts were harvested after 18.5 hours of induced (Doxycycline 1μg/ml) expression of human bHLH-PAS family members cDNA in 293Flp-TRex® cells, which for (B) AhR and (C) HIF1α expression also included co-treatment with ligand YH439 (10μM) or hypoxic (<1% O_2) growth conditions, respectively. 50μg whole cell extracts were separated by 8% SDS-PAGE followed by sequential immunoblot analysis of proteins as indicated. Symbols; # = ARNT2 (75kDa) cross-reactivity with anti-ARNT MA-515 mAb, and ε = residual ARNT1 signal on anti-RPT1 imunoblot. ARNT1 detected on a duplicate immunoblot following SIM1.myc induction. Data representative of that from two independently derived polyclonal cell lines for each bHLH-PAS family member, human SIM2s.myc and SIM2L.myc (Myc tagged), and untagged human AhR and HIF1α, or one independently derived SIM1.myc polyclonal cell line. SIM1.myc data generated by A. Raimondo, 2008.

approximately 16 hours for ARNT1 in DU145/Control cells (**Figures 3.15A & C**). However, the half-life of ARNT1 was greatly extended beyond the 20 hour time-course of this experiment in DU145/SIM2s.myc cells, indicating dramatically enhanced protein stability (**Figures 3.15A & C**). The extent to which ARNT1 protein is 'stabilised' in DU145/SIM2s.myc cells above that in DU145/Control cells was predicted to be approximately 10-fold ($t_{1/2}$ ~175h) from extrapolation of the mean (n=3) of ARNT1 levels in DU145/SIM2s.myc cells with up to 20h CHX treatment (**Figure 3.15D**). There is, however, no significant difference in mean ARNT1 levels from 0 to 20h after CHX treatment (P=0.11, paired students TTEST; **Figure 3.13.C**) indicating no change in ARNT1 levels over this time, thus this extrapolation is likely to be inaccurate and the SIM2s-dependent increase in ARNT1 half-life much greater 10-fold. Intriguingly, the (regular non-enhanced) half-life of ARNT1 in DU145 cells of 16h is much longer than that found for ARNT1 in previous studies. Specifically, pulse chase experiments of transiently expressed mouse Arnt1 in (monkey kidney) COS-7 cells found the $t_{1/2}$ to be 10.8h [131]. Interestingly in this same study, a mutant form of mArnt1 found in Hepa1 C4 cells that fails to heterodimerise with mAhR characterised by a Gly (G) to Asp (D) residue change at 326, was found to have an enhanced degradation rate of 3.5h from transient expression pulse chase experiments in COS-7 cells [131]. The degradation rate of endogenous ARNT1 has also been reported to be 4.8h from quantitation of western blot analyses of ARNT1 following CHX treatment in human (hepatoma) Hep3B cells [120]. Due to the variation in these studies, there is no consensus for the turnover rate of ARNT1, and this variation may reflect differences between the mouse and human homologues, or perhaps more likely, the cell contexts in which these studies were conducted. Indeed, the higher ARNT1 half-life in the prostate cancer DU145 cells used here may already reflect the effect of elevated endogenous levels of SIM2s expression found to be characteristic of prostate cancers and tumour derived cell lines [52, 80, 81, 93]. This supposition could be tested via the assessment of ARNT1 degradation in a SIM2s-negative expressing context, such as upon siRNA-mediated knockdown of

endogenous SIM2s in DU145 cells, or upon comparison of ARNT1 half-life in non-tumourigenic primary prostate epithelial cells (PrECs).

As shown in **Figure 3.10B**, increased SIM2s-mediated *ARNT2* transcription may account for the increase in ARNT2 protein in the cell lines where *ARNT2* mRNA levels were found to be up-regulated upon SIM2 expression. However, *ARNT2* mRNA levels remained unchanged in PANC-1 cells upon SIM2s.myc expression where ARNT2 protein levels greatly increased (**Figures 3.8B** and **3.9A**) (refer **section 3.2.3**), indicating that ARNT2 protein levels may also be regulated via SIM2s activities in a similar manner as ARNT1. Interestingly, increased ARNT2 protein stability is also evident in DU145/SIM2s.myc cells, as the mean (n=3) $t_{1/2}$ of ARNT2 was extended from <4 hours in DU145/Control cells (**Figure 3.15A**), to 10-11 hours (**Figures 3.15Bii & E**). This finding shows that ectopic SIM2s expression also allows for enhanced ARNT2 stabilisation. Consequently, this finding provides evidence for a potential mechanism of ARNT2 regulation that may account for the increase in ARNT2 seen in PANC-1 cells where *ARNT2* mRNA levels are unchanged upon SIM2 expression (**Figure 3.9B**), consistent with current findings for SIM2-dependent stabilisation of ARNT1. Moreover, these data are also particularly interesting as it indicates that multiple mechanisms are simultaneously contributing to enhancing ARNT2 protein levels in these cells.

Interestingly, the half-life of ARNT2 extends to mirror that of ectopically expressed SIM2s.myc (~10-11h, **Figures 3.15Bi & F**), whereas, ARNT1 stabilisation extends well beyond this. Whether this correlation between the turnover of endogenous ARNT2 and SIM2s.myc protein levels is co-incident or indicative of alternate post-translational SIM2s-requiring mechanism(s) of stabilisation for ARNT1 and ARNT2 that may also be connected to the rate of SIM2s.myc degradation, remain to be determined. Furthermore, it still remains to be specifically determined whether or not mechanisms of increased translation are working in conjunction with those of protein stabilisation in the SIM2-mediated regulation of ARNT protein levels.

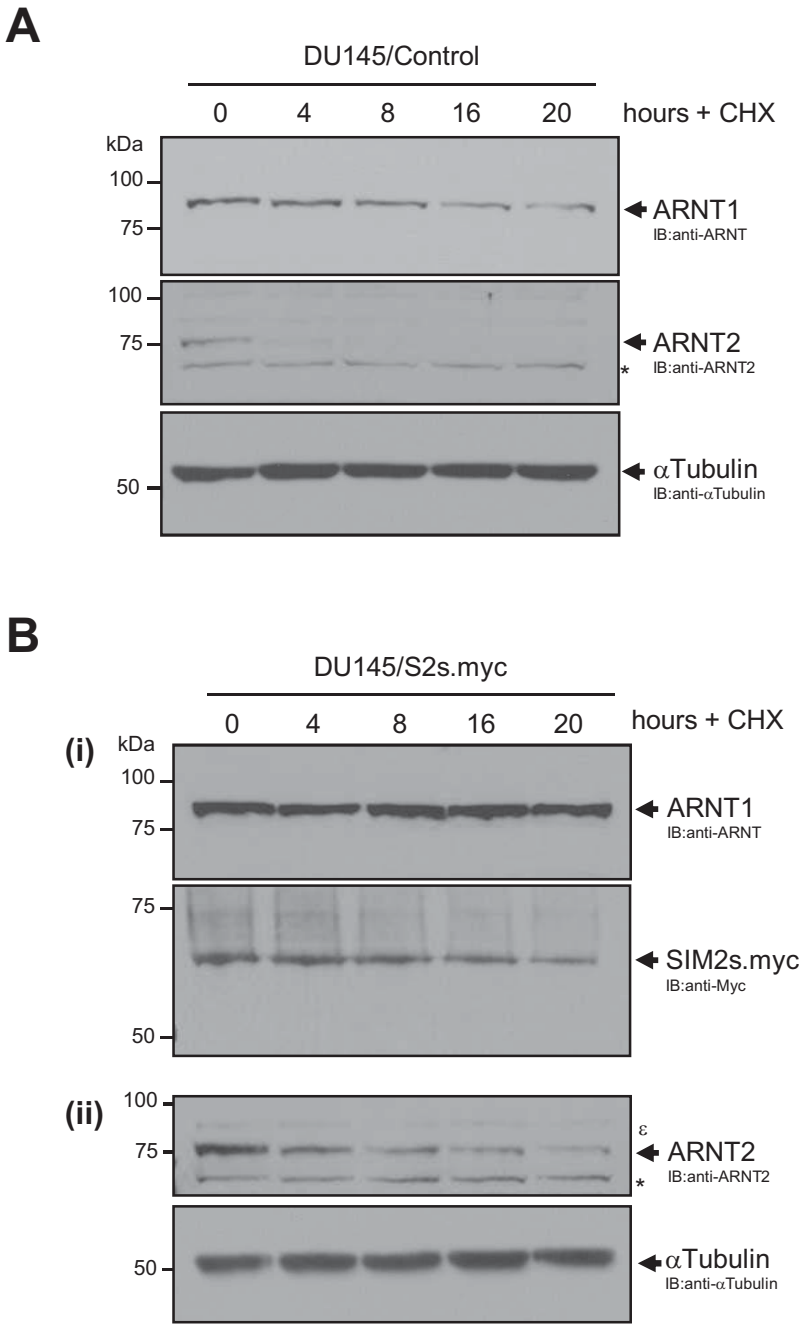

FIGURE 3.15: *The average $t_{1/2}$ of endogenous ARNT1 is greatly extended in SIM2s.myc expressing DU145 cells, as is that of ARNT2 which mirrors the average $t_{1/2}$ of stably expressed SIM2s.myc.*

DU145 cells with or without stable ectopic expression of myc tagged SIM2s were treated with 60ug/ml cyclohexamide (CHX) for the specified times, lysed, and whole cell extracts (WCE) normalised for equal protein concentration. (A) 60µg or (B) 50µg [(i) and (ii) independent blot sets] of WCE were separated by 8% SDS-PAGE, followed by sequential immunoblot analysis of proteins as indicated. Representative experiment data set from three independent experiments, except Control ARNT1 analysis, n=2. * = non-specific background band. ε = residual ARNT1 (~87kDa) signal from previous immunoblot with anti-ARNT mAb.

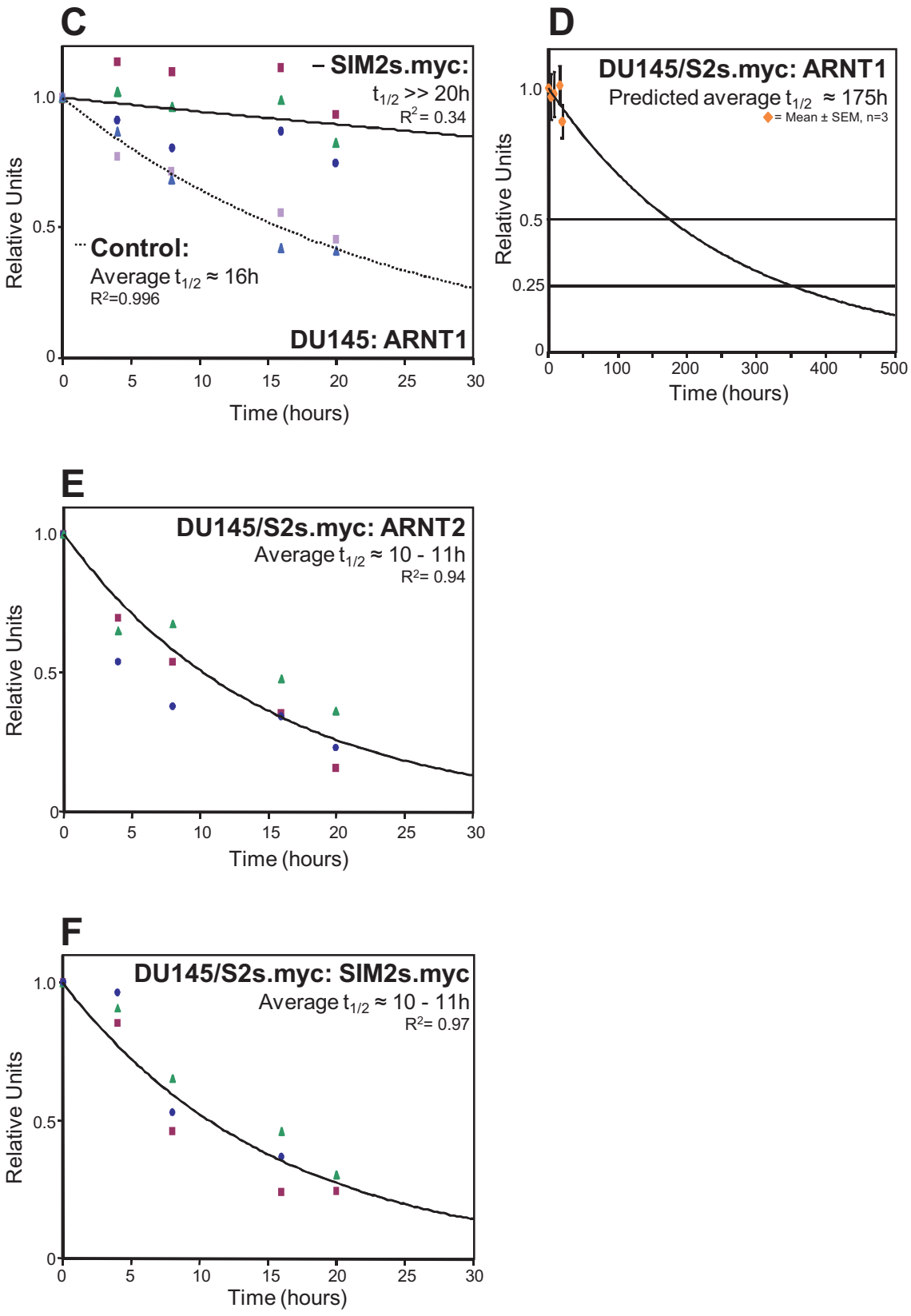

FIGURE 3.15 continued: *The average $t_{1/2}$ of endogenous ARNT1 is greatly extended in SIM2s.myc expressing DU145 cells, as is that of ARNT2 which mirrors the average $t_{1/2}$ of stably expressed SIM2s.myc.*

(C,D, E & F) Quantification of specific immunoblot bands for proteins as shown in (A) and (B) with densitometry and graphed with respect to time using EXCEL. Logarithmic decay curve was fitted to the mean data of independent experiments all displayed on graphs. ARNT1 $t_{1/2}$ estimated for DU145/Control (puromycin resistant) cells from average of n=2,■ &▲; and ARNT1, ARNT2 and SIM2s.myc $t_{1/2}$ estimated from average of n=3,■ , ▲& ●. SIM2s.myc was measured using anti-Myc (rabbit polyclonal) (■& ▲) or anti-hSIM2s (goat polyclonal) (●) antibodies.

These studies also find the half-life calculated here for human SIM2s.myc of ~10-11h (**Figure 3.15F**) to be much longer than that the previously reported of 2h for transiently expressed mSim2L.myc calculated from pulse chase experiments in 293T cells [59], which is quite a striking difference for two highly homologous proteins. As the $t_{1/2}$ of the short isoform of SIM2 in humans, or mice, has not been investigated or reported on prior to these findings, it remains to be determined if there are cell-type, or species specific modes of SIM2 regulation. Alternatively, this difference in stability of the two isoforms may provide the first insight into potential alternate mechanisms of regulation for the two highly homologous isoforms of SIM2, which in all likelihood, would impact on their respective transcriptional activities and functions.

Exactly how SIM2s contributes to ARNT1 and ARNT2 stabilisation, whether it is facilitating post-translational modifications, and/or co-factor binding to ARNT to prevent degradation, whether via direct or indirect interactions remain to be investigated. A possible means by which ARNT may be stabilised in a SIM-specific manner may be via the recruitment of as yet unidentified SIM-specific co-factors to the SIM/ARNT dimer via the highly conserved SIM bHLH-PAS domains, or facilitating the recruitment of previously identified ARNT1-stabilising co-factors such as BRCA1 [119], which then function to mediate post-translational modifications to ARNT and/or provide a complex that protects ARNT from degradation. However, the fact that ectopic SIM2s is largely interacting directly with 'stabilised' ARNT 1 and ARNT2, as indicated by co-immunoprecipitation studies in several prostate carcinoma cell lines (**Figure 3.11**), may be indicative of SIM2s mediating protein stabilisation via direct interactions with ARNT. The bHLH-PAS region is the region of highest amino acid conservation between ARNT1 and ARNT2 (**Figure 3.1**)[8, 109], and thus may be the region that confers the ability of SIM2 to stabilise both ARNT1 and ARNT2. Indeed, others have shown that ARNT-mediated stabilisation of HIF1α is conferred through the bHLH-PAS domain of ARNT [24]. Dimerisation between SIM2 and ARNT occurs via the N-terminal bHLH-PAS domains of each protein

[9, 34, 35]. Human SIM homologues share 87.2% (mouse 89.4%) amino acid identity in their N-terminal DNA-binding and dimerisation (bHLH-PAS) domains, but only 18% (mouse 15.3%) in the carboxy-terminal half [38]. Bioinformatic alignment of N-terminal bHLH-PAS regions of human HIF1α (1-329) [132] and AhR (1-385) [133], to that of SIM2 (1-351) [38], shows only 39% and 26% amino acid identity, respectively (Data not shown. Accession numbers for sequences used; NM_001530, NM_001621 & NM_005069). Thus, in light of the emerging evidence supporting a SIM-specific mechanism of regulation of ARNT, the mode of interaction and mechanism of stabilisation may likely to be conferred via the SIMs' specific capacity to interact with ARNT via these highly conserved PAS domains, in a manner unique to SIM and not shared by other class I bHLH-PAS family members. Indeed, *in vitro* yeast two-hybrid studies using GAL4 activation domain and DNA-binding domain fusion proteins show that the heterodimerisation between Sim1 and Sim2 with either Arnt1 or Arnt2 is much more efficient than that between Arnt 1 and Arnt2, and AhR [34]. However, although Sim2 dimerises with Arnt1 more efficiently than HIF1α, Sim1 does not, and the interaction between HIF1α and Arnt2 is much stronger than that between Sim1 and Sim2 with Arnt2 [34]. Thus the strength of SIMs' interactions with ARNT may not fully account for the ability of SIM2 to stabilise ARNT, however, the specificity of the interaction with ARNT may confer the stabilisation just as ARNT is able to protect HIF1α from Hsp90-dependent degradation via the specificity of binding conferred through the bHLH-PAS [24].

The studies presented here for the first time specifically show a clear association between SIM2s expression and increased stability of ARNT1 in prostate DU145 cells and strong evidence of a mechanism of SIM2-dependent ARNT1 regulation in other tissue and tumour-type derived cell lines from the kidney, and pancreatic and prostate tumours. This may be indicative of the potential for multiple and/or alternate mechanisms of ARNT1 stabilisation that may be dependent on the specific differential molecular expression profile of cells, such as those found in cell lines derived from tumours.

Regulation of class II bHLH-PAS family members by a class I family member is unprecedented. The current studies presented here are the first to provide any evidence for cross-regulation of ARNT by other bHLH-PAS family members from a series studies arising following the unexpected observation of an increase in endogenous ARNT1 protein levels upon ectopic expression of bHLH-PAS class I family member SIM2s. The work presented here shows novel mechanisms of SIM-dependent ARNT1 stabilisation, and also for the first time SIM2s-mediated mechanisms of enhanced stabilisation and gene expression levels of ARNT2. These findings present a fascinating new insight into the regulation of ARNT by SIM2s as part of what is emerging to be the complex, cross-regulatory roles of the bHLH-PAS family. Determining the mechanisms and physiological relevance of SIM(2)-dependent stabilisation and regulation of ARNT remains a fascinating line of investigation. The full plethora of ARNT activities remain to be described. However, as ARNT is central to mediating the transcriptional responses of developmentally vital factors such as HIF1α, AhR and SIM2 [5], and is also implicated in the progression of diseases such as cancer via co-mediation of the hypoxia response [134], as is SIM2s itself [43, 52, 53, 80-82, 91]. These novel insights presented here into the regulation of ARNT potentially implicate SIM2 into these functions of ARNT. Further understanding these inter-dependent relationships between bHLH-PAS family members will ultimately impact on future research into the roles and requirements of ARNT in both development and disease.

CHAPTER 4

Searching for novel gene targets of SIM2 in cancer

4.1 INTRODUCTION

Pancreatic, colon and prostate adenocarcinomas are three of the most lethal of human cancers. Select up-regulation of the short isoform of Single-minded 2 (SIM2s) has been identified in carcinoma derived cell lines and solid tumours of these cancer types [43, 80, 81, 91-94] and the expression status of SIM2s is emerging as an interesting candidate for a solid tumour marker of these tumour types. Several independent microarray studies find *SIM2* to be one of the most consistently up-regulated gene products in prostate tumours, while not being expressed in corresponding benign tissue [81, 93, 94]. Analysis of human clinical samples revealed that elevated SIM2s protein levels in prostate tumours significantly correlated to increased tumour aggression and a dramatic drop in estimated survival, highlighting the potential use of SIM2s levels as a novel marker of aggressive prostate cancer [81]. Studies have linked differential SIM2s expression to tumour cell survival and growth [43, 53, 91], however the molecular mechanisms of SIM2s function in these cancers is unknown. Whether changes in SIM2s expression levels are required for tumour initiation and/or tumour maintenance remain important questions that need to be answered for its potential use as an early detection marker and a target for the development of chemo-preventative therapeutics.

Knowledge of how and why SIM2s expression may promote tumour progression and aggression could be gained from an understanding of its transcriptional activities and the genes it regulates, and consequently how the differential regulation of gene products by SIM2s may link SIM2s to disease pathogenesis. However, few *bona fide* target genes have been described for the mammalian SIM2 orthologues, and these only appeared in the literature in 2008 [48, 82]. Recently, we described *Myomesin* 2 (*MYOM2*) as a direct target of SIM2 transcription following microarray studies of human kidney 293T cells with, and without, stable ectopic expression of a constitutively active chimera of mouse Sim2L (mSim2/AD.myc) [48]. Interestingly our report [48] showed positive gene regulation by mSim2L and hSIM2s on the human *MYOM2*

promoter via a specific binding element [48]. These data suggest, for the first time that SIM2 harbours both transactivating and, as previously described, repressive capabilities [34, 41, 47, 48, 82]. However, there are no reports of changes in *MYOM2* expression being associated with oncogenesis, indeed data mining of recently published genome-wide analysis of pancreatic cancer shows no change in *MYOM2* expression levels between tumour and tumour derived cell lines and normal tissue controls [96]. Hence the SIM2-mediated regulation of *MYOM2*, which codes for a myosin binding protein that is expressed in muscle sarcomeres and characterised as an intracellular member of the immunoglobulin superfamily [49, 50], does not provide any insight into how SIM2 may be playing a functional role in the tumourigenesis of the pancreas, prostate, or any other type of solid tumour where SIM2 is misregulated.

Interestingly, during the course of the present study the gene *SLUG* was found to be a direct target of SIM2s-repression in breast cancer MCF-7 cells in 2008 [82]. Contrary to prostate, pancreatic and colon cancers, a reduction or loss of SIM2s expression is associated with increased breast tumourigenicity, and as the alleviation of *SLUG* repression drives cancer growth via SLUG-mediated EMT (epithelial mesenchymal transition) this work links the functional loss of SIM2s with tumour progression for the first time [53, 82]. Converse to breast cancers, loss of SIM2s in pancreatic and colon cancer cells, and colon cancer cell xenografts, has been found to be associated with decreased tumour cell survival [43, 91]. Microarray analysis following antisense-mediated knockdown of SIM2s in colon cancer RKO revealed *GADD45alpha* (growth arrest and DNA damage gene), a key stress response gene associated with apoptosis, to be repressed in a SIM2s-mediated manner , however it has not been defined as a direct target of SIM2s-repression [91]. Thus, prior to the studies presented here, direct SIM2s target genes in the tumour context of enhanced levels of SIM2s expression, such as cancers of the prostate, pancreas or colon [43, 52, 80, 81, 91, 93, 94, 96] remained to be identified. Consequently, any insight into how and why SIM2s may be playing a role in the progression of these cancer types via an understanding of the genes it

regulates represented a novel avenue to advance knowledge of SIM2s transcription and its putative role in tumourigenesis.

The following studies were undertaken to determine novel targets of SIM2s transcriptional activities in a tumour cell context in the hope of ultimately discovering if there is a mechanistic role and functional requirement for SIM2s in the development of these solid tumour types.

4.2 RESULTS & DISCUSSION

4.2.1. Experimental approach for the identification of novel targets of SIM2s regulation in human Prostate carcinoma derived cells

Prostate cancer cells were chosen for these experiments for at the time these studies were initiated, several independently published microarray studies had found SIM2 to be the second most consistently up-regulated gene in prostate tumours, while not being expressed in corresponding benign tissue [81, 93, 94], thus providing the most comprehensive set of independent findings associating SIM2s up-regulation in any tumour type. Likewise, no studies had, or since have, looked at the molecular roles and requirements for SIM2s in prostate cancer, thus providing an uncharted paradigm to determine how SIM2s may fit into the developmental program of this tumour type.

This study sought to understand how aberrantly high levels of SIM2s in prostate cancer [80, 81, 93, 94], which correlates to tumour aggression [81], may promote tumour growth and/or maintenance by seeking to discover direct target genes of SIM2s using microarray studies of independently derived prostate carcinoma

cell lines upon stable ectopic expression of SIM2s. Similarly, ectopic expression of mSim2 in mice has been useful for constructing a biochemical paradigm to aid elucidation of the role of mSim2 in development and the eitology of Down Syndrome [71, 86]. Modern DNA microarray technologies for large-scale profiling of changes in gene expression of the entire transcriptome has developed greatly since it was first established in 1995 [135] and is now a routinely used method for such studies. The discovery of direct target genes of transcription factors have been successfully found following microarray analysis of cells in which the factor has been constitutively overexpressed, such as *Cyclin K* as a target of p53 [136], and indeed *MYOM2* as a target of SIM2 [48]. The studies here were designed to incorporate duplicate experiments utilising two prostate carcinoma derived cell lines for cross-comparison purposes to determine if a 'gene set' that is differentially regulated observed upon ectopic SIM2s expression is common to prostate cancer cells, and not necessarily the outcome of a cell-type specific response, as the former potential finding may provide indicators of how SIM2s may function in the oncogenesis of all solid tumour types where SIM2s is aberrantly misexpressed (**Figure 4.1B**). Analysis of *SIM2s* mRNA levels in common human prostate carcinoma cell lines by semi-quantitative RT-PCR revealed somewhat lower expression of endogenous *SIM2s* in DU145 and LNCaP cells compared to PC3AR+ cells (**Figure 4.1A**). Consequently these two former cell lines were chosen from which to engineer independently derived polyclonal cell pools exhibiting stable ectopic expression of carboxy terminal myc tagged human SIM2s (SIM2s.myc) to emulate an aberrant increase in SIM2s in prostate cancers compared to benign samples as previously observed from several studies by others [81, 93, 94]. This was achieved using the pEF-IRES-puro vector integration and expression system which routinely provides high levels of transgene expression following selection for successful integration indicated by Puromycin antibiotic resistance in cells [102]. This method has previously provided successful stable ectopic expression of the constitutively nuclear mammalian SIM homologues in cultured cells [48, 59, 60][S. Woods, PhD Thesis 2004]. Puromycin resistant control (Control) pools were generated by incorporation of the empty expression vector in these cells. As described

in **Chapter 3**, ectopic expression of SIM2s.myc in these cells resulted in a concomitant increase in endogenous levels of the obligate partner factor ARNT (**Chapter 3, Figure 3.2A**). Moreover, co-immunoprecipitation experiments revealed endogenous ARNT dimerises with SIM2s.myc in the derived DU145 and LNCaP cells. Importantly, analysis of supernatant following immunoprecipitation revealed that although SIM2s.myc was not immunodepleted from LNCaP/SIM2s.myc whole cell extracts using this method, nor was endogenous ARNT, suggesting that for the major proportion of ectopic SIM2s.myc endogenous ARNT was not limiting the formation of SIM2s.myc/ARNT heterodimers. Furthermore, endogenous ARNT protein remained in excess of SIM2s in DU145 cells. (Refer to **Chapter 3**, **Figure 3.11**). Consequently further ectopic expression of the obligate partner factor ARNT was not required to obtain near-complete and complete heterodimerisation of ectopic SIM2s in LNCaP and DU145 cells, respectively, to promote SIM2s/ARNT activity.

The design of the microarray experiment is represented in **Figure 4.1B**. The two independently derived puromycin resistant polyclonal cell lines were developed for both SIM2s.myc over expression and empty-vector control. These cell lines were created for a minimum of two independent pair-wise comparisons between control and SIM2s.myc expression, to serve as biological replicates. For example, Control polyclonal cell lines B and C, compared to SIM2s.myc polyclonal cell lines D and E (refer to **Figure 4.1C**). To control for variation due to cell culture growth conditions, each polyclonal cell line was cultured in duplicate to obtain two independently derived samples for microarray analysis (refer to **Figure 4.1B**, independent samples coloured in blue and black). Each microarray chip is hybridised with differentially labelled cDNA samples of both a Control and SIM2s.myc polyclonal cell line using the Cy3 or Cy5 fluorofore labels. Differential gene regulation was then determined from a measure of the predominant hybridised fluorescent product. Dye swap labelling reactions on biological replicates, and between independently

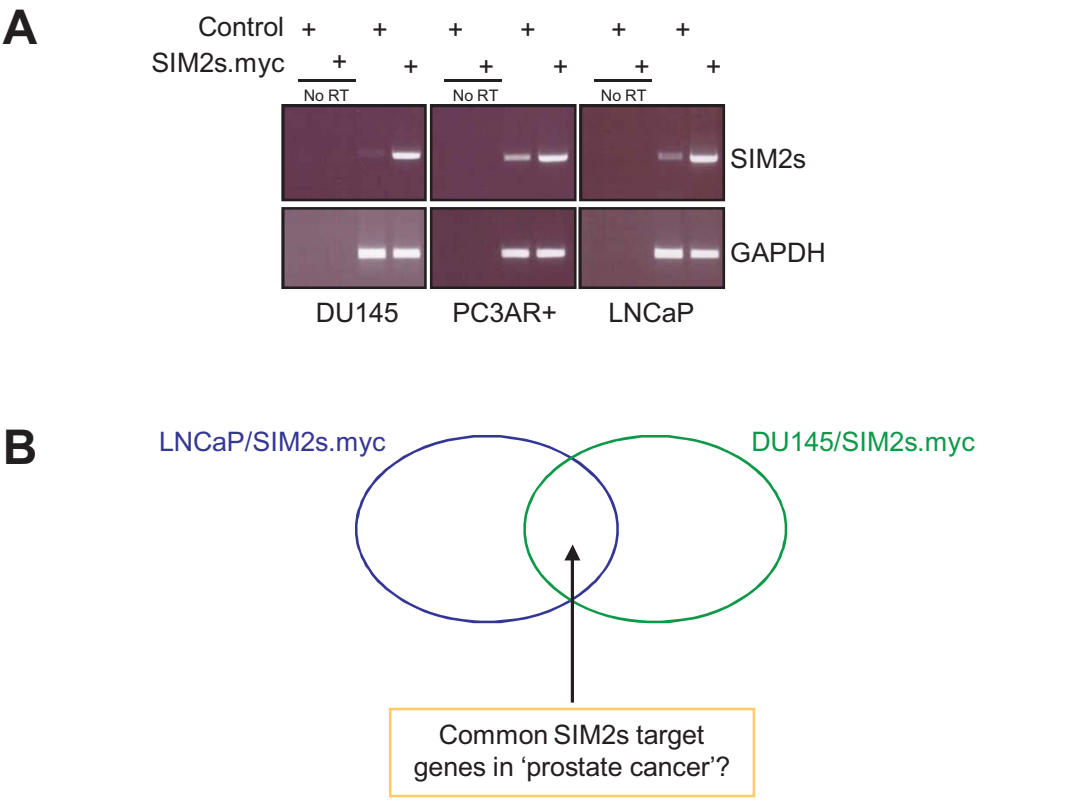

FIGURE 4.1: *Microarray approach for the identification of differentially regulated genes upon aberrant expression of SIM2s in Prostate carcinoma derived cells.*

(A) Assessment of *SIM2s* mRNA levels in human prostate carcinoma derived cell lines. Representative semi-quantitative RT-PCR of *SIM2s* mRNA levels with and without, stable ectopic SIM2s.myc expression. SIM2s PCR used limiting cycles of 35x, equal cDNA template used, synthesised from same amounts of total RNA extracts. GAPDH PCR used 25x cycles. Amplicons separated by EtBr stained 1% agarose gel electrophoresis. All SIM2s images obtained at the same UV light intensity. (B) Combinatorial analysis to ultimately identify a common set of genes regulated by SIM2s in 'prostate cancer', and not those specific to either LNCaP or DU145 cells. (C) Biological replicates for both 10µg/ml puromycin resistant Control, ie: cell lines B & C, and stable human SIM2s.myc (Myc tagged) expression, ie: cell lines D & E, are independently derived polyclonal cell lines, compared for identification of differential gene regulation by microarray analysis requiring 4 x19k human cDNA oligo microarray chips for pairwise analyses which includes, Cy3/Cy5 dye swap analysis of biological replicates, and of independent RNA extractions, **1** & **2**, of each polyclonal cell line. 20µg of total RNA extract for each sample condition were prepared from 80-90% confluent cell monolayers and supplied to the 'Adelaide Microarray Centre', Adelaide, South Australia, for cDNA synthesis with Cy-dye labelling, followed by hybridisation to human 19K oligo microarray chips, and subsequent data analysis.

derived samples from the same biological sample served as internal dye-labelling and hybridisation controls for the microarray (**Figure 4.1C**).

Although a number of genes were differentially regulated in 293T upon mSim2/AD.myc expression in a fashion that may link SIM2 to a potential functional role in cancer progression, as will be discussed later, the cDNA microarray used in that study was only capable of detecting 8000 mRNA species, thus the spectrum of differential gene regulation to be observed was limited. The development of a cDNA microarray platform that represented 19000 mRNA species provided an excellent opportunity to obtain a more comprehensive profile of differential gene regulation upon SIM2 overexpression. Also, by analysing the effects of stable ectopic expression of the short isoform of human SIM2 in a solid tumour cell context, there is the potential for insights into isoform specific transcriptional targets to emerge.

4.2.2. Identification of putative targets of SIM2s from microarray studies of human prostate carcinoma LNCaP±SIM2s.myc cells

4.2.2.1. LNCaP microarray results and semi-quantitative RT-PCR validation

The data obtained for differential gene regulation upon SIM2s.myc expression in LNCaP cells was assessed for genes with the highest fold change in expression and/or that may link SIM2s expression and transcriptional activities with a role in tumour growth. The top 30 genes are shown in **table 4.1**. Note the 22.3 fold increase in SIM2 message, although the oligonucleotide tag for SIM2 on the array does not allow for distinguishing between endogenous or ectopic SIM2s mRNA levels, nor differences in SIM2 isoform expression. Interestingly, prostate specific antigen (PSA), which is represented twice on the microarray, appears twice in the top 30 to be up regulated upon SIM2s.myc expression (rank 9 and 22) greater than 2-

fold. Increases in serum measures of PSA is regularly used as a diagnostic for the onset and progression of prostate cancer [137] (for reviews see [138, 139]), thus this immediately highlighted a link between SIM2s expression and prostate cancer. Likewise, changes in expression of other genes consistent with a link for SIM2s in cancer included; the down regulation of matrix metalloproteinase 16 (*MMP16* or *MT3-MMP*), as MT-MMP protein family members, including MMP16, have been found to be generally downregulated in prostate carcinomas [140]; the down regulation of the B-cell translocation gene 1 (*BTG1*) due to its role as an antiproliferative agent in the regulation of angiogenesis [141]; also the up regulation of heat shock 70kD protein 10 (HSPA10 or otherwise known as HSPA8 & HSC71) which had been reported in 2004 to be enhanced at the protein level in cisplatin (an anti-tumour agent) resistant cervical carcinoma A431/Pt cells compared to cisplatin-susceptible control A431 cells [142]. Elevated levels of protein tyrosine phosphatase (PTP) receptors are associated with tumour development and are the target for the development of cancer therapeutics (for review see [143, 144]). Consequently the up-regulation of PTP receptor type R (PTPRR), the most dramatic differential regulation observed upon SIM2s.myc expression of 3.9-fold, was of interest for further validation. The down regulation of *TMEFF2* (transmembrane protein with EGF-like and two follistatin-like domains 2), also known as TENB2, was of note as *TMEFF2* expression is associated with disease progression and androgen independence in prostate cancer [145]. Interestingly however, conflicting links between SIM2s expression and differential gene regulation were also observed, such as the 2.8-fold down regulation of G antigen, family B, 1 (prostate associated) mRNA (GAGEB1), also known as GAGE-9 or P antigen family, member 1 (PAGE1) (rank 7, **Table 4.1**). *GAGEB1*/*PAGE1* was first characterised as a gene involved in LNCaP prostate cancer progression model in 1998 where its mRNA levels were found to significantly increase with tumour cell line metastatic potential and aggression [146]. Likewise, *XAGE1*, a member of the XAGE subfamily of the GAGE family to which *GAGEB1*/*PAGE1* belongs, is also down regulated (1.9-fold) upon SM2s.myc expression, and as *in situ* profiling of *XAGE-1* mRNA expression in prostate carcinomas has shown it to be up regulated compared to matched normal

tissue [146], together the microarray data is not consistent for a link between SIM2s expression and the regulation of these GAGE family members and the progression of prostate tumours. Most intriguingly however was the up regulation of *S100P* (S100 calcium-binding protein P) (rank 10, **Table 4.1**) which at the time this list was generated was emerging as a early marker for pancreatic cancer and was also identified as being upregulated in prostate cancer [147-149], thus highlighting a potential shared mechanism through which SIM2s may contribute to the changes in the genetic profile of both these cancer types.

To validate the microarray findings for the effect of SIM2s.myc expression on the gene expression profiles of the above mentioned genes, semi-quantitative (sq) RT-PCR analysis was carried out on cDNA samples generated from independently extracted total RNA samples of polyclonal LNCaP/Control line A and LNCaP/SIM2s.myc line A (referred to hereafter as the 'A' cell line set) used for the microarray. *MMP16*, *XAGE1*, *PTPRR*, *PSA*, *S100P* and *TMEFF2* all showed changes in mRNA levels consistent with the microarray analysis, however, *BTG1* and *HSPA10* failed to show any difference in gene expression upon stable expression of SIM2s.myc as indicated in the microarray, and *GAGEB1* was slightly down regulated upon SIM2s expression in opposition to the microarray findings (**Figure 4.2A**). Consequently, the latter three genes were excluded from further investigation. These differences in expression between sqRT-PCR results and microarray analyses indicated the expected potential for variation in gene expression profiles between the independently derived SIM2s.myc polyclonal cell lines, thus a number of selected putative targets were selected for further validation studies. This included independent sqRT-PCR analysis of the other cell lines used for the microarray, LNCaP/Control cell line B and LNCaP/SIM2s.myc cell line B (the 'B' cell line set). **Figure 4.2B(i)** lanes 2 and 3 show the differential gene regulation between the Control and SIM2s expressing B cell lines; consistently *MMP16* and *PTPRR* and to a slightly lesser extent, *PSA*, were found to be regulated in the same manner as indicated from the microarray and in the 'A' cell line set (**Figure 4.2A**). Interestingly however, *S100P* was found to be down regulated in LNCaP/SIM2s.myc B cells

TABLE 4.1: *Top 30 differentially regulated genes, plus others of interest, on expression of SIM2s in human prostate LNCaP cells.*

Rank	ID	Name - all Homo sapiens	Fold Change	+ SIM2s	M	A	B
1	NM_005069	Single-minded (Drosophila) homolog 2 (SIM2), transcript variant SIM2, mRNA	22.3	Up	4.48	12.28	3.4802
2	AK022868	axin interactor, dorsalisation associated (AIDA)	2.3	Up	1.19	11.42	2.6659
3	AL137506	ELOVL family member 7, elongation of long chain fatty acids (yeast) (ELOVL7)	1.9	Up	0.94	10.53	2.131
4	NM_005941	matrix metalloproteinase 16 (membrane-inserted) (MMP16) mRNA	1.9	Down	-0.96	9.46	2.1162
5	NM_020411	XAGE-1 protein (XAGE-1), mRNA	2.9	Down	-1.53	9.66	2.0328
6	NM_003548	H4 histone family, member N (H4FN) mRNA	1.7	Up	0.77	9.79	1.7747
7	NM_003785	G antigen, family B, 1 (prostate associated) (GAGEB1), mRNA	2.8	Down	-1.51	9.97	1.7134
8	NM_002849	protein tyrosine phosphatase, receptor type, R (PTPRR), mRNA	3.9	Up	1.97	9.69	1.6985
9	S75755	PSA=prostate-specific antigen [human, breast cancer specimen, mRNA Partial, 569 nt]	2.4	Up	1.29	11.17	1.4167
10	NM_005980	S100 calcium-binding protein P (S100P), mRNA	2.0	Up	1.01	9.63	1.3184
11	NM_004457	Fatty-acid-Coenzyme A ligase, long-chain 3 (FACL3) mRNA	1.6	Up	0.70	11.01	1.2823
12	NM_001731	B-cell translocation gene 1, anti-proliferative (BTG1) mRNA	1.7	Down	-0.77	12.46	1.1536
13	NM_006597	heat shock 70kD protein 10 (HSC71) (HSPA10) (HSPA8), mRNA	1.7	Up	0.80	13.11	0.9038
14	AF299075	synaptotagmin IV mRNA, complete cds	2.0	Up	0.96	9.55	0.8668
15	AB032962	G protein-coupled receptor 158 (GPR158), partial cds	1.6	Up	0.67	9.52	0.8603
16	NM_016192	putative transmembrane protein with EGF-like and two follistatin-like domains 2 (TMEFF2), mRNA	2.3	Down	-1.21	10.84	0.8393
17	AF237700	Ran binding protein 2 mRNA, partial cds	1.6	Up	0.68	10.61	0.7383
18	NM_006943	SRY (sex-determining region Y)-box 22 (SOX22), mRNA	1.4	Down	-0.51	11.1	0.4124
19	NM_005656	Transmembrane protease, serine 2 (TMPRSS2) mRNA	1.5	Up	0.61	10.23	0.3574
20	NM_018235	CNDP dipeptidase 2 (metallopeptidase M20 family) (CNDP2)	1.5	Up	0.58	10.88	0.3434
21	AL109729	abhydrolase domain containing 2 (ABHD2)	1.5	Up	0.61	10.48	0.3123
22	M26663	Homo sapiens prostate-specific antigen mRNA, complete cds (PSA)	2.1	Up	1.07	11.73	0.3108
23	NM_006267	RAN binding protein 2 (RANBP2), mRNA	1.4	Up	0.54	10.07	0.2869
24	AF070623	RALY RNA binding protein-like (RALY2)	1.7	Down	-0.76	8.81	0.248
25	NM_007011	putative transmembrane protein (HS1-2), mRNA	1.4	Up	0.50	10.81	0.1989
26	NM_018376	nipsnap homolog 3B (C. elegans) (NIPSNAP3B), mRNA	1.6	Down	-0.68	10.33	0.1915
27	AF216292	endoplasmic reticulum lumenal Ca2+ binding protein grp78 mRNA, complete cds	1.6	Up	0.64	11.85	0.0325
28	NM_001355	D-dopachrome tautomerase (DDT), mRNA	1.4	Up	0.50	11.41	0.0322
29	NM_005530	Isocitrate dehydrogenase 3 (NAD+) alpha (IDH3A) mRNA	1.4	Up	0.47	10.57	0.0083
30	NM_016029	CGI-86 protein (LOC51635), mRNA	1.8	Up	0.85	12.38	-0.0149
43	NM_001398	Homo sapiens enoyl Coenzyme A hydratase 1, peroxisomal (ECH1) mRNA	1.9	Up	0.95	11.74	-0.3612
45	NM_001995	Fatty-acid-Coenzyme A ligase, long-chain 1 (FACL1), mRNA	1.6	Up	0.64	10.48	-0.3822
		remaining list	< 1.7				

Independently validated putative targets by sqRT-PCR highlighted in red. Raw data supplied from the Adelaide Microarray Centre, SA. The M value is the log2 ratio between the 2 samples, and the A value is the average intensity in both channels (log2), across all the microarrays. The B value is a log-odds score. Statistical P-values not supplied.

compared to the control (**Figure 4.2B**), contrary to the microarray data and validation in the 'A' cell line set. Likewise, when analysed in third set of independently derived Control and SIM2s.myc expressing polyclonal cell lines, cell line set 'C' not used for the microarray experiment, a reduction in *S100P* expression upon ectopic SM2s expression was also observed (**Figure 4.2B(ii)**), indicating that the up regulation reported from the microarray was due to the apparently aberrant dramatic increase in *S100P* in the LNCaP/SIM2s.myc A cell line, inconsistent with two other independently derived SIM2s.myc expressing cells. The repression of *MMP16*, the slight increase in PSA and the dramatic increase in *PTPRR* upon SIM2s expression was also consistent upon validation using the independent cell line set 'C' not used in the microarray (refer to lanes 2 & 3, **Figure 4.2C** for *PTPRR* levels, and lanes 2 & 4, **Figure 4.3A** for *MMP16* and PSA representative data). The repression of *XAGE*-1 was found to be unchanged in all other cell line sets tested upon SIM2s.myc expression (data not shown) thus was not further investigated as a putative target of SIM2s in these studies.

4.2.2.2. Independent validation studies and investigating SIM specificity in the regulation of putative SIM2s target genes in LNCaP cells.

The mouse orthologues of human SIM2 and SIM1 are highly conserved in their DNA binding and dimerisation regions (refer to Introduction **Chapter 1, Figure 1.3A**), and *in vitro* studies show shared abilities to bind the same promoter derived consensus sequences [34, 38, 41, 46, 48, 59, 129], thus there is the potential for shared target genes. There is a however a high level of divergence in the carboxy-terminal regions of the homologues which confer their transcriptional properties (refer to **Figure 1.3A, Chapter 1**) indicating possible divergent roles in the regulation of the same genes via a common DNA binding site. Yet targeted deletion studies of both Sim2 and Sim1 in mice have shown that the homologues are not developmentally redundant [58], thus how the SIMs may confer specificity for DNA-binding and gene

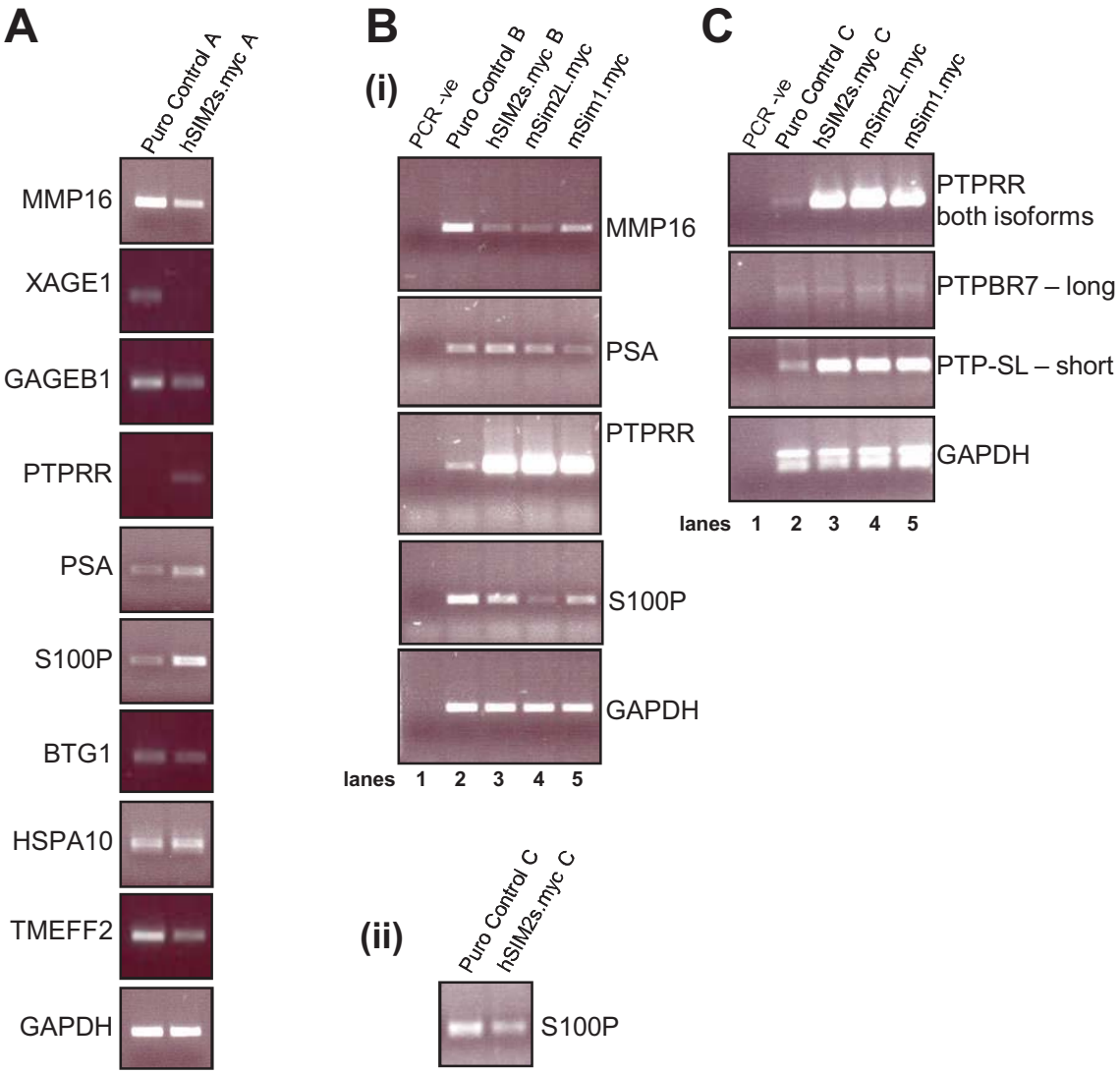

FIGURE 4.2: *Validation of differential gene regulation observed from microarray analysis of LNCaP cells with ectopic expression of SIM2s.myc and analysis of potential mammalian homologue SIM specificity of differential regulation.*

(A) Preliminary validation of putative SIM2s targets utilising independently derived RNA/cDNA from Control (puromycin resistant) and SIM2s.myc stable polyclonal cell pools used in the microarray. Note converse regulation of S100P in pools C, which were not used in the array. (B) Preliminary investigation of mammalian SIM homologue specificity of select putative targets. Independently derived RNA/cDNA of Control and SIM2s.myc polyclonal pools B which were used in the microarray. (C) Identification of specific differential regulation of the short isoform of PTPRR by mammalian SIM homologs in LNCaP cells.Semi-quantitative RT-PCR analysis of differentially regulated genes from independently derived polyclonal cell lines, as described, with, or without, stable ectopic expression of myc tagged human SIM2s in human prostate LNCaP cells. Preliminary analysis only of differential regulation of putative human SIM2short targets in polyclonal LNCaP cell with stable ectopic expression of (murine) mSIM2Long and mSIM1 (myc tagged). All PCR reactions past robust controls. No RT controls not shown. PCR amplicons of expected size identified following 1% agarose electrophoresis, stained with EtBr. Limiting cycles of PCR used: GAPDH, PSA & HSPA10 20x; MMP16 & S100P 25x; XAGE-1, GAGEB1, PTPRR, PTPBR7,PTP-SL, BTG1 & TMEFF2 30x;

regulation is an open question. In an attempt to gain an insight into the potential specificity for SIM2s regulation of these putative target genes from the microarray, LNCaP polyclonal cell lines with stable expression of the c-terminal myc tagged long isoform of mouse Sim2 (mSim2L.myc) and Sim1 (mSim1.myc) were engineered and assessed in a preliminary screen by sqRT-PCR for differential gene regulation. *PTPRR* gene expression was found to be up regulated in all SIM expressing cell lines, and similarly *S100P* expression appeared to be down regulated. Interestingly, the repression of *MMP16* appeared to be SIM2 specific, with mSim1.myc expression having little effect compared to Control. Likewise, the slight increase in *PSA* mRNA levels observed upon SIM2s.myc expression appeared to be SIM2 isoform specific as mSim2L.myc expression appeared to have no effect, yet the stable over expression of mSim1.myc did appear to result in a down regulation of PSA expression (**Figure 4.2B(i)**, compare lanes 2-5). There are two isoforms of PTPRR, the long isoform, PTPBR7, and the short, PTP-SL, that arise from alternate transcription start sites [150, 151]. The microarray oligonucleotide and validation PCR primers used for these studies do not differentiate between the two isoforms. Despite limited links to a role in tumour development in the literature, the dramatic change in expression levels upon SIM expression highlighted PTPRR as an interesting candidate as a direct target of SIM transcriptional activities. To identify if there was a SIM homologue specific profile of *PTPRR* isoform gene expression, both isoforms were analysed by sqRT-PCR in the stable SIM expressing LNCaP cell lines. Expression of the long isoform, *PTPBR7*, was unchanged upon SIM expression, whereas the short isoform, *PTP-SL* was dramatically up regulated, yet not in a SIM homologue or isoform specific manner (**Figure 4.2C**).

4.2.2.3. siRNA-mediated knock down studies to determine how intimately SIM2s expression is associated to the differential regulation of putative target genes in LNCaP cells.

Following the validation of differential gene regulation upon SIM2s.myc expression in LNCaP cells, assessing if the effect of ectopic SIM2s expression on the expression of these genes was indicative of endogenous SIM2s activities, and perhaps whether or not the regulation is the outcome of direct SIM2s-mediated transcription, was examined next. Both ectopic and endogenous SIM2s were targeted for siRNA knockdown in the LNCaP puromycin resistant Control and SIM2s.myc expressing cell lines not used in the microarray using synthesised double stranded siRNA oligonucleotides; siSIM2s-1759 to specifically target SIM2s, and a scrambled non-specific control oligonucleotide, siControl. The effect of 72 hours treatment with the siRNAs on *SIM2s* expression and on the expression levels of the putative targets was assessed by sqRT-PCR. **Figure 4.3**, **panel (i)** indicates an approximate reduction of endogenous and ectopic *SIM2s* mRNA levels of 50%. The up regulation of *S100P* expression detected upon endogenous and ectopic knockdown of SIM2s was consistent with SIM2s-mediated repression of *S100P* (**panel (ii)**). Interestingly, where the microarray and independent validation studies showed *MMP16* to be repressed upon SIM2s.myc expression, siRNA knockdown of SIM2s.myc resulted in a further reduction in *MMP16* levels, which was also reflected upon siRNA knockdown of endogenous SIM2s (**panel (iii)**). These results were inconclusive as to the nature of SIM2s-mediated regulation of *MMP16*, and thus further clarification studies are required if it is to be pursued in the future as a putative target of SIM2 regulation.

Unlike the regulation of *S100P*, the level of SIM2s.myc knockdown achieved had no effect on the induction of *PTP-SL*, which failed to be detectable in the LNCaP/Control cell line (**panel (iv)**). Similarly, no effect of SIM2s knockdown was observed on the expression levels of *PSA* (**panel (v)**). These preliminary data indicate that the induction of *PTP-SL* and PSA upon SIM2s.myc expression in LNCaP cells may not be a result of direct regulation by SIM2s, but perhaps a secondary or downstream effect of SIM2s expression.

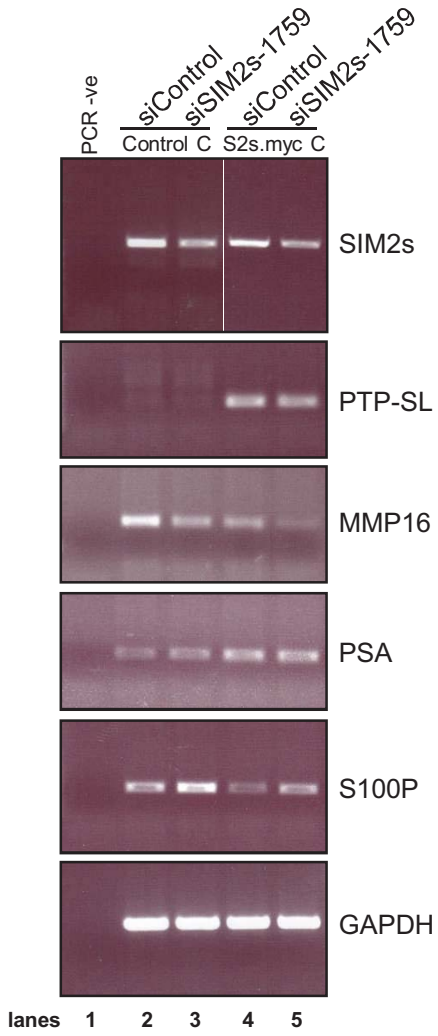

FIGURE 4.3: *S100P is a putative direct target of SIM2s activities in prostate carcinoma cell lines. Preliminary observations of the increase in S100P mRNA levels on siRNA knockdown of endogenous and ectopic SIM2s in LNCaP cells, whereas PTP-SL and PSA levels remain unchanged. MMP16 levels change conversely to expectations.*

Subconfluent cells were treated 2x100nM siRNA 24 hours apart, then total RNA was extracted 72hrs after first treatment followed by semi-quantitative RT-PCR analysis. Limiting cycles of PCR used: GAPDH, MMP16 & S100P 25x; PTP-SL 30x; endogenous SIM2s (lanes 2 & 3) 33x, ectopic SIM2s (lanes 4 & 5) 25x.

Or perhaps the absence of any effect on *PTP-SL* and *PSA* induction upon treatment with siSIM2s-1759 may also be indicative of the level of SIM2s knock down achieved was not sufficient to reduce SIM2s activities associated with the regulation of these genes.

Due to either inconsistent results or lack of any effect upon siRNA-mediated knockdown of SIM2s, *MMP16*, *PTP-SL* and *PSA*, were not further investigated as putative direct target genes of SIM2s transcription. The consistent results indicating *S100P* is down regulated in a SIM2s-responsive manner highlighted it as a potential candidate for future investigation.

4.2.3. Microarray studies in human prostate carcinoma DU145±SIM2s.myc cells

4.2.3.1. Analysis of microarray data and independent validation studies.

As outlined in **figure 4.1**, a second microarray experiment of the same design as that for LNCaP cells was planned for another prostate carcinoma derived cell line, DU145, to not only validate the LNCaP microarray, but to ultimately identify a common gene set that is regulated in a SIM2s-dependent manner in prostate cancer. The outcome of combined statistical analysis of these two experiments will be detailed in **section 4.2.4**, however, consideration of these data is only relevant following the internal validation of the microarray profiling changes in gene expression upon SIM2s.myc expression in DU145 cells. As was carried out for the LNCaP microarray data set (**section 4.2.1**), the following studies sought to determine if the changes in gene expression upon ectopic SIM2s.myc in DU145 cells by microarray were consistent by sqRT-PCR detection in an independent polyclonal cell line. A select number of putative target genes were analysed due to links and implications in the literature that connect these genes to tumourigenesis and the degree of change in expression levels upon SIM2s.myc expression. Of particular interest was *PHLDA1*/*TDGA51* (pleckstrin homology-like domain, family A, member 1/T-cell death-associated gene 51), which was

represented twice, by two independent oligonucleotides for detecting this gene, inside the top 10 ranking genes, at position 5 and 8, indicating a consistent 2.3-fold down regulation upon stable SIM2s expression in the DU145 cells (**Table 4.2**). In itself this representation inside the data list is a form of internal validation, and consistently, was found to have reduced expression in an independent SIM2s.myc over-expressing DU145 polyclonal cell line by sqRT-PCR (**Figure 4.4A(i)**). At the time of these studies the literature did link PHLDA1 with prostate or colon cancers, however, reports existed of increased *PHLDA1* expression in pancreatic cancer [152, 153]. These studies were in apparent opposition to how enhanced levels of SIM2s may correlate to PHLDA1 levels in pancreatic cancer. Yet *PHLDA1* remained an intriguing subject as a putative target of SIM2s as it had been described to play an essential role in the induction of apoptosis in T-cells [154], and its down regulation was associated with resistance to apoptosis in melanoma [155], which may reflect cancer specific roles. The role of PHLDA1 in apoptosis was a key indicator suggesting that putative SIM2s-mediated down regulation of a pro-apoptotic factor as a potential mechanism by which SIM2s may promote prostate and/or colon tumour growth. Likewise, the reduced levels of the established pro-cell death factor *BNIP3* (BCL2/adenovirus E1B 19kD-interacting protein 3) [156-158] upon SIM2s expression observed from the microarray (**Table 4.2**, rank 14), and independently validated (**Figure 4.4A(ii)**), also provides a potential mechanism for SIM2s-mediated resistance to tumour cell death. And again similiarly, the stress inducible *IER3/IEX-1* (immediate early response gene X-1), which functions to promote cell death when over expressed, was also confirmed to be repressed upon ectopic SIM2s.myc expression (**Table 4.2**, rank 96 2.46-fold down regulation, and **Figure 4.4A(iii)**). Repression of *IEX-1* is associated with reduced apoptosis, however, other varied roles for IEX-1 have also been described in cell cycle regulation and particularly, cell survival. Interestingly, these pro- and anti-apoptotic activities occur in a cell context and stress-specific manner (for review [159]).

TABLE 4.2: *Top 30 differentially regulated genes, plus others of interest, on expression of SIM2s in human prostate DU145 cells.*

Rank	ID	Name – all Homo sapiens	Fold Change	+ SIM2s	M	A	P.Value	B
1	NM_005069	single-minded (Drosophila) homolog 2 (SIM2), transcript variant SIM2, mRNA	32.90	Up	5.04	12.31	0.000001	8.49
2	AF278532	beta-netrin mRNA, complete cds	3.78	Down	-1.92	9.89	0.002	5.92
3	NM_001432	epiregulin (EREG) mRNA	2.97	Down	-1.57	10.63	0.002	5.59
4	NM_003954	mitogen-activated protein kinase kinase kinase 14 (MAP3K14), mRNA	1.84	Up	0.88	10.21	0.003	5.31
5	NM_007350	pleckstrin homology-like domain, family A, member 1 (PHLDA1), mRNA	2.28	Down	-1.19	10.41	0.005	4.76
6	NM_002539	ornithine decarboxylase 1 (ODC1) mRNA	2.99	Up	1.58	13.34	0.005	4.47
7	X75684	T ransmembrane 4 L six family member 1 (TM4SF1) (TL27) mRNA	1.82	Down	-0.87	13.17	0.006	4.36
8	AK026181	Pl eckstrin homology-like domain, family A, member 1, mRNA (PHLDA1)	2.30	Down	-1.20	10.75	0.006	4.33
9	NM_001975	enolase 2, (gamma, neuronal) (ENO2), mRNA	1.72	Down	-0.78	10.56	0.007	4.22
10	M59040	Human cell adhesion molecule (CD44) mRNA, complete cds	1.89	Down	-0.92	10.88	0.007	4.05
11	NM_014767	sparc/osteonectin, cwcv & kazal-like domains proteoglycan (testican) 2 (SPOCK2)	6.11	Up	2.61	10.34	0.007	4.01
12	NM_005100	A kinase (PRKA) anchor protein (gravin) 12 (AKAP12), mRNA	1.87	Down	-0.90	10.43	0.015	3.45
13	NM_000291	phosphoglycerate kinase 1 (PGK1) mRNA	2.14	Down	-1.10	11.96	0.026	2.97
14	NM_004052	BCL2/adenovirus E1B 19kD-interacting protein 3 (BNIP3), mRNA	2.14	Down	-1.10	11.87	0.035	2.69
15	AF043290	Lymphocyte membrane associated protein (8B7) mRNA, complete cds	1.83	Up	0.87	9.31	0.043	2.45
16	NM_001748	calpain, large polypeptide L2 (CAPN2) mRNA	1.78	Down	-0.83	11.86	0.043	2.42
17	NM_003280	Troponin C, slow (TNNC1) mRNA	1.94	Up	0.96	10.58	0.046	2.33
18	NM_002610	pyruvate dehydrogenase kinase, isoenzyme 1 (PDK1), mRNA	1.52	Down	-0.60	9.74	0.051	2.16
19	NM_001423	epithelial membrane protein 1 (EMP1) mRNA	1.69	Down	-0.76	8.89	0.051	2.16
20	AB037784	arylacetamide deacetylase-like 1 (AADACL1), partial cds	1.52	Down	-0.60	10.21	0.052	2.10
21	NM_014391	cardiac ankyrin repeat protein (CARP), mRNA	2.08	Up	1.06	12.58	0.061	1.84
22	AJ008139	NIK gene, exon 3, 3'	1.47	Up	0.56	10.26	0.065	1.82
23	AK023772	Thrombospondin, type I, domain containing 4 (THSD4)	1.80	Down	-0.85	10.08	0.065	1.81
24	NM_015956	CGI-28 protein (LOC51073), mRNA	1.58	Up	0.66	12.33	0.072	1.69
25	NM_006824	nucleolar protein p40 (P40), mRNA	2.45	Up	1.29	12.35	0.081	1.50
26	NM_000700	annexin A1 (ANXA1) mRNA	1.51	Down	-0.60	12.04	0.081	1.48
27	NM_003479	protein tyrosine phosphatase type IVA, member 2 (PTP4A2) mRNA	1.60	Down	-0.68	11.38	0.081	1.46
28	Z24725	mitogen inducible gene mig-2, complete CDS	1.55	Up	0.63	11.82	0.081	1.46
29	AK023015	WD repeat domain 54 (WDR54)	1.58	Down	-0.66	10.66	0.090	1.35
30	NM_001255	Cell division cycle 20, S.cerevisiae homolog (CDC20) mRNA	1.51	Up	0.60	12.16	0.090	1.31
36	AK001362	discoidin, CUB and LCCL domain containing 2 (DCBLD2)	2.35	Down	-1.23	10.64	0.108	1.01
42	NM_005749	Transducer of ERBB2 1 (TOB1), mRNA	1.64	Down	-0.71	11.89	0.122	0.76
50	NM_002276	keratin 19 (KRT19) mRNA	2.07	Down	-1.05	11.61	0.131	0.56
63	NM_004789	LIM HOX gene 2 (LHX2) mRNA	2.17	Up	1.12	10.00	0.168	0.12
71	D29810	discoidin, CUB and LCCL domain containing 2 (DCBLD2)	2.58	Down	-1.37	13.01	0.192	-0.09
76	NM_001657	amphiregulin (schwannoma-derived growth factor) (AREG) mRNA	2.38	Down	-1.25	12.44	0.218	-0.26
78	NM_014585	solute carrier family 11, member 3 (SLC11A3), mRNA	3.18	Up	1.67	9.47	0.218	-0.30
96	NM_003897	Immediate early response 3 (IER3), mRNA	2.46	Down	-1.30	11.52	0.262	-0.66
122	NM_001912	cathepsin L (CTSL) mRNA	2.33	Down	-1.22	11.41	0.275	-0.92
151	NM_003843	sciellin (SCEL) Mrna [contains LIM domain]	3.12	Down	-1.64	10.93	0.292	-1.14

Independently validated putative targets by sqRT-PCR highlighted in red. Raw data supplied from the Adelaide Microarray Centre, SA. The M value is the log2 ratio between the 2 samples, and the A value is the average intensity in both channels (log2), across all the microarrays. The B value is a log-odds score. Statistical P-value shown in both tables. Significance, $P \leq 0.05$.

The microarray of the top thirty differentially regulated genes showed a predominance of down regulation upon SIM2s.myc expression (**Table 4.2**), however strikingly, greatest fold-change observed in expression levels was the up regulation of *SPOCK2* (sparc/osteonectin, cwcv & kazal-like domains proteoglycan (testican) 2) by 6-fold (**Table 4.2**, rank 11). Independent validation consistently showed enhanced *SPOCK2* mRNA levels upon ectopic expression of SIM2s in DU145 cells (**Figure 4.4A(iv)**). This level of differential regulation highlighted *SPOCK2* as a putative target gene of interest, also supported by a report that SPOCK2 is required to facilitate cell migration in human glioma U251 cells by inhibiting interference of membrane-type 1 matrix metalloproteinase (MT1-MMP) [160], the latter of which has been shown to promote prostate DU145 and LNCaP cell *in vitro* migration and xenograft metastasis, and is a suggested target for preventing cancer metastasis [161]. Considered together, the interesting hypothesis arises that perhaps enhanced levels of SIM2s indirectly promote MTI-MMP-mediated mechanisms of cell migration via the up regulation of *SPOCK2* to aid aggressive prostate cancer development. Interestingly, the SIM2s-associated repression of *Epiregulin* (*EREG*) (**Table 4.2**, rank 3, 2.97-fold down regulation, and **Figure 4.4A(v)**), and *AREG* (*amphiregulin*) (**Table 4.2**, rank 76, an unvalidated fellow EGF family ligand for ERBB family receptors which clusters in the same region of chromosome 4 with *EREG* [162]), also supports a putative role for SIM2s in the development of the more aggressive prostate tumours. Specifically, a study by Tørring et al (2005) revealed that AREG and EREG are upregulated in human prostate CWR22 cell mouse xenografts following castration, a process which ultimately lead to a decrease in tumour size [163], indicating that elevated levels of EREG and AREG levels are associated with hormone-sensitive prostate tumour cell-death processes. Similarily, *EREG* expression was found to be elevated upon microarray analysis of prostate carcinoma PC3 cells treated with MG132, an agent found to promote prostate tumour cell death [164], thus also associating elevated EREG with cell death processes. These findings considered in reference to the correlation bewteen SIM2s expression and repressed *EREG* and *AREG* mRNA levels, provides a preliminary basis for the notion of a putative mechanism by which SIM2s inhibits the up

regulation of these ligands via their transcriptional repression, which consequently renders the tumour insensitive to androgen-ablation therapy, thus providing the opportunity for the tumour to transform into a recurrent aggressive androgen-insensitive tumour. Unfortunately, this link does not apparently translate to a potential role for SIM2s in the development of pancreatic cancers where both ligands have been reported to be upregulated [152, 165]. Indeed EREG is reported to stimulate pancreatic cancer cell growth [165]. Despite not fulfilling the profile of a putative target through which SIM2s-mediated regulation may drive the progression of prostate and pancreatic solid tumours, the high ranking nature and extent of change in gene regulation indicated in the microarray data, highlighted it as an interesting candidate for investigation.

In summary, putative SIM2s target genes selected from the DU145 microarray data for independent validation by sqRT-PCR included, *PHDA1/TDAG51*, *BNIP3*, *IER3/IEX-1*, *SPOCK2* and *EREG*. All genes displayed the same mode of differential regulation upon stable ectopic SIM2s expression in an independent polyclonal cell line consistent with that observed in the microarray.

4.2.3.2. Investigating the SIM specificity of putative target gene regulation in DU145 cells

To discern if other Sim species might also regulate the target genes obtained by microarray , a selection of the independently validated putative SIM2s targets were assessed for mRNA expression upon stable ectopic expression of carboxy-terminally myc tagged murine orthologues of full length Sim2 (mSim2L.myc) and Sim1 (mSim1.myc) in DU145 cells. These preliminary studies revealed that the mRNA levels of *BNIP3* were found to be slightly reduced upon expression of all SIM homologues. However, human SIM2s conferred greater repression than mSim2L, and yet interestingly, a similar level of reduced BNIP3 was observed upon both mSim1 and hSIM2s expression (**Figure 4.4B(i)**), indicating that the regulation of BNIP3 may be a shared gene target of all SIM factors. *EREG* expression was found to be repressed to the same

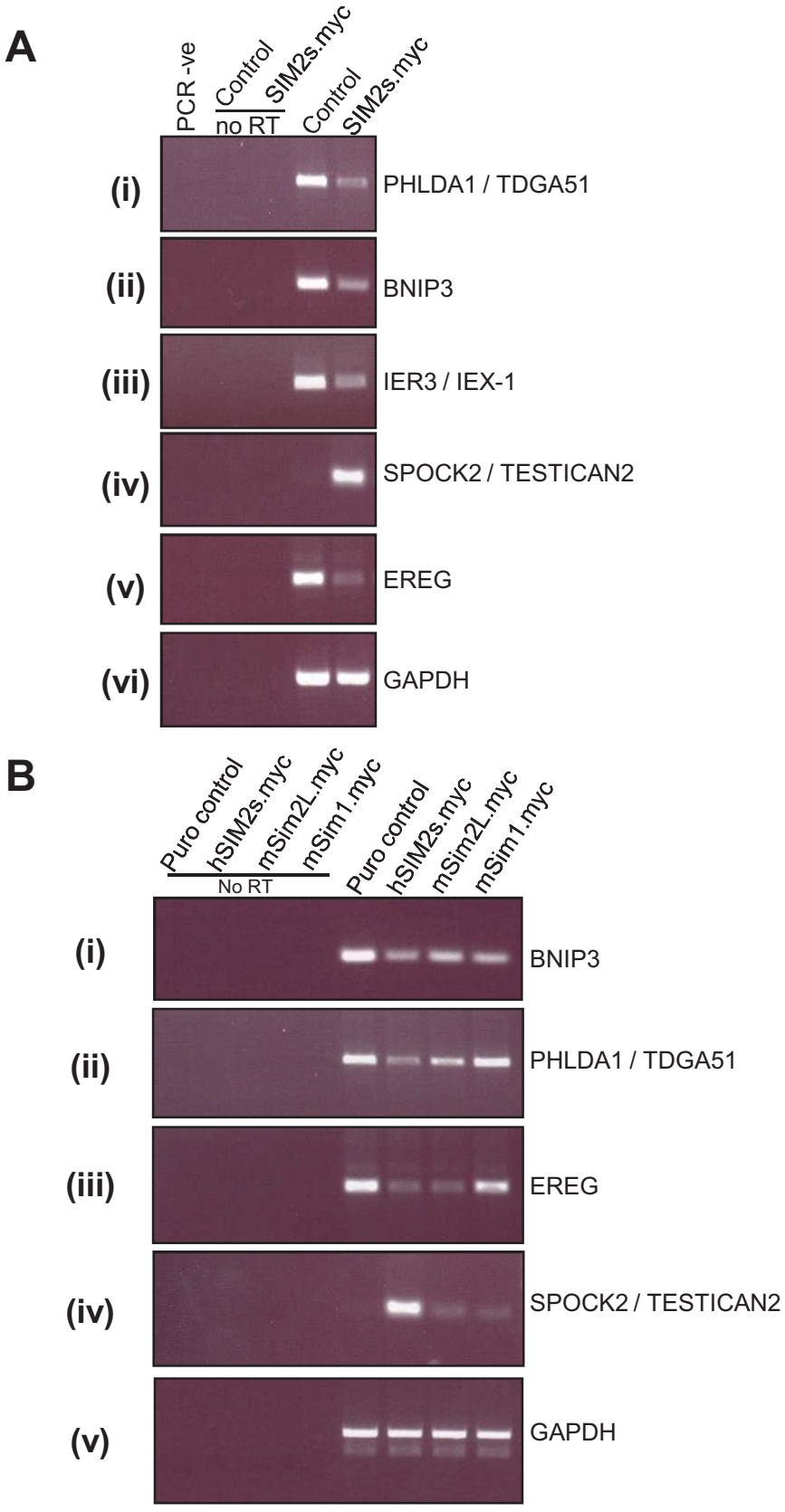

FIGURE 4.4: (A) *Independent validation of candidate SIM2s target genes identified from microarray studies on prostate DU145±SIM2s.myc expression. (B) Preliminary investigation into specificity of differential gene regulation by mammalian SIM homologues stably expressed in DU145 cells.*

cDNA from independently derived polyclonal DU145 cell line for human SIM2s.myc expression, not used in the microarray, or with stable ectopic expression of murine SIM2Long.myc and mSIM1.myc, analysed by semi-quantitative RT-PCR to validate the differential regulation of observed in microarray analyses, compared to a polyclonal puromycin resistant Control cell line. Limiting cycles of PCR used: GAPDH & BNIP3 25x, all others 28x.

extent by both isoforms of SIM2, however was unaffected by mSim1 expression (**Figure 4.4B(ii)**). Likewise, mSim1 expression had no effect on *PHLDA1* mRNA levels, thus *PHLDA1* is repressed in a manner specific to SIM2, and from this experiment, most potently by human SIM2s (**Figure 4.4B(iii)**). Interestingly, the striking upregulation of *SPOCK2* expression was found to be specific to the short isoform of SIM2 (**Figure 4.4B(iv)**). Due to absence of any effect on mRNA levels associated with ectopic mSim1 expression, these latter three genes may be interesting candidates for the future study of SIM2 transcriptional specificity that may perhaps lead to insights of how these non-redundant family members function in development.

4.2.4. SIM2s-mediated regulation of a prostate cancer 'gene set'?

4.2.4.1. Combined analysis of LNCaP and DU145 microarray data & Limitations of microarray analyses

In an effort to identify a direct target gene(s) of SIM2s transcription common to prostate cancer development microarray data of differential gene regulation upon stable ectopic expression of SIM2s from two prostate carcinoma derived cell lines, LNCaP and DU145 cells, were subjected to composite statistical analysis, carried out the Adelaide Microarray Centre, SA, to derive if common patterns of gene regulation occurred between the cell lines to eliminate potential cell-type specific responses. Initial inspection of the independent lists does not reveal any striking similarity in the ranking profile of differential gene regulation between the two microarray experiments (refer to **Tables 4.1 & 4.2**). **Table 4.3A** lists the top thirty genes derived from composite analysis of both microarray experiments. It is interesting to observe in the top thirty differentially regulated genes from combined analysis shows some genes that are common to those shown in either **table 4.1** or **4.2**, representing genes of interest from each of the LNCaP or DU145 microarray data sets, respectively, but not to both (refer to highlighted examples in **Table 4.3A**). **Table 4.3B** contains a list of

selected putative target genes of interest from each microarray experiment, including those independently validated, as they were found to be differentially regulated upon combined analysis. The down regulation of *PHLDA1*, first identified from the DU145 microarray experiment, was shown to rank highly upon combined analysis (**Table 4.3A**, rank 7, ↓1.8-fold). As indicated in the far right column of **Tables 4.3A & B**, *PHLDA1* also appears to be down regulated in LNCaP cells upon SIM2s expression, however ranking very low at 689, with only 1.5-fold reduction in mRNA levels. However, when gene expression of *PHLDA1* was assessed in LNCaP±SIM2s.myc cells, *PHLDA1* mRNA failed to be detected (**Figure 4.5**, panel ii, lanes 9 & 10). Interestingly, where the combined analyse show *SPOCK2* to be up regulated an average of 2.6-fold upon combined analysis, analysis of the individual data sets reveals that *SPOCK2* mRNA levels are unchanged in LNCaP/SIM2s.myc cells, confirmed by independent sqRT-PCR validation (**Figure 4.5**, panel i, lanes 9 & 10), which indicates the combined analyses is revealing misleading indicators of shared modes of regulation of putative target genes across both cell lines. In a similar manner, combined analysis indicates *IER3/IEX-1* is downregulated in both cell lines, however examination of microarray data from LNCaP cells indicates *IER3* expression levels remain unchanged in LNCaP/SIM2s.myc cells (**Table 4.3B**), and indeed, are undetectable by sqRT-PCR in LNCaP cells (**Figure 4.5**, panel iv, lanes 9 &10). Together these findings not only reveal distinct differences in the genetic profiles of these two prostate carcinoma derived cell lines, but also the limitation or flaw in the way the results of the combined assessment of the two microarray experiments transpire. Namely it appears these results largely represent the average of fold change observed between each microarray. Thus dramatic changes observed in either microarray data set, such as the 6.11-fold increase of *SPOCK2* in DU145/SIM2s.myc cells, would bias the result and instead of ranking genes in a fashion showing consistent modes and degree of differential gene regulation upon ectopic SIM2s expression shared between the two microarray experiments, inappropriately attributes a shared degree of differential regulation. Indeed the absence of statistical significance of these combined analyses, as indicated by the P value, beyond the first gene listed below SIM2s, *H4FN* (H4 histone family,

TABLE 4.3

(A) *Top 30 differentially regulated genes from combined analysis of LNCaP and DU145 microarray data upon SIM2s.myc expression.*

Rank	ID	Name - all Homo sapiens	Fold Change	+ SIM2s	P.Value	Rank position & fold change in individual arrays
1	NM_005069	single-minded (Drosophila) homolog 2 (SIM2), transcript variant SIM2, mRNA	28.2	Up	7.6E-07	
2	NM_003548	H4 histone family, member N (H4FN) mRNA	1.5	Up	0.07	
3	NM_002812	proteasome (prosome, macropain) 26S subunit, non-ATPase, 8 (PSMD8)	1.4	Up	0.35	
4	NM_001975	enolase 2, (gamma, neuronal) (**ENO2**), mRNA	1.5	Down	0.35	DU145: #9 ↓1.72 / LNCaP:
5	L02922	Human tropomyosin isoform hTM5a mRNA, exon 1	1.4	Up	0.35	
6	X75684	Transmembrane 4 L six family member 1 (TM4SF1). (**TL27**)	1.8	Down	0.35	DU145: #7 ↓1.8 / LNCaP:
7	NM_007350	Pleckstrin homology-like domain, family A, member 1 (**PHLDA1**)	1.8	Down	0.35	DU145: #5 & #8 ↓2.3 / LNCaP: #689 ↓1.5
8	NM_004457	Fatty-acid-Coenzyme A ligase, long-chain 3 (**FACL3**) mRNA	1.4	Up	0.35	LNCaP: # 11 ↑1.6 / DU145:
9	NM_017606	zinc finger protein 395 (ZNF395), mRNA.	1.3	Down	0.35	
10	NM_006287	Tissue factor pathway inhibitor (TFPI), mRNA	1.3	Down	0.44	
11	U81001	Human SNRPN mRNA, 3' UTR, partial sequence	1.3	Up	0.48	
12	NM_006579	emopamil-binding protein (sterol isomerase) (EBP), mRNA	1.3	Up	0.48	
13	NM_003528	H2B histone family, member Q (H2BFQ)	1.4	Up	0.57	
14	NM_006010	arginine-rich, mutated in early stage tumors (ARMET)	1.2	Up	0.58	
15	NM_005749	Transducer of ERBB2, 1 (**TOB1**), mRNA	1.4	Down	0.62	DU145: #42 ↓1.64 / LNCaP:
16	NM_006219	phosphoinositide-3-kinase, catalytic, beta polypeptide (PIK3CB) mRNA	1.2	Up	0.62	
17	NM_001539	heat shock protein, DNAJ-like 2 (HSJ2) mRNA	1.2	Up	0.62	
18	X75692	H.sapiens (TL21) mRNA from LNCaP cell line. Dystonin (DST)	1.2	Up	0.62	
19	NM_018490	G protein-coupled receptor 48 (GPR48), mRNA	1.3	Up	0.62	
20	NM_016040	CGI-100 protein (LOC50999), mRNA	1.2	Up	0.62	
21	AK023971	cDNA FLJ13909 fis, clone Y79AA1000065. ch16 open reading frame 59	1.3	Down	0.62	
22	NM_001355	D-dopachrome tautomerase (DDT), mRNA	1.3	Up	0.62	
23	NM_001874	carboxypeptidase M (CPM), mRNA	1.4	Down	0.62	
24	NM_012229	5'-nucleotidase (purine), cytosolic type B (NT5B), mRNA	1.2	Up	0.62	
25	NM_016418	neurofibromin 2 (merlin) (NF2)	1.3	Up	0.62	
26	NM_005643	TATA box binding protein-associated factor, RNA pol II, I, 28kD (TAF2I)	1.2	Up	0.62	
27	AK026874	cDNA: FLJ23221 fis, clone ADSU01965. ch1 open reading frame 54	1.2	Down	0.62	
28	NM_003543	H4 histone family, member H (H4FH) mRNA	1.6	Up	0.62	
29	AJ011409	mRNA for hypothetical protein, partial. ch21 open reading frame 104	1.3	Down	0.62	
30	NM_006597	heat shock 70kD protein 10 (HSC71) (**HSPA10**) (HSPA8), mRNA	1.6	Up	0.62	LNCaP: # 13 ↑1.7 / DU145:
		Positions in independent array lists:				
		DU145/S2s array				
67	NM_003548	Homo sapiens H4 histone family, member N (H4FN) mRNA	1.30	Up	0.186	
		LNCaP/S2s array				
6	NM_003548	Homo sapiens H4 histone family, member N (H4FN) mRNA	1.7	Up	-	

TABLE 4.3 continued.
(B) *Ranked positions of selected putative targets of interest from independent LNCaP & DU145 microarrays upon Combined microarray analysis.*

Rank	ID	Name - all Homo sapiens	Fold Change	+SIM2s	P.Value	Rank position & fold change in individual arrays
7	NM_007350	**PHLDA1**	1.8	Down	0.35	DU145: #5 & #8 ↓2.3 / LNCaP: #689 ↓1.5
32	NM_001432	**EREG**	1.9	Down	0.62	DU145: #3 ↓2.97 / LNCaP: #1563 ↓1.2
36	AJ008139	NIK gene, exon 3, 3'	1.3	Up	0.62	
76	NM_003785	**GAGEB1**	1.8	Down	0.62	
109	NM_003954	mitogen-activated protein kinase kinase kinase 14 (MAP3K14)	1.4	Up	0.62	
118	AK001362	discoidin, CUB and LCCL domain containing 2 (DCBLD2)	1.7	Down	0.62	
121	NM_016192	**TMEFF2**	1.6	Down	0.62	
177	M59040	Human cell adhesion molecule (CD44)	1.4	Down	0.62	
201	NM_014391	Cardiac ankyrin repeat protein (CARP)	1.5	Up	0.62	
240	NM_002610	pyruvate dehydrogenase kinase, isoenzyme 1 (PDK1)	1.3	Down	0.62	
254	NM_002276	Keratin 19 (KRT19) mRNA	1.5	Down	0.62	
281	NM_014767	**SPOCK2**	2.6	Up	0.62	DU145: #11 ↑6.11 / LNCaP: #14497 ↑1.0
309	NM_002539	ornithine decarboxylase 1 (ODC1)	1.7	Up	0.62	
323	AF278532	beta-netrin mRNA	2.0	Down	0.63	
327	S75755	PSA	1.6	Up	0.63	
371	NM_001657	amphiregulin (schwannoma-derived growth factor) (AREG)	1.7	Down	0.65	
409	NM_005941	MMP16	1.4	Down	0.66	
421	NM_002849	PTPRR	1.9	Up	0.66	
596	NM_004052	**BNIP3**	1.5	Down	0.67	DU145: # 14 ↓2.14 / LNCaP: #2777 ↓1.2
606	NM_003897	**IER3**	1.7	Down	0.67	DU145: # 96 ↑2.46 / LNCaP: #9176 ↓1.1
650	NM_005980	**S100P**	1.4	Up	0.68	LNCaP: # 10 ↑2.0 / DU145: # 12777 ↓1.04
833	NM_001912	cathepsin L (CTSL)	1.6	Down	0.69	
895	NM_020411	XAGE-1	1.6	Down	0.70	
1114	NM_006824	nucleolar protein p40 (P40)	1.5	Up	0.75	
1125	NM_000291	phosphoglycerate kinase 1 (PGK1)	1.4	Down	0.75	
1161	AK022868	axin interactor, dorsalisation associated (AIDA)	1.4	Up	0.75	
1621	D29810	discoidin, CUB and LCCL domain containing 2 (DCBLD2)	1.5	Down	0.79	
1676	NM_004789	LIM HOX gene 2 (LHX2)	1.4	Up	0.79	
2711	NM_001731	BTG1	1.2	Down	0.84	
3608	AL137506	ELOVL7	1.2	Up	0.85	

(A) Genes of interest due to appearance in top 30, or high differential regulation from both LNCaP or DU145 microarray data highlighted in bold. (B) Genes analysed from the DU145 and LNCaP microarrays across three prostate cell lines by sqRT-PCR are indicated in green and blue, respectively. Raw data supplied from the Adelaide Microarray Centre, SA. Statistical P-value shown in both tables. Significance, $P \leq 0.05$.

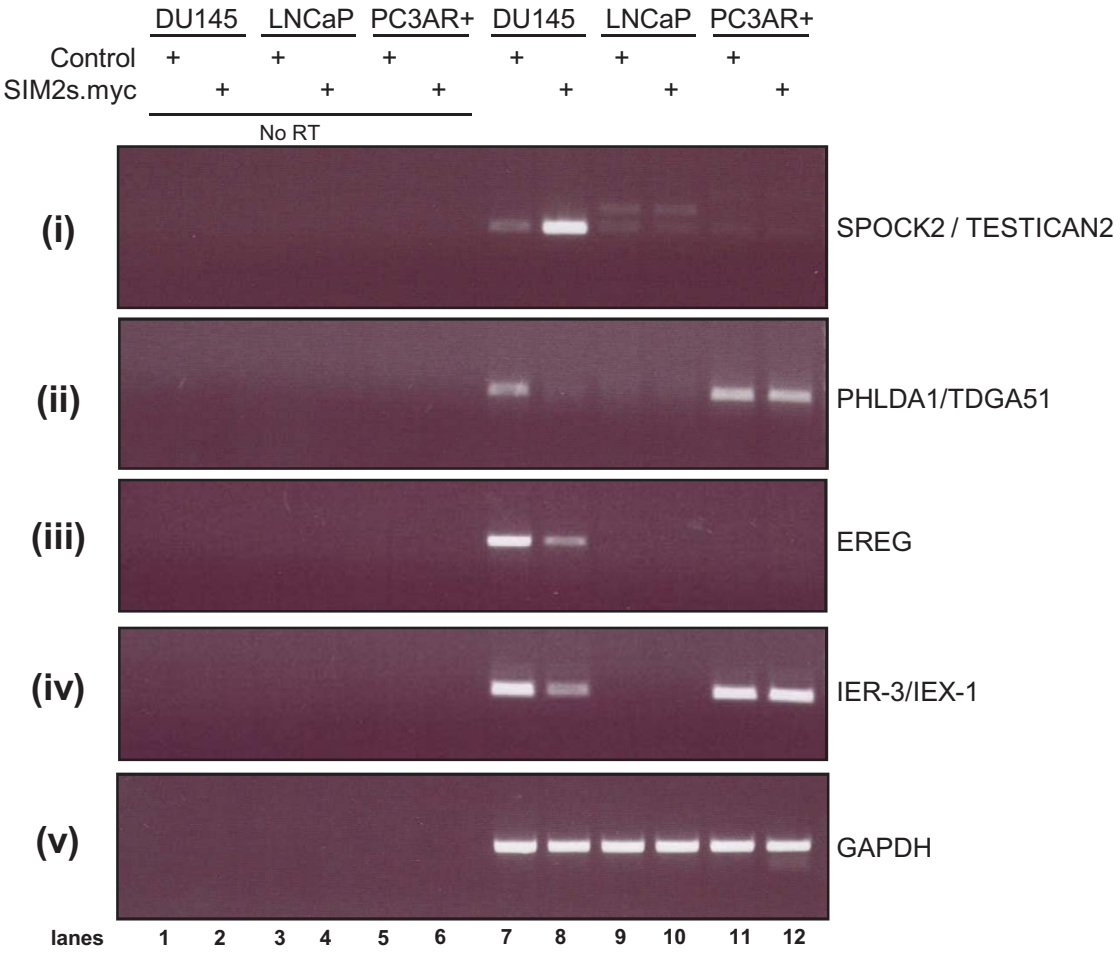

FIGURE 4.5: *Differences in the genetic expression profiles between prostate carcinoma derived cell line lines revealed upon semi-quantitative RT-PCR assessment of differential regulation of putative SIM2s targets from DU145±SIM2s.myc microarray in LNCaP and PC3AR+ prostate carcinoma cell lines with, or without, stable ectopic expression of human SIM2s.myc.*

cDNA from independently derived polyclonal human DU145, LNCaP & PC3AR+ cell lines ± human SIM2s.myc expression, analysed by semi-quantitative RT-PCR to validate the differential regulation of genes found from DU145 microarray studies, compared to a polyclonal puromycin resistant Control cell lines. GAPDH gene expression serves as loading control. No RT controls shown. Limiting cycles of PCR used: GAPDH 25x, SPOCK2/TESTICAN2 30x, all others 28x.

member N, **Table 4.3A**), is a supporting indicator that the fold-changes in gene expression level reported upon combined analysis are not necessarily representative differential gene regulation in both cell lines.

4.2.4.2 Close examination of differential gene regulation of putative SIM2s target genes in LNCaP, DU145 and PC3AR+ prostate carcinoma derived cell lines

As the combined analysis of the LNCaP and DU145 microarray data sets failed to provide indicators of shared modes of gene regulation upon SIM2s expression, these studies were extended a little further to definitively ascertain if the putative SIM2s target genes of interest from each microarray are cell-type specific or not. As afore mentioned, a common mode of transcriptional regulation across a number of independently derived prostate carcinoma cell lines would provide a compelling indicator that misregulation of that gene is commonly associated to SIM2s misexpression, and perhaps consequently to prostate carcinogenesis. Highlighted in **table 4.3B** are the putative target genes of interest chosen from each microarray experiment which were analysed for differential regulation by sqRT-PCR upon stable ectopic expression of SIM2s in LNCaP, DU145 and a third prostate carcinoma derived cell line, PC3AR+ cells. These were selected due to the degree of differential regulation found in their respective microarray experiments, and/or for their connection to a potential role for SIM2s in solid tumours, with the aim to exclude cell-type specific changes in gene regulation and determine if any may link SIM2s to prostate tumourigenesis in general. Of the selected putative targets identified and validated from the DU145 microarray shown in **Figure 4.4**, none displayed a shared mode differential regulation across all prostate carcinoma cell lines, in fact all where highly divergent between cell lines (**Figure 4.5**). The findings from this limited screen ultimately excluded these putative target genes from further investigation at this time as it was within these stringent parameters that a future gene candidate for studying the transcriptional roles of SIM2s would be conducted. The global assessment of the transcriptome across many prostate tumour

samples and derived cell lines compared to normal controls [93, 166], have thus far only been published in part. Access to these entire data sets would have greatly aided definitively ascertaining if there is indeed a correlation between high levels of SIM2s in prostate cancers and the observed levels of these putative targets. If such analyses are conducted in the future, this may provide supporting evidence for distinguishing between the differential gene regulation observed in DU145/SIM2s.myc cells as being cell-type specific or perhaps reflective of gene regulation events occurring in tumours where SIM2s is aberrantly up regulated. Until such analyses, these candidate putative target genes remain the potential subject of future investigation.

4.2.4.3 S100P and BNIP3 are differentially regulated in a consistent manner in LNCaP, DU145 and PC3AR+ prostate cancer cells upon stable ectopic expression of SIM2s

Interestingly, the predominant down regulation of *S100P* initially observed in LNCaP/SIM2s.myc cells was also found to occur in DU145/SIM2s.myc cells by PCR despite the DU145 microarray data indicating no change (**Figure 4.6**, and refer to **Table 4.3B**). The down regulation of *S100P* was also further validated in PC3AR+/SIM2s.myc cells (**Figure 4.6**). These data support the notion that *S100P* gene expression is regulated in a SIM2s-responsive manner. Unfortunately, the predominant repressive mode of *S100P* gene regulation due to SIM2s expression does not link a functional role for SIM2s into the genetic fingerprint of prostate, pancreatic or gastric cancer development where S100P is found to be upregulated [148, 149, 167-169]. Consequently, *S100P* was not studied further as a putative target of SIM2s transcription in this solid tumour context. Whether this change in *S100P* expression in response to SIM2s reflects mechanisms of regulation that may occur in an alternate context to tumourigenesis, such as during certain developmental processes, remains an open question.

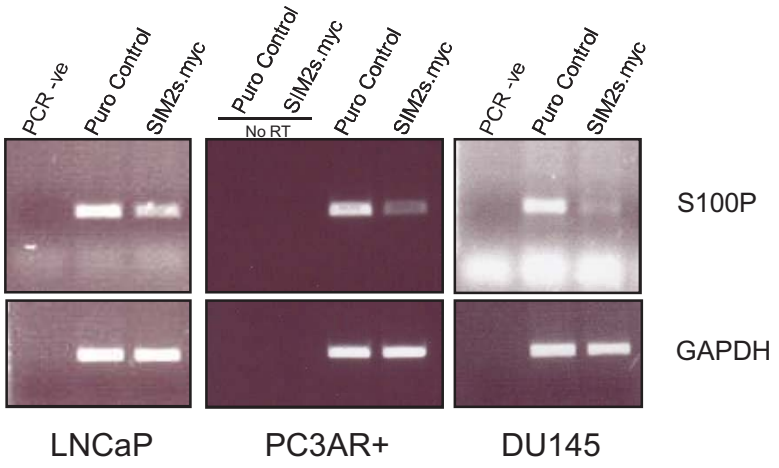

FIGURE 4.6: *S100P mRNA is found to be repressed on stable SIM2s.myc expression in the three independent prostate carcinoma cell lines, LNCaP, PC3AR+ and DU145*

Semi-quantitative RT-PCR analysis of S100P mRNA levels in polyclonal cell lines with stable expression of myc tagged SIM2s, compared to puromycin resistant Control lines as indicated. GAPDH indicates equal loading. * = primer dimers. GAPDH mRNA detected using 25x (limiting) cycles of PCR, S100P levels detected in LNCaP & PC3AR+ cDNA samples using 25x cycles, and 30x cycles in DU145 cDNAs.

Of all the putative validated target genes investigated, one did fit the proforma for further investigation as a direct target of SIM2s transcription. Message levels of the pro-cell death gene, *BNIP3*, where found to be repressed upon stable ectopic expression of SIM2s in all three prostate tumour lines tested (data not shown and **Figure 5.1**, **Chapter 5**), in a manner consistent with that indicated by the microarray data (see summary notes in **Table 4.3B**). Interestingly, in an independent study by others *BNIP3* message levels were also reported to increase 2.3-fold upon antisense knock down of SIM2s in colon carcinoma RKO cells by microarray [91], thus providing supportive data consistent for SIM2s-mediated repression of *BNIP3* expression. Likewise, microarray analysis of 293T cells with stable ectopic expression of the constitutively active mSim2/AD.myc protein, which contains the activation domain (AD) of mouse AhR in place of the Sim2L C-terminal repression regions, revealed a 1.55-fold increase in *BNIP3* mRNA (S. Woods, PhD thesis 2004), which again supports the notion that *BNIP3* gene expression may be regulated in a SIM2 responsive manner. These microarray findings, and the independent validation studies shown here, provided consistent indicators of SIM2-mediated regulation of *BNIP3* and consequently a compelling basis for further study investigating the notion that SIM2s-mediated repression of the pro-cell death factor BNIP3 may functionally link high levels of SIM2s expression with tumour cell survival. These studies are described in **Chapter 5**.

4.2.5 Identifying inherent limitations of sensitivity in the microarray approach used for the present study

It was apparent upon analysis of all the microarray data that the fold changes in gene expression reported did not consistently correspond to the change in levels observed upon sqRT-PCR analysis. Particular examples of note include the distinct 'switching on' of *SPOCK2* in DU145/SIM2s.myc cells (see **section 4.2.3**). The microarray data indicated a 6-fold increase in levels upon SIM2s expression, however,

SPOCK2 mRNA was undetectable in the Control cell line following 40 cycles of PCR (refer to **Figure 4.5**). Another example; the absence of any report of a change in the expression of *S100P* in DU145/SIM2s.myc cells by microarray which was indeed evident upon PCR detection (refer to **Figure 4.6**, and **Table 4.3B**), and as was discussed in the previous chapter (**Chapter 3**), the consistently observed up regulation in *ARNT2* mRNA levels in response to ectopic SIM2s.myc expression in both LNCaP and DU145 cells was not detected by microarray (data not shown). This is clearly evident upon comparison of the reported difference in SIM2 levels between the Control and SIM2s.myc cell lines by microarray, and the fold-change calculated following quantitative-PCR (qPCR) analysis. The microarray oligonucleotide for the detection SIM2 does not differentiate between ectopic or endogenous SIM2, or between the two isoforms. SIM2 levels were reported to be enhanced 22.3 and 32.9-fold in the LNCaP and DU145 SIM2s.myc expressing cell lines, respectively, by microarray (**Figure 4.7**, **A(i)** & **B(i)**), whereas specific qPCR analysis of *SIM2s* mRNA levels reveals a significantly greater fold change, namely an average of 1150-fold and 700-fold, respectively (**Figure 4.7**, **A(ii)** & **B(ii)**). Together, these results indicate the dramatically reduced sensitivity of detection of changes in gene expression by the microarray approach used here, and consequently a limitation of this experimental system for discovering subtle, yet potentially biologically important, changes in gene expression.

4.2.6 Summary Comments

Aberrantly elevated levels of SIM2s have been found to be characteristic of aggressive prostate tumours [80, 81, 166]. Consequently SIM2s was stably over-expressed in LNCaP and DU145 prostate carcinoma cells to profile changes in gene expression by microarray that occur when SIM2s is highly misexpressed in cells of this tumour type. These studies were designed to aid the discovery novel targets of SIM2s

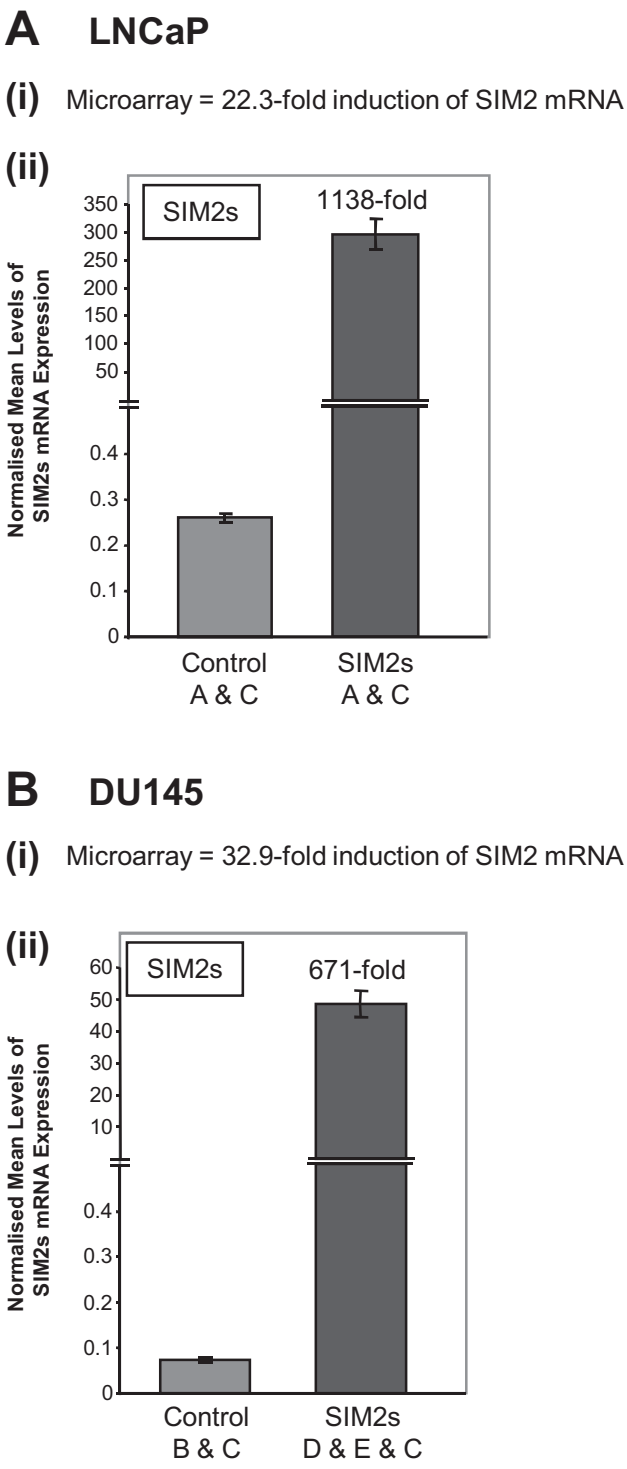

Figure 4.7: *Microarray determination of SIM2s mRNA over-expression in LNCaP (A) and DU145 (B) polyclonal cell lines is approximately 50x & 20x less than that determined by quantitative PCR, respectively, indicating the much reduced sensitivity of microarray analysis for changes in mRNA expression levels.*

cDNA synthesised from total RNA extracts of puromycin resistant polyclonal cell lines used for qPCR analysis of *SIM2s* mRNA normalised to *POL2RA* levels. qPCR data graphed using 'Qgene' software. SIM2s.myc cell lines not used in the microarray for independent validation studies are also assessed and included in data analysis to show consistency of *SIM2s* mRNA overexpression levels across independently derived polyclonal cell lines for each cell type. Error bars SEM. (Aii) Data representative of two independent experiments, performed in triplicate, (Bii) n=3 independent experiments, performed in triplicate.

transcription that may provide an insight into how SIM2s may play a role in the tumourigenesis of the prostate, and also potentially of the colon and pancreas.

A number of interesting candidate target genes for SIM2s emerged from these studies, and although not investigated further beyond the studies presented here, it is interesting to observe that since the time of these studies reports have recently emerged in the literature that further support the implication that SIM2s may play a role in their regulation. Particularly, positive *IER3/IEX-1* expression in pancreatic cancer has recently been found to correlate to better prognosis and patient survival [170]. Consequently, it may be inferred that negative IER3 expression does not correlate to a better patient outcome, indeed a negative correlation between *IER3* expression and tumour invasiveness was also observed [170]. This study provides a new supporting link consistent for a putative role for SIM2s in the repression of IRE3, as found in DU145/SIM2s.myc cells in the present study, thus perhaps a role for SIM2s in the development of more aggressive cancers. Conversely however, the latest genome-wide global analysis of pancreatic cancer [96] further supports previous findings of significant *PHLDA1*, *EREG* [152, 153, 165] and *S100P* [148, 149, 167-169] up regulation in this cancer type, thus providing more evidence to discount the apparent down regulation of these genes upon SIM2s expression in prostate cancer cell lines as being indicative of a transcriptional role for SIM2s shared across the progression of these two tumour types.

Intriguingly however, recent studies have also revealed potential new contexts in which SIM2 may regulate selected genes highlighted in our microarray study. A study by Kim *et al* (2007) showed *EREG*, *AREG* and *SLUG* to all be significantly upregulated upon induced overexpression of the transcription factor WT1 by microarray. Further study found these genes to be direct targets of WT1 transcription [171]. These findings are of particular interest as *SLUG* has recently been described as a direct target of SIM2s repression [82], and the microarray studies presented here in **section 4.2.2** indicate that *EREG* and *AREG* are also

repressed in response to SIM2s expression. Interestingly, WT1 binds to region of the *EREG* promoter between -171 to +200 [171], which from bioinformatic analyses, also contains a putative 5'-AACGTG-3' SIM2 Response Element (S2RE) at +39 (data not shown), which may function as a site through which SIM2s may play a direct role in the regulation of *EREG*, and perhaps more significantly, do so by opposing function of WT1. The region where WT1 was found to bind the *SLUG* promoter, -714 to -205, by Kim and colleagues does not correlate to -2800 to -2247 of the *SLUG* promoter where SIM2s was found to bind [82]. However, the region of WT1 binding does containa number of E-boxes, as reported by Laffin and co-workers (2008), but were not analysed for SIM2s binding [82]. These E-boxes can function as sites for SIM2s DNA-binding and mediation of SIM2s-transcription, as found during the studies presented in **Chapter 5**, and as such could also be sites through which SIM2s may interfere with the role of WT1 in the regulation of *SLUG*. Intriguingly, SIM2 was found to be overexpressed in a subclass of syndromic Wilms Tumours that have mutant loss-of-function WT1 and characterised by a gain-of-function mutant beta-catenin (CTNNB1) [172] which perhaps indicates a specific context where SIM2 may preferentially have the opportunity regulate these genes in the absence of functional WT1 in kidney cancer.

The microarray studies described in this chapter were carried out to facilitate the discovery of a novel direct target of SIM2s transcription. Not only to further determine the molecular mechanisms of SIM2s-mediated gene regulation, but importantly, to provide a novel insight into how increased SIM2s activities may be implicated in the initiation, and/or maintenance and progression of tumours of the prostate, pancreas or colon. To this end, several interesting candidate target genes were investigated, however, ultimately SIM2s-mediated repression of the pro-cell death gene, *BNIP3*, initially observed in DU145 cells, was selected for more comprehensive studies as detailed in the following chapter (**Chapter 5**) describing this work.

CHAPTER 5

SIM2s regulation of the pro-cell death gene *BNIP3*

5.1 INTRODUCTION

Microarray experiments revealed down regulation of Bcl-2 nineteen-kilodalton interacting protein (BNIP3) mRNA upon ectopic expression of SIM2s, which was independently validated by semi-quantitative RT-PCR in DU145/SIM2s.myc stable expressing cells not used for the microarray study (refer to **Chapter 4**, **Figure 4.4B** and **Figure 5.2**). At the time these studies were initiated, BNIP3 had long been regarded as a pro-cell death BH3-only Bcl-2 family member [for review see [173]]. However since that time, BNIP3 has been implicated in three types of cell death; apoptotic, necrotic and autophagic arising from a number of alternate pathways. BNIP3 homodimers bind to the outer mitochondrial membrane via its TM domain, causing an increase in ROS (reactive oxygen species) and loss of mitochondrial membrane potential ($\Delta\psi$m), and the release of cytochrome c leading to the induction apoptotic, necrotic and autophagic cell death pathways. Also, BNIP3 has been found to mediate Beclin-1 induced autophagic cell death via sequestering Bcl-2 away from Beclin-1, and via binding to Rheb and consequently inhibiting the ability of Rheb to activate mTOR (for review see [174])(**Figure 5.1**). Autophagy is a cellular response to stressful stimuli, such as hypoxia and starvation, which can result in cell death, or interestingly cell survival outcomes, reflected in evidence from cancer studies where autophagy plays roles in both tumour suppression and tumour growth (for review see; [175, 176]). The precise molecular mechanisms that occur in response to specific stress stimuli, and/or tumour microenvironment, that regulate autophagy to either prevent or promote tumourigenesis remain to be determined. In pancreatic and colon tumours, notably tumour types were SIM2s is found to aberrantly up-regulated [52, 80], the loss of BNIP3, either by hypermethylation or transcriptional repression, correlates to inhibition of cell death, tumour progression, chemoresistance and worsened prognosis *in vivo* [177-184]. In contrast, up-regulation of BNIP3 sensitizes carcinoma cells, including those of the pancreas, to hypoxia-induced cell death [185-187]. Unfortunately, there is no current understanding of how regulation of BNIP3 affects prostate cancer progression and patient outcomes. However, these findings suggest a putative role

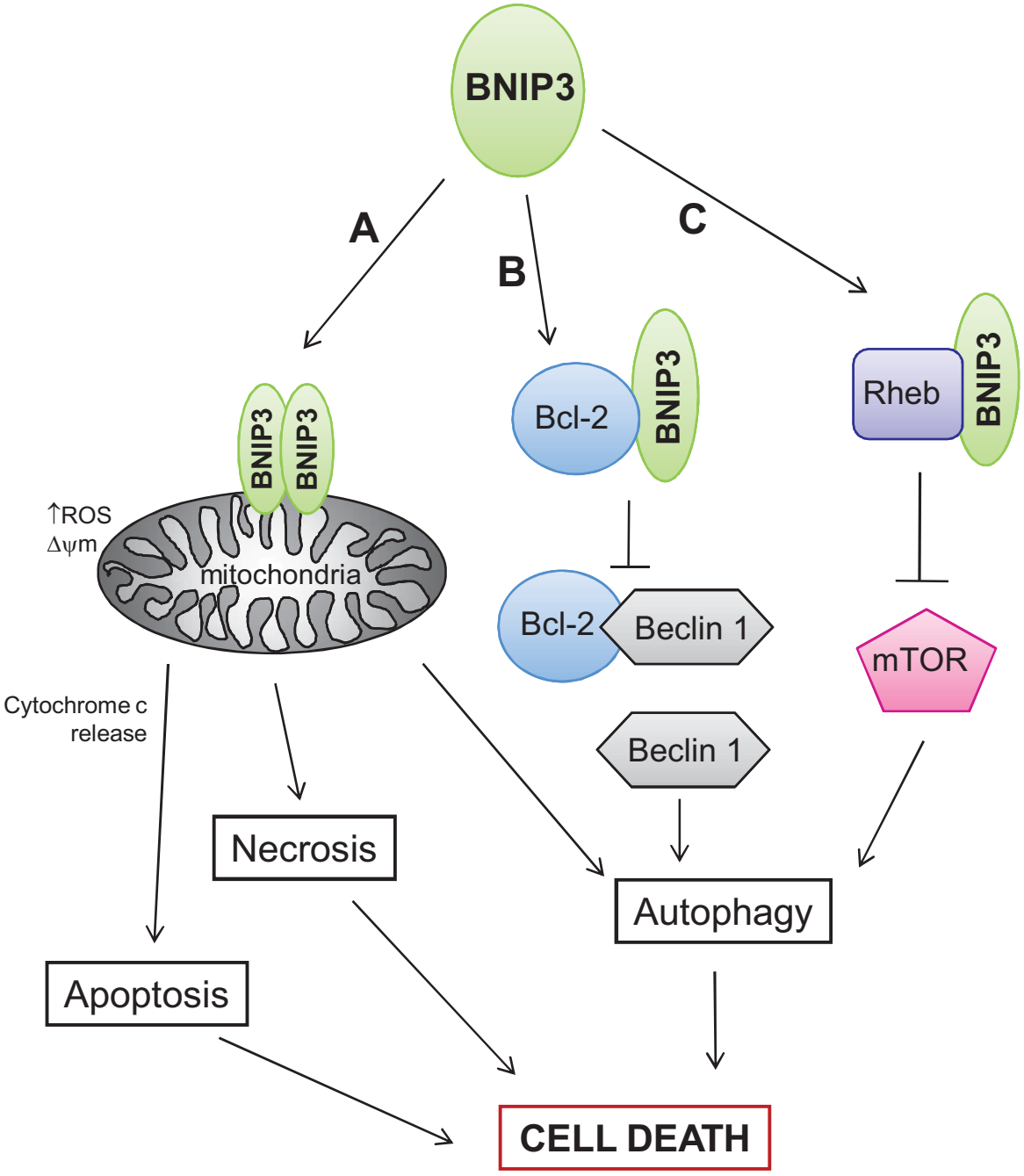

FIGURE 5.1: *BNIP3 induces the three types of cell death.*

(A) BNIP3 homodimers bind to the outer mitochondrial membrane via its TM domain, causing an increase in ROS (reactive oxygen species) and loss of mitochondrial membrane potential ($\Delta\psi m$), and the release of cytochrome c leading to the induction apoptotic, necrotic and autophagic cell death pathways. (B) BNIP3 mediates Beclin-1 induced autophagic cell death via sequestering Bcl-2 away from Beclin-1. (C) Autophagic cell death also occurs as a result of BNIP3 binding to Rheb and thus inhibiting the ability of Rheb to activate mTOR.

Figure adapted from review by Burton and Gibson (2009) *Cell Death and Differentiation*. Advance online publication 9 January 2009

for SIM2s in cancer via repression of *BNIP3*, with inhibition of BNIP3-mediated cell-death being a possible mechanism of tumour progression.

The following studies sought to determine if the gene *BNIP3* was a direct target of SIM2s repression, and the mechanisms by which this occurs. And furthermore, investigate the functional outcomes associated with SIM2s-mediated down-regulation of *BNIP3* in prostate cancer cells.

5.2 RESULTS & DISCUSSION

5.2.1 Validation of the *BNIP3* gene as a target of repression by SIM2s

As down-regulation of BNIP3 associated with ectopic SIM2s expression was first identified in prostate carcinoma DU145 cells, further studies were required to assess if this was indeed a general, and not cell-type specific, response. Excitingly, further validation of *BNIP3* repression upon stable ectopic expression of SIM2s in other human prostate carcinoma derived cell lines; PC3AR+, and to a lesser extent in LNCaP, and across tumour cell types, in the pancreatic cancer lines CFPAC and PANC-1, was found (**Figure 5.2**). Repression was evident at both the message and protein levels in these carcinoma derived cell lines (**Figures 5.2 A&B,** respectively). Stable and transient expression of hSIM2s also repressed *mBNIP3* expression in mouse NIH3T3 fibroblasts and mouse P19 embryonic carcinoma cells, respectively (**Figure 5.2**). siRNA-mediated knock down of stably expressed SIM2s, using two independent siRNA oligonucleotides, alleviated BNIP3 repression as shown by western analysis in PC3AR+/SIM2s.myc cells (**Figure 5.3Ai**), which was also evident at the RNA level (**Figure 5.3Aii**). Likewise, BNIP3 levels were enhanced upon treatment of parent prostate PC3AR+ and DU145 cells for specific siRNA-mediated

knockdown of endogenous SIM2s in a consistently moderate manner at the protein level (**Figure 5.3B**) and as shown for DU145 cells, also at the mRNA level (**Figure 5.3C**). Taken together, these data strongly indicate that BNIP3 silencing is downstream of SIM2s activity.

5.2.2 Investigating the possible indirect mechanism of SIM2s-mediated repression of BNIP3 via promoting hyper-methylation of the *BNIP3* promoter

Silencing of BNIP3 has previously been found to occur in colon and pancreatic tumours via hypermethylation of the CpG island contained within the regulatory region of the human *BNIP3* promoter (**Figure 5.4Bi**), indeed this methylation has been shown to inhibit the hypoxic induction of BNIP3 expression in cell lines of these cancer types [181, 183, 184]. Descriptions of the mechanisms by which this occurs remain to be reported. Perhaps methylation of the CpG motif within the HRE (underlined [5'-CACGTG-3']) inhibits HIF1α/ARNT binding recognition. There are no reports of this mechanism of BNIP3 silencing in prostate carcinomas. At the time these studies were initiated there was no understanding of any mechanisms of transcriptional regulation of BNIP3 in normoxia. As *BNIP3* expression was silenced upon ectopic expression of SIM2s.myc, the possibility of an indirect mechanism of SIM2s-mediated silencing of *BNIP3* via promoting hyper-methylation of the *BNIP3* promoter was investigated in human prostate carcinoma DU145 cells. Utilising epigenetic genomic DNA sodium bisulphite conversion and sequencing techniques, no change in promoter methylation at CpG sites with stable SIM2s ectopic expression was found (**Figure 5.5**). This finding indicated that *BNIP3* expression levels must be regulated in another manner, and not silenced due to changes in promoter methylation. Consequently, potential direct mechanisms of SIM2s transcriptional repression of *BNIP3* were investigated.

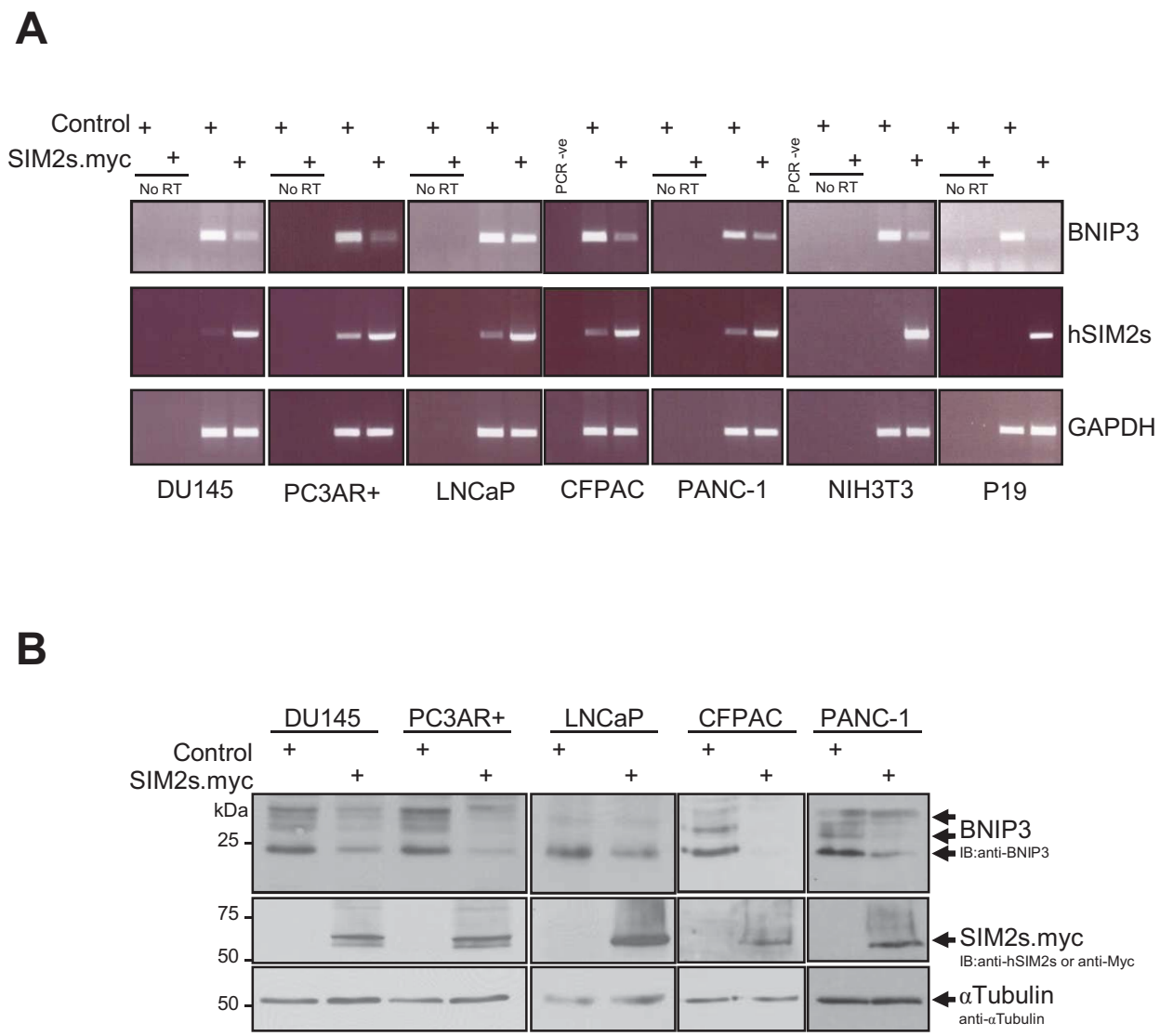

FIGURE 5.2: *BNIP3 levels decrease upon stable ectopic expression of SIM2s.myc.*

(A) Decrease in *BNIP3* mRNA measured by semi-quantitative (sq) RT-PCR of human prostate DU145, LNCaP and PC3AR+, and pancreatic CFPAC and PANC-1, carcinoma cell lines and mouse NIH3T3 fibroblast and embryonic carcinoma P19 cell lines. cDNAs made from total RNA extracts from puromycin resistant or parent control cell lines and cells with either stable or transient over-expression of human SIM2s.myc were analysed by semi-quantitative RT-PCR. Single amplicons separated 1% agarose gel electrophoresis, stained with EtBR. PCR cycles used: GAPDH 25x in human cells, 30x in mouse derived cell lines; BNIP3 25x, except pancreatic lines, 30x, and 35x & 40x in NIH3T3 & P19 cells, respectively; SIM2s in human cells 35x, 25x and 30x in NIH3T3 and P19 cells, respectively. (B) BNIP3 protein levels decrease on ectopic expression of SIM2s.myc in human prostate DU145, LNCaP and PC3AR+, and pancreatic CFPAC and PANC-1, carcinoma cell lines. 35µg WCE from puromycin resistant Control cells or cells with stable ectopic expression of SIM2s.myc were separated by 12% SDS-PAGE, and then subjected to immunoblot detection of proteins as marked.

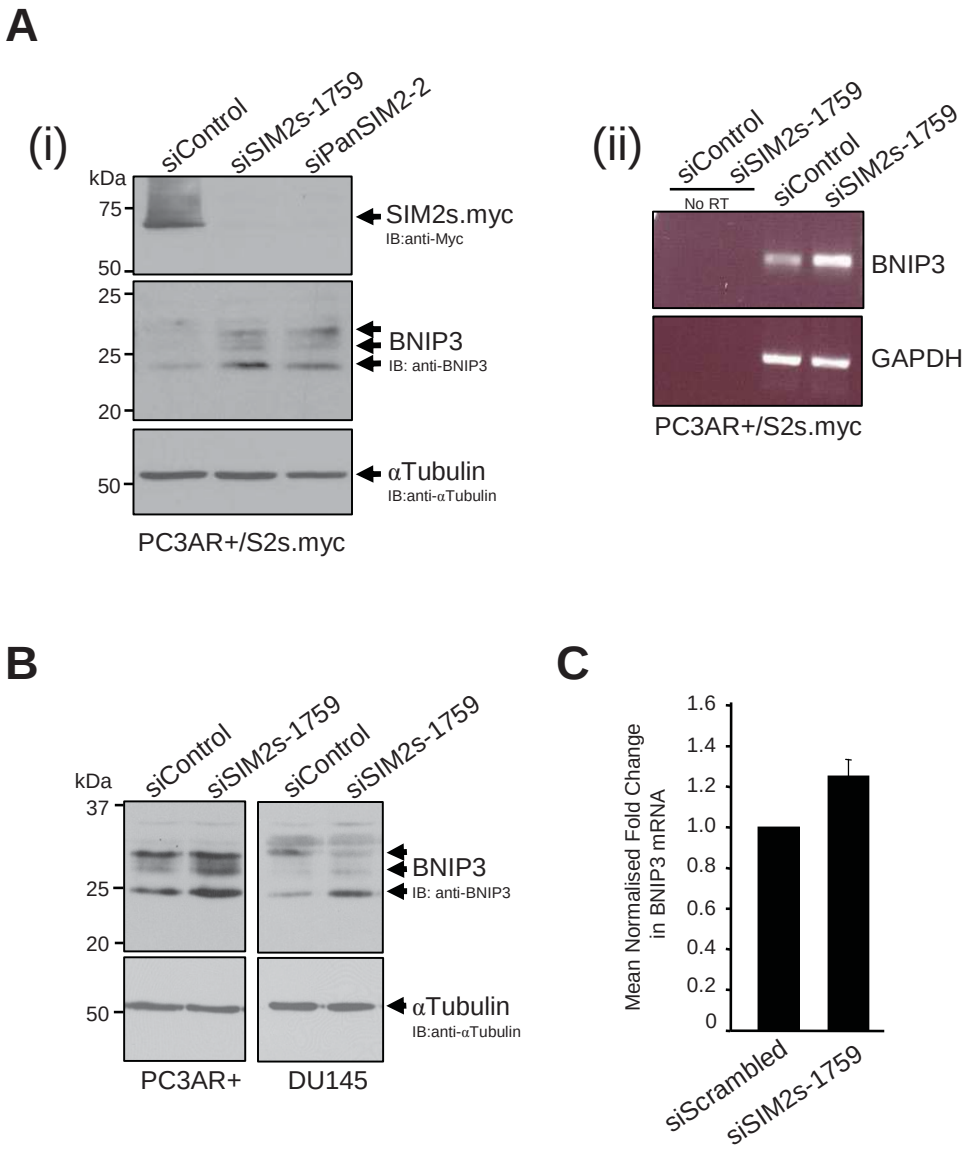

FIGURE 5.3: *Repression of BNIP3 is downstream of SIM2s activities.*

(A) Repression of BNIP3 is alleviated on siRNA knockdown of ectopic hSIM2s.myc (S2s.myc). (Ai) Two independent siRNA oligonucleotides, siSIM2s-1759 & siPanSIM2-2, and a scrambled control siRNA were used to treat PC3AR+/SIM2s.myc cells in 2x100nM doses 24h apart. (Ai) WCE or (Aii) total RNA, were harvested 72h after first treatment. (i) 35µg WCE separated by 12% SDS-PAGE, followed by sequential immunoblot analysis of BNIP3, hSIM2s.myc, and αTubulin as loading control. Representative of n=3. (ii) Semi-quantitative RT-PCR of BNIP3 *mRNA,* compared to *GAPDH* mRNA levels as loading control, separated by 1% agarose gel electrophoresis. No RT = no reverse transcriptase controls. (B & C) BNIP3 levels are enhanced in a manner consistent with siRNA-mediated knockdown of endogenous SIM2s. (B) Western analysis of BNIP3 levels in parent PC3AR+ and DU145 cell lines following transfection of siSIM2s-1759. 12% SDS-PAGE separation and immunoblot analysis of 35µg WCE. Representative of n=2 for each cell line. (C) Quantitative-PCR assessment of the fold-change in *BNIP3* mRNA levels following induced expression of siSIM2s-1759 in DU145 cells. n=3, error bars SEM.

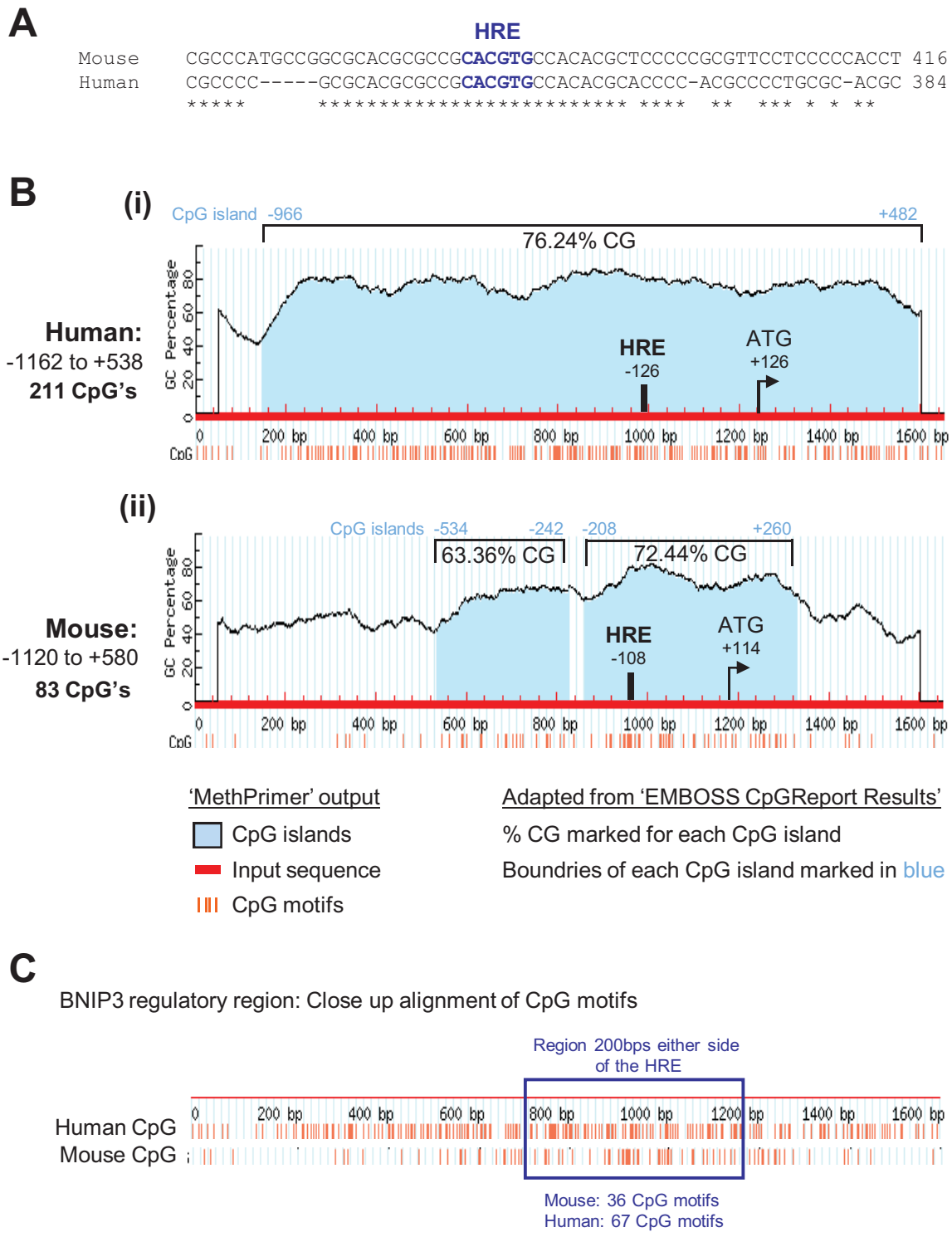

FIGURE 5.4: *Bioinformatic analysis of the CpG content of mouse and human BNIP3 promoter and regulatory regions.*

(A) Proximal promoter HRE and surrounding sequence is conserved between mice and humans. (B) The human (i) BNIP3 regulatory region is more CG rich, and has 2.5x more CpG motifs than that of mouse (ii). Online bioinformatic tools: EMBL EMBOSS http://www.ebi.ac.uk/emboss/cpgplot/ and 'Methprimer' http://www.urogene.org/methprimer/index1.html, both predicted the same CpG islands. Input sequences for 1700 bp of the *BNIP3* regulatory regions analysed are shown. Human sequence analysed previously defined CpG island by Okami *et al* (2004) *Cancer Res*. 64(15): 5338-46. Graphs generated by Methprimer and subsequently annotated to include EMBOSS results and positions of proximal promoter HRE and ATG translation start site. (C) Closer analysis of the CpG content in the region surrounding the HRE in mice and humans. Vertical red lines represent CpG motifs, number present in 200bp region indicated.

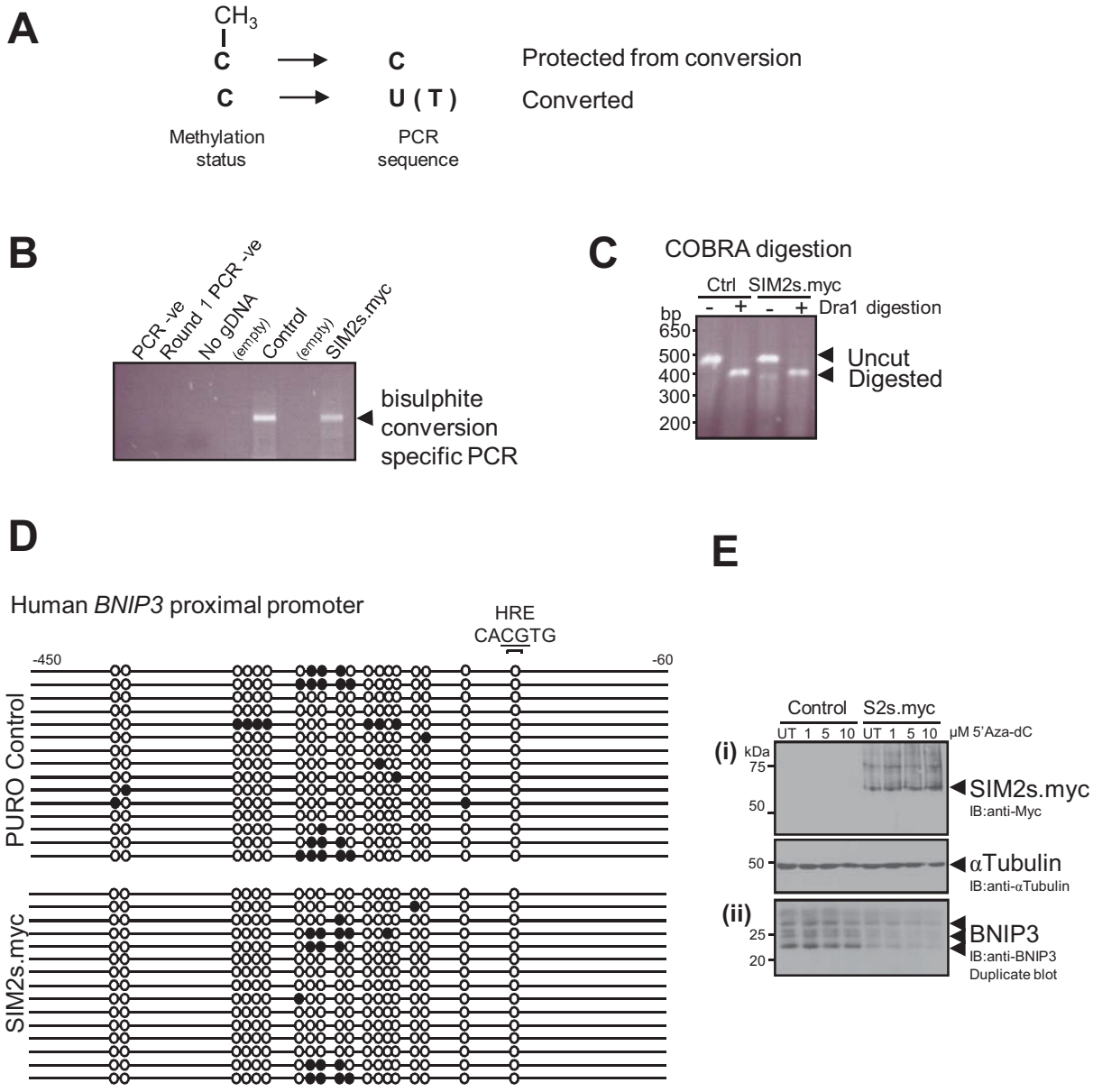

FIGURE 5.5: *Stable ectopic expression of SIM2s in human prostate carcinoma DU145 cells does not promote silencing of BNIP3 via hypermethylation of the CpG island in the regulatory region of BNIP3.*

Analysis of human BNIP3 methylation status with and without stable ectopic expression of SIM2s.myc in prostate carcinoma DU145 cells by epigenetic analysis. Data represents three independent sodium bisulphite conversions of three independent genomic DNA preparations (n=3) from DU145 cells. (A) Methylated cytosines [C] are protected from bisulphite conversion and will be detected by PCR as C, whereas unmethylated C are converted to uracil [U], which following PCR is sequenced as a thymine [T]. (B) Bisulphite conversion specific PCR amplicons produced using bisulphite conversion specific primers designed by online software design tool 'MethPrimer' were (C) tested for complete conversion using COBRA analysis, a measure of the bisulphite creation of a Dra1 restriction enzyme site, 5'-TTTAAA-3' (unconverted DNA 5'-CCCAAA-3'). (D) Individual clones sequenced over the proximal promoter of human BNIP3 containing the HRE. 19/60 CpG motifs represented here from this region are only motifs which differed in methylation status between clones, or were contained inside the HRE. All other motifs were unmethylated. Dark and light circles denote methylated and unmethylated motifs, respectively. (E) Treatment with increasing amounts of de-methylating 5'Aza-dc to DU145/SIM2s.myc cells does not increase repressed protein levels of BNIP3 consistent with SIM2s not promoting hypermethylation as indicated by bisulphite sequencing data. (i) 8% and (ii) 12% duplicate SDS-PAGE separation of 28μg of WCE made following 48h treatment with 0, 1, 5 or 10μm 5'Aza-dc. Immunoblot detection of proteins as indicated. Representative of n=2.

5.2.3 SIM2s binds to the HRE, and not the intronic S2RE, in the proximal promoter of *BNIP3*

SIM2 has been shown to exhibit crosstalk with HIF by binding to the *EPO* HRE in a synthetic reporter gene [59]. Therefore the previously identified HRE (5'-CACGTG-3') in the proximal promoter of *BNIP3* [183, 187, 188] was investigated as a putative site for SIM2s binding (also see **Figure 5.4A**). Utilising a bioinformatic approach, further possible sites through which SIM2s might directly mediate repression of *BNIP3* were identified, in particular, the novel S2RE, recently identified by us in the promoter of Myomensin2 (section 5.2.3) [48]. Functional intronic DNA-binding sites for dSim have been previously identified for the regulation of *slit* [77]. Intriguingly, a putative S2RE was found to be conserved within the first intron of *BNIP3* in human, predicted chimp, rat and mouse genes in a positional manner as is the HRE (**Figure 5.6**). This site was termed S2RE 'site 1'. Other putative S2RE sites were identified upstream of the HRE in the rat, and a second S2RE (site 2) downstream of S2RE site 1 identified in mouse (**Figure 5.6**).

Bioinformatic analysis of the region of the mouse *BNIP3* promoter corresponding to the previously defined CpG island by Okami and co-workers (2004) in the human promoter showed a markedly reduced CG content (**Figure 5.4B,** compare (i) and (ii), and as shown in blue in **Figure 5.6**), making it ultimately a more amenable region for PCR analysis of chromatin immunoprecipitation (ChIP) assays and the generation of *BNIP3* promoter luciferase reporter constructs (**Figure 5.6**). These methods were used initially to examine if the mechanism of SIM2s repression of *BNIP3* was via direct binding at the identified HRE and S2RE sites. Stably expressed hSIM2s in mouse NIH3T3 cells results in *mBNIP3* repression as observed in human carcinoma cell lines (**Figure 5.2A**). Human SIM2s was found bound to the proximal promoter HRE, and interestingly, neither of the downstream intronic S2REs of the *mBNIP3* promoter in normoxic growth

conditions by ChIP (**Figure 5.7A**). HIF1α binding at these sites was not examined as HIF1α protein is rapidly degraded in normoxia [189] and not detectable in these cells in these growth conditions (**Figure 5.8A**), nor do ChIP studies by others find HIF1α to be bound to the *BNIP3* promoter in normoxia [187]. Luciferase gene expression under the control of 1kb of the *mBNIP3* promoter (**Figure 5.6**) in NIH3T3 cells shows that SIM2s transcriptional repression requires a functional HRE, as HRE mutant constructs fail to be repressed, despite the presence of a functional S2RE (**Figure 5.7B**), indicating that the S2RE is not required for SIM2s mediated repression of *BNIP3.* The level of repression observed was not as great as expected in comparison to the repression observed on the endogenous promoter by measures of *BNIP3* mRNA in these cells (**Figure 5.2**), which may be indicative of the requirement for other regulatory elements/co-factor binding not present in the promoter region of the reporter gene. Taken together, this shows for the first time functional SIM2s recognition of an endogenous HRE.

5.2.4 SIM2s attenuates the hypoxic induction of BNIP3

BNIP3 is hypoxically up-regulated in a wide variety of tumours and tumour derived cell types [190] and has long been established as a target gene of HIF1α/ARNT1 via binding to the HRE in the proximal promoter [188]. To ascertain if SIM2s-mediated repression of *BNIP3* via the HRE seen in normoxic growth conditions has any impact on the ability of hypoxia to induce BNIP3 expression, human prostate carcinoma and mouse fibroblast cells stably expressing hSIM2s were subjected to 16 hours growth in a hypoxic chamber (< 1% O_2) and BNIP3 protein levels assessed by western analysis. Across all lines, while hypoxic induction of HIF-1α was clearly seen, induction of BNIP3 was attenuated in hSIM2s.myc expressing cells as compared to control cells (**Figure 5.8A**). This suggests SIM2s may directly interfere with HIF1α activities in hypoxia. This interference appears to be despite the marked reduction of SIM2s.myc protein levels during hypoxic treatment (**Figure 5.8A**, panel set ii.). This reduction in SIM2 protein levels during hypoxia has been

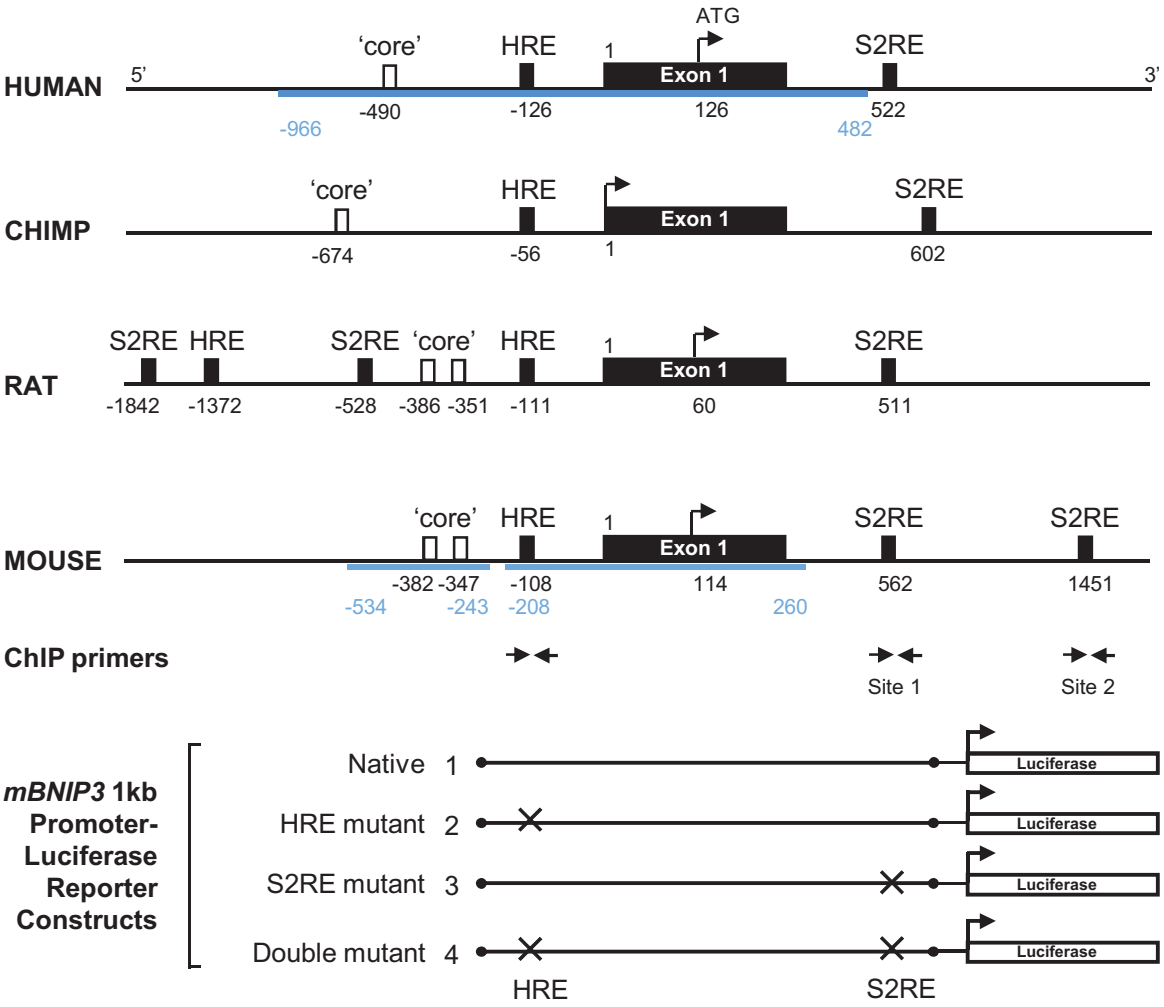

FIGURE 5.6: *Schematic diagram of bioinformatically identified conserved binding consensus sequences in the regulatory region of the BNIP3 gene which includes the proximal promoter, the first exon and part of the first intron, in human, (predicted) chimp, rat and mouse.*

HRE = Hypoxia Response Element, 5'-CACGTG-3'
S2RE = SIM2 Response Element, 5'-AACGTG-3' [human and (predicted) chimp, CACGTT]
'Core' = core element, all 5'-(G)ACGTG-3'
CpG islands as defined by 'Methprimer' and 'EMBL EMBOSS' analyses are shown in blue.
Sites of ChIP analyses, and segment of the regulatory region studied by luciferase reporter analyses of *mBNIP3* regulatory region are also shown.

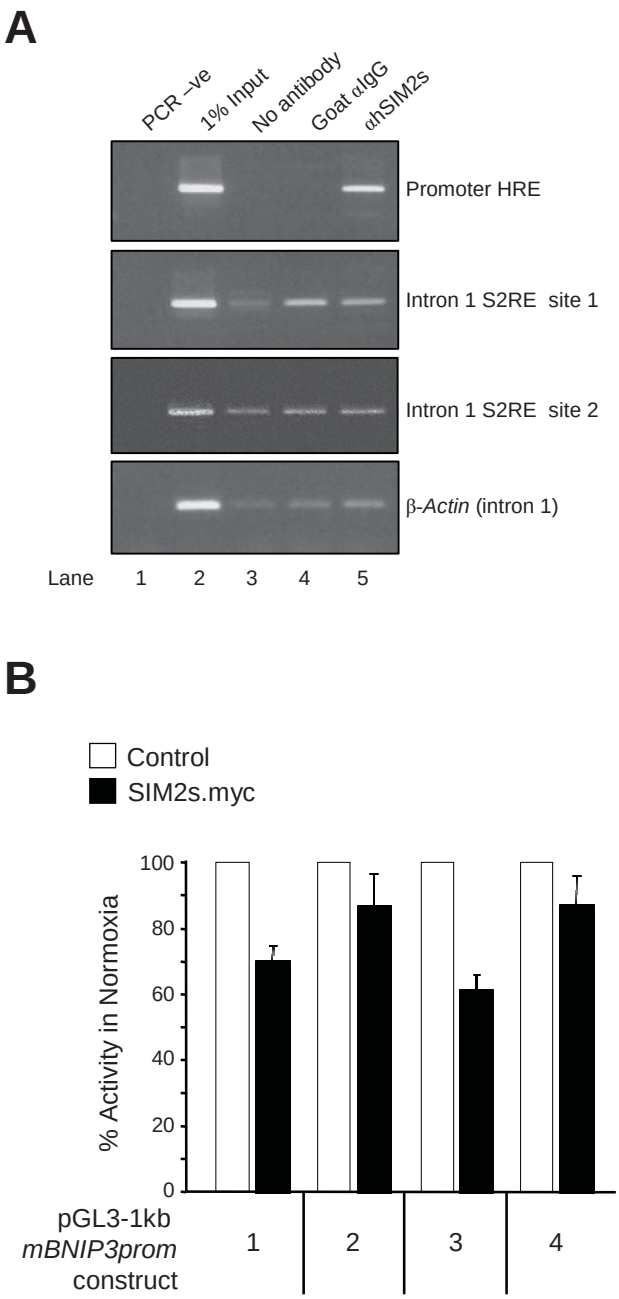

FIGURE 5.7: *(A) SIM2s.myc is found at the proximal promoter HRE, and not the downstream intronic S2RE's, on the endogenous mouse BNIP3 promoter. (B) The HRE in mBNIP3 proximal promoter, and not the intronic S2RE, is required for SIM2short repression of 1kb mBNIP3prom-Luciferase reporter activity in normoxic growth conditions.*

NIH3T3 cells with stable ectopic expression of human SIM2s.myc compared to empty vetctor Control stable cell line. (A) PCR analysis of ChIP of SIM2s.myc binding activities on the *mBNIP3* regulatory region, compared to β-Actin (intron 1) PCR as background control. Representative n=2. (B) Stable cell lines were transfected with each reporter construct (details see Figure 5.5) and allowed to grow under normal growth conditions for 24hrs. Ratios of luciferase reporter activity were calculated relative to co-transfected beta-galactosidase, and data represented as percent reporter activity where reporter activity in control cell line is normalised to 100%. Error bars SEM, n=4.

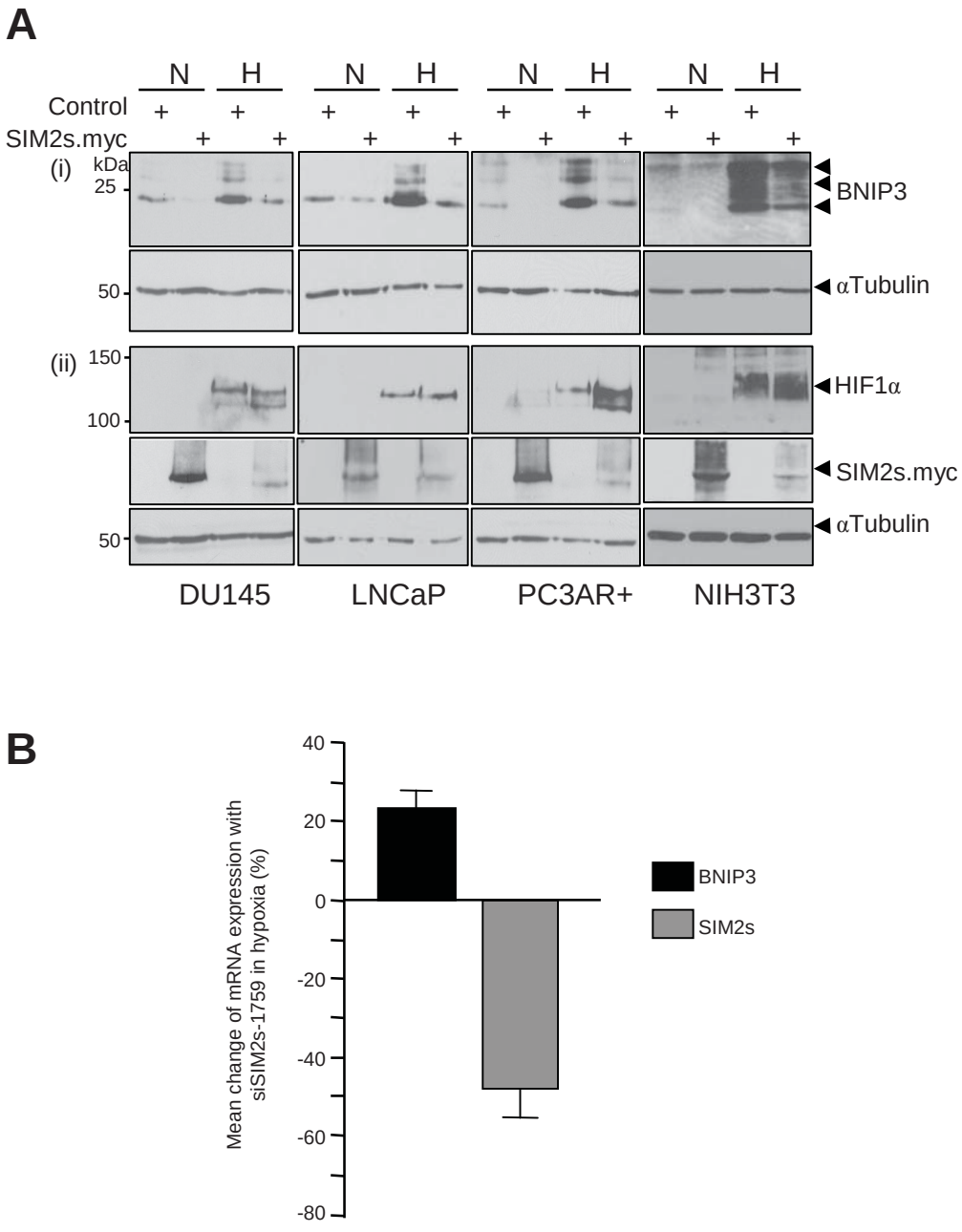

FIGURE 5.8: *(A) Stable ectopic expression of hSIM2s attenuates the hypoxic induction of BNIP3 in human Prostate DU145, LNCaP and PC3AR+ carcinoma cell lines, and mouse NIH3T3 fibroblasts. (B) siRNA-mediated knockdown of endogenous SIM2s in PC3AR+ cells enhances the hypoxic induction of BNIP3.*

(A) Whole cell extracts were made from both puromycin resistant empty-vector Control cells and cells engineered for SIM2s.myc stable expression, grown under usual normoxic (N) growth conditions, or treated with 16hrs hypoxia (H) (<1% O_2), then 35µg subjected to (i) 12% and (ii) 8% duplicate SDS-PAGE separation, and sequential immunoblot blot analysis of proteins as labelled. Representative of n=3 for each human, and n=2 mouse, cell lines. (B) Quantitative-PCR assessment of the fold-change in *BNIP3* mRNA levels in PC3AR+ cells relative to *hPOL2RA* expression levels following 2x100nM treatments of siSIM2s-1759 or siRNA scrambled control, and harvested 72hrs after first treatment where the cells were subjected to <1% oxygen (hypoxia) for the final 8hrs. n=3, error bars SEM.

previously observed, presumably a result of hypoxia induced global reduction in translation [59]. Consistent with ectopic SIM2s attenuation of hypoxic BNIP3 induction, siRNA mediated knockdown of endogenous *SIM2s* mRNA in human prostate PC3AR+ cells, results in a statistically significant moderate increase in the hypoxic induction of *BNIP3* mRNA (**Figure 5.8B**)(the same result found with the use of a second SIM2s-specifc siRNA oligonucleotide, siSIM2s-2a, data not shown), and consistently, to the same extent (an approximate 25% increase) as observed in normoxic DU145 cells (**Figure 5.3C**). Together, these studies indicate an endogenous role for SIM2s in the regulation of *BNIP3* in normoxic and hypoxic conditions.

5.2.5 SIM2s attenuates hypoxic induction of BNIP3 via activities when bound to the HRE

Following from the observation that SIM2s expression correlates to an attenuation in hypoxic induction of BNIP3 (**Figure 5.8**), further studies sought to investigate if these conditions led to alternate mechanisms, and/or sites of activity, of SIM2s-mediated repression. To examine if the binding site profile of SIM2s to the *BNIP3* regulatory region changed in hypoxia, subconfluent NIH3T3 cells with and without stable expression of hSIM2s.myc were treated with 8 hours hypoxia and subsequently used for ChIP analysis of HIF1α and hSIM2s.myc binding on the endogenous *BNIP3* regulatory region. Clear PCR enrichment for endogenous HIF1α binding at the HRE in control cells was observed, but HIF1α was not found to bind to the downstream, putative S2RE (**Figure 5.9**). Interestingly, this finding is consistent with the previous studies by Woods *et al* (2008) which found HIF1α was not able to confer transcriptional regulation of a reporter gene via an S2RE site [5'-AACGTG-3'] which is highly similar to previously defined HRE hexamer sequences [5'-T/CAGTG-3'], and together these studies may contribute to future work to further define target sequence specificity of the bHLH/PAS heterodimers. Furthermore, transient transfection of the luciferase reporter gene containing the 1kb *mBNIP3* promoter (**Figure 5.10A**), for 24 hours followed by a

final 16 hours of hypoxia, showed hypoxic induction of the promoter requires the HRE, while the S2RE alone is unable to mediate hypoxic induction of the reporter gene (**Figure 5.10A**, compare columns a & g). Interestingly, in NIH3T3/hSIM2s.myc cells, both endogenous HIF1α and hSIM2s were found to be present at the HRE, and again, not at the downstream intronic putative S2RE (**Figure 5.9**) by ChIP. This shows that hSIM2s absolute preference for the HRE does not change in hypoxia. Consistent with stable ectopic expression of SIM2s attenuating hypoxic induction of BNIP3 in human carcinoma and mouse fibroblast cells (**Figure 5.8A**), transient expression of human SIM2s markedly attenuated the hypoxic induction of the *mBNIP3* promoter driven reporter gene approximately 4-fold (**P<0.01) (**Figure 5.10A**, compare columns a & c). This activity required the presence of the functional HRE, while the downstream S2RE was not required, nor sufficient, to mediate regulation (**Figure 5.10A**; compare columns a & c reporter construct 1, g & i, reporter construct 2).

5.2.6 Ectopic expression of SIM2L also mediates repression of BNIP3 via the HRE

The two isoforms of human SIM2, SIM2s and SIM2L, share identical DNA binding, and dimerisation motifs [38], thus it is highly likely that they share target genes, as was observed in SIM2 regulation of *MYOM2* [188] (and refer to **Chapter 1**, **Figure 1.4A**). Independently derived polyclonal cell lines for stable ectopic expression SIM2L in human prostate PC3AR+ cells also show repression of normoxic endogenous protein levels of BNIP3 like SIM2s, however, SIM2L mediated repression was not to the same extent as that conferred by SIM2s over-expression (**Figure 5.12A**). Likewise, transient expression of human SIM2L was also able to attenuate hypoxic induction of the 1kb *mBNIP3* promoter (**Figure 5.10A**; compare columns a, c & e), and like SIM2s, this activity was also dependent on the presence of the functional proximal promoter HRE, and not the downstream S2RE (**Figure 5.10A**; columns g and k). It is likely that SIM2L is also able to

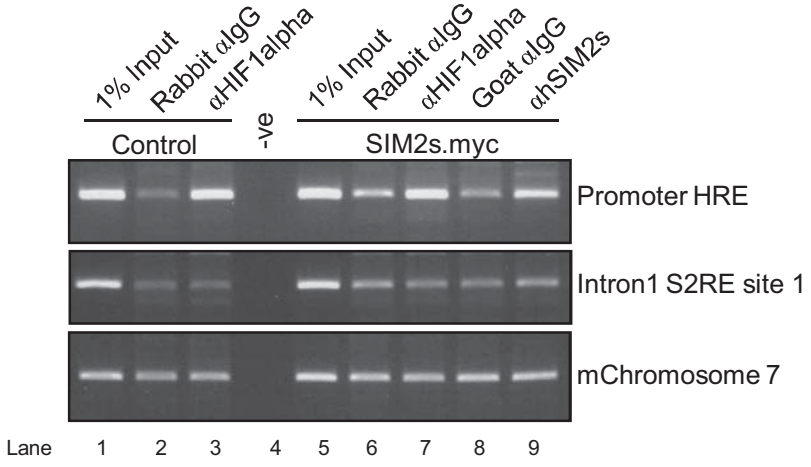

FIGURE 5.9: *SIM2s and endogenous HIF1α bind to the endogenous BNIP3 proximal promoter HRE, but not the downstream S2RE, during hypoxia in NIH3T3 cells.*

Chromatin immunoprecipitation (ChIP) analyses were performed with HIF1α and hSIM2s antibodies using NIH3T3 cells without (Control), or with stable hSIM2s.myc expression, following 8h growth in a hypoxic chamber (<1% O_2). Single amplicons were identified by 2.5% agarose gel electrophoresis. PCR analysis of chromosome 7 (Chr7), a region 3kb upstream of the *mBNIP3* promoter, serves as a negative and background loading control, as do immunoprecipitations with IgG antibodies. 1% input chromatin is included as a positive PCR control (lanes 1 and 5). Negative PCR (-ve) control shown (lane 4). Representative of two independent experiments.

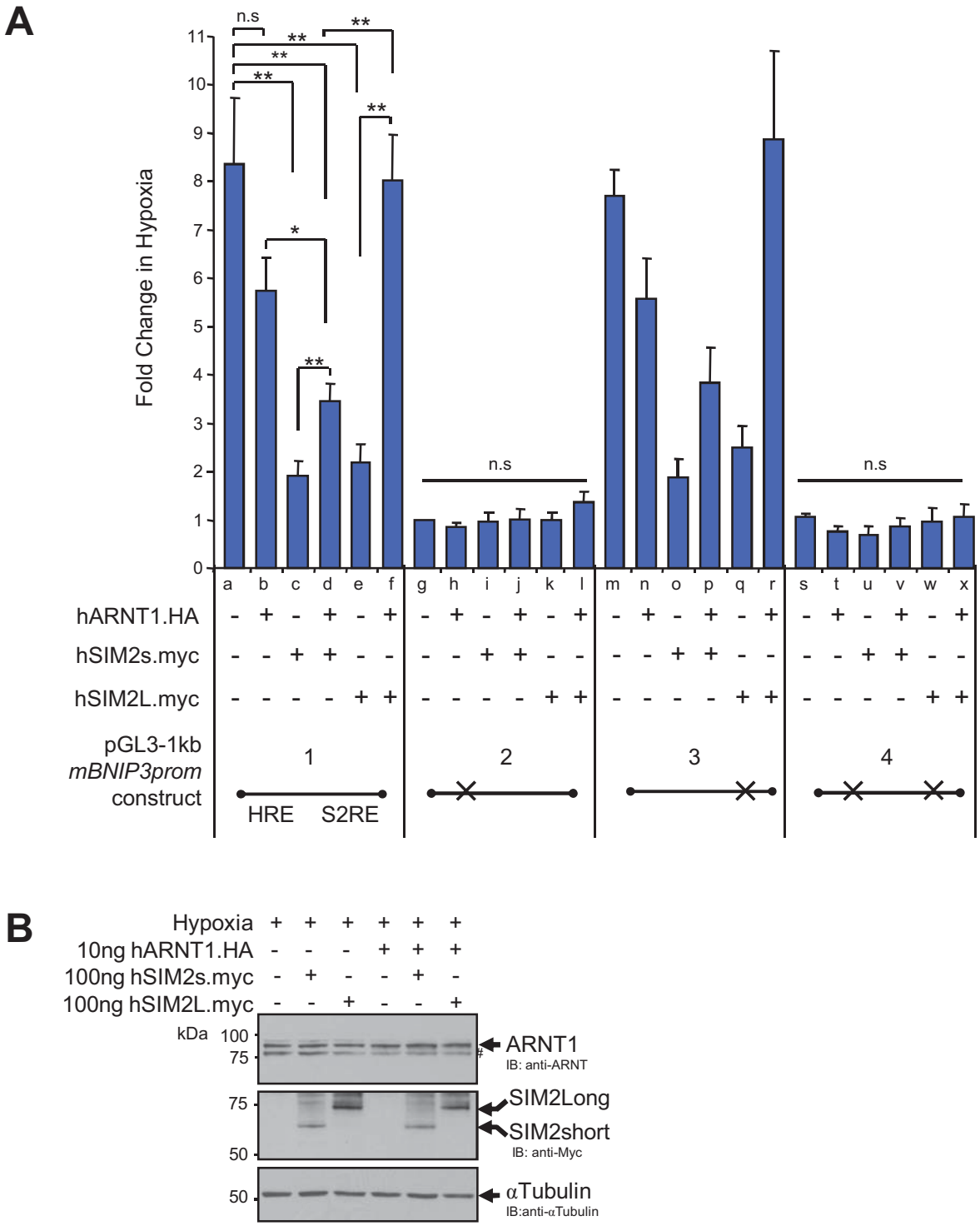

FIGURE 5.10: *Human SIM2 attenuates hypoxic transcriptional induction of mBNIP3 promoter driven luciferase via HRE specific binding activities in the proximal promoter of mBNIP3, and sequestration of obligate HIF1α partner factor, ARNT1.*

(A) NIH3T3 cells were transfected and left for 24hrs, then followed by 16hrs growth in hypoxia (<1% O_2). Ratios of luciferase reporter activity were normalised to co-transfected beta-galactosidase. Data normalised to pGL3-Basic-empty vector controls and represented as fold change above pGL3-Basic-1kb *mBNIP3*prom-HREmutant/empty vector control =1 (column g). Error bars represent SEM, n=4. Significance * P≤0.05, ** P≤0.01, n.s = no significance. Unpaired, two-tailed, Students T-TEST was used. (B) 50µg WCE were obtained from duplicate transfections and hypoxic treatments (as described in (A)) and separated by 8% SDS-PAGE, and then subjected sequential immunoblot detection of proteins as marked. Note, transient expression of ectopic ARNT1 (10ng) is not detectable above endogenous ARNT levels. # = cross reactivity of anti-ARNT MA-515 (ARNT1 ~ 87kDa) with ARNT2 (~75kDa).

bind directly to the HRE however this is yet to be tested experimentally. Interestingly, western analysis showed higher levels of SIM2L protein compared to SIM2s in this reporter system (**Figure 5.10B**). Taken together, these data indicate that there are apparent differences in the potency of ectopic SIM2s.myc and SIM2L.myc mediated repression of *BNIP3*. Indeed, it should be noted that in human prostate DU145 cells, where stable ectopic expression of SIM2s consistently results in reduced BNIP3 protein levels, stable ectopic expression of SIM2L resulted in variable effects on BNIP3 protein levels, indeed in two out of three independently derived polyclonal cell lines, SIM2L failed to have any effect on BNIP3 levels (**Figure 5.12B**).

Neither of the human SIM2 isoforms conferred any transcriptional activity via the S2RE in the first intron of *mBNIP3*. Whether there is any significance to this highly conserved putative S2RE motif inside the first intron of the *BNIP3* gene in mammals, and if it confers potential bHLH-PAS factor-mediated regulation , remains an open question.

5.2.7 SIM2 repression of BNIP3 in hypoxia may also be mediated by sequestering the common partner factor ARNT1 from HIF1α

ChIP data shows SIM2s is present, as is HIF1α, at the HRE in hypoxia (**Figure 5.9**). This indicates that SIM2s and HIF1α may be competing for the HRE, with SIM2s/ARNT physically interfering with HIF1α/ARNT (HIF1) binding activities, perhaps by limiting the availability of the HRE for HIF1. The long isoform of murine SIM2 has been previously shown to interfere with the transcriptional activities of HIF1α in an *in vitro* reporter context via sequestration of the class II partner factor, ARNT1, from HIF1α [9, 59]. To test if this mechanism may also contribute to human SIM2s and SIM2L repression of hypoxic induction of the *mBNIP3* promoter, human ARNT1 was co-transfected with each isoform of SIM2 to ascertain if there are any differences in promoter driven luciferase activity in hypoxically treated NIH3T3 cells. The minor addition of

human ARNT1 alone (undetectable above endogenous levels, **Figure 5.10B**) caused a consistent, however not statistically significant, decrease in the HIF1 mediated hypoxic induction of the *mBNIP3* promoter (**Figure 5.10A**, compare columns a & b, m & n). However, addition of human ARNT1 with SIM2 alleviated the repression exerted by SIM2 alone (**Figure 5.10A**, compare c & d, and e & f) yet to differing extents between SIM2 isoforms (**Figure 5.10A**, compare d & f). SIM2L repression was completely alleviated on addition of ARNT1 (**Figure 5.10A**, compare a, b & f). However, this same increase in ARNT1 with SIM2s was not able to completely interfere with SIM2s attenuation of the hypoxic induction of the *mBNIP3* 1kb promoter (**Figure 5.10A**, compare a & d, and b & d). These regulatory outcomes of both isoforms with excess ARNT1 both require the functional HRE, and not the intronic S2RE of the *BNIP3* regulatory region (**Figure 5.10A**). These data suggest the following; that not only is SIM2s present at the HRE, but when ARNT is limiting, SIM2 may sequester endogenous ARNT from HIF1α, thus interfering with the formation of functional HIF1α/ARNT heterodimers, thus contributing to the SIM2 mechanism of *BNIP3* repression, and furthermore, in light of the differing protein levels of each SIM2 isoform in this system (**Figure 5.10B**), SIM2L is not able to do so with the same potency as SIM2s. The addition of excess ARNT may allow for the formation of more HIF1α/ARNT heterodimers, which are then able to 'out compete' SIM2/ARNT from the HRE. HIF1α/ARNT heterodimers are less successful when competing against SIM2s/ARNT, thus the latter may have enhanced binding capabilities and transcriptional activities at this site via the aid of SIM2 isoform specific partner factors which remain to be identified. Conversely, this experiment may indicate alternate mechanisms of *BNIP3* regulation by each SIM2 isoform independent of ARNT1 sequestration. Due to the identical DNA binding sequences of the two isoforms, it is highly likely SIM2L also binds to the HRE, indeed this study shows the functional HRE, and not the intronic S2RE, is required to exert SIM2L effects (**Figure 5.10A**). However, SIM2L binding at the HRE, with and without excess ARNT1, is yet to be formally characterised experimentally. This knowledge would help define how SIM2L may play a role in the regulation of *BNIP3*. And in light of the evident difference in the potency, and variability, of SIM2L to

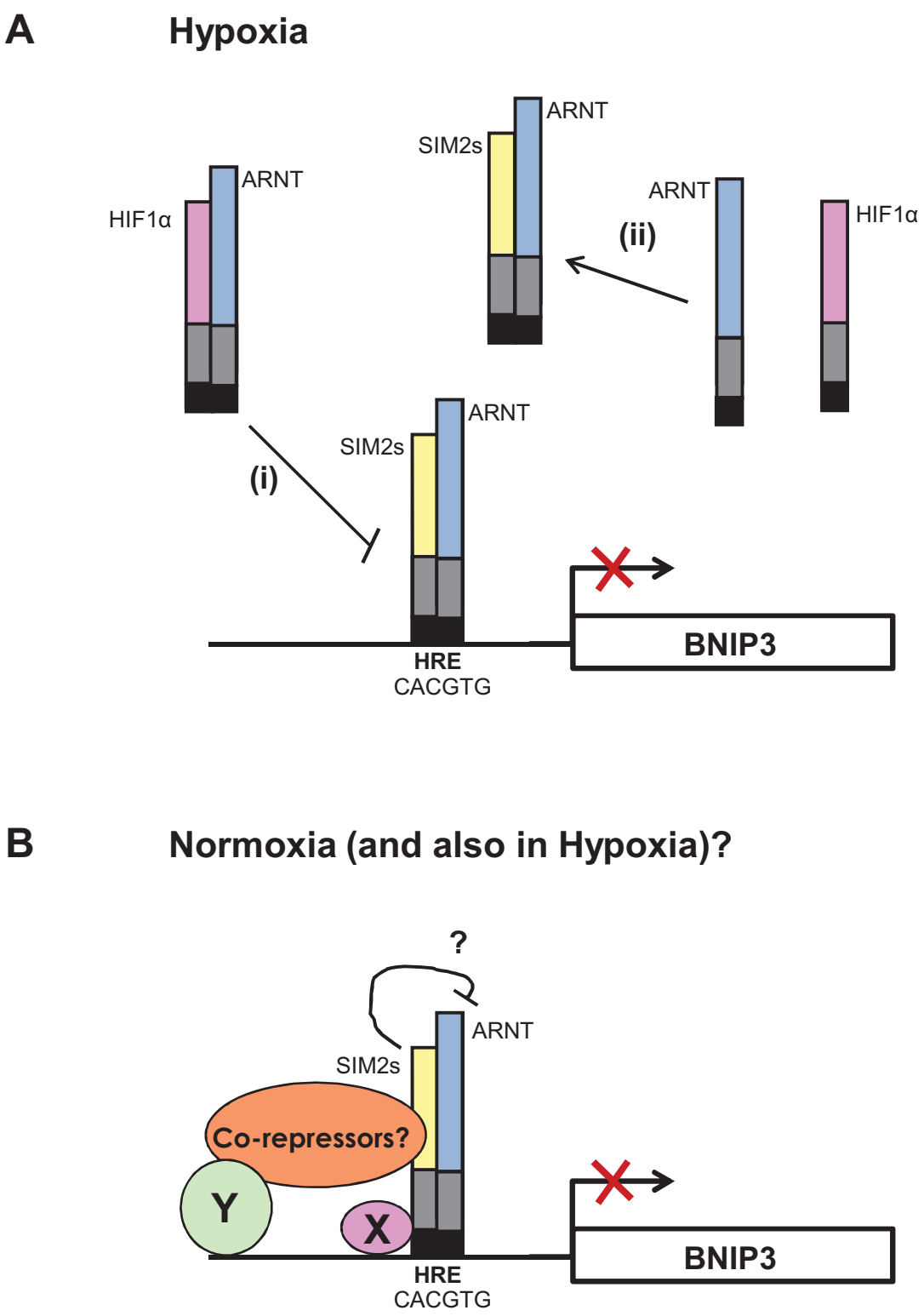

FIGURE 5.11: *Summary of suggested mechanisms of SIM2s-mediated repression of BNIP3 from endogenous promoter ChIP experiments and mBnip3promoter driven luciferase reporter studies.*

(A) Under hypoxic conditions, SIM2s attenuates BNIP3 induction via (i) directly binding on the HRE, and (ii) SIM2s sequestration of ARNT from HIF1α, and consequently interfere with the capacity of HIF1 to bind at the same response element. (B) In normoxic conditions, where there is no HIF1α, SIM2s binds the HRE, however, possible activities of SIM2s, including the repression of ARNT transactivational properties, and/or co-regulatory requirements remain to be determined, and may or may not differ between Normoxic and Hypoxic conditions.

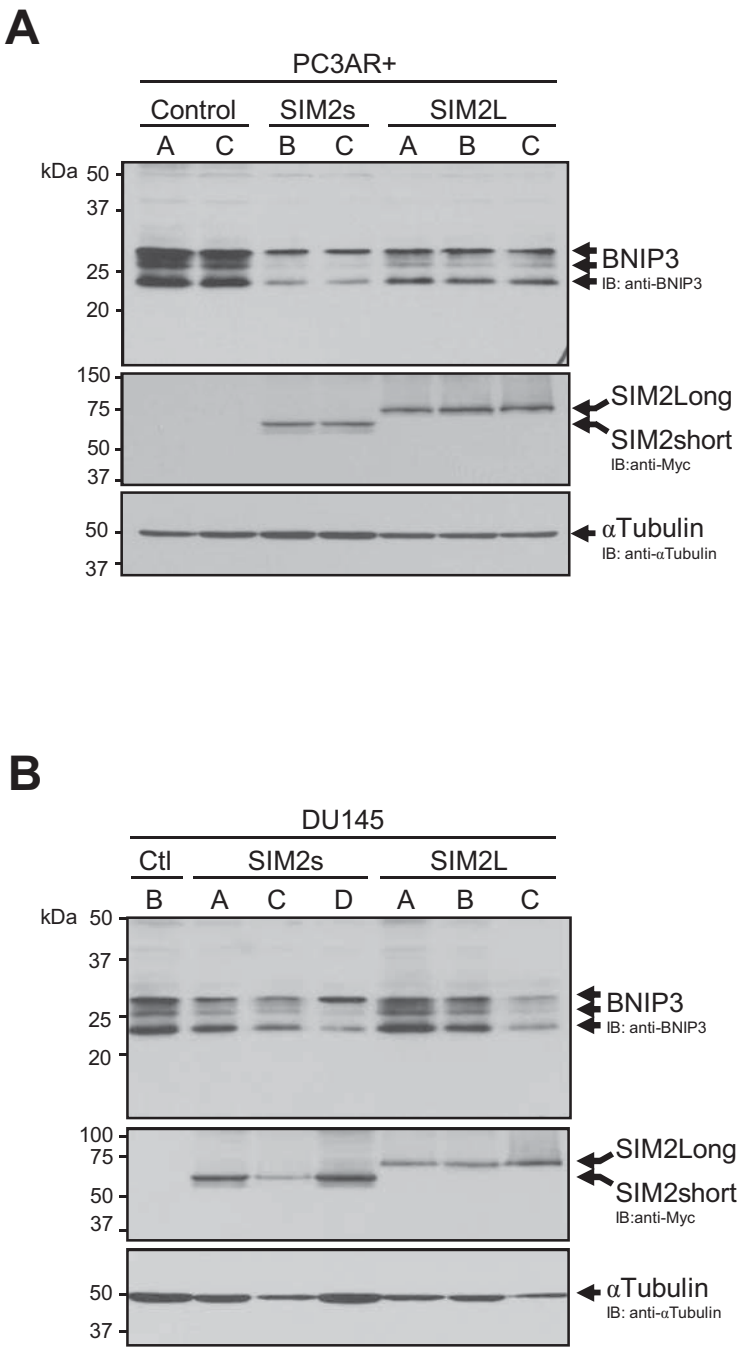

FIGURE 5.12: *Analysis of BNIP3 protein levels on stable ectopic expression of human SIM2L.myc in prostate PC3AR+ (A) and DU145 (B) carcinoma cell lines.*

12% SDS-PAGE separation of 35µg whole cell extracts, followed by sequential immunoblot detection of endogenous BNIP3, exogenous, myc tagged SIM2 and α-tubulin for loading control.

mediate regulation of *BNIP3* (**Figure 5.10** and **5.12**), it would be fascinating to further understand how the regulation of *BNIP3* by SIM2L may differ from that conferred by SIM2s, and ultimately insight into how the roles of each isoform may diverge.

In summary, these data suggest that SIM2 mediated repression of *BNIP3* in hypoxia may also involve competition for ARNT from HIF1α. This is the first evidence of SIM2 repression in the regulation of an endogenous target gene utilising this mechanism. The mechanisms of SIM2s-mediated repression of BNIP3 suggested from endogenous promoter ChIP experiments and mBnip3-promoter driven luciferase reporter gene studies in summarised in **Figure 5.11**.

5.2.8 SIM2s expression protects from prolonged hypoxia mimetic induced cell death in human prostate carcinoma PC3AR+ cells

As outlined in the introduction **section 5.1** and **figure 5.1**, autophagic and apoptotic cell death programmes are not mutually exclusive, and BNIP3 has been implicated in both mechanisms (for review see; [174, 176]). Aleman and colleagues have shown that cell death resulting from SIM2s antisense treatment of colon cancer RKO cells was apoptotic, being largely dependent on the activities of caspases 9 and 10 [91]. Mechanisms of autophagic cell death, however, have not been investigated, despite Aleman and co-workers also reporting an increase in *BNIP3* mRNA levels by microarray in SIM2s antisense treated RKO cells (see supplementary information [91]). This report is consistent with the current findings of this thesis of a role for SIM2s in the repression of *BNIP3*, and together supports the hypothesis that SIM2s-mediated repression of *BNIP3* may attenuate BNIP3-mediated cell-death processes to promote carcinogenesis.

Prolonged hypoxia induces cell death via an autophagic pathway involving the HIF1α mediated up-regulation of BNIP3 [186, 187]. Thus the possibility that SIM2s expression, concomitant with its repression of *BNIP3*, enhances tumour cell survival under prolonged hypoxic conditions was investigated next. Recently, the enhanced degradation of sequestosome 1 (SQSTM1/p62) has been found to occur under conditions of hypoxia-induced autophagy [191]. Reduced protein levels of SQSTM1/p62 were found following prolonged (44h) treatment of human prostate PC3AR+ cells with the hypoxia mimetics DMOG (dimethyloxallyl glycine, a hydroxylase inhibitor), consistent with previous reports [191], and DP (Dipyridyl, an iron chelator), compared to DMSO vehicle control, indicating the induction of hypoxia-activated autophagy in these cells using these 'hypoxia' mimetics (**Figure 5.13A**). Treatment with both hypoxia mimetics induced BNIP3 protein levels, however, the levels of DP-induced BNIP3 were slightly variable (**Figure 5.14A**, compare columns 1 & 5 to 3). Utilising a WST-1 reagent assay system which quantifies mitochondrial function as a measure of cell survival and growth, it was found that ectopic expression of SIM2s.myc in human prostate PC3AR+ cells resulted in increased cell survival in these hypoxia-activated autophagic conditions. Cells expressing SIM2s.myc maintained significantly higher mitochondrial function from 18 to 36 hours of DP treatment, whereas control cell viability dropped dramatically by 36 hours (**Figure 5.13B**). Intriguingly, from 18-36 hours of DMOG treatment, SIM2s.myc expressing cells showed an increase in mitochondrial function, indicating cell proliferation (**Figure 5.13B**). Ultimately, PC3AR+/SIM2s.myc cells were able to maintain increased cell survival and mitochondrial function above PC3AR+/Control cells in hypoxia-activated autophagic conditions induced by 44 hours of prolonged treatment with either of the hypoxia mimetics, and was concomitant with maintained SIM2s-mediated repression of BNIP3 (**Figure 5.13B** & **5.14A**).

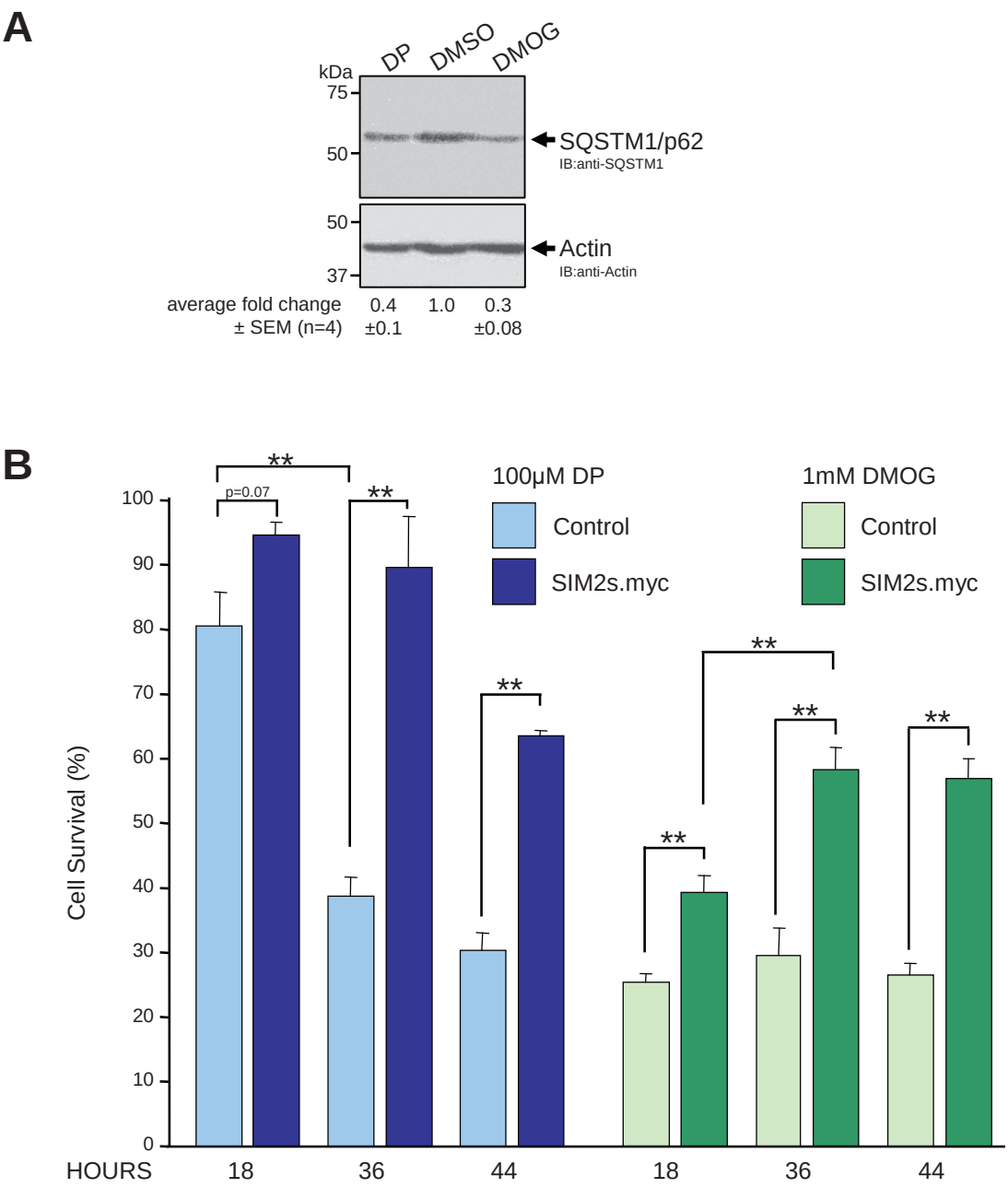

FIGURE 5.13: *Ectopic SIM2short expression protects prostate carcinoma PC3AR+ cells from prolonged hypoxia mimetic autophagy-induced cell death.*

(A) Prolonged (44h) treatment with hypoxia mimetics 100uM DP, or 1mM DMOG, compared to DMSO vehicle in PC3AR+ cells induces the turnover of SQSTM1/p62, a marker of hypoxia–induced autophagy. Anti-SQSTM1/p62 western-blot (35μg WCE) analysis representative of n=4 independent experiments. Relative average fold change of p62 levels compared to DMSO control of quantified chemiluminenest immunoblot data normalised to Actin protein using Image Quant v5.2. n=4. (B) Two independently derived puromycin resistant PC3AR+ polyclonal cell lines without (Control), and with stable expression of hSIM2s.myc were treated with hypoxia mimetics or DMSO control as described above. Analyses of cell survival from 18 to 44 hrs of hypoxia mimetic treatment were performed using optimised WST-1 reagent assay system (Roche) as per manufacturers' instructions. Cell survival (mitochondrial activity) is represented as the average percent of respective DMSO vehicle treated Control or SIM2s.myc cells at each time point. n=3 independent experiments. Error bars SEM. Unpaired, two-tailed students T-Test. Significance; ** $P \leq 0.01$. Values of non-statistically significant (n.s) P values are also indicated.

5.2.9 The hypoxic induction of the autophagy marker LC3-II fails upon ectopic SIM2s expression in PC3AR+ cells.

BNIP3, which localises to the mitochondria, has been shown to induce mitochondrial autophagy, or mitophagy, mitochondrial dysfunction and cell death in mouse embryonic fibroblasts (MEFs) [192, 193]. Thus inherent in the WST-1 assay system for cell viability which measures mitochondrial function, is the potential ability to not only correlate SIM2s-mediated repression of BNIP3 with attenuation of hypoxia-induced cell death, but more specifically with a functional outcome of BNIP3 activities at the mitochondria as part of hypoxic autophagic processes, although this assay has not been previously exploited to this end. Thus, to ascertain if SIM2s enhanced cell survival and mitochondrial activity, associated with BNIP3 repression, is via attenuation of hypoxia-induced autophagic cell-death processes reported to be mediated by BNIP3 [186, 187] the processing and induction of protein levels of the autophagy marker, LC3-II [194, 195] was specifically analysed. The studies shown here indicate that both DP and DMOG induce cell-death in the context of activated hypoxia-induced autophagy by measurement of SQSTM1/p62 protein levels (**Figure 5.13**). Likewise, others have found DMOG treatment to induce autophagy to a similar level as hypoxia by the measurement of LC3-puncta [187], however, any further effects of DP induced 'hypoxia' on autophagic cell-death processes have not yet been reported. Interestingly, after 44 hours of prolonged DMOG treatment or exposure to growth conditions of less than 1% oxygen (hypoxia), LC3-II levels were consistently induced in PC3AR+/Control cells, but not in PC3AR+/SIM2s.myc cells (**Figure 5.15**). These data strongly suggest that the hypoxic induction of autophagy is inhibited in SIM2s expressing cells, concomitant with BNIP3 repression (**Figures 5.15 & 5.14A**, respectively). Treatment with DP, however, resulted in equal induction of LC3-II protein between control and SIM2s expressing cells, and interestingly to a greater extent than that induced with DMOG treatment in control cells (**Figure 5.15A** & **B**). Despite apparent equal induction of LC3-II in control and SIM2s expressing cells, SIM2s expression is still able

protect cells from prolonged DP-induced autophagic cell-death, indicates that alternate mechanisms also exist for SIM2s mediated protection from prolonged 'hypoxia'-induced cell death concomitant with BNIP3 repression. Taken together, these data link increased SIM2s expression with enhanced cell survival during hypoxic stress, concomitant with BNIP3 repression, and the attenuation of hypoxia-induced autophagic cell-death processes.

Intriguingly, these experiments clearly showed that attenuation of HIF1α-mediated hypoxic induction of BNIP3 due to the ectopic expression of SIM2s was despite a dramatic increase in HIF1α protein levels associated with SIM2s expression (**Figure 5.14B**). This striking finding reveals further insights into how SIM2s may function in tumours to modulate HIF1α activities to aid tumour development. Namely, in conjunction with attenuating HIF1α activities on BNIP3, and stabilising HIF1α protein levels, SIM2s may allow for HIF1α to direct its activities away from promoting cell death, and towards aiding tumour survival and invasivness via the upregulation of HIF1α-mediated angiogenic pathways [196](see **section 5.2.10** below and **Figure 5.16**). Further discussion of potential roles for SIM2s in the regulation of HIF1α and the implications for an alternate role for SIM2s in tumourigenesis is contained within the following chapter, **chapter 6**.

5.2.10 SIM2s repression of BNIP3: Correlation to tumourigenesis and patient prognosis?

Mechanistic roles for SIM2s and BNIP3 in cancer remain to be fully defined, however, deregulation of both factors are emerging as select solid tumour markers and are associated with poor prognostic outcomes [80-82, 174]. As previously discussed, decreased BNIP3 levels and poor prognosis [177, 182, 183] clearly correlates with elevated SIM2s expression [43, 80] in pancreatic cancer. Moreover, consistent with our

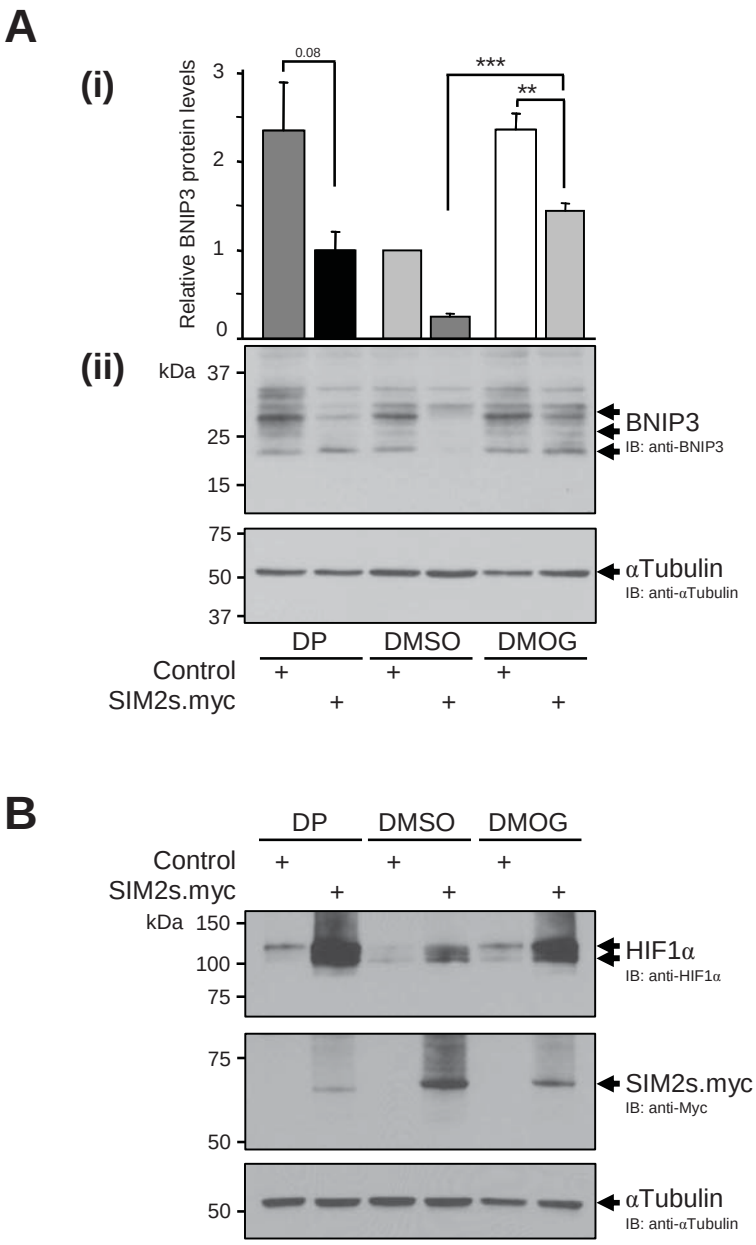

FIGURE 5.14: *(A) BNIP3 protein levels remain repressed with SIM2s.myc expression in PC3AR+ cells after 44 hours of prolonged hypoxic treatment with either DP or DMOG, compared to DMSO vehicle control treatment despite the apparent increase in HIF1α protein levels associated with SIM2s expression (B).*

Subconfluent cells with, or without, stable ectopic expression of SIM2s, ('SIM2s.myc' or 'Control', respectively) were treated with DMSO vehicle control or either of the hypoxia mimetics, DP or DMOG, or for 44 hours. (A) 35µg of whole cell extracts were separated by (A) 12% or (B) 8% SDS-PAGE, then subjected to immunoblot analysis of proteins as indicated. (A) Quantification from chemiluminescent immunoblot analyses of three independent experiments, western anlaysis of BNIP3 protein levels (all species indicated by the arrows), was normalised to alpha-tubulin protein levels, and shown as relative expression of DMSO treated control cell line levels, using ImageQuantv5.2 software. n=3, representing two independently derived polyclonal cell lines for both puromycin resistant control and stable SIM2s.myc expression. Error bars SEM. Two-tailed, unpaired student T-TEST was used. Significance, ** P<0.01, *** P<0.001.

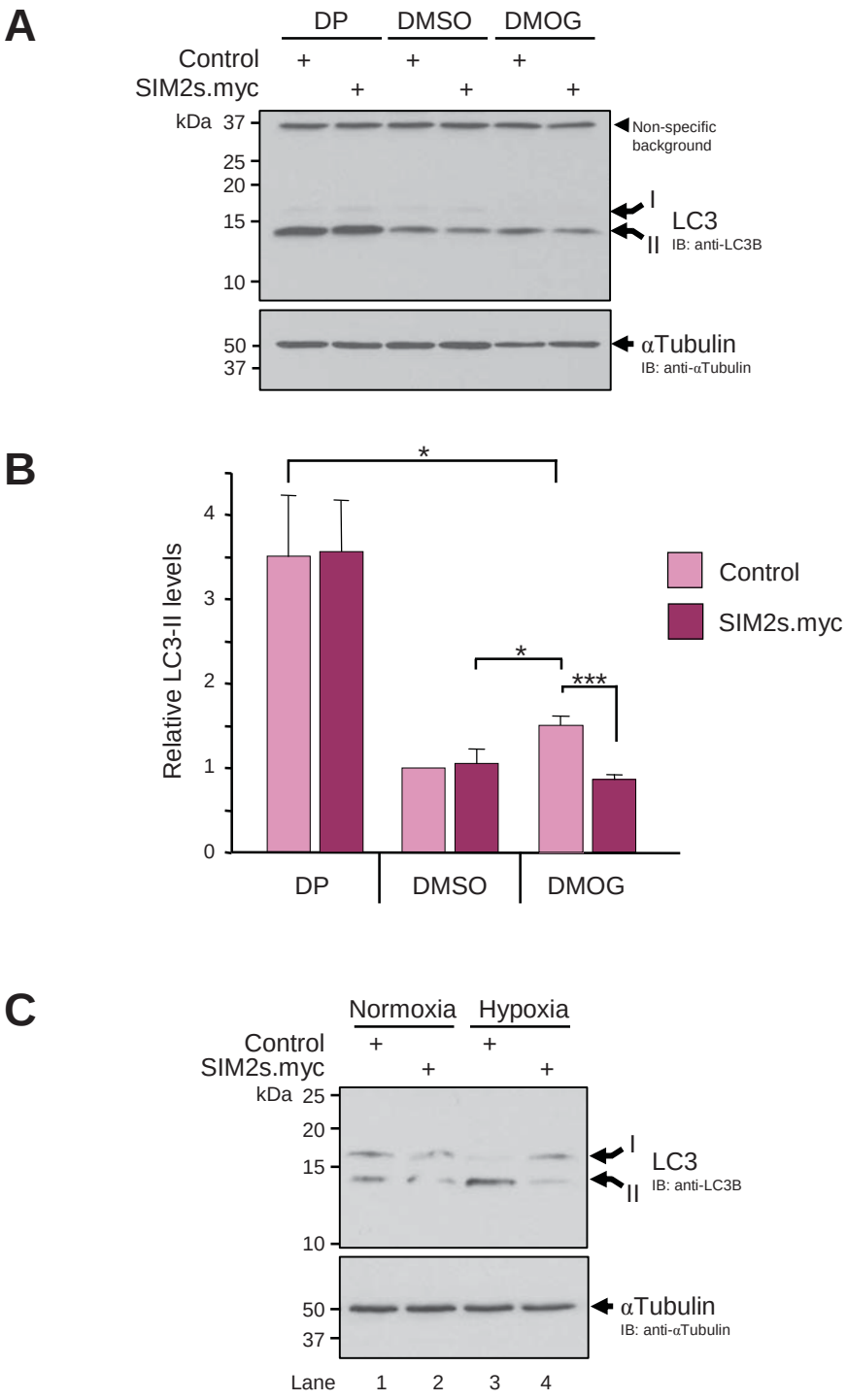

FIGURE 5.15: *Analysis of autophagy marker protein LC3-II levels after 44 hours of prolonged 'hypoxia' in prostate PC3AR+ cells, with or without (Control), stable ectopic expression of SIM2s.*

Subconfluent cells with, or without, stable ectopic expression of SIM2s, ('SIM2s.myc' or 'Control', respectively) were treated with DMSO vehicle control or either of the hypoxia mimetics, DP or DMOG, or left untreated (normoxia) or subjected to hypoxic growth conditions (Hypoxia < 1% O_2) for 44 hours. (A&C) 35 or 40 µg of WCE were separated by 15% SDS-PAGE, then subjected to immunoblot analysis of proteins as marked. (B) Quantification of western anlaysis of LC3-II protein levels (lower species as marked, ~14kDa), was normalised to both alpha-tubulin and anti-LC3B non-specific background (as indicated at approximately 35kDa) protein levels, and shown as relative expression of DMSO treated control cell line levels. n=3, representing two independently derived polyclonal cell lines for both puromycin resistant control and stable SIM2s.myc expression. Error bars SEM. Two-tailed, unpaired student T-TEST was used. Significance, * P≤0.05, ** P<0.01, *** P<0.001. (C) Representative of n=2 independent experiments.

findings others have reported, although not validated, in RKO colon cancer cells an up regulation of *BNIP3* mRNA following antisense knockdown of endogenous SIM2s, concomitant loss of cell-viability (refer to supplementary data in [91]). Unlike SIM2s [81], there is no understanding of how BNIP3 levels correlate to prostate tumour cell survival or prognosis. Independent studies reported on the 'Oncomine®Research' database (www.oncomine.org) offer an insight into the genetic profile of prostate cancer progression in which *SIM2* mRNA levels are significantly elevated in early stage carcinomas and advanced metastatic and hormone-refractory cancers compared to normal tissue controls, whereas corresponding BNIP3 levels remain unchanged until the onset of metastatic and hormone-refractory disease [197, 198]. These insights lead to the proposal that SIM2s may function to initially repress and/or inhibit *BNIP3* expression in competition with HIF1α with the onset hypoxic growth conditions, thus attenuate hypoxic cell death processes to allow prostate tumour development (**Figure 5.16**). Once alternate pro-tumourigenic HIF1α-mediated pathways are established in advanced tumours (reviewed by [134]) SIM2 may be unable to effectively compete with increasing levels of HIF1α to moderate the regulation of *BNIP3* (**Figure 5.16**). This putative model for SIM2s moderation of HIF1α activities, as evidenced here via SIM2s cross-talk on the endogenous HRE of hypoxia inducible *BNIP3*, provides a possible novel mechanism which allows for the apparent opposing functions of HIF1α [134] in the tumourigenesis of cancers with aberrant levels of SM2s.

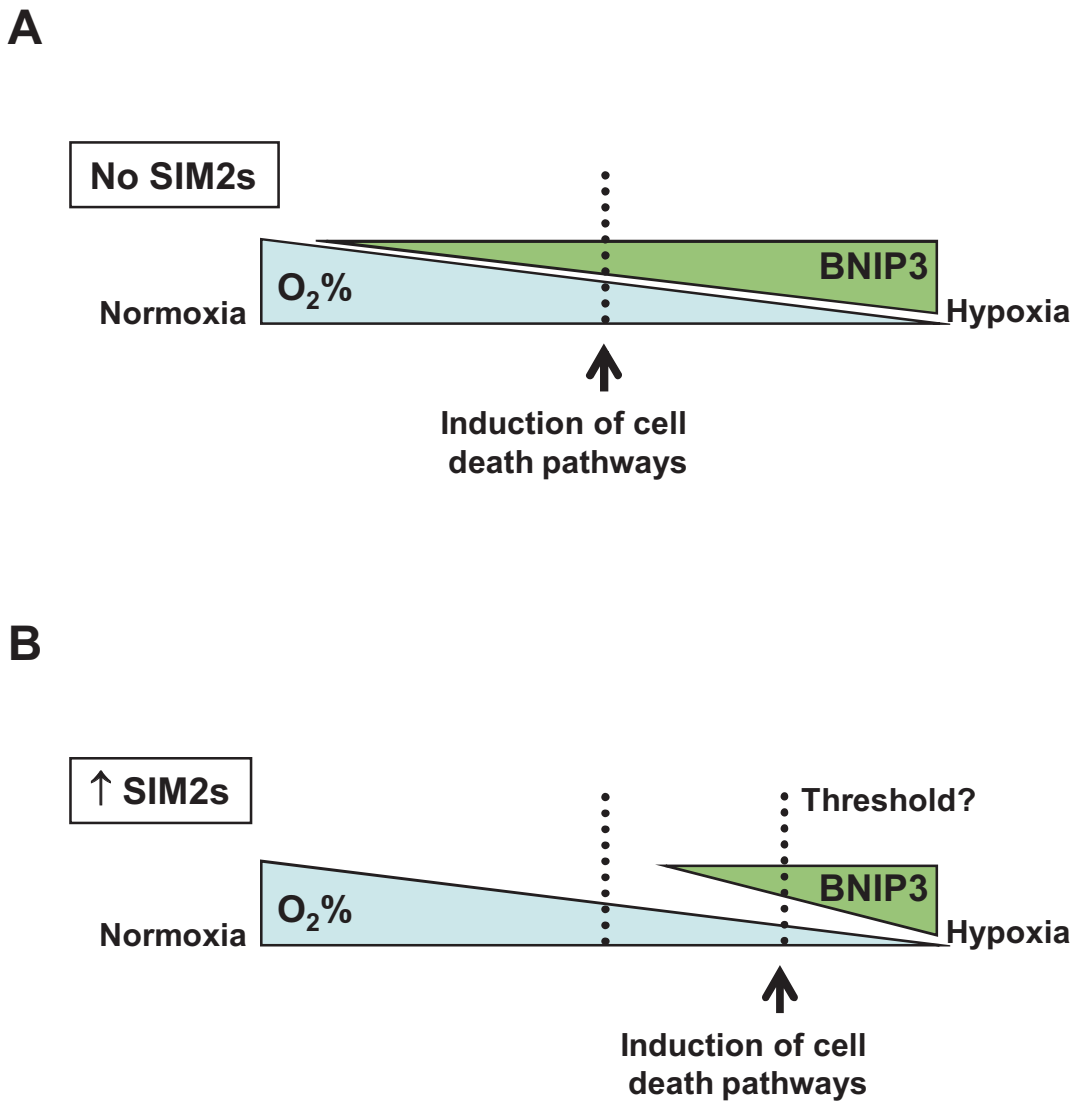

FIGURE 5.16: *The threshold at which the HIF1α-mediated hypoxic induction of BNIP3 would initiate cell death processes (A), may be delayed in tumours with aberrant levels of SIM2s via SIM2s-mediated direct repression of BNIP3 (B) thus allowing for tumour growth. SIM2s modulation of HIF1α-mediated hypoxic induction of BNIP3 via cross-talk on the endogenous HRE provides a possible novel mechanism which allows for the apparent opposing functions of HIF1α in tumourigenesis.*

CHAPTER 6

Novel findings for SIM2s activities in the Hedgehog & Androgen signalling pathways, and the regulation of HIF1a:

Further implications of roles for SIM2s in tumourigenesis

6.1 Hedgehog Signalling and SIM2 in Cancer:

6.1.1 INTRODUCTION

Extensive studies in vertebrate and cell culture model systems has lead to the current comprehensive understanding of the highly conserved components and mechanisms of Hedgehog (Hh)-signalling following Hh ligand activation. The Hh signalling pathway is directly linked to cell growth and differentiation processes and is essential for executing the cell fate decisions required for metazoan embryonic pattern formation and the homeostasis of adult tissues (for reviews see [199-201]). Consequently, the Hh pathway and its components are associated with a number of malformation and disease states (for review, [200]), and recently, mechanisms of tissue repair, stem cell renewal, and aberrant Hh activation with the pathogenesis of a number of tumour types (for review [202-206]). Hh signalling confers changes in gene transcription in response to the long and short range signalling of the Hh ligands, such as the mammalian Sonic, Indian or Desert Hedgehog (Shh, Ihh and Dhh, respectively) [201, 207]. Signalling is mediated by the effectors, and downstream targets of Hh signalling, the latently cytoplasmic zinc-finger GLI-kruppel family of transcription factors. First identified as the Ci (cubitus interruptus) protein in *Drosophila*, three mammalian homologues have been identified and denoted Gli1, Gli2 and Gli3 in mice (GLI1, GLI2 and GLI3 in humans) [103, 208, 209]. All confer transcriptional activation properties, and with the exception of Gli1, repression also. The positive or negative function of the Gli2 and Gli3 factors in response to the Hh-signal is context dependent and directed by specific modes and outcomes of proteolysis that arise in response to the Hh signal (reviewed in [199-201]) (**Figure 6.1**). In turn, the Gli factors themselves are gene targets of Hh-signalling, for example, *Gli1* is a target of Gli3 transactivation activities in response to Shh [200, 210]. Shh activated signalling inhibits both the transcription of *Gli3* and the formation of the Gli3 repressor (reviewed in [200]) to drive active signalling via the upregulation of Gli1. Conversely however, *Shh* gene expression itself is

thought to be downstream target of Gli3 repression as suggested by the ectopic expression of *Shh* observed in the developing dorsal neural tube [211] and anterior limb bud [212] of mouse embryos with targeted deletion of *Gli3*. Indeed, in *Drosophila* the absence of Hh ligand the Gli orthologue Ci (cubitus interuptus) is cleaved to its repressor form and directly inhibits *hh* gene expression (reviewed in [199, 201]). In this manner the Hh pathway is capable of autoregulation, and Gli3-mediated transcriptional repression of *Gli1* and *Gli2*, as seen during kidney patterning [213], is another mechanism of pathway repression. Likewise, down-regulation of Hh-signalling activities occurs via the Hh-signalling dependent Gli-mediated gene up-regulation of the transmembrane Hh ligand sensor protein, *Ptch1* (*Patched1*). For example, the over expression of Ptch has been shown to attenuate the induction of Shh-signalling target genes and consequently normal neural tube patterning [214]. Prior to Hh ligand binding, Ptch represses the signal transduction activity of the seven-transmembrane Hh pathway 'switch' protein, Smo (Smoothened) [199, 215-217] (**Figure 6.1**). Together these mechanisms of gene regulation directed by the Gli factors contribute to the ability of the Hh-pathway to confer a level of autoregulation as simply depicted in **figure 6.1**.

A number of significant studies have recently emerged citing the importance of increased Hh-pathway activity in the pathogenesis of many tumour types [200, 202], however, the mechanisms that initiate Hh-pathway activities in these cancers remain to be determined. Aberrant Hh-signalling is intimately associated with the initiation and progression of digestive tract tumours, including the pancreas [95, 204, 218-221], and prostate [98, 100, 222-224], which are strikingly the same tumour types in which SIM2s is found to aberrantly misexpressed [43, 52, 80, 81, 92-94, 96]. This correlation is perhaps more than coincidence as similar findings have been reported for the importance of SIM2s in tumour cell survival and association with an aggressive disease outcome in these tumour types [43, 81], which considered together highlights the potential for a shared functional link between SIM2s expression and Hh-pathway activities in these cancers. Specifically, treatment with antisense hSIM2s in pancreatic and colon cancer derived cell lines inhibits

tumour cell, and xenograft, growth and promotes apoptosis [43, 52, 91], indicating the essential requirement of SIM2s expression for tumour cell preservation. Similarly, inhibition of Hh signalling using the antagonist cyclopamine [225] (refer to **Figure 6.1**) in pancreatic carcinoma xenografts and cell lines results in cell death [219-221, 226, 227], indicating the essential requirement for an active Hh-pathway for the survival of tumour cells of this cancer type. An apparent functional link between SIM2s and Hh-signalling is also evident in prostate cancer, namely where there is a strong correlation between elevated SIM2s protein levels and prostate cancer aggression [81], as there is likewise with Hh-pathway activation in advanced prostate tumours [228]. Hh-signalling activation via the over-expression of Gli1 transforms cultured primary prostate epithelial cells (PrEC) and enhances cell proliferation and invasiveness [98] indicating that Shh-signalling may be a mechanism for prostate tumour initiation. Consistently, cyclopamine-induced inhibition of Hh-signalling also results in prostate cancer cell death [100] showing the requirement for Shh for cell survival and consequently inciting further investigation of the potential of cyclopamine as a treatment for advanced prostate cancer [229]. However, the essential requirement for SIM2s in prostate cancer initiation and cell survival is yet to be determined. Although there is strong data showing the requirement for SIM2s expression in human colon cancer RKO cell derived tumour xenograft survival [91], there exists conflicting data as to the essential nature of Hh-signalling in tumour derived cell lines of the colon [221, 227, 230], thus firm evidence for the dual requirements of SIM2s and Hh-signalling in this cancer type remains to be shown. In essence, there exists a compelling putative functional link between SIM2s and Hh-pathway signalling for pancreatic carcinoma cell survival and progression of disease, and up to point in prostate cancer. Thus at the time these studies were initiated, and even still to this day, the correlation for the dual, and perhaps linked, requirements for SIM2s expression and Hh-signalling for pancreatic tumour cell survival remains the firmest.

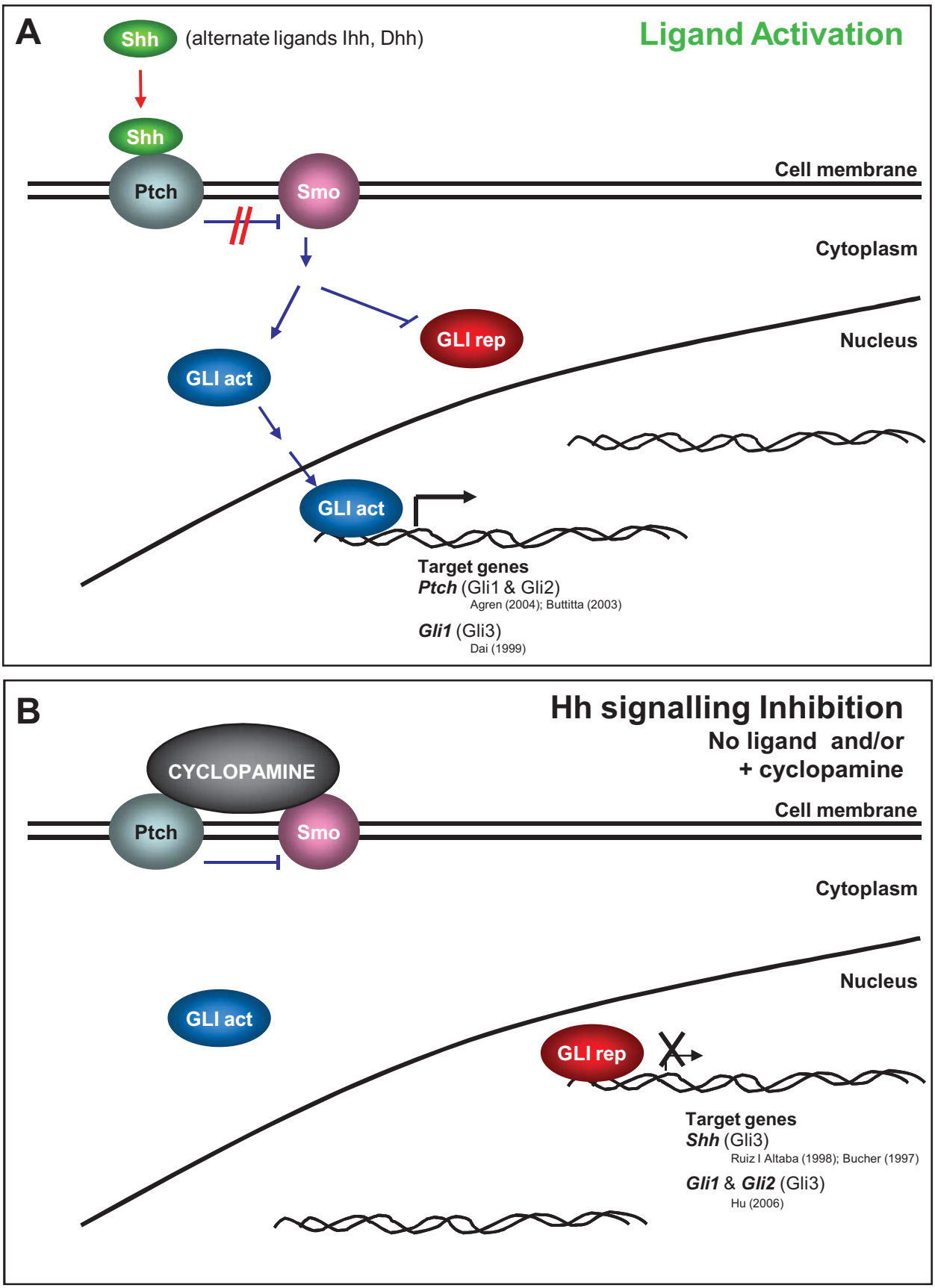

FIGURE 6.1: *Simplified view of the Hh-signalling pathway: GLI Transcription factors are downstream targets and mediators of autocrine Hh signalling in Hh responsive cells. (A) Upon ligand binding to Ptch, repression of Smo is alleviated to allow downstream signalling via the Gli transcriptional regulators. (B) Cyclopmaine is an antagonist of Hh-pathway signalling via inhibition of Smo transduction. Without ligand activation, Ptch continues to interfere with Smo at the outer membrane.*

Smo (Smoothened); Ptch (Patched); Shh, Ihh, Dhh (Sonic, Indian and Desert hedgehog, respectively); GLI1act (GLI activators: Gli1,2 and 3); GLIrep (GLI repressors: Gli3 and Gli2).

Neither human SIM2 isoforms (long or short) were detectable in the normal pancreas, nor was SIM2s detected in early pancreatic BPH (benign pancreatic hyperplasia) samples, however, levels were greatly elevated in pancreatic carcinoma derived cells [43, 52, 80]. This finding has very recently been validated in the most comprehensive global genomic analysis to date of clinical samples of pancreatic carcinomas compared to benign and normal tissue [96]. Similarly, there are no detectable levels of *Shh* in the normal pancreas, indeed active Hh signalling has been found to inhibit normal pancreatic development and is excluded from the developing pancreas as well as the mature organ to ultimately play a role in controlling embryonic pancreatic expansion [231, 232]. However, abnormal *Shh* expression and subsequent Hh signalling in PanINs (pancreatic intraepithelial neoplasia, non-invasive precursor lesions) has recently been shown to be an early and late mediator of pancreatic tumour genesis [219]. These PanIN lesions develop in a stepwise sequence of carcinogenesis, from the early PanIN-1 precursor lesions, to intermediate PanIN-2 lesions, and then become severe PanIN-3 lesions before onset of metastatic disease. All pancreatic cell types arise from *IPF1 (or PDX1* insulin promoter factor 1/pancreatic and duodenal homeobox 1) expressing cells (for review [233]), and as all ductal carcinomas express IPF1 the possibility arises that PanINs may stem from undifferentiated precursor cells [95]. Critical stages of known genetic mutation common to all invasive pancreatic ductal adenocarcinomas have been identified in PanIN (for reviews, [95, 203, 234]). Initially there is the early activation of K-RAS (Ras-Raf-MEK signalling) and expression of HER2/NEU in PanIN-1 lesions. Studies in mice reveal that *K-RAS* mutation alone will cause low frequency metastasis, however for invasive tumours this is followed by the intermediate stage inactivation of the $p16^{ink4a}$/$p19^{Arf}$ (Ink4a/Arf in human) locus (PanIN-2) [235, 236]. These are tumour suppressor genes located on the same locus which result from alternative reading frames, and are critical for the retinoblastoma (Rb) and p53 pathways, respectively. $p16^{ink4a}$ functions to control cell cycle progression by inhibiting the phosphorylation of Rb required for transcription of cell cycle promoting genes. $p19^{Arf}$ is proposed to be part of an autoregulatory loop that controls the levels of p53 in the cell, as high levels of $p19^{Arf}$ result in inhibition of p53

expression and in turn, high levels of p53 represses the $p19^{Arf}$ promoter. $p19^{Arf}$ binds MDM2 thus preventing the MDM2/p53 interaction which normally results in p53 degradation. The initial mechanism of $p16^{ink4a}/p19^{Arf}$ inactivation in cancer is in many cases found to be either loss of one or both alleles [235, 237, 238] (for reviews see [95, 239]). However, the promoter for both genes has been found to be silenced by methylation in the absence of any cell abnormality [238]. The resulting deregulation of p53, along with that of the tumour suppressor SMAD4, characterises the late genetic events (PanIN-3), driving the change from severe to invasive pancreatic cancer (for review, [234]). Mouse models of PanINs have also revealed the activation of the normally quiescent Notch pathway which mediates TGFα [240], as well as expression of both matrix metalloproteinase (MMP7) and cyclooxygenase 2 (COX2) (for review see [95]). Abnormal *Shh* expression and Hh signalling are now also implicated in this genetic profile of PanIN as early and late mediators of carcinogenesis [95, 219, 220]. These findings initially emerged from the analysis of pancreata from three week old mice with directed misexpression of *Shh* under the control of the Ipf/Pdx promoter which had developed pancreatic lesions that phenocopy those found during the development of human pancreatic cancer [219]. Four years following this finding, roles for Shh at multiple stages of pancreatic adenocarcinoma development have been further corroborated by Morton and colleagues (2007) [220].

Although the literature provides compelling evidence of a correlation between the overlapping expression profile and survival outcomes due to SHH and SIM2s expression in pancreatic carcinomas and tumour cells, it remains unknown what role, if any, SIM2s plays in pancreatic tumourigenesis and whether its expression may, or may not be, required in PanIN development to promote the onset of invasive cancer as is so for SHH. Overlapping expression patterns of SHH and SIM2 have been observed previous to the correlations mentioned here in pancreatic and prostate tumours. In the E10.5 mouse embryo, Ema *et al* (1996b) showed that the two murine *Sim* mRNA expression patterns were distributed within regions of *Shh* expression [34].

Interestingly, mSim2 expression was seen to precede and overlap with *Shh* expression in regions of the diencephalon and zona limitans *i*ntrathalamica (ZLI), whereas *mSim1* expression was subsequent to that of S*hh* [71]. *Sim1* expression doesn't appear to be directly downstream of Hh signalling, as in the developing somites, *Sim1* expression is normal in *Gli2*$^{-/-}$/*Gli3*$^{-/-}$ embryos [216]. In *mSim2*$^{-/-}$ and *mSim1*$^{-/-}$/*mSim2*$^{-/-}$ mice *Shh* expression remained normal, therefore mSim1 and mSim2 are not essential for *Shh* expression [71]. However, significantly, misexpression of *mSim2* in the dorsal CNS of transgenic mice resulted in the ectopic expression of *Shh* [71]. The data from the Epstein *et al* (2000) study indicate that mSim2 activity is sufficient to induce *Shh* transcription. These data provide a potential mechanism that may link SIM2s and SHH expression observed in pancreatic cancer survival. As aberrant misexpression of murine Sim2 is sufficient to upregulate Shh expression, if SIM2s becomes aberrantly misexpressed in pancreatic carcinomas, it may regulate and/or maintain SHH expression, and thus SIM2s and downstream SHH expression and activities are linked for tumour cell survival.

The following studies sought to determine if SIM2s expression is linked to the activities of the Hh-pathway in a cancer context, and if ectopic expression of SIM2s can initiate PanIN development in the pancreata of mice.

6.1.2 RESULTS & DISCUSSION

6.1.2.1SIM2s and the regulation of SHH

To initially investigate if ectopic expression of human SIM2s could similarly regulate the expression of SHH in cancer cells as has been found for mSim2L misexpression in the developing mouse brain [71], and further, subsequently influence the Hedgehog signalling pathway, SIM2s was stably over-expressed in a number of human cell lines corresponding to tissues or carcinoma types which are known to express

endogenous levels of SIM2s [48, 52, 80, 81, 93, 96]. These cell lines included human embryonic kidney 293A, human prostate carcinoma DU145, LNCaP and PC3AR+, and human pancreatic carcinoma CFPAC and PANC-1 derived cell lines (refer to **Chapter 5**, **Figure 5.1**). Strikingly, SHH levels were found to be dramatically increased to detectable levels upon stable ectopic expression of SIM2s (SIM2s.myc) in independently derived polyclonal cell lines, compared to empty-vector Control cell lines, by western blot analysis of (50µg) whole cell extracts from 293A and LNCaP cells (**Figure 6.2A**). Likewise, this associated increase in endogenous SHH levels upon stable expression of SIM2s was further validated in DU145 cells compared to empty-vector control cells, however, SHH failed to be detected with or without SIM2s.myc expression in PC3AR+ cells despite analysis of 70µg of whole cell extracts (**Figure 6.2B**). A reduction in enhanced endogenous SHH protein levels upon siRNA-mediated knockdown of SIM2s.myc (siSIM2s-1759), compared to scrambled siRNA controls (siControl), confirmed the direct relationship between increased SHH levels and ectopic expression of SIM2s as distinctively shown here in DU145/SIM2s.myc cells (**Figure 6.2C**).

To examine if the increase in SHH observed at the protein level was due to increased transcription and/or mRNA stability of *SHH*, *SHH* mRNA levels were assessed by well controlled semi-quantitative (sq) reverse-transcriptase (RT)-PCR of cDNA synthesised from total RNA extracts from prostate DU145 cells, with and without stable SIM2s.myc expression. A faint, but distinct, amplicon for *SHH* at the expected size was observed only in cDNA samples from DU145/SIM2s.myc cells, and not DU145/Control cells (**Figure 6.3A**, lane 10 compared to lane 9). Although SHH was unable to be detected by western blot analysis of whole cell extracts from pancreatic carcinoma CFPAC±SIM2s.myc cells (data not shown) as found for PC3AR+±SIM2s.myc cell extracts (see above, **Figure 6.2B**), a distinct upregulation of *SHH* message levels was also found upon ectopic SIM2s expression in CFPAC cells compared to levels in the parent cell line (Control) (**Figure 6.3B**, lanes 13 & 14 respectively). Semi-quantitative-RT-PCR assessment of *ARNT1* and

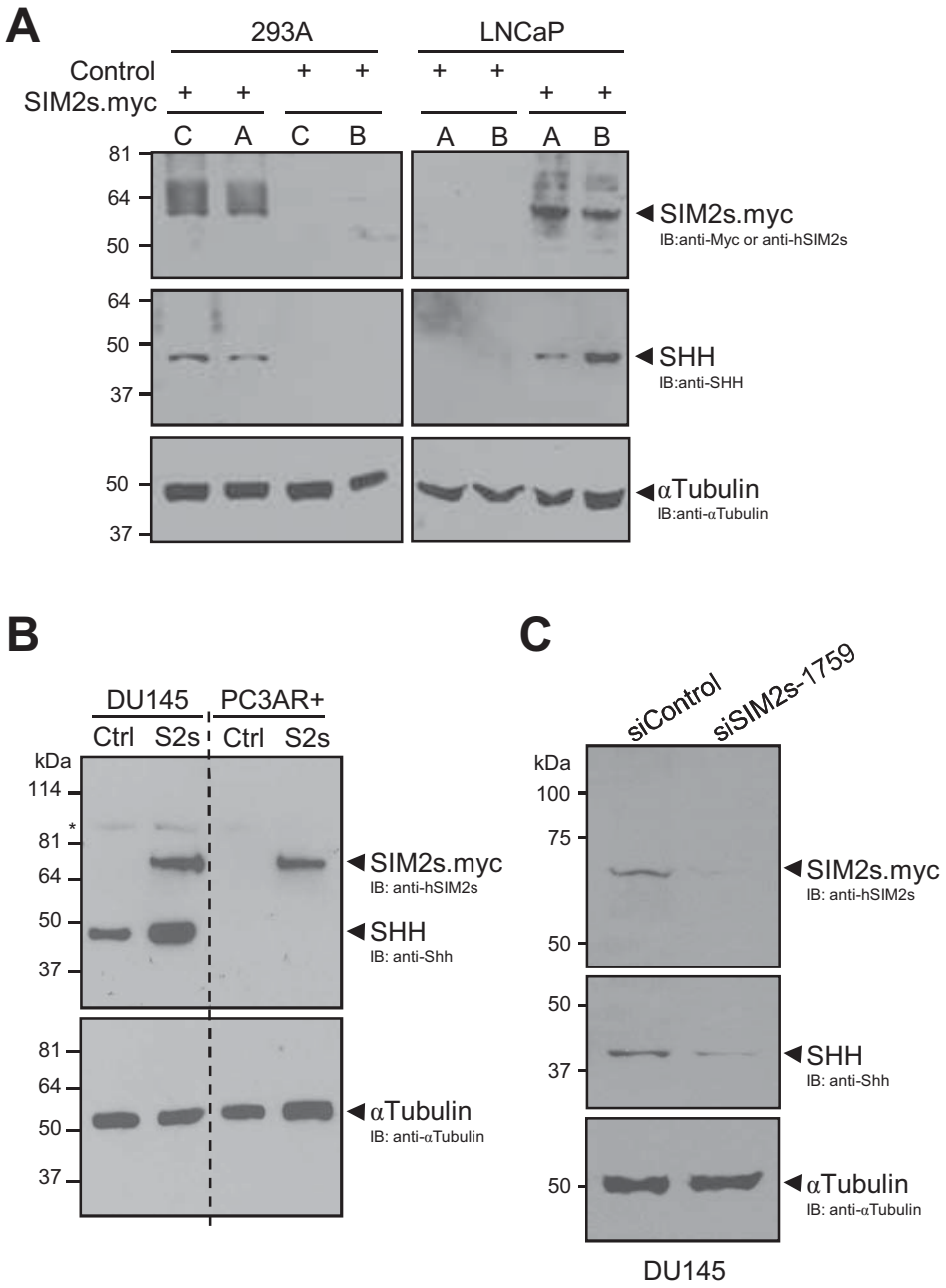

FIGURE 6.2: *(A) An increase in endogenous protein levels of SHH is observed with stable expression of myc tagged human SIM2s (SIM2s.myc) in embryonic kidney 293A and prostate carcinoma LNCaP independently derived polyclonal cell pools. (B) SHH protein also increases with stable expression of SIM2s in prostate DU145, but not in PC3AR+ carcinoma cells, where SHH levels are undetectable. (C) SHH protein levels decrease upon siSIM2s-1759 siRNA-mediated knockdown of ectopic SIM2s in prostate DU145/SIM2s.myc polyclonal cells, compared to scrambled control (siControl) siRNA controls.*

(A&C) 50µg or (B) 70µg of whole cell extracts from independently derived polyclonal pools for SIM2s.myc (S2s), or puromycin resistant (Control/Ctrl) cell lines, were separated by 8% SDS-PAGE, followed by immunoblot analysis of proteins as marked. Doted line denotes were marker lane has been spliced out. * = non-specific background band. Representative of minimum 3 independent experiments. (C) Cells were treated 2x100nM siSIM2s-1759, 24h apart, then whole cell extracts were made 72h after first treatment. Representative of minimum 3 independent experiments per cell line.

ACTIN mRNA levels were used as cDNA template input/loading controls. These data indicate that SIM2s may confer regulation of *SHH* at the mRNA or transcription level.

As aforementioned, expression of mSim2L has previously been shown to be sufficient, but not necessary, for the expression of *Shh* in the embryonic mouse brain [71]. Likewise, these studies show that ectopic expression of human SIM2s in human carcinoma cell lines also appears to be sufficient for the upregulation of SHH levels. Thus, to determine if endogenous SIM2s is necessary for *SHH* expression in carcinoma derived cell lines, unlike in the developing mouse brain [71], prostate LNCaP cells were treated with siSIM2s-1759 siRNA for specific knockdown of SIM2s, or a scrambled control siRNA (siControl), and subsequently endogenous *SIM2s* and *SHH* mRNA levels were assessed by sq-RT-PCR. Excitingly, this preliminary study revealed a reduction in *SHH* mRNA levels concomitant with siRNA knockdown of endogenous SIM2s (**Figure 6.3C**). Further studies in LNCaP, and other prostate and pancreatic carcinoma cell lines, to validate this finding were inconclusive due to inconsistencies in the efficacy of transiently transfected siRNA oligonucleotides to knock down endogenous SIM2s in these cells (data not shown) (see **Figure 6.2C** above). This preliminary observation is in part consistent with that previously proposed by Epstein and co-workers (2000) [71] who showed in transgenic mice that ectopic expression of mSim2L enhanced expression of a *lacZ* reporter gene driven by the Shh Brain Enhancer-1 (SBE1) – 1.3kb genomic fragment from mouse *Shh* intron 2, indicating mSim2L is sufficient to activate *Shh* transcription [71]. The authors of this study report that *in vitro* gel shift studies failed show evidence of mSim2/Arnt binding within the 532bp region of the SBE1 said to confer reporter activity. This sequence does not contain any putative sites for potential mSim2L/Arnt binding, hence the transcriptional upregulation of *Shh* was proposed to be mediated indirectly [71]. Yet, the potential for mSim2L-mediated regulation via direct binding activities outside of this region, with the requirement of another factor(s) that functions through the 532bp fragment identified, was not explored. Not available to Epstein and colleagues in 2000 is the readily accessible

bioinformatic genomic DNA screening and analysis now available since completion of the human genome project in 2004 [241]. Analysis of genomic DNA 10kb upstream, and 2kb downstream, of the start of exon 1 from both human and mouse *SHH* gene revealed a number of putative sites for SIM2/ARNT binding containing the core 5'-ACGTG-3' sequence. A number of sites were identified in the human *SHH* putative regulatory region analysed, however, only three sites were identified in the mouse. These sites are of particular interest as they are conserved between species, also in a positional manner. In particular, two CME 5'-TACGTG-3' sites approximately 10kb upstream of exon 1, and 1.5kb downstream of the start of exon 1 inside intron 1 (**Figure 6.4**, each site marked with an asterix). Also, a core 5'-ACGTG-3' site is also positionally conserved approximately 6.5kb upstream of exon 1 (**Figure 6.4**, marked with a # symbol). The nature of this site conservation highlights a potential *bona fide* role of these sites for *SHH* gene regulation, perhaps in a manner as is found for HIF1α-mediated regulation via the conserved hypoxia response element (HRE) of *BNIP3* in humans, rats and mice [187, 188](and see findings in **Chapter 5**). In light of this new bioinformatic information, and considering the preliminary finding here that SIM2s may be essential for *SHH* expression in LNCaP cells (**Figure 6.3C**), until it is definitively shown otherwise in the future, contrary to that observed by Epstein and colleagues (2000) the short isoform of SIM2 at least may have a direct role in the regulation of *SHH* gene expression in a tumour context.

6.1.2.2 Effect of ectopic SIM2s expression on the activities of the Hh signalling pathway in prostate and pancreatic carcinoma cell lines

The transcriptional activators GLI1 and GLI2 translocate to the nucleus upon Hh ligand activation of pathway signalling and are key mediators of the Hh-pathway response (for review [205]). Expression of the *GLI1* gene itself is also upregulated upon overexpression of SHH and Hh-signalling activation via direct GLI2 transactivation, and is thus regarded as a marker of active Hh-signalling [105, 205] (**Figure 6.1**). Therefore with this in mind, *GLI1* mRNA levels were examined by sq-RT-PCR in DU145 and CFPAC cells

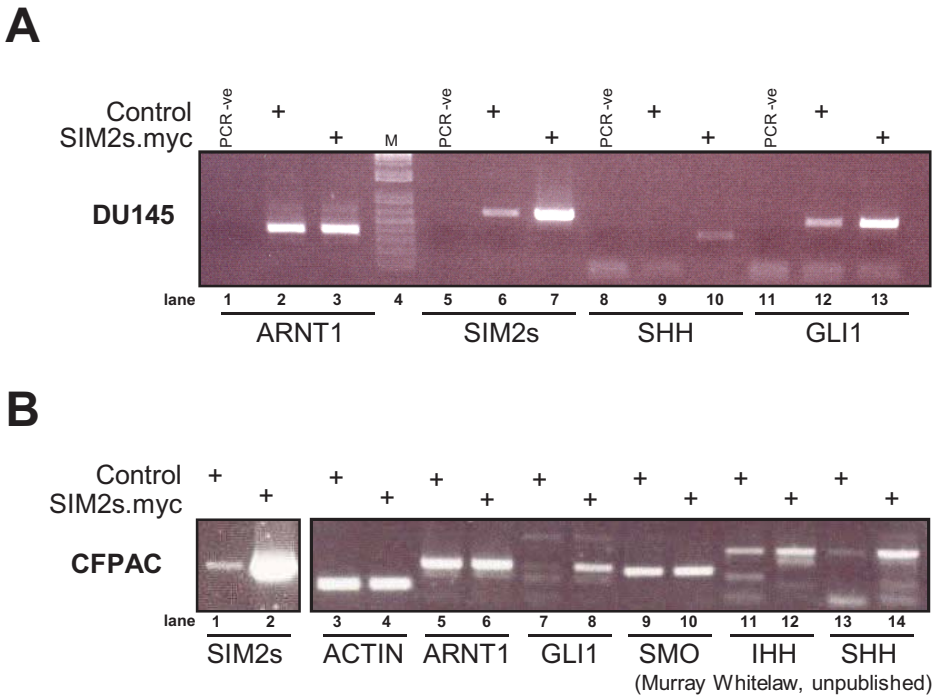

FIGURE 6.3: *Expression of Hedgehog signalling pathway factors are up-regulated in human carcinoma cell lines upon stable ectopic expression of SIM2*.

(A & B) Stable ectopic expression of myc tagged human SIM2s (SIM2s.myc) in pancreatic CFPAC and prostate DU145 carcinoma cells results in increased mRNA expression of Hedgehog signalling factors as indicated. ARNT1 mRNA levels serve as loading control.

(C) Preliminary observation: SHH mRNA levels decrease with siRNA knockdown of endogenous SIM2s in LNCaP cells. Cells were treated 2x100nM siSIM2s-1759 or scrambled control siRNA (siControl), 24hrs apart, then total RNA extracts made 72h after first treatment. (A-C) Semi-quantitative (sq) RT-PCR analysis from cDNA made from total RNA extracts. PCR amplicons identified following EtBr stained 1% agarose gel electrophoresis. M= marker. No RT control PCR reactions not shown. –ve = no cDNA template PCR negative control. GAPDH, ARNT and ACTIN mRNA levels serve as cDNA input/load control

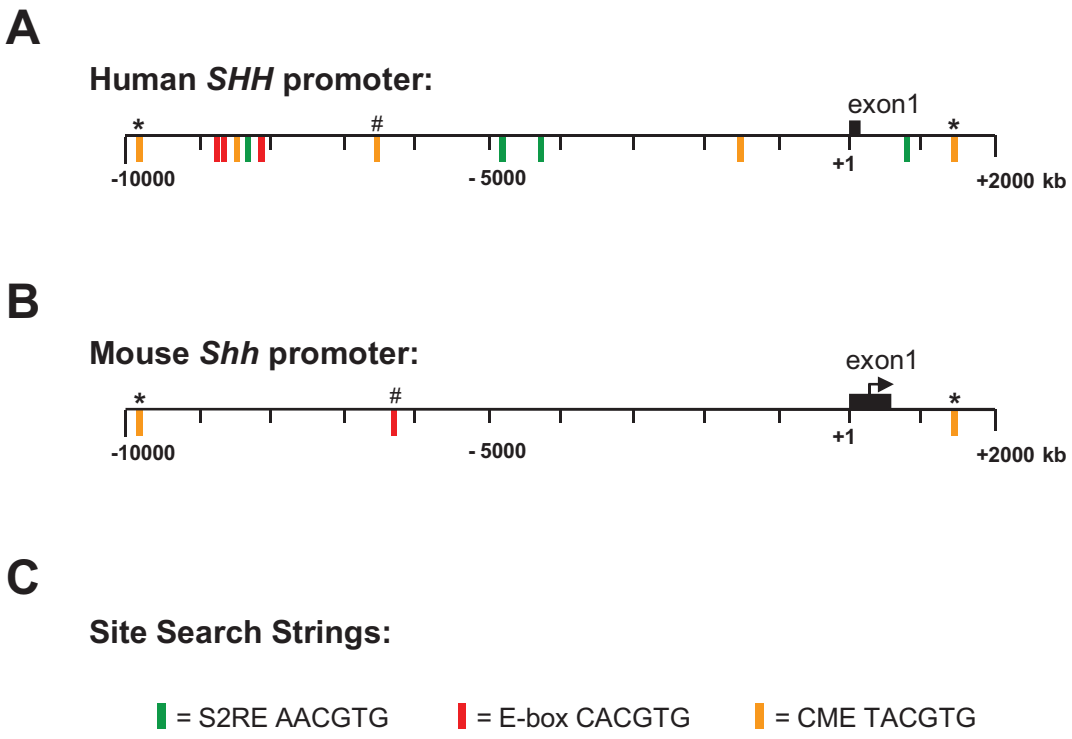

FIGURE 6.4: *Bioinformatic identification of putative binding sites for SIM2s/ARNT-mediated regulation of SHH gene expression in humans and mice.*

Genomic DNA sequence upstream of (A) *hSHH*, accession number NM_000193, and (B) *mShh*, accession number NM_009170, sourced from online resource Human (and Mouse) BLAT (http://genome.ucsc.edu/cgi-bin/hgBlat?command=start) and both strands scrutinised using 'TESS (Transcription Element Search System)' (http://www.cbil.upenn.edu/cgi-bin/tess/tess) for putative sites using the search strings as indicated in (C). * = positionally conserved sites of same sequence, # = site containing a core ACGTG, conserved in a positional manner.

with and without ectopic expression of SIM2s to ascertain if the upregulation of SHH observed in these cells correlates to functional activation of Hh signalling. *GLI1* mRNA were found to be distinctly upregulated in both DU145 and CFPAC SIM2s expressing polyclonal cell lines compared to empty-vector or parent line control cells (**Figure 6.3A & B**, lanes 12 & 13, and 7 & 8, respectively). Message levels of the Hh signalling ligand IHH, and the cell membrane receptor SMO have previously been found to upregulated 35-fold and 1.6-fold, respectively, by quantitative RT-PCR analysis of pancreatic tumour samples compared to normal tissue levels [226]. In a similarly consistent manner in pancreatic carcinoma cell line CFPAC, which as previously been shown to not to express any endogenous levels of *SHH*, *IHH* or *GLI1* [221], preliminary assessment of the levels of these genes in the CFPAC/SIM2s.myc polyclonal cell line by sq-RT-PCR revealed an increase in *IHH* mRNA, however, from this method of analysis no change in *SMO* mRNA levels was observed, when compared to the parent CFPAC cells (**Figure 6.3B**, lanes 9 to 12). It must be noted at this juncture that in contrast to the evidence of increased levels of SHH protein upon ectopic SIM2s expression in LNCaP and DU145 cells, and increased *SHH* and *GLI1* mRNA in DU145/SIM2s.myc cells presented here, microarray studies conducted subsequent to this work in these cell lines (see **Chapter 4**) failed to show any change in the mRNA levels of *SHH* or *GLI1* upon ectopic expression of SIM2s (data not shown). However, as the studies discussed in **Chapter 4**, **section 4.2.5** show, detection of differential changes in mRNA levels by the microarray has greatly reduced sensitivity compared to PCR methods. Consequently the absence of changes in the Hh signalling factors in the microarray may be attributable to this limitation of microarray.

In summary, increased message levels of the Hh signalling activating ligands *IHH* and *SHH*, as well as the transcriptional target and important mediator of Hh-signalling, *GLI1*, appear to be downstream of ectopic SIM2s expression, which together further implicates SIM2s with the activation of Hh signalling in these tumour cell lines.

Cyclopamine is a specific Hh-pathway antagonist (refer **Figure 6.1**), and treatment of human digestive tract, pancreatic, and prostate carcinoma derived cell lines and mouse xenografts of these cancer types with cyclopamine has been shown to result in induced apoptosis, and decreased cell viability, invasive potential, and tumour volume [98, 100, 219, 221, 227, 228]. These reflect the extremely similar set of outcomes observed upon antisense-mediated knockdown of endogenous SIM2s in similar solid tumour-derived cell lines and xenografts of these types [43, 52, 91]. To further examine if ectopic SIM2s is indeed linked to activation and/or maintenance of the Hh-pathway, the effect of the Hh-signalling inhibitor, cyclopamine, on the growth of cultured prostate and pancreatic cancer cells, with and without stable ectopic expression of SIM2s, was investigated. Pancreatic PANC-1 cells were chosen as they have detectable endogenous levels of the activating ligand SHH (**Figure 6.5A**), and others have previously shown a dramatic 5-fold reduction in cell viability following treatment with cyclopamine in these cells, indicating their responsiveness to Hh-signalling [221]. Likewise, prostate DU145 cells which also have detectable levels of SHH (**Figure 6.5A**) that increase upon SIM2s expression (**Figure 6.2**), have also been shown by others to be highly susceptible to loss of cell viability following treatment with cyclopamine compared to cells treated with the structurally similar control drug, tomatidine [98]. As Hh-pathway stimulation via the expression of the diffusible form of SHH, SHH-N, has been shown to partially rescue cyclopamine induced colon carcinoma cell death *in vitro* [227] it was hypothesised that the enhanced levels of SHH observed upon SIM2s expression, for example in DU145 cells, may contribute to resistance to cyclopamine in SIM2s.myc cells. Consistent with these previous reports, cell viability and growth, assessed by the number of adherent cells, was dramatically reduced in PANC-1 and DU145 cells following treatment with cyclopamine compared to tomatidine control treated cells (**Figure 6.5B**, compare panels i & ii, and v & vi, respectively). Excitingly, cells with stable ectopic expression of SIM2s.myc appeared unaffected by treatment with cyclopamine, displaying no discernable difference in growth compared to tomatidine controls (**Figure 6.5B**, compare panels iii & iv, and

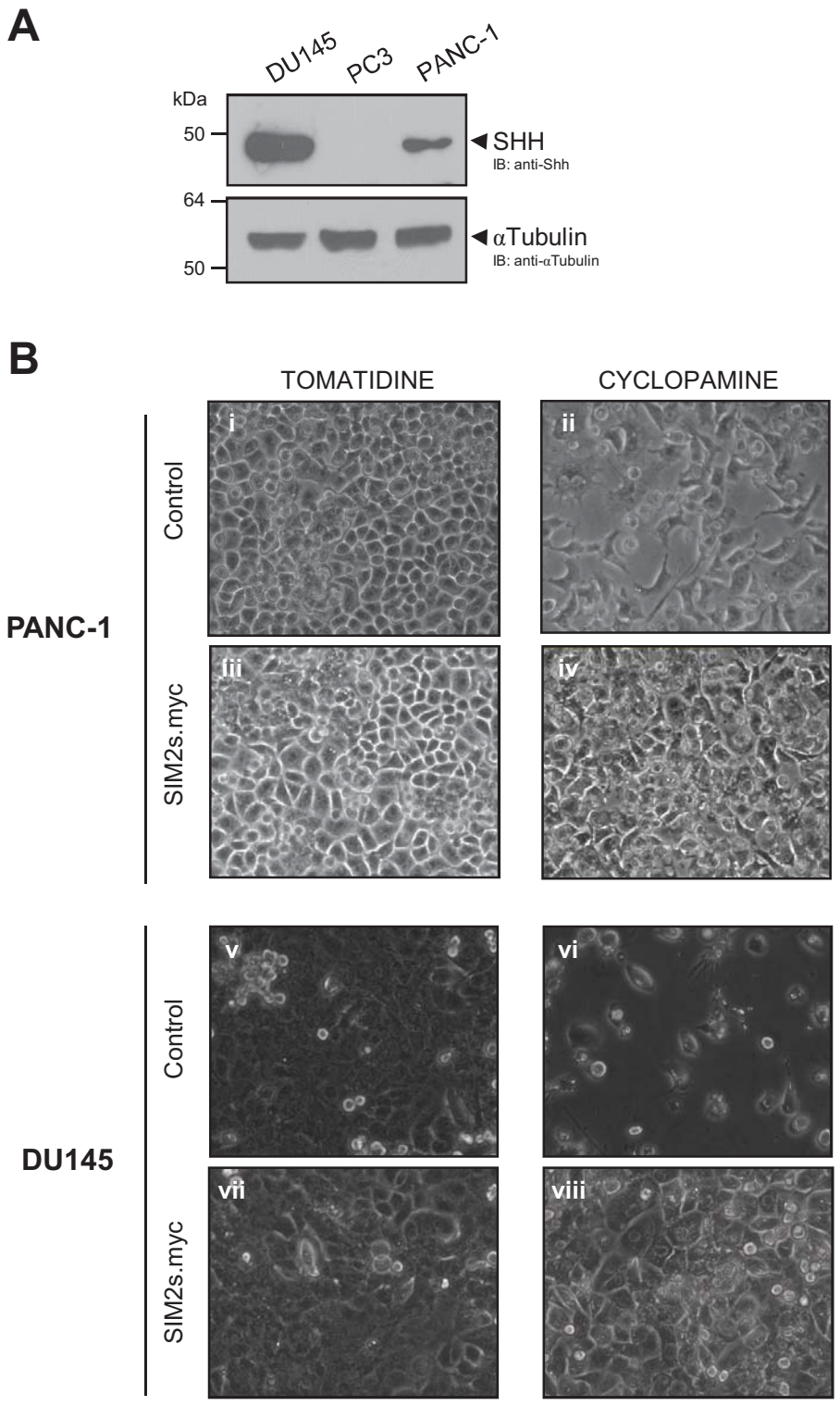

FIGURE 6.5: *Preliminary Observation: Stable ectopic expression of SIM2s in human pancreatic, PANC-1, and prostate, DU145, carcinoma cell lines correlates to increased cell survival on treatment with the Hedgehog Signalling Pathway inhibitor, Cyclopamine.*

(A) Immunoblot analysis of Shh in parent prostate DU145 & PC3AR+, and pancreatic PANC-1, carcinoma cell lines. 80µg of whole cell extracts were separated by 8% SDS-PAGE followed by immunoblot detection of proteins as indicated. (B) 10uM Cyclopamine, compared to 10uM Tomatidine control treatments. Cells first treated at 50% confluency, and media replaced every three days and growth monitored. PANC-1±SIM2s.myc cells treated for 12days; DU145 puromycin resistant control line treatment time 7days, and SIM2s.myc line treatment time 15 days shown here. 200x images, size not relative between cell types.

vii & viii). This outcome is consistent with the hypothesis that SIM2s contributes to Hh-pathway activation and maintenance, perhaps via the upregulation of SHH levels.

However, as afore mentioned, treatment with Shh-N only partially rescues colon cancer derived cells from cyclopamine induced cell death [227]. Cyclopamine directly binds and interferes with the signal transduction properties of the Hh-pathway surface receptor SMO [242], and requires expression of the SMO repressor, and fellow membrane Hh receptor, *PTCH* [98, 221, 227], to inhibit Hh-signalling (**Figure 6.1B**). Cyclopamine can inhibit the Hh-pathway irrespective of SHH expression across a number of pancreatic and other digestive tract tumour-derived cell lines [219, 221], thus maintained activation of Hh-signalling upon treatment with cyclopamine can be conferred downstream of PTCH and SMO. A reduction in *GLI1* mRNA is associated with cyclopamine treatment, indicating reduced Hh-pathway activity [100] and studies by others have shown a potent rescue from cyclopamine in prostate 22RV1 cells upon overexpression of GLI1, and not by an altered inactive form of GLI1 (GLI^{zfd}) [98]. Likewise, in DU145 cells CMV-driven GLI1 expression confers resistance to the cyclopamine-induced reduction in cell viability [228], and the findings presented here also appear to show this same outcome upon constitutive expression of SIM2s in these same cells (**Figure 6.5B**). Therefore, given GLI1 is upregulated upon ectopic SIM2s expression highlights the further possibility that SIM2s may be driving Hh-pathway signalling and protecting from the cyclopamine-induced cell death downstream of SMO via direct, or indirect, regulation of *GLI1* [71].

Active Hh signalling in cultured cells has been measured by others via luciferase gene expression driven by a SHH-responsive GLI-dependent synthetic promoter containing eight repeats of the GLI response element, 5'-GAACACCCA-3' (8xGliRE-LucII), derived from the mouse *HNF*-3β minimal floor plate enhancer [105, 221, 243]. This tool was utilised to further investigate if ectopic SIM2s expression does indeed correlate to enhanced and/or maintained Hh signalling; perhaps via the upregulation of SHH expression and

subsequently GLI1 activities, and/or by directly affecting GLI activities. Mouse fibroblast NIH3T3 Hh-signalling responsive cells [243] were transiently transfected with expression vectors for human SIM2s, or human GLI1 as a positive control, and any changes in the transcriptional activation of the 8xGliRE driven reporter gene was subsequently analysed by dual luciferase assay. Ectopic expression of hSIM2s was consistently found to correlate to an increase in transactivating GLI-dependent reporter activity, to varying degrees, across three independent experiments (representative experiment shown if **Figure 6.6Ai**). Although the level of SIM2s-induced activation of the reporter varied, so too did the degree by which ectopic hGLI1 was able to activate the reporter (data not shown). Thus, when the data are assessed in terms of the capacity of hGLI1 to transactivate directly, being denoted as 100%, in each given experiment, ectopic hSIM2s was consistently found to induce approximately 5% of the capacity of ectopic hGLI1, or in other terms, hGLI1 was able to consistently induce 21.5-fold [±3.4 SEM] (n=3) greater than hSIM2s (**Figure 6.6Aii**, in-set graph). SIM2s-mediated activation of the 8xGliRE-luciferase reporter was of a much lower potency compared to that of ectopic hGLI1. This may be indicative of a putative indirect mechanism of pathway activation, perhaps via the upregulation of SHH levels and/or the direct, but mild, up-regulation of GLI1 itself, to initiate pathway activation which results in the up-regulation of endogenous GLI-activator transcription factors in these cells, and perhaps confers protection from cyclopamine-induced cell death. SIM2s/ARNT may confer direct transcriptional regulation of hGLI1 as putative sites with a core 5'-ACGTG-3' for directly conferring SIM2s/ARNT transcriptional activities were identified upon bioinformatic analysis of 13kb upstream of the start of *hGLI1*, clustered in a manner that does not immediately suggest random occurrence as four putative sites are clustered within approximately 4.5kb across the entire region of sequence investigated (expected random occurrence 4^6=1 per 4096bp) (**Figure 6.6B**). The likelihood of SIM2s being a potent regulator of GLI1 is unlikely when considered in the context of the extremely low potency of SIM2s-associated activation of the 8xGliRE-LucII reporter from these studies (**Figure 6.6Ai**). All three GLI proteins confer transactivational properties (for review [200]), thus any and/or all GLI proteins, not

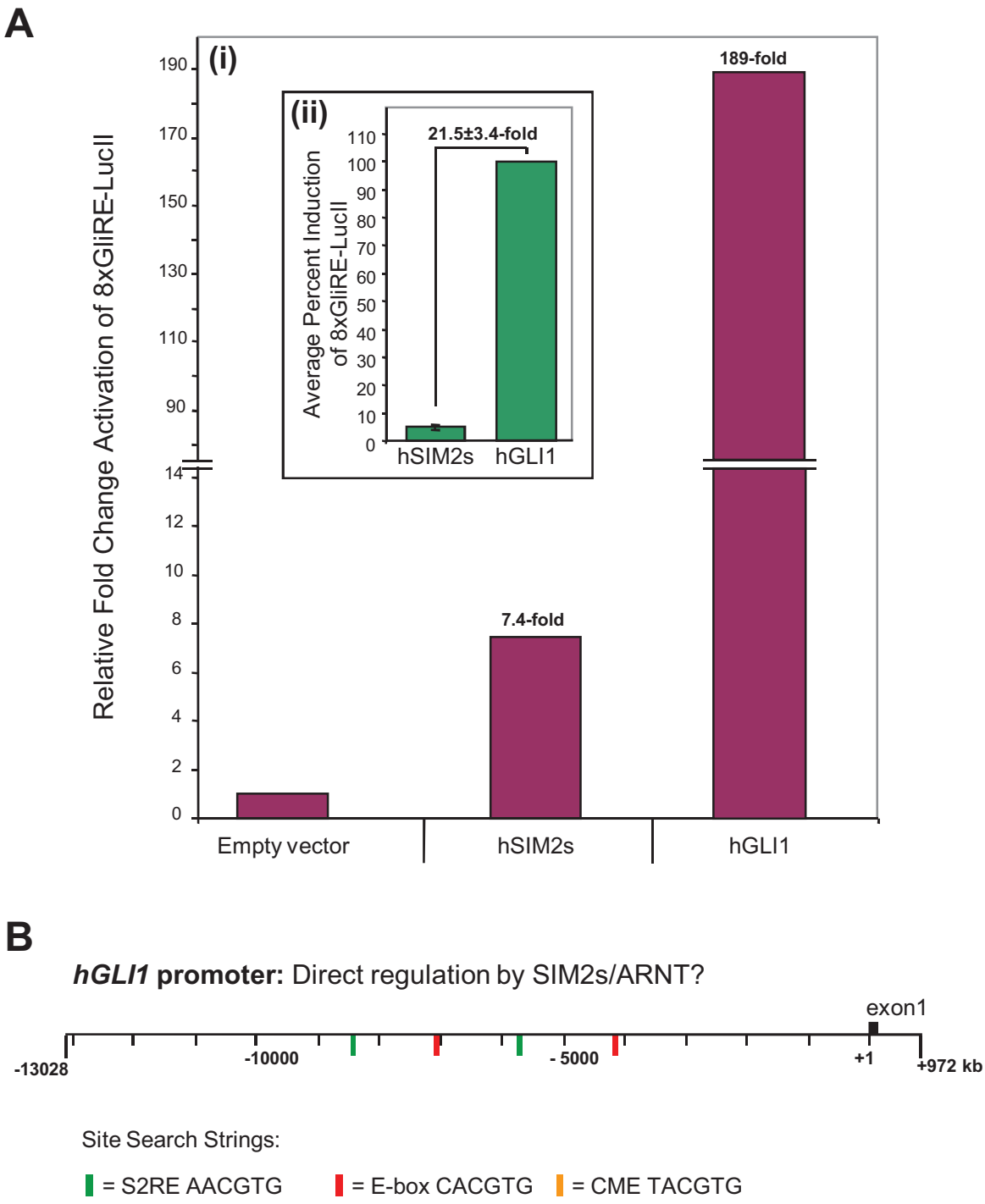

FIGURE 6.6: *Activation of Hh signalling downstream of SIM2s expression.*

(A) Activation of 8xGliBS-LucII reporter upon transient expression of human SIM2s in NIH3T3 cells normalised to pRL-TK expression. Human transient GLI1 expression serves as positive control for reporter activation. (i) Representative dual luciferase experiment (n=1) done in triplicate, and shown as fold change relative to empty-vector control. Inset graph (ii), hSIM2s consistently activated the 8xGliBS-LucII reporter to ~5% the capacity of ectopic hGLI1 activation (100%). Representative of three independent experiments (n=3), error bars/margin, SEM. (B) Bioinformatic identification of putative sites for SIM2s/ARNT-mediated activation of *hGLI1* expression. DNA sequence sourced from online resource 'Human BLAT' (http://genome.ucsc.edu/cgi-bin/hgBlat?command=start) from *hGLI1* accession number NM_005269 and both strands scrutinised using 'TESS (Transcription Element Search System)' (http://www.cbil.upenn.edu/cgi-bin/tess/tess) for site strings as indicated containing core ACGTG.

just GLI1, may be conferring the SIM2s-mediated activation of the 8xGliRE-LucII reporter (**Figure 6.6A**). It lies in future work to determine the mechanism of SIM2s-mediated upregulation of *GLI1;* whether it be (a) as a direct target of SIM2s transcription, perhaps only in response to certain environmental stimuli such as heightened cellular Hh responsiveness, or (b) indirectly through Hh-pathway activation via SIM2s-mediated SHH upregulation. It is also interesting to consider that as SIM2s may function downstream of the SHH ligand binding cell surface receptors, that the enhanced levels of SHH may be a result of SIM2s inhibiting the expression and/or formation of the GLI3 repressor, which is observed upon pathway activation [200, 205], and is associated with the repression of Shh gene expression in mice [211, 212]. Indeed, SIM2s may be promoting the expression and/or formation of the GLI3 activator, thus resulting in the up regulation of GLI1, and for that matter GLI2, levels upon SIM2s expression [210]. The potential link between SIM2 and the regulation of GLI3 and GLI2 expression and activities, and not GLI1, in specific contexts also emerges from close analysis of targeted deletion studies in mice. Mice which lack *Gli1* expression do not display any developmental defects and appear normal [244], however, it is interesting to note that in mice with targeted deletion of either Sim2 [3, 58], or Gli2, or Gli3 [245, 246], display similarly shared phenotypes of skeletal and craniofacial abnormalities; namely defects in rib development and cleft palate. Although mice which lack Gli3 are rarely born, those that are suffer respiratory distress and die shortly after birth [246] which is strikingly similar to the aerophagy-induced death observed in all *Sim2*$^{-/-}$ neonate mice [58]. Perhaps these observations of a putative relationship between SIM2s and the regulation of the GLI factors from developmental processes, considered in light of the studies presented and literature discussed here, are indeed indicative of the mechanistic roles for SIM2s in Hh-pathway activity in tumourigenesis.

In summary, **Figure 6.7** indicates the number of potential avenues by which SIM2s may enter the Hh-pathway, perhaps exclusively, or in a context specific combination, for pathway activation and/or signalling maintenance. Although the molecular mechanism(s) remains to be determined, taken together, the data

discussed from **figures 6.3** and **6.4** indicate that ectopic SIM2s expression may be linked to activation and/or maintenance of Hh-pathway signalling in cultured cells.

6.1.2.3 A role for SIM2s in tumour initiation via mediating activation of the Hh-pathway? Generating mice with directed misexpression of human SIM2s in the pancreas

Ectopic SIM2s expression also appears to be upstream of both SHH and GLI1 expression in pancreatic CFPAC and prostate DU145 polyclonal cells (**Figure 6.3A & B**), both key to Hh-signalling initiation and maintenance [205]. Misexpression of *SHH* in the pancreas results in the onset of precursor lesions in 3 week old mice [219], and ectopic expression of GLI1 in primary prostate epithelial cells (PrEC) is sufficient to transform these cells to a cancer-like state, inducing uncontrolled cell growth in culture and the formation of aggressive subcutaneous xenograft tumours in nude mice [98]. The current data suggest that SIM2s expression correlates to activation of Hh signalling in prostate and pancreatic cancer-cell types, and importantly the data suggest SIM2s contributes to cell survival via activation of this pathway as over-expression of SIM2s in SHH-positive prostate DU145 and pancreatic PANC-1 cancer cells appears to confer resistance to cyclopamine-induced cell-death (**Figure 6.5**). Given the compelling correlation from the literature between the requirements for both active Hh-signalling [219, 226] and SIM2s expression in pancreatic tumour cell survival [43, 52] that existed at the time of these studies, and the consistent preliminary links between SIM2s and SHH expression and Hh-pathway activation and cell survival presented here, understanding how SIM2s may function in pancreatic tumour formation and/or maintenance was more closely investigated. In particular, the following studies aimed to determine if, like Shh, ectopic SIM2s might also be sufficient to initiate pancreatic tumour formation via activation of the Hh-pathway, which ultimately may help elucidate a potential role for SIM2s in all human cancers where SIM2s is misexpressed [43, 52, 80, 81, 91, 96]. To this end human SIM2s cDNA was ectopically expressed under the control of the pancreatic endoderm specific *IPF* promoter in the pancreas of mice. These mice were developed in collaboration with

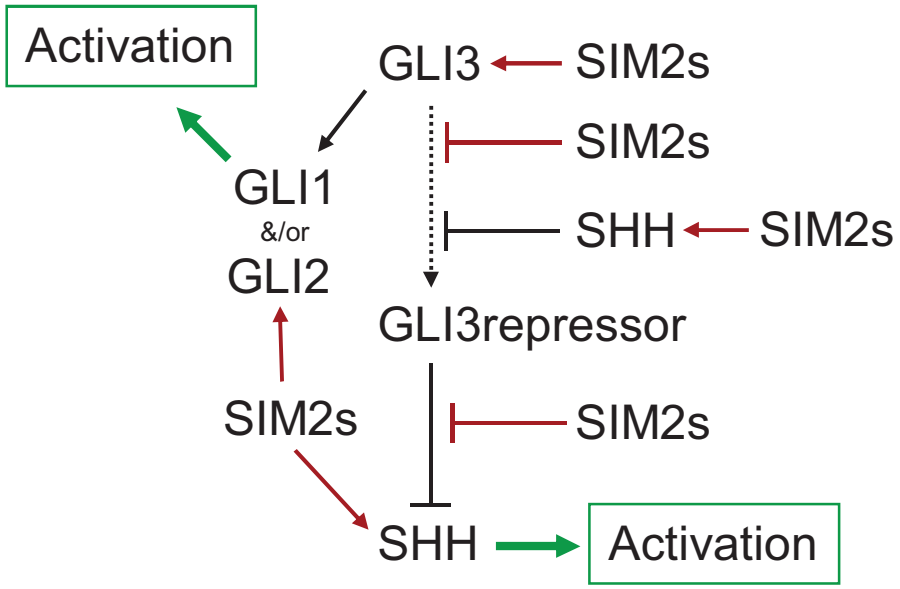

FIGURE 6.7: *Putative mechanisms by which SIM2s may interact with components of the Hh pathway (indicated in red) to initiate and/or maintain active signalling.*

Dotted line indicates proteolytic event to gain repressor form of GLI3
Solid black line = mechanisms of transcriptional regulation and or pathway activities, direct &/or indirect

L. Poellinger (Karolinska Institute, Stockholm, Sweden), and H. Edlund and co-workers (University of Umeå, Sweden), the latter of whom initially developed this method for ectopic expression of *Shh* in the pancreas [247] (**Figure 6.8A**) which resulted in the formation of pancreatic precursor cancer lesions as later identified by Thayer and colleagues [219]. Successful integration of the hSIM2s transgene was determined following PCR analysis of genomic DNA as shown for identification of transgenic F1 pups in **Figure 6.8B** from founder mice, 7191, 7192 and 7183. The pancreata of hSIM2s.myc transgenic F1 mice were next analysed by immunofluorescence for ectopic expression of hSIM2s compared to wild-type (WT) littermate controls. As hSIM2s was under the control of the *IPF* promoter, SIM2s expression was expected to co-localise with endogenous IPF. In general, staining for hSIM2s (red) appeared to be enhanced in all transgenic pups compared to WT littermates, however, despite the commercial anti-hSIM2s antibody (Santa Cruz) being previously established to successfully detect ectopic hSIM2s.myc in the nucleus of cultured cells by immunofluorescence (IF) (S. Woods, unpublished), distinct cellular localisation of hSIM2s cannot be determined from these analyses (**Figure 6.9**, central and right panels). Staining for hSIM2s did co-localise with IPF (green), however, in a 'regional' and not cell specific-type manner (**Figure 6.9**, right panels). For example, pancreata sections from mouse TG-7192/01 shows enhanced staining for hSIM2s in a region of high IPF expression, indeed, hSIM2s staining appears to extend beyond the region of positive IPF staining in sections from littermate TG-7192/03 (**Figure 6.9**, panels d-f, and m-r, respectively). Conversely, no hSIM2s staining was detected in some areas with IPF expression as observed in independent regions from TG-7191/02 pancreata (**Figure 6.9**, compare panels g-l, with j-l). These data appear to indicate ectopic hSIM2s protein levels in transgenic mice, however, in a somewhat indistinct manner both in terms of cellular localisation and in reference to endogenous IPF expression. As Hh signalling was found to be elevated upon SIM2s expression in cultured cells by measures of upregulated *GLI1* mRNA expression levels, GLI-dependent reporter activity, and resistance to cyclopamine-induced cell death (**Figures 6.3-6**), the pancreata of hSIM2s-transgenic mice were next analysed for enhanced GLI1 levels as a measure of Hh-pathway

activity downstream of hSIM2s expression. Consistent with *in vitro* studies, cytosolic GLI1 (green) levels appeared to be elevated in transgenic mice pancreata compared to WT littermate controls, and like hSIM2s expression with IPF, in regions with indications of ectopic hSIM2s expression, but not always necessarily cell specific (**Figure 6.10**). As a freely diffusible form of Shh (Shh-N) mediates long-range signalling [248], it is conceivable that in response to hSIM2s expression, and/or hSIM2s-activated Hh-pathway, upregulated Shh and its long-range signalling may account for this indicator of active Hh-signalling in cells where hSIM2s is not apparently expressed.

Conclusive findings from these studies of directed hSIM2s.myc misexpression in the pancreas were severely limited by the poor detection of ectopic hSIM2s by IF in the pancreatic tissue sample sections. However, despite this technical limitation, no aberrant changes in the structural morphology of the tissue or the appearance of any tumourigenic lesion-type structures were observed in the pancreas sections from three-week old *IPF-hSIM2s.myc* transgenic mice, as were found in *IPF-Shh* pancreata from the same age mice by others [219, 247] (**Figure 6.11**). The intestinal-like morphology and lesions of the pancreas from *IPF-Shh* mice [247] is apparent in **figure 6.11** from the pattern of nuclear staining of pancreata sections from these 3 week old mice. Thus even if hSIM2s was successfully expressed, alone it does not appear to confer the same potency of Hh-signalling activation, as does Shh misexpression [219], required to initiate tumour lesion formation by three weeks in the pancreas. Nor beyond this stage of development, as the hSIM2s transgenic mice failed to show any signs of ill health or impaired function of the pancreas as measured by glucose tolerance tests [249] (data not shown, H. Edlund personal communication) to a maximum of 10 months of age.

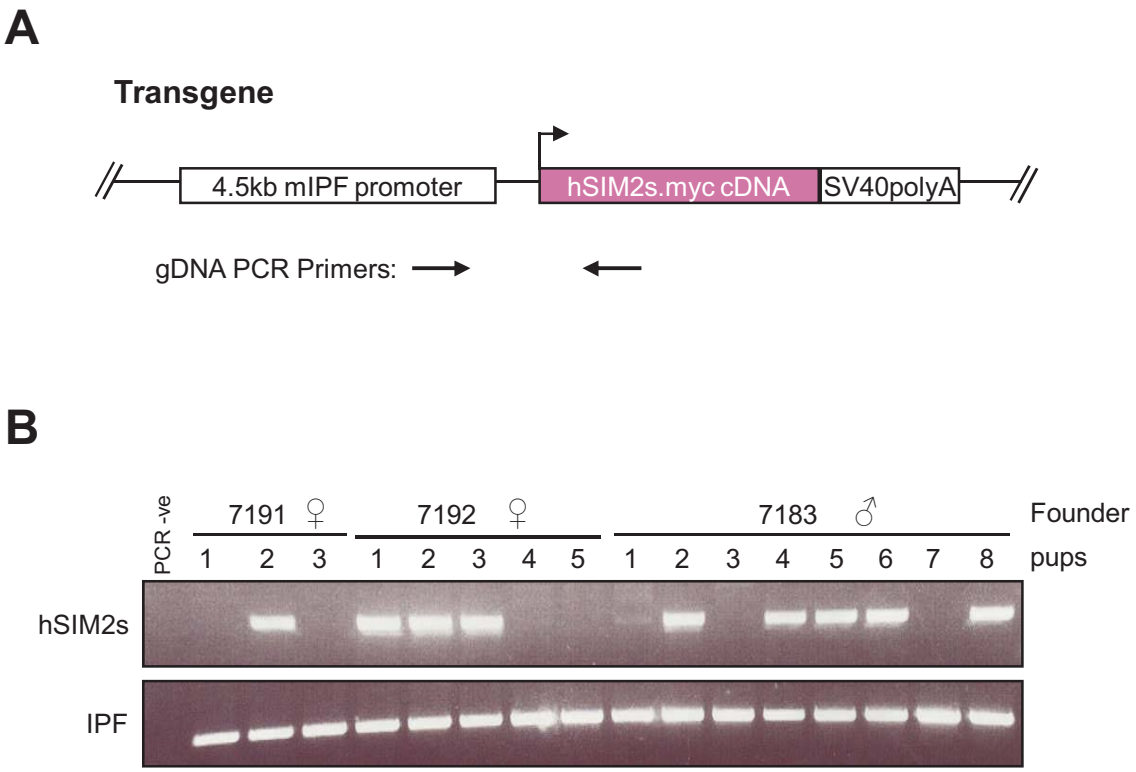

FIGURE 6.8: *Generation of transgenic mice with ectopic human SIM2s in the pancreas.*

(A) Human SIM2s.myc cDNA (3' myc tagged) expression controlled by the mouse IPF promoter for the generation of mice with hSIM2s.myc misexpression in the pancreas. (Subcloning of hSIM2s.myc into IPF driven expression construct by Murray Whitelaw). (B) Identification of transgenic mice. Genomic DNA was extracted from tail tips taken from pups of founder mice, 7191, 7192 and 7183, generated by Elisabet Palsson and Prof. Helena Edlund, University of Umeå, Sweden, then used for genomic PCR (35x cycles) detection of ectopic human SIM2s.myc expression, compared to endogenous IPF as loading control. Primers for detection of the hSIM2s transgene, indicated in part A, were designed by Elisabet Palsson.

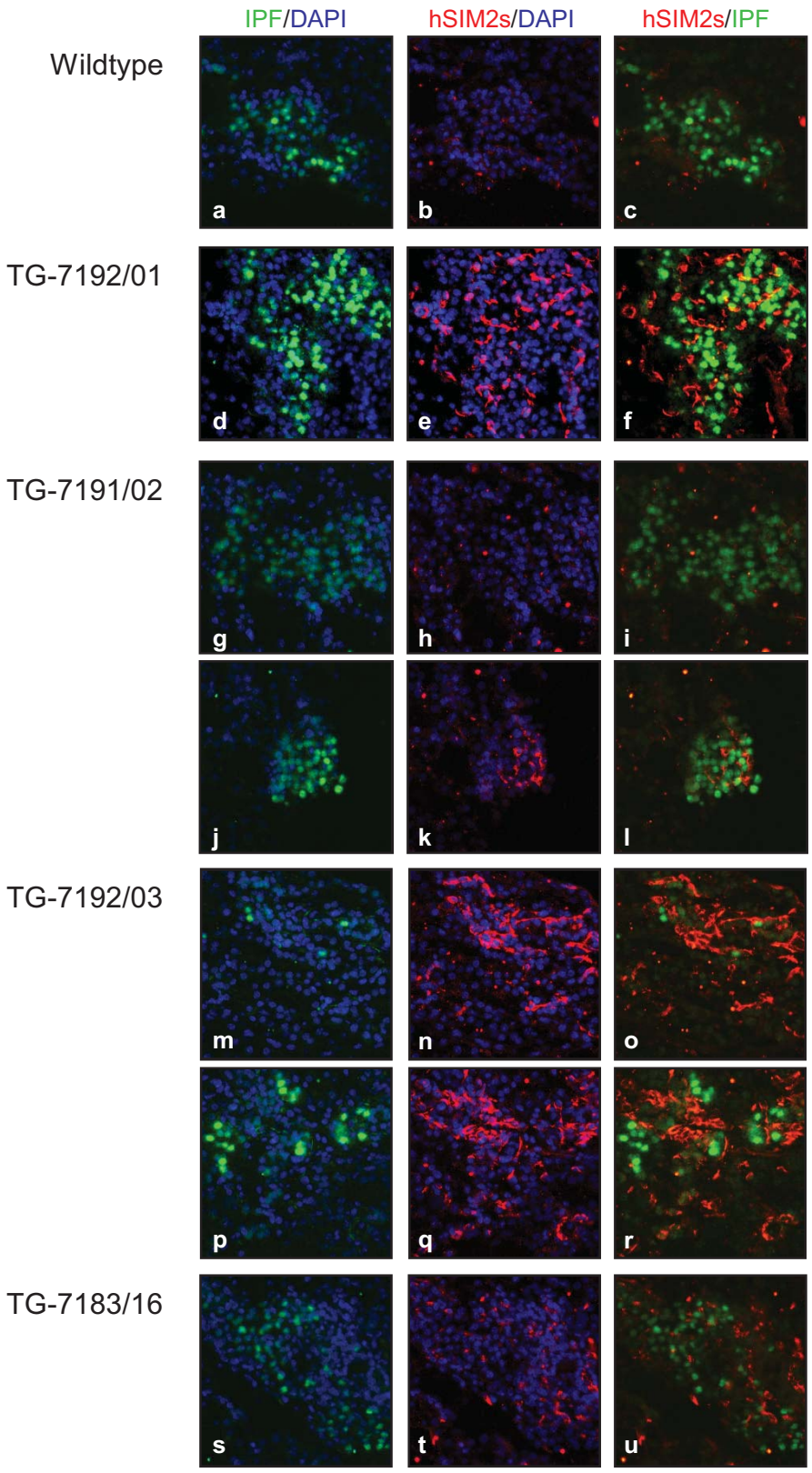

FIGURE 6.9: *Detection of transgenic human SIM2s.myc (red) expression in the pancreata from neonate pups of transgenic founders, 7191, 7192, 7183, co-stained for endogenous IPF (green), by immunofluorescence. Non-transgenic littermate is wildtype control.*

Immunofluorescent detection of hSIM2s.myc using anti-hSIM2s goat-polyclonal antibody + alexafluor594-labelled anti-goat secondary antibody (red). Endogenous IPF protein detected using anti-IPF rabbit polyclonal antibody + alexfluor488-labelled anti-rabbit secondary (green). Nuclei labelled with DAPI stain (blue). 40x confocal microscopy images.

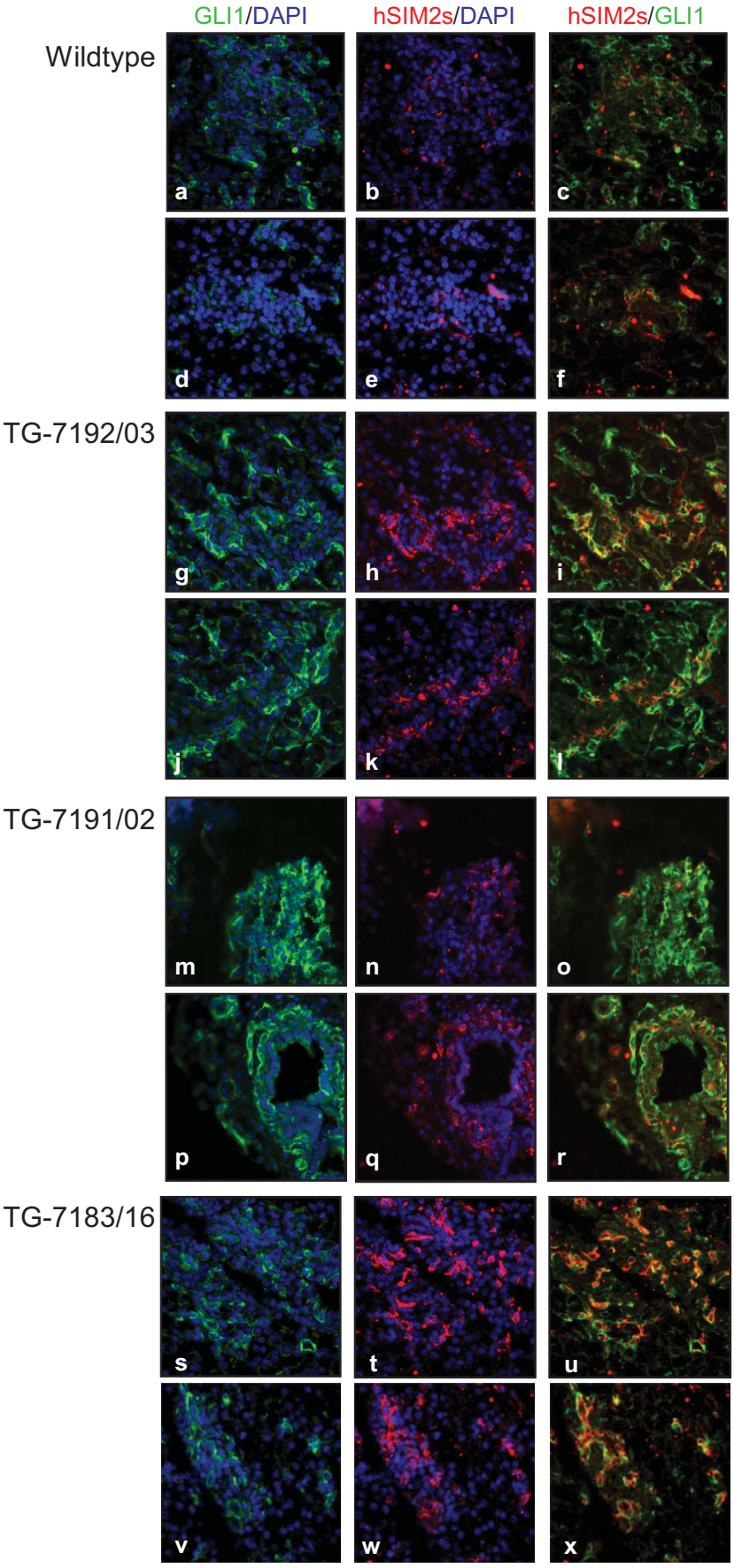

FIGURE 6.10: *Analysis of transgenic human SIM2s.myc (red) protein expression in the pancreata from neonate pups of transgenic founders, 7191, 7192, 7183, by immunofluoresence, co-stained for endogenous GLI1 (green). Non-transgenic littermate serves as wildtype control.*

Immunofluorescent detection of hSIM2s.myc using anti-hSIM2s goat-polyclonal antibody plus alexafluor594-labelled anti-goat secondary antibody (red). Endogenous GLI1 protein detected using anti-GLI1 rabbit polyclonal antibody + alexfluor488-labelled anti-rabbit secondary (green). Nuclei labelled with DAPI stain (blue). 40x confocal microscopy images.

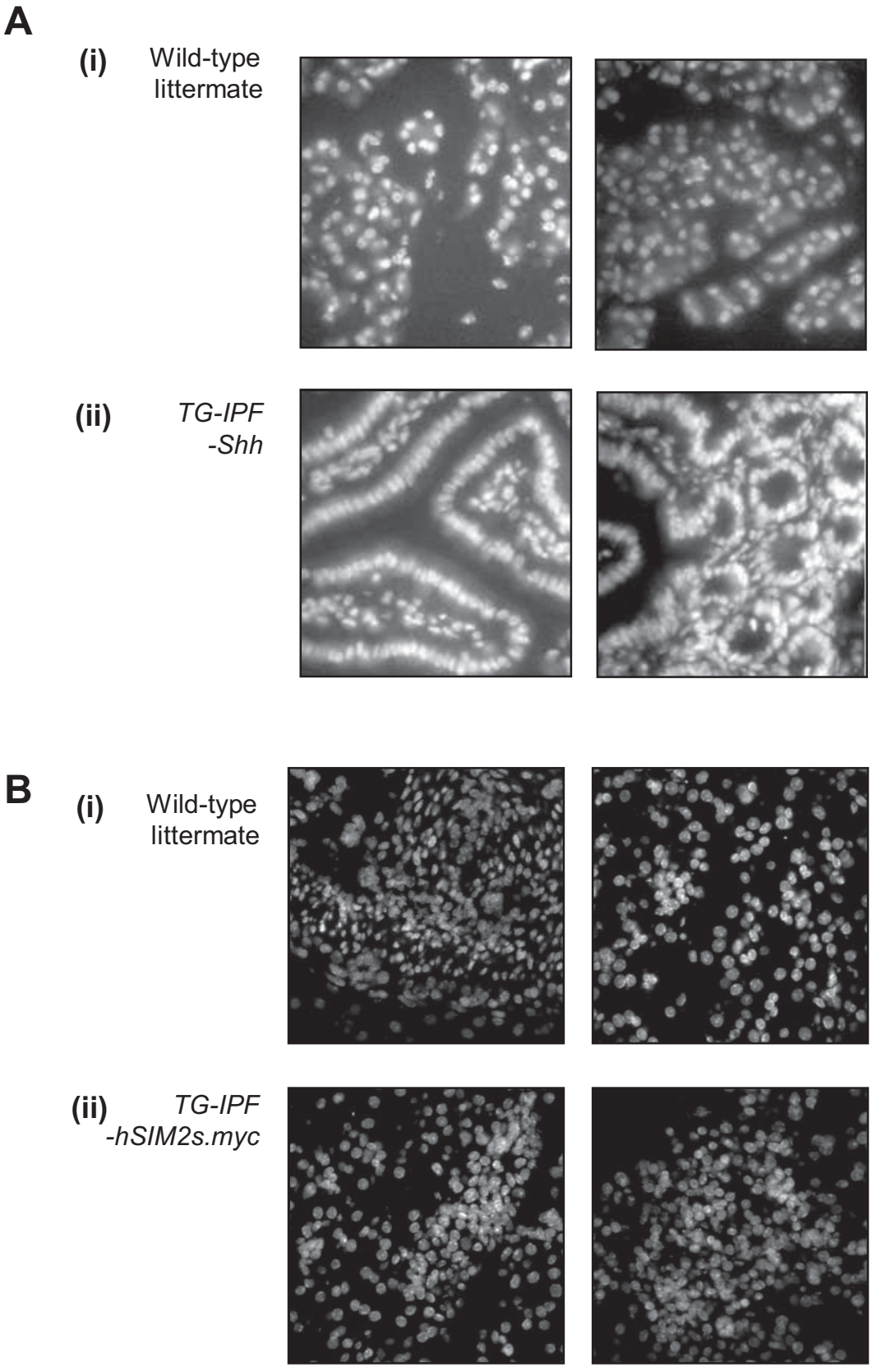

Figure 6.11: *Nuclear staining of mouse pancreas sections reveals* (A) *the dramatically altered structural morphology of the pancreas in IPF-mShh transgenic mice [1], is (B) not observed in the pancreata of transgenic IPF-hSIM2s.myc.*

Confocal microscopy images of (A) Hoerchst or (B) DAPI stained nuclei of pancreata sections from transgenic mice (ii) compared to wild-type littermate controls (i). Photos within set (A) and (B) are, respectively, to scale, but not between (A) and (B) image sets.

[1] Apelqvist, A., Ahlgren, U., & Edlund, H. (1997) *Curr Biol.* 7(10):801-4.

6.1.2.4 Summary comments on a putative role for SIM2s in Hh signalling in prostate and pancreatic cancer: Implications for tumour development

Although the *in vivo* approach used in these studies to determine if human SIM2s is capable of Hh-signalling activation and pancreatic tumour initiation in mice pancreata was inconclusive, the *in vitro* data from cell culture studies in both pancreatic and prostate carcinoma derived cell lines shown here does provide supporting evidence of a role for SIM2s in the regulation of SHH levels and Hh-pathway activities, consistent to that previously shown by Epstein and co-workers [71], but for the first time here, in a tumour cell context. It is important to remember that Sim2 was found to be sufficient, but not necessary for *Shh* expression in the developing mouse brain [71]. The sufficient nature of SIM2 upregulation of SHH does not exclude that perhaps in a tumour precursor-cell specific context, SIM2 may be able to initiate Hh-pathway activation to drive cell (and due to paracrine signalling, to surrounding cells) transformation to a tumourigenic state. However, as indicated through the discussion of these data presented here and the current literature, the possibility is evident that SIM2s may not necessarily play a role in initiating Hh-pathway activation in cancers, but function to maintain and/or hyper-induce the active signalling which ultimately drives the development of aggressive pancreatic and prostate tumours (reviewed in [250, 251]). SIM2s may perpetuate Hh-signalling via upregulation of SHH transcription, or that of the Hh pathway effectors, the GLI transcription factors (as outlined in **Figure 6.7**). However, following the observation by Epstein and co-workers that mSim2 is not necessary for *Shh* expression [71], and in light of the data presented here, it may be the Hh-pathway mediator GLI-kruppel family of transcription factors [103, 208, 209] that are required to maintain *SIM2s* expression. This would result in both factors contributing to an autoregulatory loop of Hh-signalling which may critically control tumour progression and increasing severity of the tumour (**Figure 6.7**). Perhaps this occurs in a similar way to the control of expression of *Myf5*, a bHLH skeletal muscle determining factor expressed in somites that is important for myogenic differentiation [252, 253]. *Myf5* expression is shown to initially begin under the control of the EEE (early expaxial enhancer) however,

continuation of expression is due a GLI transcription factor binding to the GLI consensus site in its EEE, thus making *Myf5* a long-range target of Shh through downstream GLI regulation [252-254]. Interestingly preliminary bioinformatics searches of the human *SIM2* promoter region for putative GLI binding sequences (a nine base pair sequence which has a probability of occurring randomly once every 262 kilobases) has found two sites within 2 kilobases - one immediately prior to the start of transcription and the other within the first intron (data not shown). The presence of these putative binding sites may be indicative of long-range Shh targeting of SIM2 via the GLI transcription factors, but this remains to be tested.

The progression of pancreatic adenocarcinoma has been defined by a series of multiple gene misregulation and/or mutation events, including activation of KRAS, and inactivation of p53 and INK4a/Arf, indeed, activating KRAS mutations are found in approximately 90% of pancreatic adenocarcinomas (for review see [95]). Mice expressing an *Ipf* promoter driven active mutant allele of *Kras* ($Kras^{G12D}$) develop pancreatic lesions which progress in the same manner as human PanINs, however at a low frequency [235, 255]. Further studies have shown that the frequency of lesions and the onset of aggressive metastatic cancer was greatly enhanced in combination with tissue specific deficiency of *Ink4a*/*Arf*, which alone does not incite pancreatic tumour formation [235], indicating a specific requirement for Kras activation in pancreatic cancer initiation and INK4a in tumour progression. It is interesting to note that the pancreatic precursor lesions from the *IPF-Shh* mouse model for pancreatic cancer also contained the *Kras* exon 12 mutation found in early human pancreatic cancers [219]. As activating mutations in *Kras* have been shown to initiate tumour formation, it is not unreasonable to infer that the disruption in *Kras* in the *Shh* transgenic mice contributed to PanIN initiation and/or development. Indeed, recent studies by Morton and co-workers (2007) have since shown that ectopic expression of Shh in pancreatic duct epithelial cells (PDEC), although able to activate Hh-signalling and enhance proliferation and cell survival in *in vitro* studies, minimally requires both loss of *Ink4a*/*Arf* and ectopic expression of activating Kras to produce tumours when transplanted into the pancreata

of mice, where Shh or mutant Kras alone are unable to incite tumour formation on this *Ink4a/Arf* deficient genetic background [220]. Thus, in light of this study which emerged following the completion of studies presented here, it is important to consider that should SIM2s function to promote tumour initiation and progression via activation and/or maintenance of Hh-signalling, it is highly likely, inferred from the lack of any phenotype in the pancreas upon ectopic expression of human SIM2s, to only do so in cooperation with other changes in the genetic profile of disease progression, such as loss of *INK4a/ARF* and/or activation of *KRAS*. Consequently, the efficiency by which SIM2s may be able to do so will only become evident from future *in vitro* and *in vivo* model studies in such genetic backgrounds. Only following such comprehensive studies can the putative role for SIM2s in Hh-pathway activation and tumourigenesis as is evident from the findings presented here, and the importance of this interaction for cancer development, be fully determined.

6.2 SIM2 and links to Androgen Receptor-dependent signalling in prostate cancer:

6.2.1 INTRODUCTION

The dependence of prostate cancer on androgens for growth and survival was first demonstrated nearly sixty years ago and since then androgen ablation therapy has been used for the treatment of advanced disease. Unfortunately however, despite early clinical remission following this treatment most patients who receive androgen ablation therapy go on to develop androgen-depletion independent (ADI) or hormone-refactory cancers for which there is no currently known cure (for reviews see [256-259]). Studies in a mouse model of prostate cancer have likewise shown, following androgen-ablation, enhanced cell proliferation rates and the development of more aggressive and metastatic disease [260, 261]. The

response to androgens is mediated by the Androgen Receptor (AR), hence the AR is implicated in mediating tumour progression [256]. AR, which is also vital for the normal development of prostate tissue, is a member of the Nuclear Receptor Superfamily of ligand dependent transcription factors. Following ligand binding, such as testosterone or dihydrotestosterone (DHT), AR undergoes a series of co-factor interactions and post-translational modifications resulting in translocation to the nucleus where it is able to bind androgen-responsive elements (AREs) to regulate the transcription of androgen-responsive genes, such as *Probasin* and *Prostate Specific Antigen* (*PSA*) [256, 262-264]. Continued AR expression and transcriptional activities have been observed in human prostate tumours after androgen-ablation therapy [265]. *AR* mRNA is up-regulated in one third of clinical samples [266], and the upregulation of *AR* expression was the only consistently differentially regulated gene found from global gene expression analyses of androgen-ablation therapy resistant human prostate cancer xenografts [267]. Increases in *AR* mRNA levels in ADI tumours [266] and stabilisation of AR in recurrent prostate tumour derived cell lines [268] results in the hyper-sensitive response of AR to low levels of residual androgens. However, what regulates *AR* mRNA levels and protein stabilisation in recurrent cancers remains to be described. Likewise, spontaneous somatic mutations in the AR following androgen deprivation therapy have also been attributed to its continued transcriptional activities despite the reduction in normal physiological levels of testicular androgens in the tumour. Mutations are commonly in the ligand binding domain and broaden AR ligand recognition beyond testicular androgens to estrogens, progestins and adrenal androgens [265, 267, 269]. Although enhanced AR levels is a marker of aggressive and metastatic disease [270], and AR expression, activation and function appears to be important for driving tumour progression [256], debate over the requirement for AR signalling in prostate tumour initiation has long been unsettled. Data thus far from mouse models shows directed ectopic expression of wild-type(wt)-AR or a promiscuous ligand binding mutant form of AR in the prostate was not sufficient to initiate tumour formation [271] and thus does not support a direct causal role for these forms of AR in tumour formation. However, directed overexpression of

AR with a gain of function mutation in the N-terminal domain, which is critical for conferring AR transcriptional output via interactions with the transcriptional machinery [272], was found to potently induce oncogenic transformation of the prostate in 100% of transgenic mice, implicating altered AR function for the first time with tumour initiation [271].

Understanding the regulation of AR levels is an important aspect of understanding the vital role for AR in the development of normal prostate tissue and prostate cancers. The androgen receptor has recently been shown to co-immunoprecipitate with ligand activated bHLH-PAS family member AhR as part of a E3-ubiquitin ligase complex in prostate (recurrent) carcinoma LNCaP cells where the (AhR-ligand activated) AhR/ARNT heterodimer was shown to be the critical mediator of AR degradation independent of androgens [273]. High expression levels of SIM2s is a putative novel marker for aggressive prostate cancer and poor prognosis [81], as are enhanced levels of AR [270]; however, a direct correlation between the expression levels and functions of these two proteins in prostate cancer progression and prognosis is yet to be formally shown. As SIM2 is known to functionally interfere other class I family members via sequestration of ARNT to repress transcription, such as from mSim1 [46] and HIF1α [9, 59](**Chapter 5**), it was hypothesised SIM2s may be able to attenuate the degradation of AR via sequestering ARNT from AhR in a similar manner to inhibit the formation and function of the AhR-E3-ligase complex, thus providing a mechanism by which AR is stabilised and able to elicit its effect on prostate cancer development. This hypothesis remains the subject of another study, however, an interesting and unexpected outcome of initial pilot studies was the observation that independent of AhR activating ligand, endogenous AR protein levels were seen to be dramatically increased in prostate PC3AR+ cells with stable ectopic expression of SIM2s.myc compared to puromycin resistant Control cells (as represented in **Figure 6.12A**). The following study was pursued in an attempt to understand how SIM2s may be regulating AR levels, independent of any potential AhR activities.

This work provides the first to link SIM2s expression with AR expression and function in prostate cancer cells, and implicates the expression of SIM2s in another signalling pathway in prostate tumourigenesis.

6.2.1 RESULTS & DISCUSSION

6.2.1.1 Endogenous Androgen Receptor is up regulated upon stable ectopic expression of human SIM2 in PC3AR+ cells.

Endogenous levels of AR protein were observed to be dramatically increased upon stable ectopic expression of SIM2s.myc in whole cell extracts from prostate carcinoma PC3AR+ cells compared to puromycin resistant control cells where little, if any, AR was detected (**Figure 6.12A**). Other prostate carcinoma cell lines were also analysed to assess the effect of SIM2s expression on AR levels. LNCaP cells showed high levels of constitutive AR expression, as previously reported by others [274], however failed to show any differences in AR levels with, and without, SIM2s.myc expression (data not shown). In contrast, no AR was detected in DU145±SIM2s.myc cells (data not shown) and is likely to be attributable to AR silencing via promoter hypermethylation previously identified in DU145 cells [275]. Western blot analyses of AR levels in three prostate carcinoma derived cell lines, PC3AR+, LNCaP and DU145, with and without stable ectopic expression of SIM2s.myc, thus far show the enhanced levels of AR associated with ectopic SIM2s expression is specific to PC3AR+ cells.

PC3AR+ cells differ from PC3AR- cells as they have detectable levels *AR* mRNA, whereas PC3AR- cells do not [276] due to partial methylation of the *AR* promoter [275, 277]. Following western analysis of AR levels in PC3AR+±SIM2s.myc cells, mRNA levels of the *AR* were examined to gain further insight into how SIM2s may be affecting AR levels. Endogenous *AR* mRNA was found to be upregulated in PC3AR+/SIM2s.myc

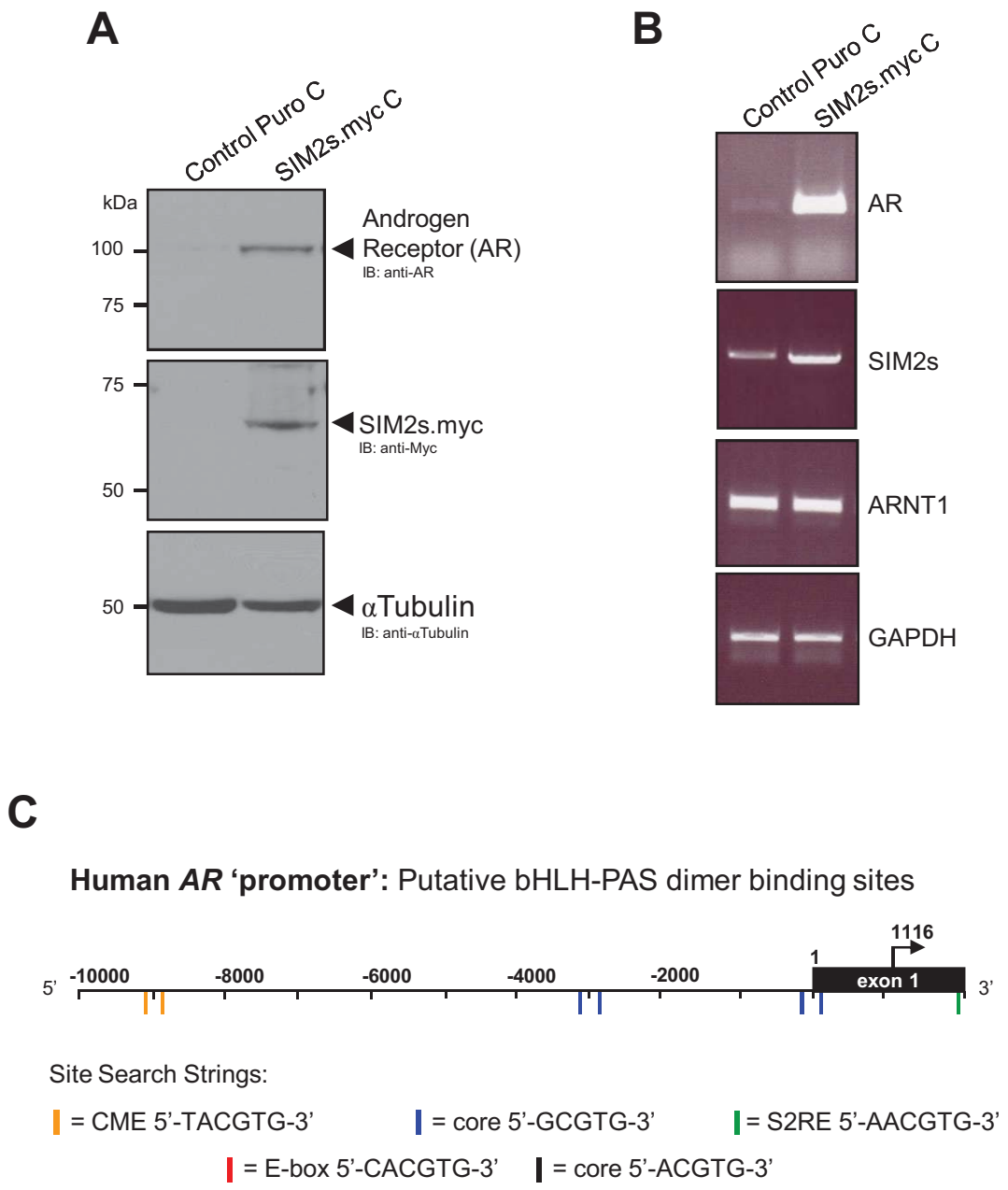

FIGURE 6.12: *Putative regulation of AR by SIM2s: Endogenous Androgen Receptor (AR) is upregulated in human PC3AR+ polyclonal cell lines upon stable ectopic expression of human SIM2s at the both the protein (A) and mRNA (B) level. (C) Bioinformatic analysis of human AR promoter reveals putative sites through which SIM2s/ARNT1 may regulate AR gene expression.*

(A) 50µg WCE from a polyclonal cell line for stable expression of myc tagged human SIM2s (SIM2s.myc) C, and puromycin resistant Control line C, were subjected to 8% SDS-PAGE and immunoblot analysis of proteins as marked. αTubulin serves as loading control. * = non-specific background band. (B) cDNA synthesised from total RNA extracts from same polyclonal cell lines in (A) was subjected to semi-quantitative RT-PCR (AR, 30x; S2s, 35x; ARNT1, 25x; GAPDH, 25x PCR cycles), and single amplicons visualised following 1% EtBr stained agarose gel electrophoresis. GAPDH and ARNT1 serve as loading controls. RT-PCR data representative of two independently derived Control and SIM2s.myc polyclonal cell lines. No-RT controls not shown. (C) Schematic of the human promoter of AR representing bioinformatically identified putative sites for bHLH-PAS dimer binding. Genomic DNA sequence sourced from online resource 'Human BLAT' (http://genome.ucsc.edu/cgi-bin/hgBlat?command=start) and both strands scrutinised using 'TESS (Transcription Element Search System)' (http://www.cbil.upenn.edu/cgi-bin/tess/tess) for site search strings as indicated.

cells, concomitant with enhanced AR protein, compared to Control cells upon analysis of independently derived polyclonal cell lines for both puromycin resistant Control and stable SIM2s.myc expression by semi-quantitative RT-PCR (**Figures 6.12A** & **B**). Message levels of *GAPDH* and *ARNT1* were used as PCR cDNA template loading controls. Whether this upregulation of *AR* mRNA is indicative of enhanced transcription or message stability upon SIM2s expression remains to be determined. Bioinformatic analyses of 10kb upstream of the start of human *AR* exon 1, and 2kb into exon 1, for putative bHLH-PAS dimer 5'-G/ACGTG-3' core binding sites [129], reveals two classical CME (central midline element) 5'-TACGTG-3' clustered approximately 9kb upstream of the start of exon 1 (210bp apart), and a single S2RE 5'-AACGTG-3' ~ 2kb into the first exon, which are putative sites for SIM2s/ARNT1 binding [41, 47, 48]. Two core 5'-GCGTG-3' sites were clustered within 350bp ~3kb upstream of exon 1, and another two within 350bp at the start of exon 1 (refer **Figure 6.12C**). While there are no previous reports of SIM2/ARNT heterodimers regulating transcription via this core site, it still may be indicative for capacity of a bHLH-PAS heterodimer to regulate the transcription [129] of *AR* via these sites. Interestingly no canonical palindromic E-box 5'-CACGTG-3' sites were found in the promoter region, thus the transcriptional upregulation of *AR* is unlikely to be directly mediated by ARNT/ARNT homodimers [118, 129].

The short and long isoforms of SIM2 only differ at the very C-terminus [38] (refer to **Figure 1.3A**, **Chapter 1**). To assess whether the effect on AR levels was specific to the short isoform of SIM2, AR protein levels were analysed by western blot from whole cell extracts of two independently derived polyclonal cell lines with stable ectopic expression of C-terminally myc tagged SIM2L (SIM2L.myc lines A & C). As was observed for SIM2s, increased AR levels were also associated with ectopic expression of SIM2L (**Figure 6.13**). Although any changes in AR mRNA levels upon SIM2L expression are yet to be investigated, stable ectopic expression of both highly homologous isoforms of SIM2 correlates to enhanced AR protein levels.

6.2.1.2 AR-dependent transcriptional responsiveness to androgen treatment in PC3AR+± SIM2s.myc cells.

Very little, if any, AR is detectable by western blot analysis of whole cell extracts from parent (and Control) PC3AR+ cells (**Figures 6.12**, **6.13** & **6.14**). This observation is consistent with reports by others using alternate anti-AR antibodies [274, 276]. Previously, Buchanan *et al* (2004) reported that the endogenous levels of AR in PC3AR+ cells were not sufficient to confer androgen responsiveness by measures of AR activity upon treatment with the androgen dihydrotestosterone (DHT) on a reporter gene driven by three tandem repeats of the minimal promoter of the androgen responsive gene, *Probasin* (PB3-luciferase) [274, 278]. To assess whether the greatly enhanced levels of AR associated with SIM2s expression are sufficient to mediate androgen responsiveness in these cells, endogenous AR activity upon treatment with DHT in PC3AR+/SIM2s.myc cells was analysed by PB3-luciferase reporter gene expression, compared to that in PC3AR+/Control cells. Irrespective of endogenous AR protein levels (**Figure 6.14A**), no reporter gene activation was observed in either PC3AR+/Control or PC3AR+/SIM2s.myc cells upon treatment with DHT (**Figure 6.14B**, compare columns a & b, with e & f). Consistent with previous reports [274], ectopically expressed wild-type AR activated PB3-luciferase expression in PC3AR+/Control cells in response to treatment with DHT (**Figure 6.14B**, compare columns c & g), thus serving as a positive control for ligand activity and indicator of intact androgen signalling in these cells. Taken together, these results suggest that the lack of endogenous AR responsiveness observed in these cells previously is not necessarily an issue of AR protein levels as reported [274], but perhaps one of a functionally defunct form of AR produced in these cells. No mutations in the DNA binding and ligand binding domains have been found from sequence analysis of AR cDNA from PC3AR+ cells [276], thus determining the nature of the 'mutation' and/or post-translational modification that renders endogenous AR unable to function, despite, or even because of, its nuclear localisation [276], in PC3AR+ cells remains a fascinating line of investigation.

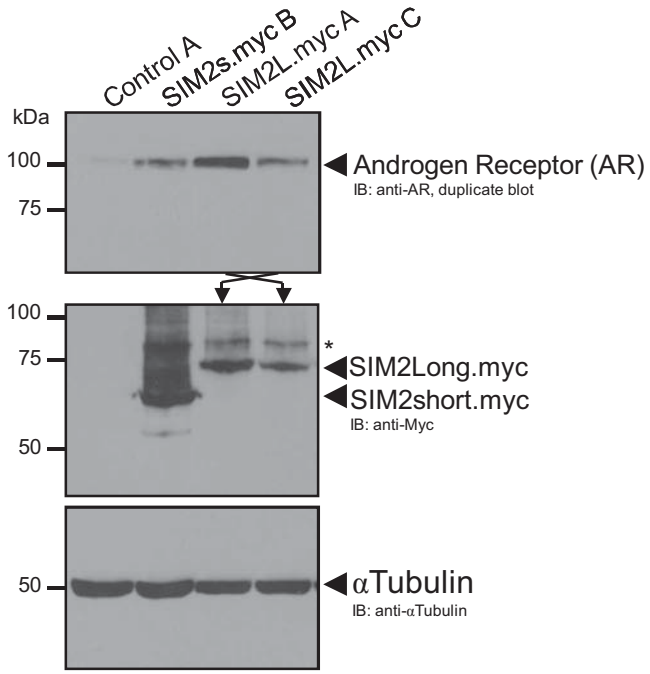

FIGURE 6.13: *Enhanced endogenous AR protein levels are also associated with stable ectopic expression of human SIM2L in PC3AR+ cells.*

50µg WCE from independently derived polyclonal cell lines Control A, SIM2s.myc B and SIM2L.myc A & C, were subjected to duplicate 8% SDS-PAGE and immunoblot analysis of proteins as marked. αTubulin serves as loading control. * = non-specific background band.

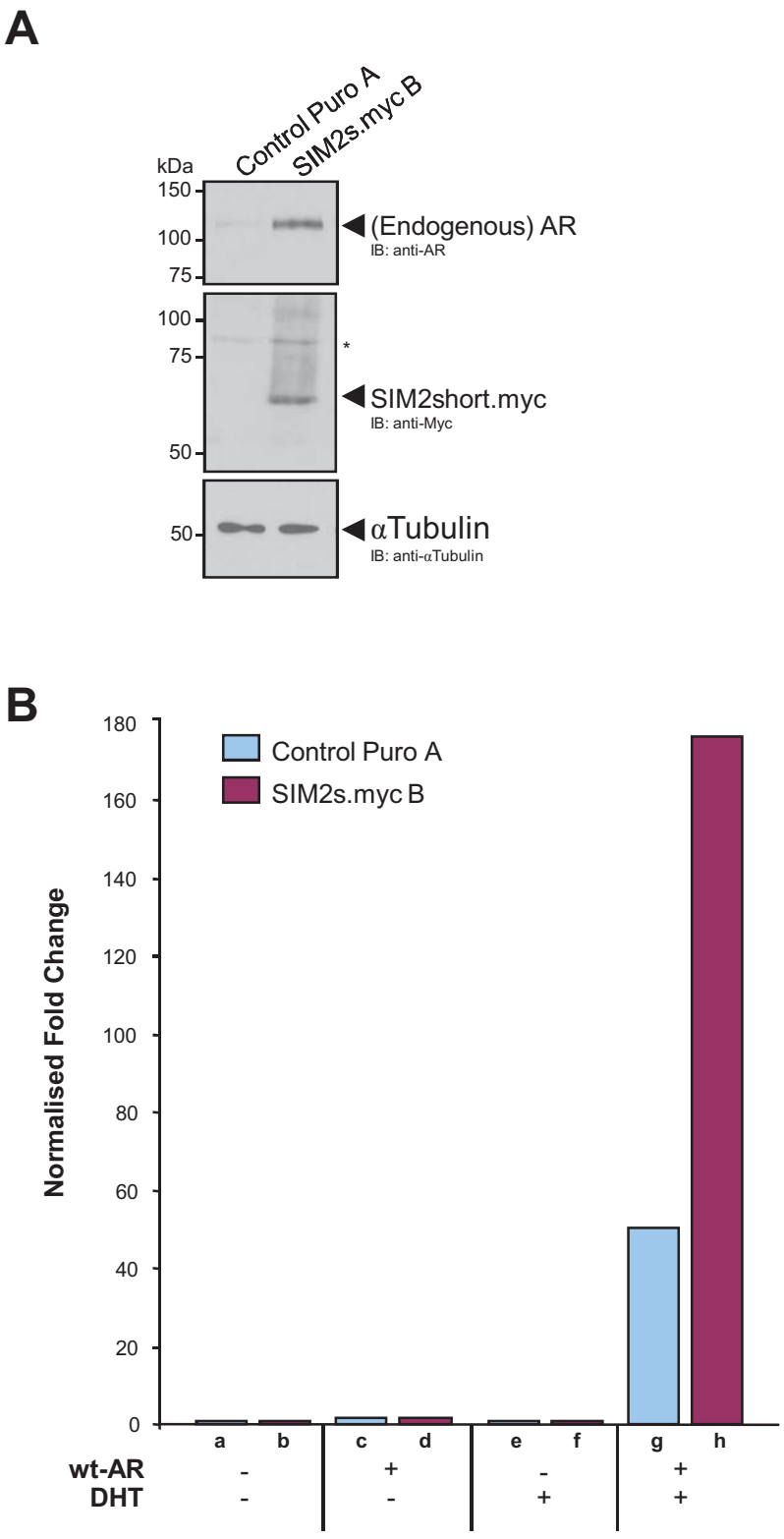

FIGURE 6.14: *Transiently expressed wild-type (wt)* AR, *and not endogenous AR, activates the Probasin (PB3) promoter to drive reporter gene expression upon treatment with AR activating ligand DHT in PC3AR+ cells, which is greatly enhanced in PC3AR+/SIM2s.myc cells.*

(A) 50µg WCE from independently derived polyclonal cell lines, puromycin resistant Control line A and stably expressing human SIM2s.myc line B were subjected to 8% SDS-PAGE and immunoblot analysis of proteins as marked. *=non-specific background band. (B) 50ng wild-type AR (wt-AR) was transiently expressed in PC3AR+ cells with, or without, stable expression of SIM2s, activated with 1µM DHT ligand. Luciferase reporter activity driven by the PB3 promoter was measured as an indicator of (wt-)AR function, normalised to co-transfected b-galactosidase. Data representative average mean fold change of n=2 independent experiments done in triplicate. Data generated with the technical assistance of A. Sullivan.

6.2.1.3 The Androgen Receptor interacts with SIM2s, and not with ARNT, in PC3AR+ cells

Unexpectedly, the level of transiently expressed wt-AR transcriptional activities on the PB3-luciferase reporter in response to treatment with DHT was much greater in PC3AR+ cells with stable expression of SIM2s, compared to Control cells (**Figure 6.14B**, compare columns g & h) inciting further investigation into the possible mechanisms by which SIM2s expression may be mediating this outcome.

The obligate bHLH-PAS partner factor ARNT1 has previously been shown to interact with another member of the nuclear receptor superfamily, the Estrogen Receptor (ER), via its ligand binding domain, and upon treatment with estrogen functions to potently co-activate ER-dependent transcriptional activities [126, 279]. There are no previous reports of ARNT1 interacting with AR to facilitate androgen-responsive transcription in this manner, however, as endogenous levels of ARNT1 are greatly increased in PC3AR+/SIM2s.myc cells (as discussed in **Chapter 3**), where elevated wt-AR transcriptional androgen responsiveness is observed (**Figure 6.14B**), a possible interaction between ARNT1 and AR was examined. Immunohistochemical staining has shown endogenous AR to be nuclear in PC3AR+ cells [276], thus this possible interaction was first initially examined independently of androgen treatment. Immunoprecipitation (IP) of endogenous ARNT1 from whole cell extracts of PC3AR+±SIM2s.myc cells failed to co-IP endogenous AR (**Figure 6.15A**, lanes 2 & 4, panels i & ii). Nor was there evidence of an interaction between ARNT1 and transiently expressed wt-AR in PC3AR+/SIM2s.myc cells (**Figure 6.15A**, lane 7, panels i & ii), indicating that ARNT1 and AR do not interact in PC3AR+ cells in these conditions. Thus far, these data do not support a model for ARNT1 co-activation of AR-dependent transcription, however, the absence of an interaction could be due to the 'defunct' nature of endogenous AR in these cells, despite being nuclear [276], or due to the absence of androgen to promote translocation of wt-AR to the nucleus. SIM2 is a nuclear protein [48, 59, 60] and interestingly these studies reveal an interaction between endogenous nuclear 'defunct' AR and SIM2s.myc (**Figure 6.15A**, lanes 5 & 8). Transient expression of wt-

AR in PC3AR+/SIM2s.myc cells slightly increases the total amount of detectable AR in whole cell extracts compared to the level of elevated endogenous AR in untransfected PC3AR+/SIM2s.myc whole cell extracts (**Figure 6.15B**, compare lanes 3 & 6, panel ii, indicative of 10% input). This slight increase is also reflected in the total amount of AR to co-IP with SIM2s.myc from wt-AR transfected whole cell extracts (**Figure 6.15A**, compare lanes 5 and 8, panel ii). Whether this latter pool of AR includes wt-AR that interacts with SIM2s.myc independent of androgen cannot be specifically determined from this experiment.

These data show that immunoprecipitation of SIM2s.myc using the anti-hSIM2s antibody (**Figure 6.15A**, lane 8, panel iii) is able to immuno-deplete endogenous ARNT1 (**Figure 6.15B**, lane 8, panel i), whereas immuno-depleteion of endogenous ARNT1 using an anti-ARNT1 antibody (**Figure 6.15A**, lane 7, panel i) does not deplete SIM2s.myc (**Figure 6.15B**, compare lanes 6 & 7, panel iii). This indicates that ectopic expression of SIM2s.myc is in excess to the (although enhanced) endogenous levels of ARNT1 in these cells. Thus, these results suggest that ARNT1 is predominantly interacting with SIM2s.myc in these cells, thus there would be little, if any, ARNT1 'available' to interact with other proteins independent of SIM2s.myc. Consequently, as all ARNT1 is equally immuno-depleted with anti-ARNT1 and anti-hSIM2s antibodies (**Figure 6.15B**, compare lanes 7 & 8 to anti-IgG control lane 6), but AR only co-IPs with SIM2s.myc which is in excess to ARNT1, these data suggest that in the absence of androgens the interaction between SIM2s and AR is independent of ARNT1. As endogenous AR in PC3AR+ cells is predominantly nuclear in the absence of ligand [276], as is SIM2s [60, 81] this interaction is likely to be nuclear, however, the amount of AR that SIM2s co-IPs is only a small fraction of the total levels of endogenous AR in PC3AR+/SIM2s.myc cells. Thus it would be interesting to ascertain not only if the AR-SIM2s ARNT-independent interaction is direct, but if it is enhanced, and/or is no longer ARNT-independent upon treatment with androgens. Although not strictly the same context, others have previously identified the requirement for estrogen ligand activation for the interaction between ARNT1 and ERα, but not between ARNT1 and ERβ [273], thus

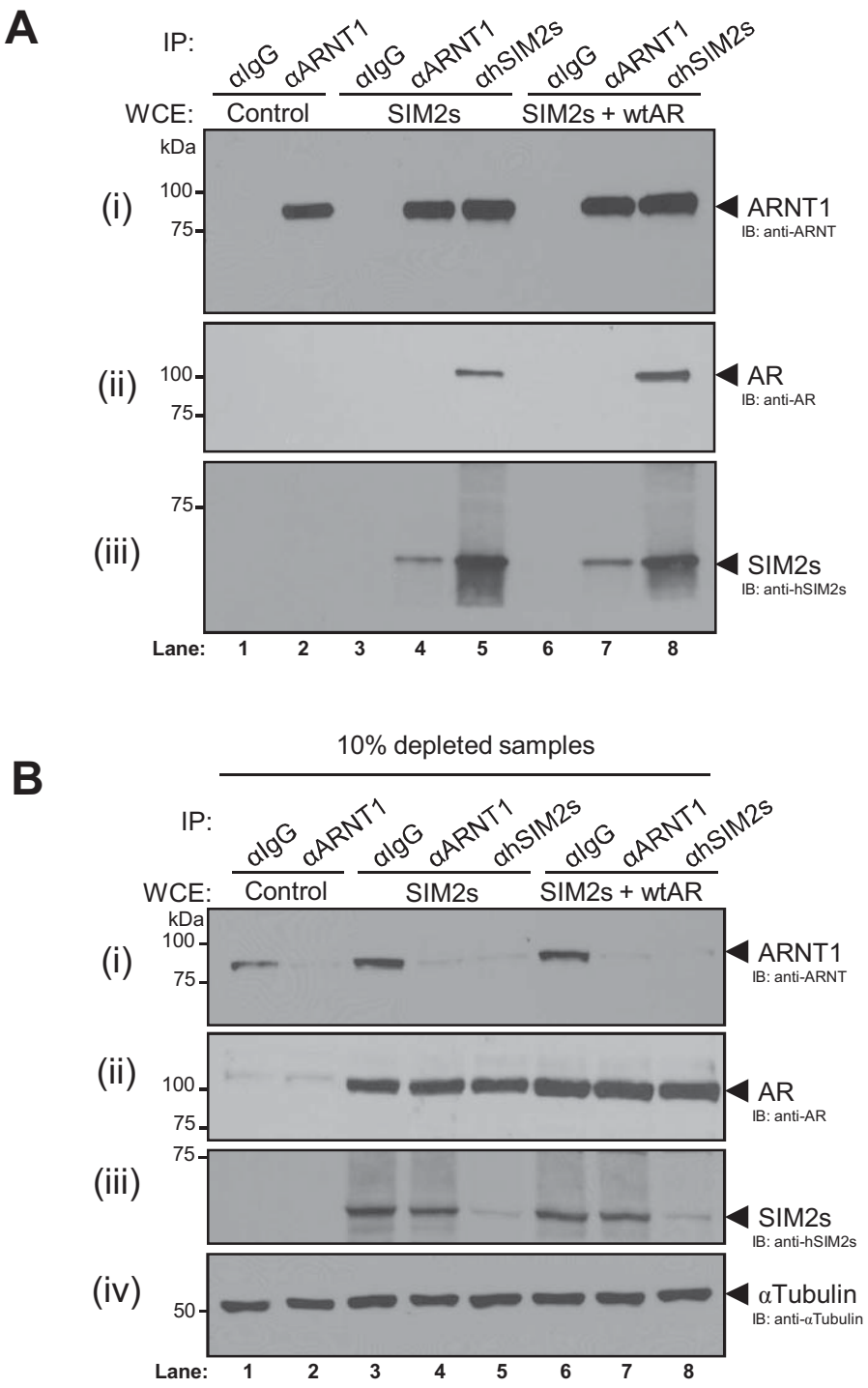

FIGURE 6.15: *SIM2s.myc co-IPs AR INDEPENDENT of endogenously stabilised ARNT1 in PC3AR+ cells.*

0.5mg WCE from PC3AR+ cells with, and without, SIM2s.myc stable expression, or PC3AR+/SIM2s.myc with transient expression of wild-type Androgen receptor (wtAR) were used to immunoprecipitate (IP) ectopic SIM2s and endogenous ARNT1, using goat polyclonal anti-hSIM2s and anti-ARNT1 antibodies compared to a matched IgG control antibody. IP's (A) and 10% depleted WCE (B) samples were subjected to 8% SDS-PAGE analysis and immunoblot detection of proteins as marked. Note, 10% depleted anti-IgG control samples for each WCE are indicative of 10% input.

indicating potential consequences of ligand activation of nuclear hormone receptors, such as AR and ER, that may facilitate the binding of ARNT1. However, ligand activated fellow class I bHLH-PAS family member AhR has previously been shown to interact with AR in a manner intrinsic to AhR, also in an androgen independent manner [280] which appears to be consistent with the SIM2s-AR interaction observed here, and provides a precedent for the capacity of AR to interact with a class I bHLH-PAS factor such as SIM2s.

In summary, these results show that ectopic SIM2s is able to interact with endogenous AR independent of ARNT and androgens in PC3AR+ cells. However, determining the physiological relevance of this interaction and how it may impact on AR-signalling in vivo remain interesting lines of future study. As others have previously shown that AhR interacts with AR in an androgen-independent manner and functions to co-activate AR-dependent gene expression [280], the androgen-independent interaction between SIM2s and AR, considered in light of the enhanced the activities of wt-AR in response to DHT treatment in PC3AR+/SIM2s cells (**Figure 6.14B**), suggests that SIM2s may also be able functioning as a co-activator of AR activities.

6.2.1.4 Summary comments on a putative role for SIM2s in AR signalling in prostate cancer: Implications for tumour development

An increase in the level of AR is a marker of aggressive prostate tumours and poor patient prognosis [270]. Likewise, increased SIM2s expression is also associated with aggressive prostate tumours and increased mortality rates [266-268]. However, no link between AR and SIM2s levels has been formally shown in the progression and disease outcome of prostate cancer. Endogenous AR protein levels were observed to be enhanced in PC3AR+ cells upon ectopic expression of SIM2s and long (**Figure 6.13** & **13**). This increase in AR may be a result of increased *AR* gene expression as *AR* mRNA was observed to be upregulated in

PC3AR+/SIM2s.myc cells (**Figure 6.12B**), however, enhanced protein stability as a result of SIM2s.myc expression is another possible mechanism that may be contributing to enhanced AR levels that is yet to be examined. A number of studies collectively show that enhanced levels of AR gene expression, which is the only consistently up-regulated message to be associated with the development of antiandrogen therapy-resistant tumours, and increased AR protein stability confers amplification the AR response to low levels of androgens [267], thus providing a mechanism for persistent AR-signalling in tumours post androgen-ablation therapy. The molecular mechanisms that aid the transition from hormone ablation-therapy responsive tumours to therapy resistant ablation-depletion independent (ADI) tumours are yet to be fully characterised. Yet, stabilised AR, with a functional ligand binding domain, is found to be both necessary and sufficient for the conversion of hormone-sensitive prostate cancers to hormone-refractory stage tumours [81, 270]. Consequently, as this current work indicates that SIM2s may be regulating AR levels, by increased transcription and /or protein stability, in PC3AR+ cells, immediately highlights a possible role for SIM2s in prostate tumour development, and perhaps significantly a key role in the transition of tumours from the hormone-sensitive to hormone-refractory stage.

Further work validating this relationship between SIM2s expression and upregulation of AR in a prostate tumour context is initially required to ascertain the significance of these findings in PC3AR+ cells. Examination of human prostate tumours pre- and post-androgen ablation therapy for potentially overlapping AR and SIM2 expression would go a long way to understanding if there is indeed a formal correlation between AR and SIM2s expression as markers of aggressive cancer [53, 82] with disease progression from androgen-sensitive to ADI tumours, and patient survival outcomes. These studies could even be extended to tumours and carcinoma derived cell lines of the breast, where conversely Porter and colleagues have shown the loss of SIM2s expression correlates to cell proliferation and tumour progression [281]. Perhaps consistent with the putative role for SIM2s in AR expression and function proposed here, loss of AR is also

associated with poor prognosis in triple-negative (Estrogen receptor/Progesterone receptor/Her2-neagtive) breast tumours (for review [281]). Moreover, AR overexpression and androgen-responsiveness in breast cancers shows anti-proliferative effects, and is associated with good prognosis [53], and again similarly, ectopic overexpression of SIM2s in breast cancer MDA-MB-435 cells also significantly reduces proliferation and invasive potential [282]. This latter correlation is weakened by the very recent findings that the MDA-MB-435 cell line has been misclassified and is actually derived from melanoma M14 cells and should no longer be regarded as a model cell system for breast cancer [283]. However, MDA-MB-435 cells are rich in AR, shares the same AR expression and localisation profile as the commonly used metastatic breast cancer cell line MDA-MB-231, and do show androgen responsive translocation of AR to the nucleus [53]. Although there are no reports of the effects in cell growth following knockdown of AR in these cells which may corroborate, ectopic expression of SIM2s in the SIM2s-negative MDA-MB-435 cell line [266, 268] may indeed still be affecting the AR-responsive pathway in these cells.

There is a myriad of factors that may contribute to enhanced AR activities in ADI tumours other than hyper-sensitivity to ligand due to increased expression levels [284], such as the upregulation of AR co-factors SRC-1 and TIF2 observed in the majority of recurrent prostate cancer samples [285], or functional EGF, KGF, IGF-1 [286] and Her2/neu [286] growth factor pathways which have all been shown to activate AR-dependent transcriptional activities in absence of treatment with androgens in *in vitro* prostate cancer cell line systems. The activation of AR independent of androgens in one study was attributed to phosphorylation of AR by Her2/neu-activated Akt [276]. The present study remarkably shows potently enhanced androgen responsive wt-AR-dependent transcriptional activities in PC3AR+ cells with ectopic expression of SIM2s (**Figure 6.14B**). This interaction, whether direct or not, between SIM2s and AR is independent of ARNT, highlighting the exciting possibility of a role for SIM2s in tumour promotion as an AR

co-activator. Moreover, and perhaps more significantly, the capacity of SIM2s to interact with AR is independent of androgens (**Figure 6.15**).

6.3 Potential Cross-regulation of HIF1α and SIM2s in tumourigenesis

6.3.1 INTRODUCTION

The regulation of HIF1α protein levels has been extensively studied, and many mechanisms, both oxygen-dependent, and oxygen-independent have been described [14, 23, 24]. Oxygen-dependent mechanisms were outlined previously in **Chapter One** (Introduction section 1.1.1). One mechanism of HIF1α stabilisation specific to protecting HIF1α from the oxygen-independent Hsp90-dependent pathway of proteasomal degradation, and not the oxygen-dependent the pVHL-pathway, is via a direct binding interaction with the ubiquitous class II bHLH-PAS common partner factor, ARNT [24]. This is the first study to describe a role for a fellow bHLH-PAS family member in the stabilisation of HIF1α. The ability of ARNT to stabilise HIF1α was found to be conferred by its capacity to heterodimerise with HIF1α via the HLH-PAS domain, thus interfering with the capacity of Hsp-90 to bind HIF1α [24]. Class I family members do not homodimerise nor heterodimerise within their class (for review [5]) and perhaps on this basis, there have been no reports of studies investigating the potential for class I family members to play roles in cross-regulation at the protein level either via direct or indirect interactions, or as a downstream effect of cellular activities.

The following studies reveal for the first time a possible mechanism for the cross-regulation of class I family members HIF1α and SIM2s. Routine western blot analysis of SIM2s.myc and endogenous HIF1α levels in prostate cancer cell lines following hypoxic growth conditions, during experiments designed to assess BNIP3 levels in response to these treatments (as discussed in **Chapter 5**), revealed startling unexpected modulation of HIF1α levels, particularly in the PC3AR+ prostate carcinoma derived cell line, concomitant with changes in SIM2s.myc expression. As such, these findings warrant individual analysis separate to the discussion on SIM2s cross-regulation of BNIP3 with HIF1α in hypoxia (see **Chapter 5**). These results, although not conclusive, for the first time implicate SIM2s expression with the stabilisation of HIF1α, and in turn, suggest a potential role for stabilised HIF1α in the regulation of SIM2s. Close analyses of the following data suggest the existence of novel mechanisms of both HIF1α and SIM2s protein regulation, and moreover together indicates the possibility of cross-regulation of protein levels between fellow class I family members in an auto-regulatory loop fashion. The pursuant implications for SIM2s expression in HIF1α-dependent responsive pathways via enhanced HIF1α stability in tumourigenesis, and likewise, the implications of possible HIF1α-mediated regulation of SIM2s and the potential impact on the role of SIM2s in prostate cancer progression, will be discussed.

6.3.2 RESULTS & DISCUSSION

6.3.2.1 Total HIF1α protein levels are enhanced in some prostate carcinoma cell lines with ectopic expression of SIM2s in hypoxia.

Analysis of HIF1α protein levels was employed as a positive control marker for hypoxic growth conditions in prostate carcinoma cell lines for the hypoxic regulation of BNIP3 which is mediated by HIF1α [287] (refer

Figures5.8A, Chapter 5). Closer analysis of this control (data reproduced in **Figure 6.16**) revealed an increase in a lower molecular weight form of HIF1α (indicated with a blue arrow) in hypoxic whole cell extracts from DU145 and PC3AR+ cells with stable ectopic expression of SIM2s (**Figure 6.16**, panels a & g), but not in samples from LNCaP stable cell lines where only the expected (higher) molecular weight band for HIF1α was observed irrespective of ectopic SIM2s.myc expression (**Figure 6.16**, panel d). The presence of this second lower band enhanced the total levels of endogenous HIF1α detected from hypoxic DU145/SIM2s.myc and PC3AR+/SIM2s.myc cells, however, in PC3AR+/SIM2s.myc cells both the upper and lower bands for HIF1α were dramatically increased after 16h hypoxia compared to PC3AR+/Control cells (**Figure 6.16**, panels a & g, compared to αTubulin controls panels c & i, respectively). These data indicate that HIF1α may have enhanced stability in some cell lines with stable ectopic expression of SIM2s. These findings were consistent across three independent experiments which included the analysis of independently derived polyclonal cell lines, with and without, SIM2s expression for each prostate carcinoma derived cell line subjected to either normoxic or hypoxic (< 1% O_2) growth conditions. A signal for HIF1α was also detectable in PC3AR+/SIM2s.myc cells in normoxia, but not in Control cells (**Figure 6.16**, slight signal panel g, compare to αTubulin load control panel i, and **Figure 6.17**, DMSO treated samples, panel i). The dramatic enhanced hypoxic stabilisation in endogenous HIF1α protein levels in PC3AR+/SIM2s.myc cells is strikingly evident, again, from western blot positive control data for HIF1α expression in PC3AR+ cells treated for a prolonged period (44h) with the hypoxia mimetics DP and DMOG analysed in conjunction with hypoxia-induced cell death experiments as discussed in **Chapter 5** (**Figure 6.17**, panel i, previously shown in part in **Figure 5.14B**, **Chapter 5**). Shorter (lighter) exposure of HIF1α immunoblots shows the presence of the lower molecular weight band in 'hypoxic' PC3AR+/SIM2s.myc samples (**Figure 6.17**, panel ii), which can be clearly seen in DMSO (vehicle control) treated PC3AR+/SIM2s.myc cells in approximately equal proportions to the expected size band (**Figure 6.17**, panel i). In Control stable cell lines, the DP and DMOG stabilised HIF1α is predominantly detectable at the expected (higher) molecular weight position, with

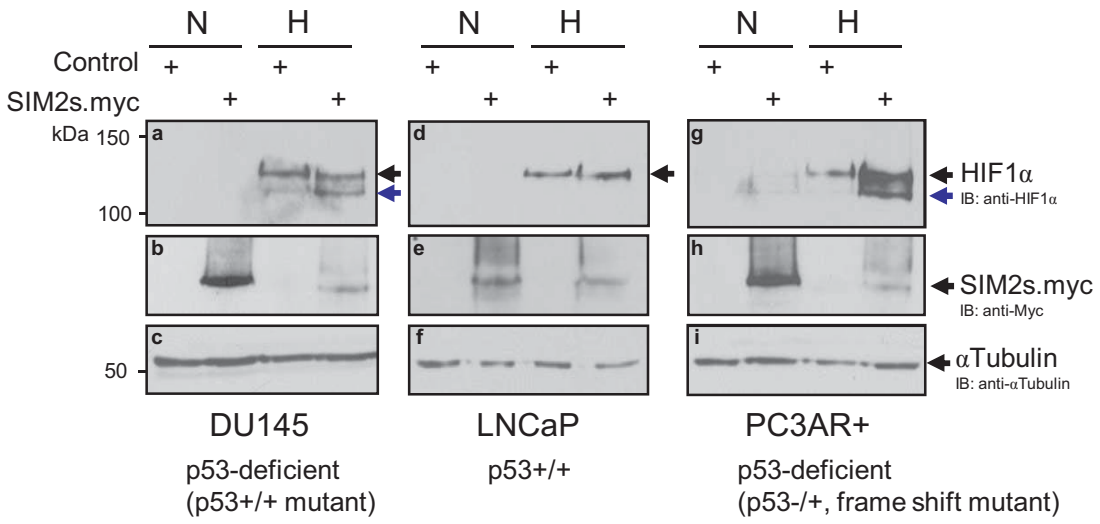

FIGURE 6.16: *Ectopic expression of SIM2s correlates to enhanced levels of total HIF1α protein, and a lower molecular weight form of HIF1α, in p53-deficient DU145 and PC3AR+, and not p53+/+ LNCaP prostate carcinoma derived cell lines in hypoxia.*

Whole cell extracts were made from both puromycin resistant empty-vector Control cells and cells engineered for SIM2s.myc stable expression, grown under usual normoxic (N) growth conditions, or 16hrs in a hypoxia chamber (H) (<1% O_2), then 35µg subjected to 8% SDS-PAGE separation, and sequential immunoblot blot analysis of proteins as labelled. Blue arrows (◄) point to lower molecular weight form of HIF1α. Representative of n=3 independent experiments.
Data previously shown as part of **Figure 5.8Aii**, **Chapter 5**.

Reference for p53 status, Isaacs *et al* (1991) *Cancer Research*, 51 (17): 4716.

a slight band at the lower molecular weight. Likewise, the expected upper band for HIF1α is also predominant over the lower form in 'hypoxic' PC3AR+/SIM2s.myc cells. Although the exact ratios of each form of HIF1α in these samples is not quantified, there does not immediately appear to be a major difference in the forms of HIF1α stabilised upon 'hypoxic' treatment, just the overall amount, between Control and SIM2s expressing PC3AR+ cells (**Figure 6.17**, panels i & ii, compare to αTubulin loading control, panel iv). Interestingly however, the data do indicate in PC3AR+/SIM2s.myc cells that there is a shift in the ratios of the forms of HIF1α 'stabilised' in normoxia and those in 'hypoxia', namely the shift from approximate equal levels of each form in normoxia, to the predominant stabilisation of the higher molecular weight species in hypoxia (**Figure 6.16**, panel g, and **Figure 6.17**, panels i & ii). Similarly, the faint band of HIF1α detectable in DMSO treated PC3AR+/Control samples is predominantly the lower form, however, this shifts to being predominantly the higher molecular weight form upon treatment with DP or DMOG (**Figure 6.17**, panel i). Taken together these observations may reflect changes in the post-translational modifications of HIF1α that occur in this cell line between oxygen-independent and oxygen-dependent mechanisms of regulation [288] and thus differences in the means by which HIF1α is then subsequently degraded, however this is far from being determined. The distinctive presence of a high molecular weight 'smear' above HIF1α upon western analysis of DP and DMOG treated PC3AR+/SIM2s.myc whole cell extracts (**Figure 6.17**, panel i), although not specifically shown here, is likely to be indicative of ubiquitylation HIF1α as it is consistent with previous immunoblot data showing ubiquitinated HIF1α [24, 289]. Therefore, this potentially shows a mechanism for SIM2s.myc-associated stabilisation of HIF1α via directly interfering with the proteasomal degradation and turnover of HIF1α, but perhaps not the ubiquitylation process itself. It would be interesting to examine the dependence of oxygen on this putative mechanism, specifically, if the apparent oxygen-independent stabilisation of HIF1α observed in normoxia in PC3AR+/SIM2s.myc cells is also working in concert with oxygen-dependent mechanisms of stabilisation in

hypoxia. In essence the question remains; is SIM2s implicated in one or multiple modes of HIF1α regulation irrespective of, or dependent on, cellular oxygen levels?

6.3.2.2 Ectopically expressed SIM2s.myc protein levels decrease upon stabilisation of HIF1α.

As previously mentioned in **Chapter 5**, a dramatic reduction in the protein levels of SIM2s.myc were observed after 16 hours of cell growth in a hypoxic (<1% O_2) chamber, compared to the levels found in cells grown in normal growth conditions in DU145, LNCaP and PC3AR+ cells, and unlike HIF1α stabilisation discussed above, independent of p53-proficiency (**Figure 6.16**, panels b, e & h, compare to αTubulin loading control, panels c, f & i. previously shown as part of **Figure 5.8A**). This observation is consistent with a previous report by others where the total protein levels of ectopically expressed carboxy-terminal myc tagged mouse homologues, mSim1 and mSim2Long, in 293T cells decreased in association with hypoxic growth conditions [13, 59]. In this study neither the mRNA levels nor half-life of mSim2L.myc protein changed with hypoxic treatment, thus the decrease in protein was attributed to general global reduction in translation found in hypoxia [59], however, it was not formally tested. Utilising the 'hypoxia' mimetics DP and DMOG to induce 'hypoxia', via the stabilisation of HIF1α through inhibition of hydroxylase and iron dependent mechanisms of HIF1α degradation, also results in a dramatic reduction in SIM2s.myc levels, compared to DMSO vehicle controls in PC3AR+ cells (**Figure 6.17**, panel iii, lanes 2, 4 & 6, compare to load control panel iv). This suggests that the loss of SIM2s protein levels may correlate more closely to the stabilisation of HIF1α, as opposed to general hypoxic reductions in translation. Indeed, these data may further support this notion as there appears to be a correlation between the level of HIF1α stabilised with each hypoxia mimetic, and the corresponding level of SIM2s.myc; specifically, HIF1α is stabilised to a greater extent following prolonged treatment with DP compared to DMOG treatment in PC3AR+/SIM2s.myc cells, and correspondingly, the levels of SIM2s.myc are much more reduced upon DP treatment, compared to that with DMOG (**Figure 6.17**, panels ii & iii, lanes 2 & 6). Together, these data may be providing an

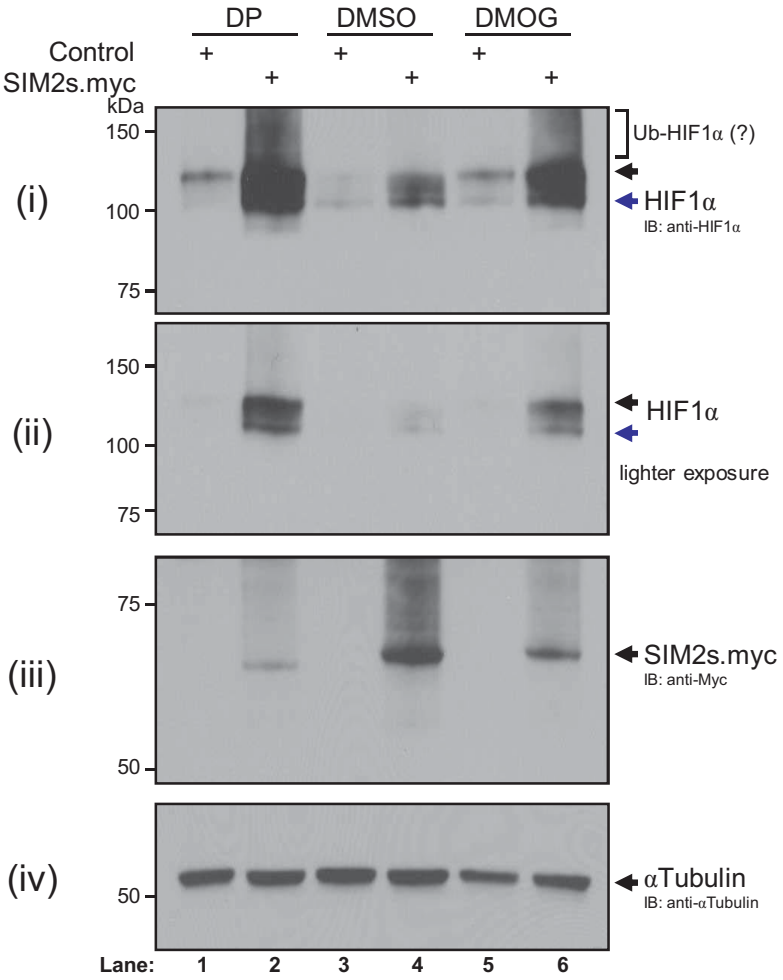

FIGURE 6.17: *Total HIF1α protein levels increase in PC3AR+/SIM2s.myc cells both in 'normoxia' (DMSO vehicle treated) and upon prolonged treatment with hypoxia mimetics, DP and DMOG compared to PC3AR+/Control.*

Subconfluent cells with, or without, stable ectopic expression of SIM2s ('SIM2s.myc' or 'Control', respectively) were treated with DMSO vehicle control or either of the hypoxia mimetics, DP or DMOG, for 44 hours and then lysed. 35µg of whole cell extracts were separated by 8% SDS-PAGE then subjected to immunoblot analysis of proteins as indicated. Blue arrow (◄) points to the lower molecular weight form of HIF1α. Potentially ubiquitinated (Ub-) HIF1α also indicated. Representative n=3 independent experiments, which includes analysis of two independently derived polyclonal Control and SIM2s.myc cell lines. Data in panels i, iii, and iv, previously shown in **Figure 5.14B**, **Chapter 5**.

intriguing novel insight into how HIF1α itself may be involved in the regulation of SIM2s protein levels. Much can be postulated regarding the potential manner by which SIM2s may be regulated downstream of HIF1α stabilisation. Possible mechanisms may include specific translational control of endogenous *SIM2* mediated by events downstream of HIF1α stabilisation. However, this work indicates that any such mechanisms of specific SIM2 translation control would not be conferred via specific 3' cap- and 5' UTR-binding events of regulatory proteins and microRNAs that together classically control translation and message stability (for reviews see [196]) as ectopically expressed SIM2s does not contain any of the 3' or 5' UTR sequences. Further possibilities may also include changes in the profile of post-translational modifications of SIM2s that may influence protein regulation.

6.3.2.3 Summary Comments on Putative Cross-Regulation of HIF1α and SIM2s: - Implications for Tumour Development

High levels of HIF1α in prostate cancer are associated with tumour development and invasive potential via mediating processes such as angiogenesis [196]. Recent studies reveal that tumours with high HIF1α do not respond well to chemo- and radiation therapies and thus is there is high interest in investigating how HIF1α contributes to tumour progression, and the potential to target HIF1α for the development of alternate chemopreventative therapeutics [290-292]. In light of this, the finding that HIF1a is dramatically stabilised in some prostate carcinoma derived cell lines upon ectopic expression of SIM2s revealed from the current study immediately highlights another mechanism by which elevated SIM2s levels found in prostate tumours [81] may be contributing to the development of aggressive prostate cancer by enhancing the activities of the HIF1α -pathway in tumours.

Mechanisms that are independent of oxygen that may account for the stabilisation seen here PC3AR+/SIM2s.myc cells in normoxia and after prolonged 'hypoxia' include the VHL-independent

regulation of HIF1α by the chaperone Hsp90 mediated pathways [24, 289]. As pharmacological inhibition of Hsp90, with the antagonist geldanamycin (GA), promotes degradation of HIF1α due to loss of HIF1α-Hsp90 interaction [24, 289], perhaps in the current context SIM2s.myc is acting directly, potentially via a direct SIM-Hsp90 interaction [47, 293], or indirectly, as an agonist for Hsp90 thus promoting stabilisation of HIF1α. Or conversely SIM2s competes with Hsp90 to bind HIF1α in a similar bHLH-PAS-mediated manner as does ARNT1 to protect HIF1α from degradation [24] (as discussed **Chapter 3**). However, in this scenario a potential SIM2s-HIF1α interaction would be independent of ARNT1 as SIM2s.myc is in excess to ARNT1 in these cells (see IP data **Figure 6.14**), and moreover unlikely, as SIM2s and HIF1α are yet to be shown to interact directly.

Loss of function of the tumour suppressor p53, commonly through mutation, is characteristic of approximately 30% of advanced prostate tumours and correlates to tumour progression, androgen-independence and worsened prognosis [81]. Likewise, enhanced expression of SIM2s in prostate tumours is also associated with aggressive tumours and worsened prognosis [294]. It is interesting to note that the enhanced stabilisation of HIF1α concomitant with ectopic expression of SIM2s appears to only occur in the prostate carcinoma lines that are p53-deficient, namely DU145 and PC3AR+ cells, and not LNCaP cells which have fully functional p53 [295] (**Figure 6.15**). This observation immediately highlights a potential requirement for this mechanism for SIM2s-associated HIF1α stabilisation, explained as follows. P53 mediates oxygen-independent proteasomal degradation of HIF1α via the human double minute 2 (Hdm2)-E3-ligase resultant of a direct binding interaction between p53 and HIF1α [296]. As such, this highlights the possibility that SIM2s expression is able to promote the stabilisation of HIF1α independently of oxygen in the absence of p53-binding mediated degradation of HIF1α via a mechanism by which HIF1α could not be otherwise stabilised when p53 is functional. Indeed, the requirement for the absence for p53 in this process could be initially assessed in the DU145 cell line which harbours a temperature sensitive form of p53, which

at 32°C it folds into the correct functional conformation [59]. Hence, if SIM2s expression no longer had associated enhanced levels of HIF1α upon induction of functional p53 in DU145 cells, in particular the enhanced levels of the lower molecular weight form of HIF1α, this would provide evidence of the involvement of p53 in attenuating the putative SIM2s-mediated mechanism of HIF1α stabilisation in an oxygen-independent manner. Ultimately, examining if there is an enhancement of HIF1α stabilisation in the p53-deficient/high-SIM2s-expressing clinical prostate tumour samples, irrespective of hypoxic microenvironments, compared to prostate tumours with low levels of SIM2s expression, with and without functional p53, would help define if the SIM2s/HIF1α/p53 relationship has any physiological relevance to tumour progression

CHAPTER 7

Final Discussion

7.1 FINAL DISCUSSION

Single-minded 2 (SIM2) is a member of the bHLH/PAS (basic Helix-Loop-Helix/Per-Arnt-Sim homology) family of transcriptional regulators [5] and is one of two mammalian homologues of *Drosophila* SIM, a mediator of central nervous system (CNS) development [34]. Functions for SIM2 in mammals remain to be fully determined, however targeted deletion of *SIM2* in mice, resulting in scoliosis, major disruptions in craniofacial structures and death shortly after birth due to a breathing defect [3, 58], demonstrates it plays important roles during development. Human *SIM2* is located in the Downs syndrome critical region of chromosome 21 [38, 39], however, how this may affect the etiology of Downs syndrome is yet to be fully elucidated [86, 88, 90].

Alternative splicing produces a short (SIM2s) protein variant in mice and humans [38, 41]. The human SIM2s (hSIM2s) splice variant arises from an alternate read-through event into the last intron of *SIM2*, resulting in a 570 amino acid protein which contains only one of the two SIM2 repression regions and a final 44 residues of unique C-terminal sequence [38]. How the minor divergence between C-termini of full length SIM2 (ie SIM2long, SIM2l), and SIM2s may confer alternate transcriptional activities or functions remain to be fully elucidated.

SIM2 heterodimerises with the common bHLH/PAS partner factor, ARNT (aryl hydrocarbon receptor nuclear translocator) to bind DNA [47]. Most of the current understanding of SIM2/ARNT transcriptional activities comes from studies of the murine long isoform (mSIM2L). Cell based reporter gene assays have shown mSIM2L to mediate repression of transcription via carboxy-terminal repression domains [9, 34, 59]. Another repressive mode of SIM2 is by sequestration of ARNT from other bHLH/PAS transcription factors, a manner

by which SIM2 can interfere with function of the Hypoxia Inducible Factor-1α (HIF1α) [59]. Conversely, on some promoters the SIM2/ARNT heterodimer can activate transcription via the transactivation domain of ARNT [41, 48]. For example, we recently discovered that human SIM2s is able to activate transcription of the *Myomesin 2* (*Myom2*) gene, via binding to a novel non-canonical E-box 5'-AACGTG-3' sequence in the promoter, which we have termed the S2RE (SIM2 response element) [**Chapter 1**] [48]. Similarly, the murine homologue of hSIM2s, which overall shares 87% protein identity, yet only 20% in the unique C-terminal region to hSIM2s, has also been shown to activate a CME (central midline element) (5'-TACGTG-3') driven reporter gene [41]. Thus it is apparent that SIM2 functions as both a transcriptional activator and repressor, however understanding how specificity of regulation is conferred in response to differing environmental or cell-signalling contexts, remains to be determined.

The expression status of SIM2s is emerging as an interesting candidate for a solid tumour marker. Select up-regulation of SIM2s has been identified in solid tumours of the pancreas, colon and prostate [43, 80, 81, 91]. Although the focus has mainly been on SIM2s in these tumour types, *SIM2L* mRNA has also been found to be expressed in tumours and tumour derived cell lines of the pancreas [43] and in prostate tumours [81], but not in corresponding normal cell lines or benign tissue samples. Several independent microarray studies find *SIM2* to be the second most consistently up-regulated gene in prostate tumours, while not being expressed in corresponding benign tissue, [81, 93, 94]. *SIM2* over-expression in human pancreatic carcinoma samples and derived cell lines compared to normal ductal epithelium controls has also recently been found in the most comprehensive genome wide analysis to date [96]. Compellingly, Halverson *et al* (2007) find elevated SIM2s protein levels significantly correlates to increased prostate tumour aggression and a dramatic drop in estimated survival, thus the authors propose SIM2s levels as a novel marker of aggressive prostate cancer. Studies by Narayanan and colleagues have strongly linked SIM2s expression with the survival of tumour derived cell lines of the pancreas and colon, where antisense mediated

knockdown of SIM2s in cell culture and mouse xenograft models results in cell death and a decrease in tumour size [43, 52, 80, 91]. Conversely however, *SIM2s* has recently been found to be repressed in breast cancer tumours [53]. In contrast to the colon and pancreatic tumour derived cell lines tested, loss of SIM2s in MCF-7 breast cancer cells correlates to cell survival via the activation of SLUG mediated EMT (epithelial mesenchymal transition) [53, 82]. Whether changes in SIM2s expression levels are required for tumour growth and/or tumour maintenance, and how SIM2s expression and transcriptional activities fit into the molecular profile of disease progression, is in need of further investigation.

This thesis sought to identify the molecular mechanisms by which aberrant levels of SIM2s expression in solid tumours of the prostate and pancreas may promote tumour development, thus providing a paradigm to gain greater knowledge and understanding of the transcription regulating activities and functional roles of SIM2.

One directed approach to addressing these aims was via investigating how the activities of SIM2s may be implicated in the known tumour promoting Hedgehog (Hh) signalling pathway as described in **Chapter 6**. Ectopic expression studies of mSim2L in the developing brain by Epstein and co-workers (2000) implied that the Sim family members may be involved in hedgehog signalling via the up regulation of the signalling ligand, Shh (sonic hedgehog). Increased activity of the Hedgehog (Hh) signalling pathway is one of the mechanisms driving tumourigenesis in cancers of the pancreas, gastric tract and prostate (for recent reviews see [204, 218, 251]). Studies by others have found that aberrantly enhanced Hh-signalling is required for prostate and pancreatic tumour cell survival, and interestingly, that ectopic *Shh* expression was sufficient to promote tumourigenic transformation of cultured primary prostate cells and the formation of precursor lesions in the pancreata of mice [98, 100, 218, 219, 224, 229]. These are notably tumour types were SIM2s is also aberrantly up regulated [43, 80, 81, 93, 94]. Thus considered together, these observations invoked

the possibility that in prostate and pancreatic carcinomas, independently activated SIM2s may lead to activation of Hh-signalling via up-regulation of Shh levels, and if so would reveal a novel role for SIM2s in the genesis of these tumour types. This constituted the premise for one of the directed approaches to examine how SIM2s may play a role in these cancer types. These studies are described in **Chapter 6**. ***In vitro* cell culture studies in human carcinoma derived cell lines of the pancreas and prostate did further support that SIM2s levels are closely linked to those of SHH, even at the endogenous level, and to Hh-pathway activation and/or maintenance, perhaps via indirect regulation of the activities of the Hh-pathway mediators, the GLI family members.** However, despite these initial findings an *in vivo* approach involving the development of transgenic mice for directed expression of human SIM2s in pancreatic precursor cells, like that developed for Shh that resulted in pancreatic tumour lesions [219, 247], failed to show any phenotype to indicate that aberrant expression of SIM2s is enough to initiate tumourigenic lesions in the pancreas. As found by Epstein and co-workers previously [71], these studies similarly suggested possible mechanisms of regulation of *Shh* by SIM2s and indeed the regulation of *SIM2s* by Shh and Hh-signalling. The possibility that activated Hh-signalling may play a role in the regulation of SIM2s expression, perhaps at the transcriptional level via GLI activities, would help explain why SIM2s levels are aberrantly up regulated in these tumours. However, as the normally quiescent Notch pathway is also activated during PanIN development and shown to drive cancer growth [240, 297-299], an alternate mechanism of *SIM2s* regulation may lie in possible tumour type specific Notch-signalling mediated mechanisms [62, 64, 66, 68, 70], which in turn may require SHH [72].

Knowledge of direct gene targets of SIM2 and the functional outcomes of their regulation in tumour cells are key to understanding how SIM2 may ultimately function in tumours where it is misregulated. It is interesting to note that human SIM2s-mediated repression of the *SLUG* gene in breast cancer cells has been recently reported [82]. Although the exact DNA-binding element required for SIM2s/ARNT was not defined, nor was

the mode of SIM2s-mediated repression, these studies did link SIM2s to the regulation of SLUG-mediated EMT (epithelial mesenchymal transition) [53, 82], a well characterised developmental mechanism emerging as a driver of solid tumour growth and metastasis [300]. However, at the time the studies of this thesis were initiated no direct target genes of SIM2s had been identified and consequently there was no understanding about the molecular mechanisms or pathways through which SIM2s may be contributing to tumour cell survival

.

Aberrantly high SIM2s levels in human prostate carcinomas correlates to tumour aggression and worsened prognosis [81]. Thus in an attempt to further understand this correlation, and perhaps identify novel mechanisms by which SIM2s may function in all tumour types where it is up-regulated, the second directed approach to investigating this in the form of a target gene discovery project was embarked upon, as described in **Chapter 4**. Microarray analysis of differential gene regulation upon stable ectopic expression of SIM2s in prostate carcinoma cell lines, followed by independent validation experiments in multiple cell lines, lead to **the identification of the HIF1α direct target gene, BNIP3 [174, 188, 301, 302], as a novel direct target of SIM2s repression (Chapter 5). These studies reveal SIM2s cross-talk on an endogenous HRE, for the first time, and attenuation of HIF1α activities in the regulation of *BNIP3* as a possible novel mechanism for SIM2s in tumourigenesis.** These studies couple a role for SIM2s in promoting tumour cell survival, consistent with reports by others [43, 91], and the direct SIM2s-mediated transcriptional repression of *BNIP3* with the attenuation of hypoxia-induced cell-death processes, particularly hypoxia-induced autophagic cell death, in prostate cancer PC3AR+ cells. During the course of these studies, new insights into the transcriptional regulation of *BNIP3* in both normoxic and hypoxic conditions were reported. Interestingly, Tracy *et al* (2007) reported that the hypoxic induction of *BNIP3* was also attenuated via direct pRB binding of E2F-1 on the promoter of BNIP3 which prevented hypoxia-induced autophagic cell death [187]. E2F-1 has been found to bind the promoter of BNIP3, together with HIF1α in hypoxia, and promotes

BNIP3 expression and consequently activation of cell death processes [187, 303]. Similarly, recently published works from Kirshenbaum and colleagues also report a novel transcriptional mechanism of *BNIP3* silencing which results in the inhibition of ventricular myocyte and pancreatic carcinoma cell death via direct NFkappaB binding activities on the promoter of *BNIP3* which inhibits E2F-1 DNA-binding [303-305]. It will be interesting to see from future work if, and how, the players of these independently identified and divergent mechanisms of transcriptional regulation of *BNIP3* gene expression, including the novel findings from this thesis implicating SIM2, orchestrate the regulation of BNIP3 to ultimately control cell-death processes under conditions of cellular stress or in tumour development. Furthermore, identifying any co-regulatory SIM2-binding protein(s) in the regulation of *BNIP3* would also provide important novel insights into how SIM2 may mediate transcription in general, especially with respect to the potential for differential regulation by the two isoforms of SIM2.

In pursuit of experimentally addressing these two defined lines of investigation, several highly unexpected and unprecedented findings emerged that revealed unforeseen avenues of study which lead to the suggestion of novel roles and activities of SIM2, in particular SIM2s, in development and cancer.

A striking unexpected finding of note was **the observation of enhanced levels of endogenous HIF1α protein in hypoxically treated human prostate DU145 and PC3AR+ cells stably expressing SIM2s**, as discussed in **Chapter 6**. This observation is particularly interesting on several counts; firstly, no fellow class I bHLH-PAS factor has previously been reported to aid stabilisation of HIF1α. And secondly, SIM2s was still able to compete with this endogenous increase in HIF1α to repress *BNIP3* via the HRE and attenuate its hypoxic induction. Much future work is required to determine if these preliminary data are indicative of cross-regulation between HIF1α and SIM2s levels in the cell, and if it is a mechanism that may ultimately help to promote tumourigenesis. However, considered together these findings support the notion of SIM2s-

mediated modulation of HIF1α beyond the competition for target gene regulation. Namely, in conjunction with attenuating HIF1α-mediated cell death process via completion for *BNIP3* regulation, SIM2s may further function to divert HIF1α activities away from provoking tumour death and towards facilitatating HIF1α-mediated pro-tumourigenic processes such as angiogenesis to tumour growth via the stabilisation of HIF1α. These studies reveal potential multiple mechanisms by which SIM2s may modulate HIF1α activities to ultimately drive cancer growth, and will surely influence future work into SIM2s and HIF1α target gene regulation and function in cancer and indeed development.

Also unexpectedly, a nuclear receptor, the **Androgen Receptor (AR), was found to be differentially up-regulated upon ectopic expression the SIM2 isoforms in human prostate PC3AR+ cells**, as described in **Chapter 6**. Moreover, endogenous *Probasin* promoter driven reporter gene studies showed that transiently expressed, DHT ligand activated, wtAR function was enhanced with SIM2s expression in these cells. AR was found to interact with ectopic SIM2s.myc, indicating for the first time that SIM2s may interact with other transcriptional regulators as a co-activator to enhance their activities. Unfortunately these putative regulatory relationships between SIM2s and AR did not extend beyond PC3AR+ cells in these studies, and thus it lies in future work to ascertain if these are to be found in prostate tumours, and if it provides insight into other mechanisms through which aberrant levels of SIM2s may promote prostate tumour growth. Searching the literature reveals interesting possible links between these unexpected results arising from studies of SIM2s in prostate tumour cells. For example; ChIP studies show in hypoxia HIF1α binds the promoter of *PSA* (prostate specific antigen) with the AR to drive expression of PSA [196]. Also, treatment of prostate tumour derived cells with AR activating ligand DHT results in the up-regulation of HIF1 target genes [306]. Thus perhaps SIM2s indirectly contributes to such mechanisms of gene regulation via the enhancement of AR and HIF1α protein levels, as observed in PC3AR+ upon stable ectopic expression of SIM2s, to also aid tumour development.

From what started as an intriguing observation, the study of the regulation of ARNT by the SIM family members, pursued due to the unprecedented premise of class I family member regulating the levels of the class II common partner factors, developed into a significant study of this thesis to reveal another incidence of SIM2s-mediated bHLH-PAS factor cross-regulation (**Chapter 3**). These **novel findings suggest that SIM2s is intimately linked to the post-translational stabilisation and maintenance of ARNT1 and ARNT2 protein levels in carcinoma, and non-carcinoma, derived cell lines. Furthermore, SIM2s appears to also regulate *ARNT2* message levels, and as SIM2s is found at the hARNT2 promoter, perhaps via mechanisms of induced transcription.** Of particular significance from these studies is the observation that **this regulation of ARNT appears to be specific to SIM family members**, as ARNT1 protein levels fail to increase upon induced expression and activation of AhR and HIF1α. Although possible modes of ARNT regulation by SIM are extensively discussed in Chapter 3, section 3.3, it remains for future work to define the specific molecular mechanisms by which SIM family members actually confer regulation ARNT. However, as studies thus far show that heterodimerisation with ARNT is requisite for class I family members to bind DNA and regulate gene transcription [5], these studies deeply implicate SIM in the regulation of bHLH-PAS (hetero)dimerisation, and consequently mechanisms of bHLH-PAS regulatory cross-talk and the potential to influence the activities and function of fellow family members. How this may contribute or influence bHLH-PAS-mediated developmental processes remains to be studied. **In the context of tumour development however, perhaps SIM2 is not only moderating the activities of HIF1α on *BNIP3* to promote tumour cell survival, but is also providing enhanced levels of ARNT for promoting HIF1α-mediated pro-tumourigenic processes such as angiogenesis.**

Despite SIM2 being essential for development and survival in mice [3, 58], and the more recent findings implicating differential regulation of *SIM2s* in the highly lethal tumours of the colon, pancreas, prostate and

breast contributing to tumour progression, aggression and cell survival [43, 52, 53, 80-82, 91, 93, 94, 96], very little is understood about the roles of SIM2 in development and disease. The predominant work of this thesis has revealed a novel direct target of SIM2s repression, the pro-cell death factor *BNIP3,* via cross-talk on the HRE, and consequently the promotion of tumour cell survival via the attenuation of hypoxically-induced BNIP3-mediated cell death processes. Furthermore, unexpected roles for SIM2 in the regulation of the general partner factor ARNT also greatly implicates SIM2 in the regulation and functional modulation of all bHLH-PAS factors requiring ARNT in developmental and tumourigeneic processes. The work of this thesis provides novel findings that further our understanding of SIM2 as a transcriptional regulator, new knowledge of SIM as a cross-regulator of bHLH-PAS family members, and insights into a number of roles through which SIM2s functions to facilitate tumourigenesis.

CHAPTER 8

REFERENCES

8.1 REFERENCES

1. Abbott, B.D. and A.R. Buckalew, *Placental defects in ARNT-knockout conceptus correlate with localized decreases in VEGF-R2, Ang-1, and Tie-2.* Dev Dyn, 2000. **219**(4): p. 526-38.

2. Hosoya, T., et al., *Defective development of secretory neurones in the hypothalamus of Arnt2-knockout mice.* Genes Cells, 2001. **6**(4): p. 361-74.

3. Shamblott, M.J., et al., *Craniofacial abnormalities resulting from targeted disruption of the murine Sim2 gene.* Dev Dyn, 2002. **224**(4): p. 373-80.

4. Crews, S.T. and C.M. Fan, *Remembrance of things PAS: regulation of development by bHLH-PAS proteins.* Curr Opin Genet Dev, 1999. **9**(5): p. 580-7.

5. Kewley, R.J., M.L. Whitelaw, and A. Chapman-Smith, *The mammalian basic helix-loop-helix/PAS family of transcriptional regulators.* Int J Biochem Cell Biol, 2004. **36**(2): p. 189-204.

6. Chapman-Smith, A., J.K. Lutwyche, and M.L. Whitelaw, *Contribution of the Per/Arnt/Sim (PAS) domains to DNA binding by the basic helix-loop-helix PAS transcriptional regulators.* J Biol Chem, 2004. **279**(7): p. 5353-62.

7. Zelzer, E., P. Wappner, and B.Z. Shilo, *The PAS domain confers target gene specificity of Drosophila bHLH/PAS proteins.* Genes Dev, 1997. **11**(16): p. 2079-89.

8. Hirose, K., et al., *cDNA cloning and tissue-specific expression of a novel basic helix-loop-helix/PAS factor (Arnt2) with close sequence similarity to the aryl hydrocarbon receptor nuclear translocator (Arnt).* Mol Cell Biol, 1996. **16**(4): p. 1706-13.

9. Moffett, P., M. Reece, and J. Pelletier, *The murine Sim-2 gene product inhibits transcription by active repression and functional interference.* Mol Cell Biol, 1997. **17**(9): p. 4933-47.

10. Ooe, N., et al., *Identification of a novel basic helix-loop-helix-PAS factor, NXF, reveals a Sim2 competitive, positive regulatory role in dendritic-cytoskeleton modulator drebrin gene expression.* Mol Cell Biol, 2004. **24**(2): p. 608-16.

11. Ooe, N., K. Saito, and H. Kaneko, *Characterization of functional heterodimer partners in brain for a bHLH-PAS factor NXF.* Biochim Biophys Acta, 2009.

12. Bracken, C.P., M.L. Whitelaw, and D.J. Peet, *The hypoxia-inducible factors: key transcriptional regulators of hypoxic responses.* Cell Mol Life Sci, 2003. **60**(7): p. 1376-93.

13. Kenneth, N.S. and S. Rocha, *Regulation of gene expression by hypoxia.* Biochem J, 2008. **414**(1): p. 19-29.

14. Lando, D., et al., *Oxygen-dependent regulation of hypoxia-inducible factors by prolyl and asparaginyl hydroxylation.* Eur J Biochem, 2003. **270**(5): p. 781-90.

15. Appelhoff, R.J., et al., *Differential function of the prolyl hydroxylases PHD1, PHD2, and PHD3 in the regulation of hypoxia-inducible factor.* J Biol Chem, 2004. **279**(37): p. 38458-65.

16. Salceda, S. and J. Caro, *Hypoxia-inducible factor 1alpha (HIF-1alpha) protein is rapidly degraded by the ubiquitin-proteasome system under normoxic conditions. Its stabilization by hypoxia depends on redox-induced changes.* J Biol Chem, 1997. **272**(36): p. 22642-7.

17. Huang, L.E., et al., *Regulation of hypoxia-inducible factor 1alpha is mediated by an O2-dependent degradation domain via the ubiquitin-proteasome pathway.* Proc Natl Acad Sci U S A, 1998. **95**(14): p. 7987-92.

18. Kallio, P.J., et al., *Regulation of the hypoxia-inducible transcription factor 1alpha by the ubiquitin-proteasome pathway.* J Biol Chem, 1999. **274**(10): p. 6519-25.

19. Lando, D., et al., *FIH-1 is an asparaginyl hydroxylase enzyme that regulates the transcriptional activity of hypoxia-inducible factor.* Genes Dev, 2002b. **16**(12): p. 1466-71.

20. Lando, D., et al., *Asparagine hydroxylation of the HIF transactivation domain a hypoxic switch.* Science, 2002a. **295**(5556): p. 858-61.

21. Wang, G.L. and G.L. Semenza, *Characterization of hypoxia-inducible factor 1 and regulation of DNA binding activity by hypoxia.* J Biol Chem, 1993. **268**(29): p. 21513-8.

22. Forsythe, J.A., et al., *Activation of vascular endothelial growth factor gene transcription by hypoxia-inducible factor 1.* Mol Cell Biol, 1996. **16**(9): p. 4604-13.

23. Bilton, R.L. and G.W. Booker, *The subtle side to hypoxia inducible factor (HIFalpha) regulation.* Eur J Biochem, 2003. **270**(5): p. 791-8.

24. Isaacs, J.S., Y.J. Jung, and L. Neckers, *Aryl hydrocarbon nuclear translocator (ARNT) promotes oxygen-independent stabilization of hypoxia-inducible factor-1alpha by modulating an Hsp90-dependent regulatory pathway.* J Biol Chem, 2004. **279**(16): p. 16128-35.

25. Franks, R.G. and S.T. Crews, *Transcriptional activation domains of the single-minded bHLH protein are required for CNS midline cell development.* Mech Dev, 1994. **45**(3): p. 269-77.

26. Lewis, J.O. and S.T. Crews, *Genetic analysis of the Drosophila single-minded gene reveals a central nervous system influence on muscle development.* Mech Dev, 1994. **48**(2): p. 81-91.

27. Estes, P., J. Mosher, and S.T. Crews, *Drosophila single-minded represses gene transcription by activating the expression of repressive factors.* Dev Biol, 2001. **232**(1): p. 157-75.

28. Nambu, J.R., et al., *The Drosophila single-minded gene encodes a helix-loop-helix protein that acts as a master regulator of CNS midline development.* Cell, 1991. **67**(6): p. 1157-67.

29. Thomas, J.B., S.T. Crews, and C.S. Goodman, *Molecular genetics of the single-minded locus: a gene involved in the development of the Drosophila nervous system.* Cell, 1988. **52**(1): p. 133-41.

30. Crews, S.T., *Control of cell lineage-specific development and transcription by bHLH-PAS proteins.* Genes Dev, 1998. **12**(5): p. 607-20.

31. Coumailleau, P., et al., *Characterization and developmental expression of xSim, a Xenopus bHLH/PAS gene related to the Drosophila neurogenic master gene single-minded.* Mech Dev, 2000. **99**(1-2): p. 163-6.

32. Serluca, F.C. and M.C. Fishman, *Pre-pattern in the pronephric kidney field of zebrafish.* Development, 2001. **128**(12): p. 2233-41.

33. Wen, H.J., et al., *Expression pattern of the single-minded gene in zebrafish embryos.* Mech Dev, 2002. **110**(1-2): p. 231-5.

34. Ema, M., et al., *Two new members of the murine Sim gene family are transcriptional repressors and show different expression patterns during mouse embryogenesis.* Mol Cell Biol, 1996b. **16**(10): p. 5865-75.

35. Ema, M., et al., *cDNA cloning of a murine homologue of Drosophila single-minded, its mRNA expression in mouse development, and chromosome localization.* Biochem Biophys Res Commun, 1996a. **218**(2): p. 588-94.

36. Fan, C.M., et al., *Expression patterns of two murine homologs of Drosophila single-minded suggest possible roles in embryonic patterning and in the pathogenesis of Down syndrome.* Mol Cell Neurosci, 1996. **7**(1): p. 1-16.

37. Yamaki, A., et al., *The mammalian single-minded (SIM) gene: mouse cDNA structure and diencephalic expression indicate a candidate gene for Down syndrome.* Genomics, 1996. **35**(1): p. 136-43.

38. Chrast, R., et al., *Cloning of two human homologs of the Drosophila single-minded gene SIM1 on chromosome 6q and SIM2 on 21q within the Down syndrome chromosomal region.* Genome Res, 1997. **7**(6): p. 615-24.

39. Dahmane, N., et al., *Down syndrome-critical region contains a gene homologous to Drosophila sim expressed during rat and human central nervous system development.* Proc Natl Acad Sci U S A, 1995. **92**(20): p. 9191-5.

40. Yamaki, A., et al., *Molecular mechanisms of human single-minded 2 (SIM2) gene expression: identification of a promoter site in the SIM2 genomic sequence.* Gene, 2001. **270**(1-2): p. 265-75.

41. Metz, R.P., et al., *Differential transcriptional regulation by mouse single-minded 2s.* J Biol Chem, 2006. **281**(16): p. 10839-48.

42. Coumailleau, P. and D. Duprez, *Sim1 and Sim2 expression during chick and mouse limb development.* Int J Dev Biol, 2009. **53**(1): p. 149-57.

43. DeYoung, M.P., M. Tress, and R. Narayanan, *Down's syndrome-associated Single Minded 2 gene as a pancreatic cancer drug therapy target.* Cancer Letters, 2003b. **200**(1): p. 25-31.

44. Goshu, E., et al., *Sim2 contributes to neuroendocrine hormone gene expression in the anterior hypothalamus.* Mol Endocrinol, 2004. **18**(5): p. 1251-62.

45. Michaud, J.L., et al., *Development of neuroendocrine lineages requires the bHLH-PAS transcription factor SIM1.* Genes Dev, 1998. **12**(20): p. 3264-75.

46. Moffett, P. and J. Pelletier, *Different transcriptional properties of mSim-1 and mSim-2.* FEBS Lett, 2000. **466**(1): p. 80-6.

47. Probst, M.R., et al., *Two murine homologs of the Drosophila single-minded protein that interact with the mouse aryl hydrocarbon receptor nuclear translocator protein.* J Biol Chem, 1997. **272**(7): p. 4451-7.

48. Woods, S., et al., *The bHLH/Per-Arnt-Sim transcription factor SIM2 regulates muscle transcript myomesin2 via a novel, non-canonical E-box sequence.* Nucleic Acids Res, 2008. **36**(11): p. 3716-27.

49. van der Ven, P.F., et al., *Assignment of the human gene for endosarcomeric cytoskeletal M-protein (MYOM2) to 8p23.3.* Genomics, 1999. **55**(2): p. 253-5.

50. Steiner, F., K. Weber, and D.O. Furst, *Structure and expression of the gene encoding murine M-protein, a sarcomere-specific member of the immunoglobulin superfamily.* Genomics, 1998. **49**(1): p. 83-95.

51. Carlsson, E., et al., *Myofibrillar M-band proteins in rat skeletal muscles during development.* Histochemistry, 1990. **95**(1): p. 27-35.

52. DeYoung, M.P., M. Tress, and R. Narayanan, *Identification of Down's syndrome critical locus gene SIM2-s as a drug therapy target for solid tumors.* Proc Natl Acad Sci U S A, 2003a. **100**(8): p. 4760-5.

53. Kwak, H.I., et al., *Inhibition of breast cancer growth and invasion by single-minded 2s.* Carcinogenesis, 2007. **28**(2): p. 259-66.

54. Crews, S.T., J.B. Thomas, and C.S. Goodman, *The Drosophila single-minded gene encodes a nuclear protein with sequence similarity to the per gene product.* Cell, 1988. **52**(1): p. 143-51.

55. Nambu, J.R., et al., *The single-minded gene of Drosophila is required for the expression of genes important for the development of CNS midline cells.* Cell, 1990. **63**(1): p. 63-75.

56. Michaud, J.L., *The developmental program of the hypothalamus and its disorders.* Clin Genet, 2001. **60**(4): p. 255-63.

57. Holder, J.L., Jr., et al., *Sim1 gene dosage modulates the homeostatic feeding response to increased dietary fat in mice.* Am J Physiol Endocrinol Metab, 2004. **287**(1): p. E105-13.

58. Goshu, E., et al., *Sim2 mutants have developmental defects not overlapping with those of Sim1 mutants.* Mol Cell Biol, 2002. **22**(12): p. 4147-57.

59. Woods, S.L. and M.L. Whitelaw, *Differential activities of murine single minded 1 (SIM1) and SIM2 on a hypoxic response element. Cross-talk between basic helix-loop-helix/per-Arnt-Sim homology transcription factors.* J Biol Chem, 2002. **277**(12): p. 10236-43.

60. Yamaki, A., et al., *A novel nuclear localization signal in the human single-minded proteins SIM1 and SIM2.* Biochem Biophys Res Commun, 2004. **313**(3): p. 482-8.

61. Kasai, Y., S. Stahl, and S. Crews, *Specification of the Drosophila CNS midline cell lineage: direct control of single-minded transcription by dorsal/ventral patterning genes.* Gene Expr, 1998. **7**(3): p. 171-89.

62. Morel, V. and F. Schweisguth, *Repression by suppressor of hairless and activation by Notch are required to define a single row of single-minded expressing cells in the Drosophila embryo.* Genes Dev, 2000. **14**(3): p. 377-88.

63. Leptin, M., *twist and snail as positive and negative regulators during Drosophila mesoderm development.* Genes Dev, 1991. **5**(9): p. 1568-76.

64. Chitnis, A.B., *Keeping single minded expression on the straight and narrow.* Mol Cell, 2006. **21**(4): p. 450-2.

65. Bardin, A.J. and F. Schweisguth, *Bearded family members inhibit Neuralized-mediated endocytosis and signaling activity of Delta in Drosophila.* Dev Cell, 2006. **10**(2): p. 245-55.

66. Martin-Bermudo, M.D., A. Carmena, and F. Jimenez, *Neurogenic genes control gene expression at the transcriptional level in early neurogenesis and in mesectoderm specification.* Development, 1995. **121**(1): p. 219-24.

67. Nagel, A.C., et al., *Involvement of co-repressors Groucho and CtBP in the regulation of single-minded in Drosophila.* Hereditas, 2007. **144**(5): p. 195-205.

68. Morel, V., R. Le Borgne, and F. Schweisguth, *Snail is required for Delta endocytosis and Notch-dependent activation of single-minded expression.* Dev Genes Evol, 2003. **213**(2): p. 65-72.

69. Kasai, Y., et al., *Dorsal-ventral patterning in Drosophila: DNA binding of snail protein to the single-minded gene.* Proc Natl Acad Sci U S A, 1992. **89**(8): p. 3414-8.

70. Gustafson, T.L., et al., *Ha-Ras transformation of MCF10A cells leads to repression of Singleminded-2s through NOTCH and C/EBPbeta.* Oncogene, 2009. **28**(12): p. 1561-8.

71. Epstein, D.J., et al., *Members of the bHLH-PAS family regulate Shh transcription in forebrain regions of the mouse CNS.* Development, 2000. **127**(21): p. 4701-9.

72. Baonza, A. and M. Freeman, *Control of cell proliferation in the Drosophila eye by Notch signaling.* Dev Cell, 2005. **8**(4): p. 529-39.

73. Nuchprayoon, I., et al., *GABP cooperates with c-Myb and C/EBP to activate the neutrophil elastase promoter.* Blood, 1997. **89**(12): p. 4546-54.

74. Yang, C., et al., *Regulatory interaction between arylhydrocarbon receptor and SIM1, two basic helix-loop-helix PAS proteins involved in the control of food intake.* J Biol Chem, 2004. **279**(10): p. 9306-12.

75. Crews, S., et al., *Drosophila single-minded gene and the molecular genetics of CNS midline development.* J Exp Zool, 1992. **261**(3): p. 234-44.

76. Wharton, K.A., Jr., et al., *Control of CNS midline transcription by asymmetric E-box-like elements: similarity to xenobiotic responsive regulation.* Development, 1994. **120**(12): p. 3563-9.

77. Wharton, K.A., Jr. and S.T. Crews, *CNS midline enhancers of the Drosophila slit and Toll genes.* Mech Dev, 1993. **40**(3): p. 141-54.

78. Ohshiro, T. and K. Saigo, *Transcriptional regulation of breathless FGF receptor gene by binding of TRACHEALESS/dARNT heterodimers to three central midline elements in Drosophila developing trachea.* Development, 1997. **124**(20): p. 3975-86.

79. Eguchi, H., et al., *A nuclear localization signal of human aryl hydrocarbon receptor nuclear translocator/hypoxia-inducible factor 1beta is a novel bipartite type recognized by the two components of nuclear pore-targeting complex.* J Biol Chem, 1997. **272**(28): p. 17640-7.

80. Deyoung, M.P., et al., *Down's syndrome-associated single minded gene as a novel tumor marker.* Anticancer Res, 2002. **22**(6A): p. 3149-57.

81. Halvorsen, O.J., et al., *Increased expression of SIM2-s protein is a novel marker of aggressive prostate cancer.* Clin Cancer Res, 2007. **13**(3): p. 892-7.

82. Laffin, B., et al., *Loss of singleminded-2s in the mouse mammary gland induces an epithelial-mesenchymal transition associated with up-regulation of slug and matrix metalloprotease 2.* Mol Cell Biol, 2008. **28**(6): p. 1936-46.

83. Liu, C., et al., *Identification of the downstream targets of SIM1 and ARNT2, a pair of transcription factors essential for neuroendocrine cell differentiation.* J Biol Chem, 2003. **278**(45): p. 44857-67.

84. Michaud, J.L., et al., *ARNT2 acts as the dimerization partner of SIM1 for the development of the hypothalamus.* Mech Dev, 2000. **90**(2): p. 253-61.

85. Muenke, M., et al., *Physical mapping of the holoprosencephaly critical region in 21q22.3, exclusion of SIM2 as a candidate gene for holoprosencephaly, and mapping of SIM2 to a region of chromosome 21 important for Down syndrome.* Am J Hum Genet, 1995. **57**(5): p. 1074-9.

86. Chrast, R., et al., *Mice trisomic for a bacterial artificial chromosome with the single-minded 2 gene (Sim2) show phenotypes similar to some of those present in the partial trisomy 16 mouse models of Down syndrome.* Hum Mol Genet, 2000. **9**(12): p. 1853-64.

87. Chen, H., et al., *Single-minded and Down syndrome?* Nat Genet, 1995. **10**(1): p. 9-10.

88. Rachidi, M., et al., *Spatial and temporal localization during embryonic and fetal human development of the transcription factor SIM2 in brain regions altered in Down syndrome.* Int J Dev Neurosci, 2005. **23**(5): p. 475-84.

89. Ema, M., et al., *Mild impairment of learning and memory in mice overexpressing the mSim2 gene located on chromosome 16: an animal model of Down's syndrome.* Hum Mol Genet, 1999. **8**(8): p. 1409-15.

90. Vialard, F., et al., *Overexpression of mSim2 gene in the zona limitans of the diencephalon of segmental trisomy 16 Ts1Cje fetuses, a mouse model for trisomy 21: a novel whole-mount based RNA hybridization study.* Brain Res Dev Brain Res, 2000. **121**(1): p. 73-8.

91. Aleman, M.J., et al., *Inhibition of Single Minded 2 gene expression mediates tumor-selective apoptosis and differentiation in human colon cancer cells.* Proc Natl Acad Sci U S A, 2005. **102**(36): p. 12765-70.

92. Ratan, R.R., *Mining genome databases for therapeutic gold: SIM2 is a novel target for treatment of solid tumors.* Trends in Pharmacological Sciences, 2003. **24**(10): p. 508-510.

93. Chandran, U., et al., *Differences in gene expression in prostate cancer, normal appearing prostate tissue adjacent to cancer and prostate tissue from cancer free organ donors.* BMC Cancer, 2005. **5**(1): p. 45.

94. Su, A.I., et al., *Large-scale analysis of the human and mouse transcriptomes.* Proc Natl Acad Sci U S A, 2002. **99**(7): p. 4465-70.

95. Leach, S.D., *Mouse models of pancreatic cancer: the fur is finally flying!* Cancer Cell, 2004. **5**(1): p. 7-11.

96. Jones, S., et al., *Core signaling pathways in human pancreatic cancers revealed by global genomic analyses.* Science, 2008. **321**(5897): p. 1801-6.

97. Richard, D.E., et al., *p42/p44 mitogen-activated protein kinases phosphorylate hypoxia-inducible factor 1alpha (HIF-1alpha) and enhance the transcriptional activity of HIF-1.* J Biol Chem, 1999. **274**(46): p. 32631-7.

98. Karhadkar, S.S., et al., *Hedgehog signalling in prostate regeneration, neoplasia and metastasis.* Nature, 2004. **431**(7009): p. 707-12.

99. Anguita, E., et al., *Globin gene activation during haemopoiesis is driven by protein complexes nucleated by GATA-1 and GATA-2.* Embo J, 2004. **23**(14): p. 2841-52.

100. Sanchez, P., et al., *Inhibition of prostate cancer proliferation by interference with SONIC HEDGEHOG-GLI1 signaling.* Proc Natl Acad Sci U S A, 2004. **101**(34): p. 12561-6.

101. Drabsch, Y., et al., *Mechanism of and requirement for estrogen-regulated MYB expression in estrogen-receptor-positive breast cancer cells.* Proc Natl Acad Sci U S A, 2007. **104**(34): p. 13762-7.

102. Hobbs, S., S. Jitrapakdee, and J.C. Wallace, *Development of a bicistronic vector driven by the human polypeptide chain elongation factor 1alpha promoter for creation of stable mammalian cell lines that express very high levels of recombinant proteins.* Biochem Biophys Res Commun, 1998. **252**(2): p. 368-72.

103. Kinzler, K.W., et al., *The GLI gene is a member of the Kruppel family of zinc finger proteins.* Nature, 1988. **332**(6162): p. 371-4.

104. Berghard, A., et al., *Cross-coupling of signal transduction pathways: the dioxin receptor mediates induction of cytochrome P-450IA1 expression via a protein kinase C-dependent mechanism.* Mol Cell Biol, 1993. **13**(1): p. 677-89.

105. Sasaki, H., et al., *A binding site for Gli proteins is essential for HNF-3beta floor plate enhancer activity in transgenics and can respond to Shh in vitro.* Development, 1997. **124**(7): p. 1313-22.

106. Muller, P.Y., et al., *Processing of gene expression data generated by quantitative real-time RT-PCR.* Biotechniques, 2002. **32**(6): p. 1372-4, 1376, 1378-9.

107. Whitelaw, M., et al., *Ligand-dependent recruitment of the Arnt coregulator determines DNA recognition by the dioxin receptor.* Mol Cell Biol, 1993a. **13**(4): p. 2504-14.

108. Whitelaw, M.L., J.A. Gustafsson, and L. Poellinger, *Identification of transactivation and repression functions of the dioxin receptor and its basic helix-loop-helix/PAS partner factor Arnt: inducible versus constitutive modes of regulation.* Mol Cell Biol, 1994. **14**(12): p. 8343-55.

109. Drutel, G., et al., *ARNT2, a transcription factor for brain neuron survival?* Eur J Neurosci, 1999. **11**(5): p. 1545-53.

110. Jain, S., et al., *Expression of ARNT, ARNT2, HIF1 alpha, HIF2 alpha and Ah receptor mRNAs in the developing mouse.* Mech Dev, 1998. **73**(1): p. 117-23.

111. Aitola, M.H. and M.T. Pelto-Huikko, *Expression of Arnt and Arnt2 mRNA in developing murine tissues.* J Histochem Cytochem, 2003. **51**(1): p. 41-54.

112. Kozak, K.R., B. Abbott, and O. Hankinson, *ARNT-deficient mice and placental differentiation.* Dev Biol, 1997. **191**(2): p. 297-305.

113. Maltepe, E., et al., *Abnormal angiogenesis and responses to glucose and oxygen deprivation in mice lacking the protein ARNT.* Nature, 1997. **386**(6623): p. 403-7.

114. Keith, B., D.M. Adelman, and M.C. Simon, *Targeted mutation of the murine arylhydrocarbon receptor nuclear translocator 2 (Arnt2) gene reveals partial redundancy with Arnt.* Proc Natl Acad Sci U S A, 2001. **98**(12): p. 6692-7.

115. Sekine, H., et al., *Unique and overlapping transcriptional roles of arylhydrocarbon receptor nuclear translocator (Arnt) and Arnt2 in xenobiotic and hypoxic responses.* J Biol Chem, 2006. **281**(49): p. 37507-16.

116. Dougherty, E.J. and R.S. Pollenz, *Analysis of Ah receptor-ARNT and Ah receptor-ARNT2 complexes in vitro and in cell culture.* Toxicol Sci, 2008. **103**(1): p. 191-206.

117. Huffman, J.L., et al., *The basic helix-loop-helix domain of the aryl hydrocarbon receptor nuclear transporter (ARNT) can oligomerize and bind E-box DNA specifically.* J Biol Chem, 2001. **276**(44): p. 40537-44.

118. Arpiainen, S., et al., *Aryl hydrocarbon receptor nuclear translocator and upstream stimulatory factor regulate Cytochrome P450 2a5 transcription through a common E-box site.* J Mol Biol, 2007. **369**(3): p. 640-52.

119. Kang, H.J., et al., *BRCA1 modulates xenobiotic stress-inducible gene expression by interacting with ARNT in human breast cancer cells.* J Biol Chem, 2006. **281**(21): p. 14654-62.

120. Choi, H., et al., *Curcumin inhibits hypoxia-inducible factor-1 by degrading aryl hydrocarbon receptor nuclear translocator: a mechanism of tumor growth inhibition.* Mol Pharmacol, 2006. **70**(5): p. 1664-71.

121. Lees, M.J., D.J. Peet, and M.L. Whitelaw, *Defining the role for XAP2 in stabilization of the dioxin receptor.* J Biol Chem, 2003. **278**(38): p. 35878-88.

122. Gunton, J.E., et al., *Loss of ARNT/HIF1beta mediates altered gene expression and pancreatic-islet dysfunction in human type 2 diabetes.* Cell, 2005. **122**(3): p. 337-49.

123. Chilov, D., et al., *Induction and nuclear translocation of hypoxia-inducible factor-1 (HIF-1): heterodimerization with ARNT is not necessary for nuclear accumulation of HIF-1alpha.* J Cell Sci, 1999. **112 (Pt 8)**: p. 1203-12.

124. Lee, K.H., J.W. Park, and Y.S. Chun, *Non-hypoxic transcriptional activation of the aryl hydrocarbon receptor nuclear translocator in concert with a novel hypoxia-inducible factor-1alpha isoform.* Nucleic Acids Res, 2004. **32**(18): p. 5499-511.

125. Maltepe, E., et al., *The role of ARNT2 in tumor angiogenesis and the neural response to hypoxia.* Biochem Biophys Res Commun, 2000. **273**(1): p. 231-8.

126. Ruegg, J., et al., *The transcription factor aryl hydrocarbon receptor nuclear translocator functions as an estrogen receptor beta-selective coactivator, and its recruitment to alternative pathways mediates antiestrogenic effects of dioxin.* Mol Endocrinol, 2008. **22**(2): p. 304-16.

127. Holmes, J.L. and R.S. Pollenz, *Determination of aryl hydrocarbon receptor nuclear translocator protein concentration and subcellular localization in hepatic and nonhepatic cell culture lines: development of quantitative Western blotting protocols for calculation of aryl hydrocarbon receptor and aryl hydrocarbon receptor nuclear translocator protein in total cell lysates.* Mol Pharmacol, 1997. **52**(2): p. 202-11.

128. Okui, M., et al., *Transcription factor single-minded 2 (SIM2) is ubiquitinated by the RING-IBR-RING-type E3 ubiquitin ligases.* Exp Cell Res, 2005. **309**(1): p. 220-8.

129. Swanson, H.I., W.K. Chan, and C.A. Bradfield, *DNA binding specificities and pairing rules of the Ah receptor, ARNT, and SIM proteins.* J Biol Chem, 1995. **270**(44): p. 26292-302.

130. Lee, I.J., et al., *Transcriptional induction of the cytochrome P4501A1 gene by a thiazolium compound, YH439.* Mol Pharmacol, 1996. **49**(6): p. 980-8.

131. Numayama-Tsuruta, K., et al., *A point mutation responsible for defective function of the aryl-hydrocarbon-receptor nuclear translocator in mutant Hepa-1c1c7 cells.* Eur J Biochem, 1997. **246**(2): p. 486-95.

132. To, K.K., et al., *The phosphorylation status of PAS-B distinguishes HIF-1alpha from HIF-2alpha in NBS1 repression.* Embo J, 2006. **25**(20): p. 4784-94.

133. Lindebro, M.C., L. Poellinger, and M.L. Whitelaw, *Protein-protein interaction via PAS domains: role of the PAS domain in positive and negative regulation of the bHLH/PAS dioxin receptor-Arnt transcription factor complex.* Embo J, 1995. **14**(14): p. 3528-39.

134. Zhou, J., et al., *Tumor hypoxia and cancer progression.* Cancer Lett, 2006. **237**(1): p. 10-21.

135. Schena, M., et al., *Quantitative monitoring of gene expression patterns with a complementary DNA microarray.* Science, 1995. **270**(5235): p. 467-70.

136. Mori, T., et al., *Cyclin K as a direct transcriptional target of the p53 tumor suppressor.* Neoplasia, 2002. **4**(3): p. 268-74.

137. Downing, S., et al., *Elevated levels of prostate-specific antigen (PSA) in prostate cancer cells expressing mutant p53 is associated with tumor metastasis.* Mol Carcinog, 2003. **38**(3): p. 130-40.

138. Amling, C.L., *Prostate-specific antigen and detection of prostate cancer: What have we learned and what should we recommend for screening?* Curr Treat Options Oncol, 2006. **7**(5): p. 337-45.

139. Brand, T.C., et al., *Prostate cancer detection strategies.* Curr Urol Rep, 2006. **7**(3): p. 181-5.

140. Jung, M., et al., *mRNA expression of the five membrane-type matrix metalloproteinases MT1-MT5 in human prostatic cell lines and their down-regulation in human malignant prostatic tissue.* Prostate, 2003. **55**(2): p. 89-98.

141. Iwai, K., et al., *An anti-proliferative gene BTG1 regulates angiogenesis in vitro.* Biochemical and Biophysical Research Communications, 2004. **316**(3): p. 628-635.

142. Castagna, A., et al., *A proteomic approach to cisplatin resistance in the cervix squamous cell carcinoma cell line A431.* Proteomics, 2004. **4**(10): p. 3246-67.

143. Tonks, N.K., *Protein tyrosine phosphatases: from genes, to function, to disease.* Nat Rev Mol Cell Biol, 2006. **7**(11): p. 833-46.

144. Easty, D., W. Gallagher, and D.C. Bennett, *Protein tyrosine phosphatases, new targets for cancer therapy.* Curr Cancer Drug Targets, 2006. **6**(6): p. 519-32.

145. Glynne-Jones, E., et al., *TENB2, a proteoglycan identified in prostate cancer that is associated with disease progression and androgen independence.* Int J Cancer, 2001. **94**(2): p. 178-84.

146. Chen, M.E., et al., *Isolation and characterization of PAGE-1 and GAGE-7. New genes expressed in the LNCaP prostate cancer progression model that share homology with melanoma-associated antigens.* J Biol Chem, 1998. **273**(28): p. 17618-25.

147. Missiaglia, E., et al., *Analysis of gene expression in cancer cell lines identifies candidate markers for pancreatic tumorigenesis and metastasis.* Int J Cancer, 2004. **112**(1): p. 100-12.

148. Ohuchida, K., et al., *S100P is an early developmental marker of pancreatic carcinogenesis.* Clin Cancer Res, 2006. **12**(18): p. 5411-6.

149. Hammacher, A., E.W. Thompson, and E.D. Williams, *Interleukin-6 is a potent inducer of S100P, which is up-regulated in androgen-refractory and metastatic prostate cancer.* Int J Biochem Cell Biol, 2005. **37**(2): p. 442-50.

150. Van Den Maagdenberg, A.M., et al., *The mouse Ptprr gene encodes two protein tyrosine phosphatases, PTP-SL and PTPBR7, that display distinct patterns of expression during neural development.* Eur J Neurosci, 1999. **11**(11): p. 3832-44.

151. Chirivi, R.G., et al., *Characterization of multiple transcripts and isoforms derived from the mouse protein tyrosine phosphatase gene Ptprr.* Genes Cells, 2004. **9**(10): p. 919-33.

152. Iacobuzio-Donahue, C.A., et al., *Highly expressed genes in pancreatic ductal adenocarcinomas: a comprehensive characterization and comparison of the transcription profiles obtained from three major technologies.* Cancer Res, 2003b. **63**(24): p. 8614-22.

153. Iacobuzio-Donahue, C.A., et al., *Discovery of novel tumor markers of pancreatic cancer using global gene expression technology.* Am J Pathol, 2002. **160**(4): p. 1239-49.

154. Park, C.G., et al., *A novel gene product that couples TCR signaling to Fas(CD95) expression in activation-induced cell death.* Immunity, 1996. **4**(6): p. 583-91.

155. Neef, R., et al., *Identification of the human PHLDA1/TDAG51 gene: down-regulation in metastatic melanoma contributes to apoptosis resistance and growth deregulation.* Cancer Res, 2002. **62**(20): p. 5920-9.

156. Ray, R., et al., *BNIP3 heterodimerizes with Bcl-2/Bcl-X(L) and induces cell death independent of a Bcl-2 homology 3 (BH3) domain at both mitochondrial and nonmitochondrial sites.* J Biol Chem, 2000. **275**(2): p. 1439-48.

157. Vande Velde, C., et al., *BNIP3 and genetic control of necrosis-like cell death through the mitochondrial permeability transition pore.* Mol Cell Biol, 2000. **20**(15): p. 5454-68.

158. Greijer, A.E. and E. van der Wall, *The role of hypoxia inducible factor 1 (HIF-1) in hypoxia induced apoptosis.* J Clin Pathol, 2004. **57**(10): p. 1009-14.

159. Wu, M.X., *Roles of the stress-induced gene IEX-1 in regulation of cell death and oncogenesis.* Apoptosis, 2003. **8**(1): p. 11-8.

160. Nakada, M., et al., *Testican 2 abrogates inhibition of membrane-type matrix metalloproteinases by other testican family proteins.* Cancer Res, 2003. **63**(12): p. 3364-9.

161. Cao, J., et al., *Membrane type 1-matrix metalloproteinase promotes human prostate cancer invasion and metastasis.* Thromb Haemost, 2005. **93**(4): p. 770-8.

162. Katoh, Y. and M. Katoh, *Canonical WNT signaling pathway and human AREG.* Int J Mol Med, 2006. **17**(6): p. 1163-6.

163. Torring, N., et al., *Increase in amphiregulin and epiregulin in prostate cancer xenograft after androgen deprivation-impact of specific HER1 inhibition.* Prostate, 2005. **64**(1): p. 1-8.

164. Yang, W., et al., *Proteasome inhibition induces both pro- and anti-cell death pathways in prostate cancer cells.* Cancer Lett, 2006. **243**(2): p. 217-27.

165. Zhu, Z., et al., *Epiregulin is Up-regulated in pancreatic cancer and stimulates pancreatic cancer cell growth.* Biochem Biophys Res Commun, 2000. **273**(3): p. 1019-24.

166. Halvorsen, O.J., et al., *Gene expression profiles in prostate cancer: association with patient subgroups and tumour differentiation.* Int J Oncol, 2005. **26**(2): p. 329-36.

167. Averboukh, L., et al., *Regulation of S100P expression by androgen.* Prostate, 1996. **29**(6): p. 350-5.

168. Parkkila, S., et al., *The calcium-binding protein S100P in normal and malignant human tissues.* BMC Clinical Pathology, 2008. **8**(1): p. 2.

169. Amler, L.C., et al., *Dysregulated expression of androgen-responsive and nonresponsive genes in the androgen-independent prostate cancer xenograft model CWR22-R1.* Cancer Res, 2000. **60**(21): p. 6134-41.

170. Sasada, T., et al., *Prognostic significance of the immediate early response gene X-1 (IEX-1) expression in pancreatic cancer.* Ann Surg Oncol, 2008. **15**(2): p. 609-17.

171. Kim, H.S., et al., *Identification of novel Wilms' tumor suppressor gene target genes implicated in kidney development.* J Biol Chem, 2007. **282**(22): p. 16278-87.

172. Li, C.M., et al., *CTNNB1 mutations and overexpression of Wnt/beta-catenin target genes in WT1-mutant Wilms' tumors.* Am J Pathol, 2004. **165**(6): p. 1943-53.

173. Lee, H. and S.G. Paik, *Regulation of BNIP3 in normal and cancer cells.* Mol Cells, 2006. **21**(1): p. 1-6.

174. Burton, T.R. and S.B. Gibson, *The role of Bcl-2 family member BNIP3 in cell death and disease: NIPping at the heels of cell death.* Cell Death Differ, 2009.

175. Levine, B. and G. Kroemer, *Autophagy in the pathogenesis of disease.* Cell, 2008. **132**(1): p. 27-42.

176. Maiuri, M.C., et al., *Self-eating and self-killing: crosstalk between autophagy and apoptosis.* Nat Rev Mol Cell Biol, 2007. **8**(9): p. 741-52.

177. Erkan, M., et al., *Loss of BNIP3 expression is a late event in pancreatic cancer contributing to chemoresistance and worsened prognosis.* Oncogene, 2005. **24**(27): p. 4421-32.

178. Akada, M., et al., *Intrinsic chemoresistance to gemcitabine is associated with decreased expression of BNIP3 in pancreatic cancer.* Clin Cancer Res, 2005. **11**(8): p. 3094-101.

179. de Angelis, P.M., et al., *Molecular characterizations of derivatives of HCT116 colorectal cancer cells that are resistant to the chemotherapeutic agent 5-fluorouracil.* Int J Oncol, 2004. **24**(5): p. 1279-88.

180. Ishiguro, M., et al., *Effect of combined therapy with low-dose 5-aza-2'-deoxycytidine and irinotecan on colon cancer cell line HCT-15.* Ann Surg Oncol, 2007. **14**(5): p. 1752-62.

181. Bacon, A.L., et al., *Selective silencing of the hypoxia-inducible factor 1 target gene BNIP3 by histone deacetylation and methylation in colorectal cancer.* Oncogene, 2007. **26**(1): p. 132-41.

182. Mahon, P.C., et al., *S100A4 contributes to the suppression of BNIP3 expression, chemoresistance, and inhibition of apoptosis in pancreatic cancer.* Cancer Res, 2007. **67**(14): p. 6786-95.

183. Okami, J., D.M. Simeone, and C.D. Logsdon, *Silencing of the hypoxia-inducible cell death protein BNIP3 in pancreatic cancer.* Cancer Res, 2004. **64**(15): p. 5338-46.

184. Murai, M., et al., *Aberrant methylation and silencing of the BNIP3 gene in colorectal and gastric cancer.* Clin Cancer Res, 2005. **11**(3): p. 1021-7.

185. Abe, T., et al., *Upregulation of BNIP3 by 5-aza-2'-deoxycytidine sensitizes pancreatic cancer cells to hypoxia-mediated cell death.* J Gastroenterol, 2005. **40**(5): p. 504-10.

186. Azad, M.B., et al., *Hypoxia induces autophagic cell death in apoptosis-competent cells through a mechanism involving BNIP3.* Autophagy, 2008. **4**(2): p. 195-204.

187. Tracy, K., et al., *BNIP3 is an RB/E2F target gene required for hypoxia-induced autophagy.* Mol Cell Biol, 2007a. **27**(17): p. 6229-42.

188. Bruick, R.K., *Expression of the gene encoding the proapoptotic Nip3 protein is induced by hypoxia.* Proc Natl Acad Sci U S A, 2000. **97**(16): p. 9082-7.

189. Semenza, G.L., *HIF-1 and human disease: one highly involved factor.* Genes Dev, 2000. **14**(16): p. 1983-91.

190. Mellor, H.R. and A.L. Harris, *The role of the hypoxia-inducible BH3-only proteins BNIP3 and BNIP3L in cancer.* Cancer Metastasis Rev, 2007. **26**(3-4): p. 553-66.

191. Pursiheimo, J.P., et al., *Hypoxia-activated autophagy accelerates degradation of SQSTM1/p62.* Oncogene, 2009. **28**(3): p. 334-44.

192. Kubli, D.A., J.E. Ycaza, and A.B. Gustafsson, *Bnip3 mediates mitochondrial dysfunction and cell death through Bax and Bak.* Biochem J, 2007. **405**(3): p. 407-15.

193. Zhang, H., et al., *Mitochondrial autophagy is an HIF-1-dependent adaptive metabolic response to hypoxia.* J Biol Chem, 2008. **283**(16): p. 10892-903.

194. Mizushima, N. and T. Yoshimori, *How to interpret LC3 immunoblotting.* Autophagy, 2007. **3**(6): p. 542-5.

195. Klionsky, D.J., et al., *Guidelines for the use and interpretation of assays for monitoring autophagy in higher eukaryotes.* Autophagy, 2008. **4**(2): p. 151-75.

196. Kimbro, K.S. and J.W. Simons, *Hypoxia-inducible factor-1 in human breast and prostate cancer.* Endocr Relat Cancer, 2006. **13**(3): p. 739-49.

197. Varambally, S., et al., *Integrative genomic and proteomic analysis of prostate cancer reveals signatures of metastatic progression.* Cancer Cell, 2005. **8**(5): p. 393-406.

198. Yu, Y.P., et al., *Gene expression alterations in prostate cancer predicting tumor aggression and preceding development of malignancy.* J Clin Oncol, 2004. **22**(14): p. 2790-9.

199. Lum, L. and P.A. Beachy, *The Hedgehog response network: sensors, switches, and routers.* Science, 2004. **304**(5678): p. 1755-9.

200. Mullor, J.L., P. Sanchez, and A. Ruiz i Altaba, *Pathways and consequences: Hedgehog signaling in human disease.* Trends Cell Biol, 2002. **12**(12): p. 562-9.

201. Ingham, P.W. and A.P. McMahon, *Hedgehog signaling in animal development: paradigms and principles.* Genes Dev, 2001. **15**(23): p. 3059-87.

202. Beachy, P.A., S.S. Karhadkar, and D.M. Berman, *Tissue repair and stem cell renewal in carcinogenesis.* Nature, 2004. **432**(7015): p. 324-31.

203. Lee, C.J., J. Dosch, and D.M. Simeone, *Pancreatic cancer stem cells.* J Clin Oncol, 2008. **26**(17): p. 2806-12.

204. Morton, J.P. and B.C. Lewis, *Shh signaling and pancreatic cancer: implications for therapy?* Cell Cycle, 2007b. **6**(13): p. 1553-7.

205. Ruiz i Altaba, A., P. Sanchez, and N. Dahmane, *Gli and hedgehog in cancer: tumours, embryos and stem cells.* Nat Rev Cancer, 2002. **2**(5): p. 361-72.

206. Taipale, J. and P.A. Beachy, *The Hedgehog and Wnt signalling pathways in cancer.* Nature, 2001. **411**(6835): p. 349-54.

207. Marigo, V., et al., *Cloning, expression, and chromosomal location of SHH and IHH: two human homologues of the Drosophila segment polarity gene hedgehog.* Genomics, 1995. **28**(1): p. 44-51.

208. Ruppert, J.M., et al., *The GLI-Kruppel family of human genes.* Mol Cell Biol, 1988. **8**(8): p. 3104-13.

209. Hui, C.C., et al., *Expression of three mouse homologs of the Drosophila segment polarity gene cubitus interruptus, Gli, Gli-2, and Gli-3, in ectoderm- and mesoderm-derived tissues suggests multiple roles during postimplantation development.* Dev Biol, 1994. **162**(2): p. 402-13.

210. Dai, P., et al., *Sonic Hedgehog-induced activation of the Gli1 promoter is mediated by GLI3.* J Biol Chem, 1999. **274**(12): p. 8143-52.

211. Ruiz i Altaba, A., *Combinatorial Gli gene function in floor plate and neuronal inductions by Sonic hedgehog.* Development, 1998. **125**(12): p. 2203-12.

212. Buscher, D., et al., *Evidence for genetic control of Sonic hedgehog by Gli3 in mouse limb development.* Mech Dev, 1997. **62**(2): p. 175-82.

213. Hu, M.C., et al., *GLI3-dependent transcriptional repression of Gli1, Gli2 and kidney patterning genes disrupts renal morphogenesis.* Development, 2006. **133**(3): p. 569-78.

214. Goodrich, L.V., et al., *Overexpression of ptc1 inhibits induction of Shh target genes and prevents normal patterning in the neural tube.* Dev Biol, 1999. **211**(2): p. 323-34.

215. Agren, M., et al., *Expression of the PTCH1 tumor suppressor gene is regulated by alternative promoters and a single functional Gli-binding site.* Gene, 2004. **330**: p. 101-14.

216. Buttitta, L., et al., *Interplays of Gli2 and Gli3 and their requirement in mediating Shh-dependent sclerotome induction.* Development, 2003. **130**(25): p. 6233-43.

217. Murone, M., A. Rosenthal, and F.J. de Sauvage, *Sonic hedgehog signaling by the patched-smoothened receptor complex.* Curr Biol, 1999. **9**(2): p. 76-84.

218. Katoh, Y. and M. Katoh, *Hedgehog signaling pathway and gastric cancer.* Cancer Biol Ther, 2005. **4**(10): p. 1050-4.

219. Thayer, S.P., et al., *Hedgehog is an early and late mediator of pancreatic cancer tumorigenesis.* Nature, 2003. **425**(6960): p. 851-6.

220. Morton, J.P., et al., *Sonic hedgehog acts at multiple stages during pancreatic tumorigenesis.* Proc Natl Acad Sci U S A, 2007a. **104**(12): p. 5103-8.

221. Berman, D.M., et al., *Widespread requirement for Hedgehog ligand stimulation in growth of digestive tract tumours.* Nature, 2003. **425**(6960): p. 846-51.

222. Chen, B.Y., et al., *A mouse prostate cancer model induced by Hedgehog overexpression.* J Biomed Sci, 2006. **13**(3): p. 373-84.

223. Datta, S. and M.W. Datta, *Sonic Hedgehog signaling in advanced prostate cancer.* Cell Mol Life Sci, 2006. **63**(4): p. 435-48.

224. Fan, L., et al., *Hedgehog signaling promotes prostate xenograft tumor growth.* Endocrinology, 2004. **145**(8): p. 3961-70.

225. Incardona, J.P., et al., *The teratogenic Veratrum alkaloid cyclopamine inhibits sonic hedgehog signal transduction.* Development, 1998. **125**(18): p. 3553-62.

226. Kayed, H., et al., *Indian hedgehog signaling pathway: expression and regulation in pancreatic cancer.* Int J Cancer, 2004a. **110**(5): p. 668-76.

227. Qualtrough, D., et al., *Hedgehog signalling in colorectal tumour cells: induction of apoptosis with cyclopamine treatment.* Int J Cancer, 2004. **110**(6): p. 831-7.

228. Sheng, T., et al., *Activation of the hedgehog pathway in advanced prostate cancer.* Mol Cancer, 2004. **3**: p. 29.

229. Kumar, S.K., et al., *Targeted inhibition of hedgehog signaling by cyclopamine prodrugs for advanced prostate cancer.* Bioorg Med Chem, 2008. **16**(6): p. 2764-8.

230. Chatel, G., et al., *Hedgehog signaling pathway is inactive in colorectal cancer cell lines.* Int J Cancer, 2007. **121**(12): p. 2622-7.

231. Kim, S.K. and M. Hebrok, *Intercellular signals regulating pancreas development and function.* Genes Dev, 2001. **15**(2): p. 111-27.

232. Kim, S.K. and D.A. Melton, *Pancreas development is promoted by cyclopamine, a hedgehog signaling inhibitor.* Proc Natl Acad Sci U S A, 1998. **95**(22): p. 13036-41.

233. Murtaugh, L.C. and D.A. Melton, *Genes, signals, and lineages in pancreas development.* Annu Rev Cell Dev Biol, 2003. **19**: p. 71-89.

234. Hansel, D.E., S.E. Kern, and R.H. Hruban, *Molecular pathogenesis of pancreatic cancer.* Annu Rev Genomics Hum Genet, 2003. **4**: p. 237-56.

235. Aguirre, A.J., et al., *Activated Kras and Ink4a/Arf deficiency cooperate to produce metastatic pancreatic ductal adenocarcinoma.* Genes Dev, 2003. **17**(24): p. 3112-26.

236. Bardeesy, N., et al., *Obligate roles for p16(Ink4a) and p19(Arf)-p53 in the suppression of murine pancreatic neoplasia.* Mol Cell Biol, 2002. **22**(2): p. 635-43.

237. Bearzatto, A., et al., *p16(INK4A) Hypermethylation detected by fluorescent methylation-specific PCR in plasmas from non-small cell lung cancer.* Clin Cancer Res, 2002. **8**(12): p. 3782-7.

238. Robertson, K.D. and P.A. Jones, *The human ARF cell cycle regulatory gene promoter is a CpG island which can be silenced by DNA methylation and down-regulated by wild-type p53.* Mol Cell Biol, 1998. **18**(11): p. 6457-73.

239. Simon, B. and N. Lubomierski, *Implication of the INK4a/ARF locus in gastroenteropancreatic neuroendocrine tumorigenesis.* Ann N Y Acad Sci, 2004. **1014**: p. 284-99.

240. Miyamoto, Y., et al., *Notch mediates TGF alpha-induced changes in epithelial differentiation during pancreatic tumorigenesis.* Cancer Cell, 2003. **3**(6): p. 565-76.

241. *Finishing the euchromatic sequence of the human genome.* Nature, 2004. **431**(7011): p. 931-45.

242. Chen, J.K., et al., *Inhibition of Hedgehog signaling by direct binding of cyclopamine to Smoothened.* Genes Dev, 2002. **16**(21): p. 2743-8.

243. Taipale, J., et al., *Effects of oncogenic mutations in Smoothened and Patched can be reversed by cyclopamine.* Nature, 2000. **406**(6799): p. 1005-9.

244. Park, H.L., et al., *Mouse Gli1 mutants are viable but have defects in SHH signaling in combination with a Gli2 mutation.* Development, 2000. **127**(8): p. 1593-605.

245. Mo, R., et al., *Specific and redundant functions of Gli2 and Gli3 zinc finger genes in skeletal patterning and development.* Development, 1997. **124**(1): p. 113-23.

246. Johnson, D.R., *Extra-toes: anew mutant gene causing multiple abnormalities in the mouse.* J Embryol Exp Morphol, 1967. **17**(3): p. 543-81.

247. Apelqvist, A., U. Ahlgren, and H. Edlund, *Sonic hedgehog directs specialised mesoderm differentiation in the intestine and pancreas.* Curr Biol, 1997. **7**(10): p. 801-4.

248. Zeng, X., et al., *A freely diffusible form of Sonic hedgehog mediates long-range signalling.* Nature, 2001. **411**(6838): p. 716-20.

249. Ahlgren, U., et al., *beta-cell-specific inactivation of the mouse Ipf1/Pdx1 gene results in loss of the beta-cell phenotype and maturity onset diabetes.* Genes Dev, 1998. **12**(12): p. 1763-8.

250. Kayed, H., et al., *Hedgehog signaling in the normal and diseased pancreas.* Pancreas, 2006. **32**(2): p. 119-29.

251. Anton Aparicio, L.M., et al., *Prostate cancer and Hedgehog signalling pathway.* Clin Transl Oncol, 2007. **9**(7): p. 420-8.

252. Gustafsson, M.K., et al., *Myf5 is a direct target of long-range Shh signaling and Gli regulation for muscle specification.* Genes Dev, 2002. **16**(1): p. 114-26.

253. Teboul, L., D. Summerbell, and P.W. Rigby, *The initial somitic phase of Myf5 expression requires neither Shh signaling nor Gli regulation.* Genes Dev, 2003. **17**(23): p. 2870-4.

254. Bigelow, R.L., et al., *Transcriptional regulation of bcl-2 mediated by the sonic hedgehog signaling pathway through gli-1.* J Biol Chem, 2004. **279**(2): p. 1197-205.

255. Hingorani, S.R., et al., *Preinvasive and invasive ductal pancreatic cancer and its early detection in the mouse.* Cancer Cell, 2003. **4**(6): p. 437-50.

256. Richter, E., S. Srivastava, and A. Dobi, *Androgen receptor and prostate cancer.* Prostate Cancer Prostatic Dis, 2007. **10**(2): p. 114-8.

257. Zhu, M.L. and N. Kyprianou, *Androgen receptor and growth factor signaling cross-talk in prostate cancer cells.* Endocr Relat Cancer, 2008. **15**(4): p. 841-9.

258. Heinlein, C.A. and C. Chang, *Androgen receptor in prostate cancer.* Endocr Rev, 2004. **25**(2): p. 276-308.

259. Wang, X., et al., *Targeted treatment of prostate cancer.* J Cell Biochem, 2007. **102**(3): p. 571-9.

260. Jeet, V., et al., *Broadening of transgenic adenocarcinoma of the mouse prostate (TRAMP) model to represent late stage androgen depletion independent cancer.* Prostate, 2008. **68**(5): p. 548-62.

261. Han, G., et al., *Hormone status selects for spontaneous somatic androgen receptor variants that demonstrate specific ligand and cofactor dependent activities in autochthonous prostate cancer.* J Biol Chem, 2001. **276**(14): p. 11204-13.

262. Lee, D.K. and C. Chang, *Molecular communication between androgen receptor and general transcription machinery.* J Steroid Biochem Mol Biol, 2003. **84**(1): p. 41-9.

263. Claessens, F., et al., *The androgen-specific probasin response element 2 interacts differentially with androgen and glucocorticoid receptors.* J Biol Chem, 1996. **271**(32): p. 19013-6.

264. Kim, J. and G.A. Coetzee, *Prostate specific antigen gene regulation by androgen receptor.* J Cell Biochem, 2004. **93**(2): p. 233-41.

265. Tilley, W.D., et al., *Mutations in the androgen receptor gene are associated with progression of human prostate cancer to androgen independence.* Clin Cancer Res, 1996. **2**(2): p. 277-85.

266. Koivisto, P., et al., *Androgen receptor gene amplification: a possible molecular mechanism for androgen deprivation therapy failure in prostate cancer.* Cancer Res, 1997. **57**(2): p. 314-9.

267. Chen, C.D., et al., *Molecular determinants of resistance to antiandrogen therapy.* Nat Med, 2004. **10**(1): p. 33-9.

268. Gregory, C.W., et al., *Androgen receptor stabilization in recurrent prostate cancer is associated with hypersensitivity to low androgen.* Cancer Res, 2001. **61**(7): p. 2892-8.

269. Taplin, M.E., et al., *Mutation of the androgen-receptor gene in metastatic androgen-independent prostate cancer.* N Engl J Med, 1995. **332**(21): p. 1393-8.

270. Li, R., et al., *High level of androgen receptor is associated with aggressive clinicopathologic features and decreased biochemical recurrence-free survival in prostate: cancer patients treated with radical prostatectomy.* Am J Surg Pathol, 2004. **28**(7): p. 928-34.

271. Han, G., et al., *Mutation of the androgen receptor causes oncogenic transformation of the prostate.* Proc Natl Acad Sci U S A, 2005. **102**(4): p. 1151-6.

272. Reid, J., et al., *Conformational analysis of the androgen receptor amino-terminal domain involved in transactivation. Influence of structure-stabilizing solutes and protein-protein interactions.* J Biol Chem, 2002. **277**(22): p. 20079-86.

273. Ohtake, F., et al., *Dioxin receptor is a ligand-dependent E3 ubiquitin ligase.* Nature, 2007. **446**(7135): p. 562-6.

274. Buchanan, G., et al., *PC-3 cells with enhanced androgen receptor signaling: a model for clonal selection in prostate cancer.* Prostate, 2004. **60**(4): p. 352-66.

275. Jarrard, D.F., et al., *Methylation of the androgen receptor promoter CpG island is associated with loss of androgen receptor expression in prostate cancer cells.* Cancer Res, 1998. **58**(23): p. 5310-4.

276. Tilley, W.D., et al., *Evidence for a novel mechanism of androgen resistance in the human prostate cancer cell line, PC-3.* Steroids, 1995. **60**(1): p. 180-6.

277. Chlenski, A., et al., *Androgen receptor expression in androgen-independent prostate cancer cell lines.* Prostate, 2001. **47**(1): p. 66-75.

278. Zhang, J., et al., *A small composite probasin promoter confers high levels of prostate-specific gene expression through regulation by androgens and glucocorticoids in vitro and in vivo.* Endocrinology, 2000. **141**(12): p. 4698-710.

279. Brunnberg, S., et al., *The basic helix-loop-helix-PAS protein ARNT functions as a potent coactivator of estrogen receptor-dependent transcription.* Proc Natl Acad Sci U S A, 2003. **100**(11): p. 6517-22.

280. Ohtake, F., et al., *Intrinsic AhR function underlies cross-talk of dioxins with sex hormone signalings.* Biochem Biophys Res Commun, 2008. **370**(4): p. 541-6.

281. Conzen, S.D., *Minireview: nuclear receptors and breast cancer.* Mol Endocrinol, 2008. **22**(10): p. 2215-28.

282. Rae, J.M., et al., *MDA-MB-435 cells are derived from M14 melanoma cells--a loss for breast cancer, but a boon for melanoma research.* Breast Cancer Res Treat, 2007. **104**(1): p. 13-9.

283. Liu, Y.N., et al., *Activated androgen receptor downregulates E-cadherin gene expression and promotes tumor metastasis.* Mol Cell Biol, 2008. **28**(23): p. 7096-108.

284. Gregory, C.W., et al., *A mechanism for androgen receptor-mediated prostate cancer recurrence after androgen deprivation therapy.* Cancer Res, 2001. **61**(11): p. 4315-9.

285. Culig, Z., et al., *Androgen receptor activation in prostatic tumor cell lines by insulin-like growth factor-I, keratinocyte growth factor, and epidermal growth factor.* Cancer Res, 1994. **54**(20): p. 5474-8.

286. Wen, Y., et al., *HER-2/neu promotes androgen-independent survival and growth of prostate cancer cells through the Akt pathway.* Cancer Res, 2000. **60**(24): p. 6841-5.

287. Koh, M.Y., T.R. Spivak-Kroizman, and G. Powis, *HIF-1 regulation: not so easy come, easy go.* Trends Biochem Sci, 2008.

288. Isaacs, W.B., B.S. Carter, and C.M. Ewing, *Wild-type p53 suppresses growth of human prostate cancer cells containing mutant p53 alleles.* Cancer Res, 1991. **51**(17): p. 4716-20.

289. Isaacs, J.S., et al., *Hsp90 regulates a von Hippel Lindau-independent hypoxia-inducible factor-1 alpha-degradative pathway.* J Biol Chem, 2002. **277**(33): p. 29936-44.

290. Downing, S.R., P.J. Russell, and P. Jackson, *Alterations of p53 are common in early stage prostate cancer.* Can J Urol, 2003. **10**(4): p. 1924-33.

291. Bookstein, R., et al., *p53 is mutated in a subset of advanced-stage prostate cancers.* Cancer Res, 1993. **53**(14): p. 3369-73.

292. Heidenberg, H.B., et al., *Alteration of the tumor suppressor gene p53 in a high fraction of hormone refractory prostate cancer.* J Urol, 1995. **154**(2 Pt 1): p. 414-21.

293. McGuire, J., et al., *The basic helix-loop-helix/PAS factor Sim is associated with hsp90. Implications for regulation by interaction with partner factors.* J Biol Chem, 1995. **270**(52): p. 31353-7.

294. Rudolfsson, S.H. and A. Bergh, *Testosterone-stimulated growth of the rat prostate may be driven by tissue hypoxia and hypoxia-inducible factor-1alpha.* J Endocrinol, 2008. **196**(1): p. 11-9.

295. Ravi, R., et al., *Regulation of tumor angiogenesis by p53-induced degradation of hypoxia-inducible factor 1alpha.* Genes Dev, 2000. **14**(1): p. 34-44.

296. Bajgelman, M.C. and B.E. Strauss, *The DU145 human prostate carcinoma cell line harbors a temperature-sensitive allele of p53.* Prostate, 2006. **66**(13): p. 1455-62.

297. Kimura, K., et al., *Activation of Notch signaling in tumorigenesis of experimental pancreatic cancer induced by dimethylbenzanthracene in mice.* Cancer Sci, 2007. **98**(2): p. 155-62.

298. De La, O.J., et al., *Notch and Kras reprogram pancreatic acinar cells to ductal intraepithelial neoplasia.* Proc Natl Acad Sci U S A, 2008. **105**(48): p. 18907-12.

299. Wang, Z., et al., *Epidermal growth factor receptor-related protein inhibits cell growth and invasion in pancreatic cancer.* Cancer Res, 2006. **66**(15): p. 7653-60.

300. Hugo, H., et al., *Epithelial--mesenchymal and mesenchymal--epithelial transitions in carcinoma progression.* J Cell Physiol, 2007. **213**(2): p. 374-83.

301. Sowter, H.M., et al., *HIF-1-dependent Regulation of Hypoxic Induction of the Cell Death Factors BNIP3 and NIX in Human Tumors.* Cancer Res, 2001. **61**(18): p. 6669-6673.

302. Boyd, J.M., et al., *Adenovirus E1B 19 kDa and Bcl-2 proteins interact with a common set of cellular proteins.* Cell, 1994. **79**(2): p. 341-51.

303. Yurkova, N., et al., *The cell cycle factor E2F-1 activates Bnip3 and the intrinsic death pathway in ventricular myocytes.* Circ Res, 2008. **102**(4): p. 472-9.

304. Shaw, J., et al., *Antagonism of E2F-1 regulated Bnip3 transcription by NF-kappaB is essential for basal cell survival.* Proc Natl Acad Sci U S A, 2008. **105**(52): p. 20734-9.

305. Shaw, J., et al., *Transcriptional silencing of the death gene BNIP3 by cooperative action of NF-kappaB and histone deacetylase 1 in ventricular myocytes.* Circ Res, 2006. **99**(12): p. 1347-54.

306. Horii, K., et al., *Androgen-dependent gene expression of prostate-specific antigen is enhanced synergistically by hypoxia in human prostate cancer cells.* Mol Cancer Res, 2007. **5**(4): p. 383-91.